Institute for Geoecology

Measurement and Modelling of Water and Sediment Fluxes in Meso-Scale Dryland Catchments

Dissertation submitted to the Faculty of Mathematics and Natural Sciences at the University of Potsdam, Germany
for the degree of Doctor of Natural Sciences (Dr. rer. nat.) in Geoecology

Till Konrad Otto Francke

Potsdam, March 2009

Published online at the
Institutional Repository of the University of Potsdam:
http://opus.kobv.de/ubp/volltexte/2009/3152/
urn:nbn:de:kobv:517-opus-31525
[http://nbn-resolving.de/urn:nbn:de:kobv:517-opus-31525]

He performs wonders that cannot be fathomed, miracles that cannot be counted.
He bestows rain on the earth; he sends water upon the countryside.

Job 5, 9-10

Contents

Abstract

Water shortage is a serious threat for many societies worldwide. In drylands, water management measures like the construction of reservoirs are affected by eroded sediments transported in the rivers. Thus, the capability of assessing water and sediment fluxes at the river basin scale is of vital importance to support management decisions and policy making. This subject was addressed by the DFG-funded SESAM-project (Sediment Export from large Semi-Arid catchments: Measurements and Modelling). As a part of this project, this thesis focuses on (1) the development and implementation of an erosion module for a meso-scale catchment model, (2) the development of upscaling and generalization methods for the parameterization of such model, (3) the execution of measurements to obtain data required for the modelling and (4) the application of the model to different study areas and its evaluation. The research was carried out in two meso-scale dryland catchments in NE-Spain: Ribera Salada (200 km²) and Isábena (450 km²).

Adressing objective 1, WASA-SED, a spatially semi-distributed model for water and sediment transport at the meso-scale was developed. The model simulates runoff and erosion processes at the hillslope scale, transport processes of suspended and bedload fluxes in the river reaches, and retention and remobilisation processes of sediments in reservoirs. This thesis introduces the model concept, presents current model applications and discusses its capabilities and limitations.

Modelling at larger scales faces the dilemma of describing relevant processes while maintaining a manageable demand for input data and computation time. WASA-SED addresses this challenge by employing an innovative catena-based upscaling approach: the landscape is represented by characteristic toposequences. For deriving these toposequences with regard to multiple attributes (eg. topography, soils, vegetation) the LUMP-algorithm (Landscape Unit Mapping Program) was developed and related to objective 2. It incorporates an algorithm to retrieve representative catenas and their attributes, based on a Digital Elevation Model and supplemental spatial data. These catenas are classified to provide the discretization for the WASA-SED model.

For objective 3, water and sediment fluxes were monitored at the catchment outlet of the Isábena and some of its subcatchments. For sediment yield estimation, the intermittent measurements of suspended sediment concentration (SSC) had to be interpolated. This thesis presents a comparison of traditional sediment rating curves (SRCs), generalized linear models (GLMs) and non-parametric regression using Random Forests (RF) and Quantile Regression Forests (QRF). The observed SSCs are highly variable and range over six orders of magnitude. For these data, traditional SRCs performed poorly, as did GLMs, despite including other relevant process variables (e.g. rainfall intensities, discharge characteristics). RF and QRF proved to be very robust and performed favourably for reproducing sediment dynamics. QRF additionally excels in providing estimates on the accuracy of the predictions. Subsequent analysis showed that most of the sediment was exported during intense storms of late summer. Later floods yielded successively less sediment. Comparing sediment generation to yield at the outlet suggested considerable storage effects within the river channel.

Addressing objective 4, the WASA-SED model was parameterized for the two study areas in NE Spain and applied with different foci. For Ribera Salada, the uncalibrated model yielded reasonable results for runoff and sediment. It provided quantitative measures of the change in runoff and sediment yield for different land-uses. Additional land management scenarios were presented and compared to impacts caused by climate change projections. In contrast, the application for the Isábena focussed on exploring the full potential of the model's predictive capabilities. The calibrated

model achieved an acceptable performance for the validation period in terms of water and sediment fluxes. The inadequate representation of the lower sub-catchments inflicted considerable reductions on model performance, while results for the headwater catchments showed good agreement despite stark contrasts in sediment yield.
In summary, the application of WASA-SED to three catchments proved the model framework to be a practicable multi-scale approach. It successfully links the hillslope to the catchment scale and integrates the three components hillslope, river and reservoir in one model. Thus, it provides a feasible approach for tackling issues of water and sediment yield at the meso-scale. The crucial role of processes like transmission losses and sediment storage in the river has been identified. Further advances can be expected when the representation of connectivity of water and sediment fluxes (intra-hillslope, hillslope-river, intra-river) is refined and input data improves.

Zusammenfassung

In vielen Regionen der Erde stellt Wassermangel ein Problem für die menschliche Gesellschaft dar. Insbesondere in Trockengebieten werden jedoch Maßnahmen des Wassermanagements, wie die Wasserspeicherung in Stauseen, durch die im Fluss transportierten Sedimentfrachten negativ beeinflusst. Somit stellen eine adäquate Beurteilung von Wasser- und Sedimentflüssen eine wichtige Voraussetzung für Entscheidungen in Wassermanagement und -planung dar. Dieser Problematik widmete sich das SESAM-Projekt (Sediment Export from large Semi-Arid catchments: Measurements and Modelling). Im Rahmen dieses Projektes befasste sich diese Dissertation mit (1) der Entwicklung und Umsetzung eines Erosions-Moduls für ein Einzugsgebietsmodell auf der Meso-Skala, (2) der Entwicklung von Skalierungs- und Generalisierungsmethoden für die Parametrisierung eines solchen Modells, (3) der Durchführung von Messungen, um die notwendigen Daten für das Modell zu gewinnen und (4) die Anwendung des Modells für verschiedene Einzugsgebiete und seiner Bewertung. Die Studie umfasste zwei mesoskalige Trockeneinzugsgebiete in NO-Spanien: Ribera Salada (200 km²) und Isábena (450 km²).

Im Hinblick auf Zielstellung 1 wurde WASA-SED, ein räumlich semi-distribuiertes Modell für Wasserflüsse und Sedimenttransport, entwickelt. Das Modell simuliert Abfluss- und Erosionsprozesse auf der Hangskala, den Transport von suspendierten und Geschiebesedimenten auf der Skala von Flussabschnitten sowie Rückhalt- und Remobilisierungsprozesse von Sedimenten in Stauseen. Die vorliegende Arbeit stellt das Modellkonzept und Modellanwendungen vor und beschreibt Fähigkeiten und Grenzen des Modells.

Die Modellierung auf größeren Skalen beinhaltet das Dilemma, dass relevante Prozesse beschrieben werden müssen, gleichzeitig aber die Anforderungen an Eingabedaten und Rechenzeit realisierbar bleiben. In WASA-SED wird diesem durch die Anwendung eines innovativen Hangprofil-basierten Skalierungsansatzes Rechnung getragen, indem die Landschaft durch charakteristische Toposequenzen repräsentiert wird. Um derartige Toposequenzen hinsichtlich verschiedener Landschaftseigenschaften (z.B. Relief, Böden, Vegetation) abzuleiten, wurde in Bezug zur Zielstellung 2 der LUMP-Algorithmus (Landscape Unit Mapping Program) entwickelt. LUMP beinhaltet ein Verfahren zur Berechnung repräsentativer Hangprofile und ihrer Attribute aus einem digitalen Geländemodell und optionalen Zusatzdaten. Durch die Klassifikation dieser Hangprofile wird die Grundlage der räumlichen Diskretisierung des WASA-SED Modells bereitgestellt.

Im Zusammenhang mit Zielstellung 3 wurden Abfluss und Sedimentkonzentration (SSC) am Auslass und in einigen Teileinzugsgebieten des Isábena-Einzugsgebietes gemessen. Um den Sedimentaustrag zu bestimmen, mussten die Einzelmessung der Sedimentkonzentration interpoliert werden. Diese Arbeit vergleicht die Eignung traditioneller Eichkurvenansätze (SRCs), Generalized Linear Models (GLMs) und der nichtparametrischen Regressionstechniken Random Forests (RF) und Quantile Regression Forests (QRF). Da die beobachteten SSC-Werte stark über sechs Größenordnungen variieren, erwiesen sich die traditionellen SRCs als unzureichend. Gleichfalls versagten GLMs trotz der Einbeziehung weiterer relevanter Prozessgrößen wie Niederschlagsintensitäten und Abflusscharakteristika. RF und QRF stellten sich hingegen als sehr robust und für die Rekonstruktion der Sedimentdynamik geeignet dar. QRF liefert darüber hinaus auch Informationen zur Genauigkeit dieser Schätzungen. Die darauf aufbauende Analyse ergab, dass der Großteil der Sedimentfracht während der Starkregenereignisse des Spätsommers transportiert wurde. Spätere Niederschlagsereignisse erzeugten deutlich geringeren Austrag. Durch den Vergleich von Sedimentfrachten im Oberlauf mit Austragsmengen am Gebietsauslass konnte die Bedeutung der Sediment-

speicherung im Flussbett identifiziert werden.
Zielstellung 4 wurde bearbeitet, indem das WASA-SED-Modell für zwei Untersuchungsgebiete in NO-Spanien unter unterschiedlichen Gesichtspunkten angewendet wurde. Für das Ribera-Salada-Einzugsgebiet lieferte das unkalibrierte Modell plausible Ergebnisse hinsichtlich der Wasser- und Sedimentflüsse. Damit war es möglich, die potentiellen Änderungen dieser Größen durch verschiedene Landnutzungsszenarien zu quantifizieren. Diese wurden den prognostizierten Veränderungen, die durch Klimaänderungen hervorgerufen würden, gegenübergestellt. Im Gegensatz dazu konzentrierte sich die Anwendung im Isábena-Einzugsgebiet auf die Untersuchung der bestmöglichen Modellanpassung. Im Validierungszeitraum ergab sich eine befriedigende Modellgüte für Wasser- und Sedimentflüsse. Diese Gesamtgüte wurde maßgeblich durch die unzureichende Abbildung der Unterliegergebiete beeinflusst, wohingegen die Gebiete des Oberlaufs, trotz ihrer stark kontrastierenden Sedimentausträge, gut dargestellt wurden.
Die Anwendung des WASA-SED-Modells auf drei verschiedene Untersuchungsgebiete bestätigt die generelle Eignung des Modellkonzepts als einen sinnvollen multiskaligen Ansatz, der in einem Modell effektiv die Hangskala mit der Einzugsgebietsskala sowie den Einfluss von Flüssen und Stauseen vereint. Er stellt somit eine mögliche Grundlage für die Bearbeitung von wasser- und sedimentbezogenen Fragestellungen auf der Meso-Skala dar. Die besondere Bedeutung der Prozesse der Sickerverluste und Sedimentspeicherung im Gerinne konnten herausgearbeitet werden. Mögliche Verbesserungen betreffen die Berücksichtigung der Konnektivität von Wasser- und Sedimentflüssen (auf dem Hang, zwischen Hang und Fluss, innerhalb des Flusses) und die Qualität der Eingangsdaten für das Modell.

Chapter I:

Introduction, objectives and overview

1. Introduction and background

Large parts of the Earth surface are covered by dryland regions, where the availability of water poses limitation on natural and economic systems. According to the IPCC report (Kundzewicz *et al.*, 2007), water shortage affects large parts of Africa, the Mediterranean region, the Near East, South Asia, Northern China, Australia, the USA, Mexico, North-East Brazil, and the western coast of South America. Thus, a quarter to a third of the world population is faced with these problems. Often, water supply problems are further aggravated by a rapid increase in population and water demand. In general, the projected implications of climate change are considered to worsen the dilemma further. Traditionally, mitigating these challenges by water management has aimed to address the temporal mismatch of water demand and supply and increase the reliability of the latter by constructing reservoirs. However, by retaining runoff, the transfer of sediments trough the river network is also interrupted. Thus, besides the well-known on-site implications of erosion (e.g. soil loss, degradation of cultivated areas, etc.), a series of subsequent problems arise once the sediments reach the river. Aspects of sediment-water quality interactions, channel navigability, fish and invertebrate habitat, malfunctioning of hydropower plants, instream mining, river restoration, river aesthetics, etc. (Walling, 1977; Williams, 1989) may be affected by excess sediment input and finally lead to the loss of reservoir storage volume within relatively short time spans. For Spain, which accounts for about 2.5 % of the world's dams, Avendaño *et al.* (1997) reported that almost 10 % of reservoirs in Spain have suffered a reduction in capacity of 50 % or more. De Araujo *et al.* (2006) showed that sedimentation of reservoirs is significantly decreasing water storage and thus water supply in the North-East of Brazil. Tamene *et al.* (2006) mention considerable impairment of dam services and increased costs for reconstruction due to siltation. The associated expenditure for dam replacement has been estimated at around US$ 6 billion globally (Fan & Springer, 1993). Hence, especially in many developing countries, sustainable land management and water resource development are often impaired by the aforementioned problems (Walling *et al.* 2001). The related human interference in the natural river course also has numerous effects downstream of reservoirs due to the alteration of flow (e.g. Batalla *et al.*, 2004) and sediment transport regimen (e.g. Vericat and Batalla, 2006). Further consequences may include increased scouring of the channel, impacts on riverine ecology and a perturbation of the equilibrium between fluvial and marine processes in deltaic and coastal zones, leading to subsequent implications like contamination of aquifers, obstruction of river flow due to excessive growth of macrophytes and destruction of habitats.

Thus, due to the number and complexity of the relevant processes, the impacts of water availability and sediment related issues are often revealed at the catchment or even larger scale, where they gain importance (Lu *et al.* 2003). Consequently, there is an urgent need for catchment based erosion control and sediment management (Walling *et al.*, 2001).

Numerical modelling can provide an integrated approach to investigate, reproduce, and, ideally, predict water and sediment dynamics of meso-scale basins and provide policy-makers with scientifically founded decision support on water resources and land management, e.g. agricultural practice, afforestation, reservoir management. However, in spite of the progress in hydrological modelling in recent years, the prediction of sediment yield at the catchment scale, let alone the dynamics thereof, still faces considerable problems (de Vente *et al.*, 2006). Erosion models are mostly designed for or derived from their use at the plot or hillslope scale, which causes three major challenges (Lu *et al.* 2003, Lenhart *et al.*, 2005): firstly, the usually large number of parameters involved is generally very expensive or even impossible to ob-

tain at the meso-scale. Secondly, the parameter variability (e.g. soil properties) is large and not adequately reflected in data sources available for that scale. Thirdly, upscaling from local to large domains is non-trivial because of the predominance of different processes at different scales. The application of simplistic lumped or empirical erosion models without the explicit description of processes tries to circumvent these issues (e.g. Antronico *et al.*, 2005; Boellstorff & Benito, 2005). These approaches do not explicitly consider runoff processes, sediment storage and remobilisation in the channel network or reservoirs and thus hardly allow the quantification of sediment yields at the macro-scale. Alternatively, purely regression-based approaches are restricted to the period of currently available data and cannot be applied to different catchments or a future altered state (Bathurst, 2002), which require process-based models. For these, a hydrological model with an adequate description of runoff generation processes needs to be implemented, namely for highly erodible landscapes (Gallart *et al.*, 1997).

Consequently, an integrated assessment of water and sediment fluxes from a meso-scale catchment must, on the one hand, incorporate all relevant hydrological and sediment-related processes at hillslopes, within the river channel and in reservoirs. On the other hand, it requires effective scaling methods to describe these processes at the appropriate scale while maintaining reasonable requirements of computation times and input data. Where the latter are unavailable from existing data-sources, suitable measuring techniques need to be adapted and the respective fieldwork and monitoring campaigns have be carried out.

This objective was pursued by the SESAM-project (Sediment Export from large Semi-Arid catchments: Measurements and Modelling), funded by DFG (Deutsche Forschungsgemeinschaft). From 2005 to 2008, members of the University of Potsdam, the German Research Centre for Geosciences (GFZ) and partners from the Universities of Fortaleza (Brazil), Lleida (Catalonia, Spain) and the Forestry and Technology Center of Catalonia have been conducting research in three meso-scale dryland catchments in Spain and Brazil, aiming at monitoring and modelling water and sediment fluxes from the sources to the deposition areas. Within this context, the research presented in this PhD-thesis is embedded in the complementary work of other parts of the project.

2. Objectives

Conceptionally, the processes of water and sediment export at the meso-scale can be assigned to the components “hillslope”, “river” and “reservoir”. This thesis focuses on the hillslope component (related to objectives 1 and 2 of SESAM-project). The key questions can be phrased as

- How much water and sediment is generated in the source areas?
- How can the relevant processes be modelled? What are capabilities and limitations of such a model?

These questions are pursued by addressing the following tasks:

1. Conceptual development and implementation of an erosion module as a component for the integrated modelling of water and sediment yield at the meso-scale
2. Development of appropriate upscaling and generalisation methods for the discretisation and parameterisation of such a model
3. Collection of adequate input parameters and time series in fieldwork and monitoring campaigns
4. Parameterisation and application of the above mentioned model to the different study areas; identification of strengths and limitations

These tasks can be related to the Chapters V, IV, II-III and VI-VIII, respectively.

3. Study areas

In the course of research underpinning this thesis, three study areas were investigated: the catchments of Ribera Salada, Isábena and Benguê. However, only the outcomes of the case studies of the Ribera Salada and the Isábena are contained in this thesis. The results for the Benguê catchment (Mamede, 2008; Medeiros *et al.*, subm.) are not presented here.

The Ribera Salada catchment is situated in the foothills of the Southern Pyrenees and covers 200 km² (Fig. 2a). With altitude ranging from 746 to 2200 m a.s.l., the area has a typical Mediterranean mountainous climate, with mean annual precipitation and evaporation varying between 500-800 mm and 700-750 mm, respectively. Rivers never dry up, although flows are very low during the summer. The current vegetation is dominated by woodland, being a result of land abandonment in the 1950s and subsequent afforestation. These land-use changes and the associated hydrological implications, combined with continuously rising water demand arising from agriculture in the Ebro depression, pose a challenge for water and land management in the region. More details are given in Chapter VI.

The second study area is also located in the Pre-Pyrenees (Fig. 2a). Its 445 km² are drained by the Isábena river. The catchment features a strong climatic gradient with a mean annual precipitation of 770 mm (from 450 to 1600 mm) and an average annual potential evaporation of 550 to 750 mm, caused by altitude ranging from 450 to 2,720 m a.s.l.. Heterogenous relief, lithology (Paleogene, Cretaceous, Triassic, Quaternary) and land-use (agriculture in the valley bottoms, mattoral, woodland and pasture in the higher parts) create a diverse landscape. The abundance of Miocene marls lead to the formation of Badlands with very high erosion rates. The eroded material is efficiently transported to the Barasona reservoir at the catchment outlet. Its initial capacity of 92 hm³ has been considerably reduced by the subsequent siltation, threatening the mid-term reliability of irrigation water supply. Further aspects are given in Chapter II and III.

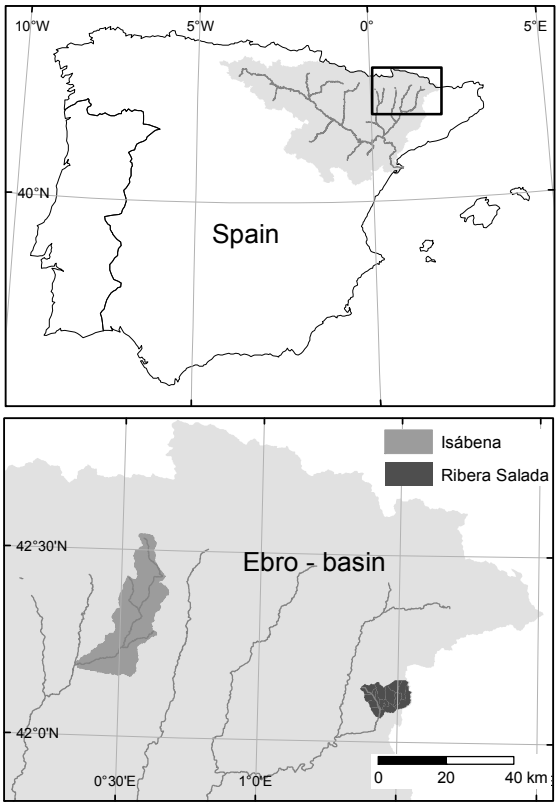

Fig. 1: Study areas.

4. Outline of the thesis

4.1. Overview of conducted work

Fig. 2 illustrates the general components of this study and their relation. Because of the different focus and basin properties, these components have been processed with varying methods and a different degree of intensity for the study areas. The most basin-specific research of this thesis was dedicated to the Isábena catchment.

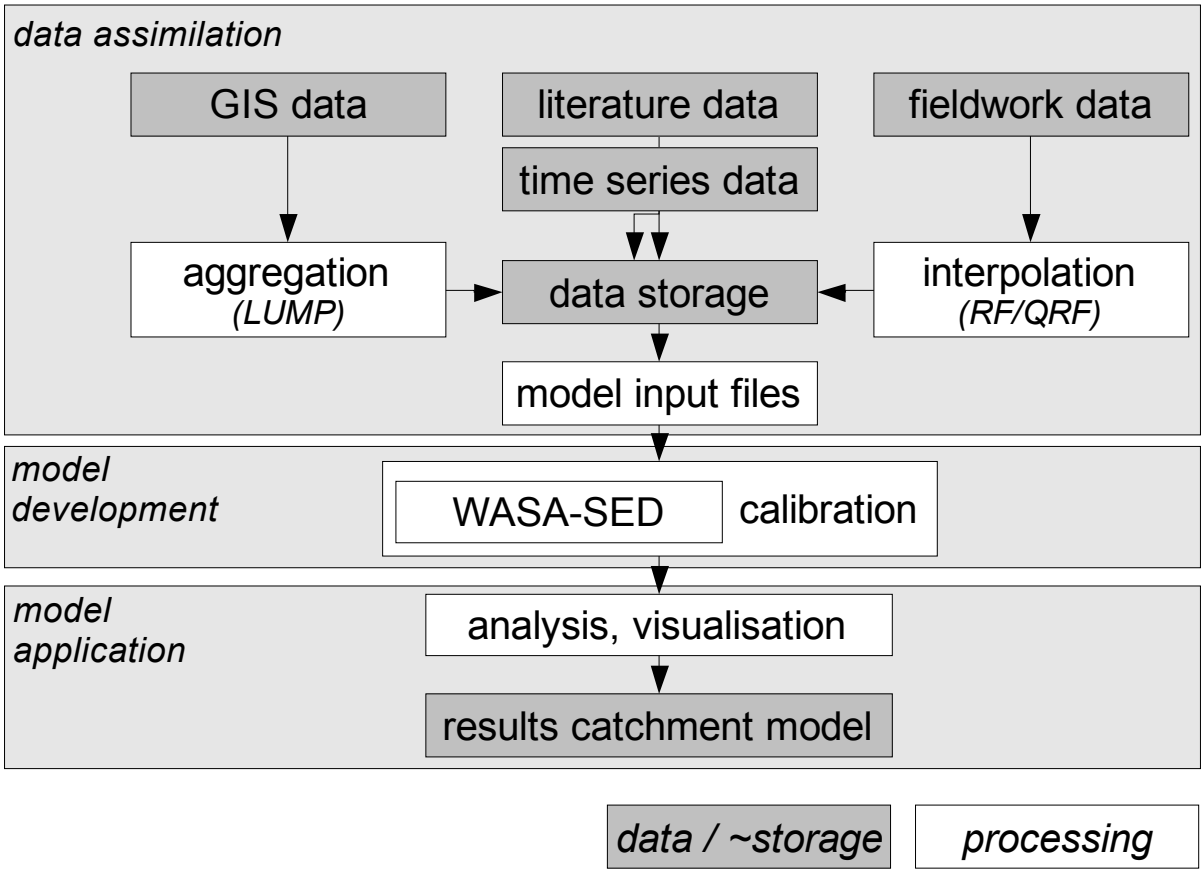

Fig. 2: Components of the presented study.

4.1.1. Data assimilation

"Data assimilation" in Fig. 2 encompasses all steps that are related to the acquisition and processing of data. Thus, it is associated to the task 2 - 4 (section 2) and served for improving process understanding (e.g. identifying sediment sources), the quantification of dynamics (e.g. amount of exported sediment) and providing parameters, input- and calibration-data for the model (e.g. hydraulic conductivity of soil).

Firstly, this comprises the actual fieldwork, i.e. the monitoring of rainfall, runoff and suspended sediment concentration (SSC) for the Isábena (see Chapter III) and the development of a technique for the interpolation of the SSC measurements was developed (step "pre-processing II", see Chapter II). Details of further fieldwork, which provided insight and data but which is not described here in detail, includes the measurement of slope angle, grain-size distribution, saturated hydraulic conductivity, the detailed monitoring of erosion and deposition rates, the determination of the volume of trapped sediment for the experimental badland catchment Torrelaribera and fieldwork measurements of vegetation and surface characteristics for the parameterisation of the vegetation and erosion characteristics of the different land-use classes (Francke, 2006).

The parameterisation of the model required further input, denoted as "GIS data", "literature data" and "Time series data". The component "GIS data" comprises the generation, acquisition and preparation of geo-data. Besides the standard chores of harmonizing datasets of topography, land-use, soils and lithology, it also included the processing of high-resolution airphotos and the delineation of badland areas for the Isábena catchment. Integrating and upscaling the geo-data resulted in the development of the LUMP algorithm (see Chapter IV), which allowed the derivation of modelling units for WASA-SED (task 2).

Finally, the component "literature data" summarizes the collection of all the semantic data that served to parameterize the objects of the geodata sets, which involved

an extensive review of data sources, especially for the vegetation and soil properties. "Timeseries data" includes acquisition, harmonizing and spatial interpolation of climate input data and the processing of discharge and sediment flux data for calibration and validation
Efficient workflow and convenient data storage was achieved by developing or adapting suitable database solutions (Chapter V, Reusser *et al.*, 2008).

4.1.2. Model development

The WASA model (Güntner, 2002; Güntner and Bronstert, 2004) provided the basis for model development (task 1). For upgrading this model to WASA-SED, numerous features associated with erosion modelling had to be implemented: erosion generation at the hillslopes using different approaches, transport capacity concept, representation of particle size distribution, etc. (see Chapter V). Furthermore, the WASA-SED model was modified in various aspects of processing time, saving and loading of model state, enhanced flexibility with and improved error checking of input files, dynamic estimation of rainfall intensity, etc.
Model calibration (step "calibration") proved successful only with a combination of Latin Hypercube search of the initial parameter estimates and subsequent application of a gradient-based approach (see Chapter VII). For this purpose, a variety of scripts has been created that serve for the parameter-specific visualisation of model performance, the automated generation of equilibrium initial conditions for WASA-SED and the interface to the PEST calibration software (Doherty, 2004).

4.1.3. Model application

The combination of these aforementioned components eventually resulted in the final catchment models for Ribera Salada (see Chapter VI), the Isábena catchment (see Chapter VII). The former focussed on the uncalibrated application to compare the effect of different climate and land-use scenarios in a relative way. In contrast, the application for the Isábena focussed on exploring the full potential of the model's predictive capabilities and comparing model results to the data collected during the monitoring.
For that purpose, software tools had to be developed to facilitate the analysis and visualisation (steps "analysis, visualisation") of the resulting model output files, including the computation of water and sediment balance, runoff coefficients, flood-based sediment yield analysis, visualisation and generation of result grids on the LU or TC-scale. The results provided a basis for the concluding discussion in Chapter VIII.

4.2. Structure of thesis, author's contributions

This thesis is cumulatively organised as illustrated in Fig. 3: Chapters II – VII were written as stand-alone manuscripts that are published or awaiting publication in international peer-reviewed journals (for full reference, see front pages of the respective chapters). These papers are reproduced here unmodified, except for cross-references which have been replaced by the respective chapter number.

Chapter I:
Introduction, objectives and overview

data assimilation

Chapter II :*Francke, López-Tarazón, Schröder*
Estimation of suspended sediment concentration and yield – development of method *(Hydrolog Process, 2008)*

Chapter III: *Francke, López-Tarazón, Vericat, Bronstert, Batalla*
Estimation of suspended sediment concentration and yield – measurements and application *(Earth Surf Process Landforms, 2008)*

Chapter IV:*Francke, Güntner, Mamede, Müller, Bronstert,*
Automated catena-based discretization of landscapes - data aggregation and upscaling *(Int J Geogr Inform Sci, 2008)*

model development

Chapter V: *Müller, Güntner, Francke, Mamede*
Modelling water and sediment export from drylands - the WASA-SED model *(Geosci Model Dev Discuss, 2008)*

model application

Chapter VI:*Müller, Francke, Batalla, Bronstert*
Effects of land-use change on runoff and sediment yield - model application for Ribera Salada catchment *(Catena, subm.)*

Chapter VII: *Francke*
Water and sediment in highly erodible catchments - model application for Isábena catchment *(Catena, in prep.)*

Chapter VIII:
Discussion and conclusion

Fig. 3: Structure of thesis (Chapter titles modified for clarity; full title of papers can be found in the appropriate chapter).

The work described in Chapters I-IV, VII and VIII has essentially been performed by the author. Significant contribution in terms of data collection by the Catalan partners (Chapters II and III) and invaluable discussions, minor drafting tasks and proofreading by the co-authors is acknowledged notwithstanding.
For Chapter V, in terms of formulation of the conceptual basis, implementation and drafting of the manuscript the author has essentially performed the task for the section on the hillslope module and significantly contributed to the general sections.
The author's contribution to Chapter VI comprises significant contributions to the preparation and processing of the data and the implementation of the model.

Chapter II

Estimation of suspended sediment concentration and yield using linear models, Random Forests and Quantile Regression Forests

Abstract

For sediment yield estimation, intermittent measurements of suspended sediment concentration (SSC) have to be interpolated to derive a continuous sedigraph. Traditionally, sediment rating curves (SRCs) based on univariate linear regression of discharge and SSC (or the logarithms thereof) are used but alternative approaches (e.g. fuzzy logic, artificial neural networks, etc.) exist.

This paper presents a comparison of the applicability of traditional SRCs, generalised linear models (GLMs) and non-parametric regression using Random Forests (RF) and Quantile Regression Forests (QRF) applied to a dataset of SSC obtained for four sub-catchments (0.08, 41, 145 and 445 km²) in the Central Spanish Pyrenees. The observed SSCs are highly variable and range over six orders of magnitude. For these data, traditional SRCs performed inadequately due to the over-simplification of relating SSC solely to discharge. Instead, the multitude of acting processes required more flexibility to model these non-linear relationships. Thus, alternative advanced machine learning techniques that have been successfully applied in other disciplines were tested.

GLMs provide the option of including other relevant process variables (e.g. rainfall intensities, temporal information) but require the selection of the most appropriate predictors. For the given datasets, the investigated variable selection methods produced inconsistent results. All proposed GLMs showed an inferior performance, whereas RF and QRF proved to be very robust and performed favourably for reproducing sediment dynamics. QRF additionally provides estimates on the accuracy of the predictions and thus allows the assessment of uncertainties in the estimated sediment yields that is not commonly found in other methods. The capabilities of RF and QRF concerning the interpretation of predictor effects are also outlined.

Keywords: suspended sediment concentration, sediment rating curve, generalised linear model, Random Forests, Quantile Regression Forests

Published as

T. Francke, J. A. López-Tarazón, B. Schröder (2008)

Estimation of suspended sediment concentration and yield using linear models, Random Forests and Quantile Regression Forests. *Hydrological Processes* **22**, 4892–4904, DOI: 10.1002/hyp.7110.

1. Introduction

Understanding the transport of sediment by streams is an important aspect related to issues of sediment-water quality interactions, reservoir siltation, water pollution, channel navigability, soil erosion and soil loss, fish and invertebrate habitat, malfunctioning of hydropower plants, instream mining, river restoration, river aesthetics, etc. (Walling, 1977; Williams, 1989). In addition, in the context of climate change, with the possibility of the progressive aridification of the climate in the Mediterranean, improving and adapting water resources management strategies is essential. For this purpose, accurate estimations of the sediment volume carried by rivers are necessary to prevent, as much as possible, problems derived from suspended sediment load circulating in rivers, especially in relation to the loss of water storage in reservoirs and water quality.

Rivers transport water and sediment from headwaters to the deposition areas, being responsible for the equilibrium between fluvial and marine processes in deltaic and coastal zones (e.g. Vericat and Batalla, 2006). Sediment can be carried downstream as bed load (particles that move along the river bed by rolling, skipping, or sliding) or as suspended load (supported by fluid flow and maintained by fluid turbulence). Bed load is flow dependent and generally accounts for around 10 % of a river's total

solid transport. In alluvial streams, bed load can contribute as little as 1 % to the total annual load, while in mountain streams it may account for more than 70 % (Meade, Yuzyk and Day, 1990). In contrast, suspended load is typically source-dependent, i.e. wash-load. It is mostly composed by particles finer than 0.062 mm in diameter, although may also include bed-material particles i.e. sand fractions, during high flows. Suspended load is the major transporting mechanism in streams worldwide. Thus sediment yields are often based on data concerning the suspended load only (Wood, 1977). However, their computation, especially when based on a limited number of measurements, is not a trivial task.

Methodological issues –state of the art

In contrast to the measurement of discharge, measurements of suspended sediment concentration (SSC) or sediment flux are relatively intricate. Besides the direct determination of SSC from water samples in the lab, various indirect *in situ* (i.e. quasi-continuous) methods such as optical, X-ray or acoustic backscatter, attenuation or laser diffraction, etc. exist.

Direct measurements, however, remain the benchmark against which other methods are calibrated (Wren, Barkdoll, Kuhnle and Derrow, 2000). They are widely used where logistic, administrative or financial issues or SSC-range inhibit the use of *in-situ* measurements. But direct measurement of SSC demands sampling, which requires manual labour or automatic water samplers and thus can only produce intermittent data.

Consequently, the estimation of sediment loads requires the integration of the continuous discharge data with discrete measurements of SSC, i.e. estimates of SSC between the observations have to be made. According to Holtschlag (2001), two approaches can be distinguished:

a) time-averaging methods / interpolators: SSC between observations is estimated from nearest neighbour, linear or spline interpolation This method is apparently suitable when SSC is measured at high frequency compared to SSC variability. For less-frequent sampling, this method may fail to reproduce SSC dynamics; for unmonitored events, no SSC-prediction can be made at all. The estimations thus obtained are consistent with the data at the times of measurement, but do not allow for the estimation of uncertainty (Holtschlag, 2001). Sivakumar and Wallender (2005) advocate using a non-linear deterministic dynamic model that builds upon a local approximation in multi-dimensional phase-space. This method yielded promising results when used with comparatively

densely sampled data but is also not suitable to predict values of unmonitored events.

b) flow weighting methods / regression estimators: SSC is estimated by regression on ancillary variables. This approach generally does not exactly reproduce the observations but can provide a formal measure for uncertainty. Commonly, linear regression on discharge data is used for this purpose (traditional 'sediment rating curve', SRC; Walling, 1984), but also other predictors can be included in multiple regression models (e.g. Cohn *et al.*, 1992; Schnabel and Maneta, 2005). Regression is often carried out on log-transformed data to improve linearity between SSC and discharge and reduce heteroscedasticity (Smith and Croke, 2005). The resulting bias often requires a correction (Crawford, 1991; Asselman, 2000) that in turn may generate additional uncertainty (Smith and Croke, 2005). The nonlinearity of the underlying processes has also been dealt with by using second and third order polynomials or power and exponential functions (Schnabel and Maneta, 2005).

However, it is generally accepted that there is no simple discharge-SSC relationship which can be addressed by a single sediment rating curve (SRC). This issue has been dealt with by fitting different curves according to season or discharge range (Sivakumar and Wallender, 2005) or using moving rating curves for sediment flux estimation (van Dijk *et al.*, 2005). Since soil loss is also highly related to other variables such as rainfall intensity (Schnabel and Maneta, 2005), especially for small ephemeral streams, accommodating these variables in models capable of using multiple predictors can greatly improve performance.

Generally, established regression estimators can also be applied for periods when no SSC observations are available as long as the necessary predictor data has been recorded (Holtschlag, 2001). *State-space-estimators* (e.g. Holtschlag, 2001) further extend this concept by considering autoregressive error components. These models can have high predictive performance (Holtschlag, 2001) but are conceptually more demanding. They require the estimation of additional parameters such as the covariances of process and measurement errors. Kisi *et al.* (2006) employed fuzzy logic to predict SSC from discharge. For SSC prediction from a set of predictors, Schnabel and Maneta (2005) applied polynomial regression and artificial neural networks. Nagy *et al.* (2002) trained artificial neural networks using stream-hydraulic parameters as predictors, which bridges the gap towards physically based approaches. Both FL and artificial neural networks are designed to address the issues of nonlinearity and have recently experienced much attention. Both approaches are non-parametric and produce range-conservative predictions but no error estimations. Fuzzy logic is more interpretable and transparent than artificial neural networks but requires a subjective or automated calibration procedure (Kisi *et al.* 2006). Kisi (2005) demonstrated the inclusion of multiple predictors (discharge and SSC of preceding time step) with fuzzy logic and artificial neural networks and obtained slightly better performance with fuzzy logic, which was also reported by Lohani *et al.* (2007).

Instead of predicting SSC, Regüés *et al.* (2000) perform multivariate linear regression on flood-related sediment yields. Though being more direct and presumably more robust in the context of yield estimations, this approach requires a comparatively large database for calibration, because multiple SSC-measurements during a flood are integrated into a single value – a process that in itself requires high-frequency sampling or one of the methods presented above.

Thus, in the context of SSC prediction and sediment yield reconstruction for intermittently monitored sites, a method should be applied that deals adequately with the nonlinear nature of the subject, includes multiple predictors and provides a measure for the uncertainty of predicted values. In the presented study, we explore the applicability of multivariate linear regression by

means of generalised linear models (GLMs) and ensemble forecasting by regression trees for SSC predictions for four sites compared to traditional methods. The characteristics of the techniques employed are briefly outlined in the following section.

1.1. Regression methods

1.1.1. (Generalised) linear regression models (GLMs)

Linear regression refers to relating a response variable Y to a set of predictors x_i in the form (e.g. Chatterjee and Price, 1991):

$$Y = b_0 + b_1 \cdot x_1 + b_2 \cdot x_2 + \ldots + b_p \cdot x_p \qquad \text{Eq. 1}$$

where the coefficients b_i are adjusted to obtain an optimum fit. Each predictor x_i may consist of an unmodified or transformed value, such as the logarithm of the discharge. An advantage of linear regression is its easy implementation: in the univariate case, the model can be set up in most spreadsheet application; multivariate regression may require slightly advanced software. The obtained regression coefficients allow the interpretation of the predictors' influence. Linear regression models are computationally efficient and can also predict confidence intervals for the obtained coefficients and the predicted data, if the underlying statistical assumptions are met. These include normal distribution of error terms, homoscedasticity, independence of observations, (i.e. absence of autocorrelation) and absence of multicollinearity (e.g. Quinn and Keough, 2002). In practice, however, these assumptions often do not hold (e.g. Asselman, 2000; Holtschlag, 2001), which impedes an analysis of the uncertainties in parameters and predictions (Smith and Croke, 2005).

Generalised linear models (GLMs), in contrast, extend this concept by transforming the response variable with a link function and accommodating response variables with non-normal conditional distributions (e.g. Fox, 2002).

Therefore, applying an appropriate link function that ensures at least some of the above mentioned prerequisites (homoscedasticity, appropriate distribution of error terms) can potentially remedy these limitations. Furthermore, when applying the model for prediction, suitable link functions can confine the range of predictions to a reasonable interval (e.g. positive SSCs only), inhibiting physically implausible results.

1.1.2. Regression trees, Random Forests, Quantile Regression Forests

Classification and regression trees (a.k.a. CARTs) are a non-parametric statistical technique for classification and regression problems (Breiman *et al.*, 1984). A CART is a rule-based classifier that partition observations into groups having similar values for the response variable, based on a series of binary rules (splits) constructed from the predictor variables (Hastie *et al.* 2001). It is constructed as a binary decision tree by recursive data partitioning, which can include both categorical and continuous data. In case of continuous response variables, i.e. regression trees, model predictions are obtained by calculating the average of the response variable in the respective terminal leaf of the tree. Model selection usually is carried out by cross-validation which also yields a realistic estimate of model performance. Advantages of regression trees include the ability to deal with nonlinearity and interactions as well as their interpretability. Regression trees imply no assumptions about the distribution of the data. They are capable of handling non-additive behaviour, for which linear models require pre-specified interactions (De'ath & Fabricius, 2000). A disadvantage of regression trees is their instability with respect to small changes in the training data. To overcome this problem, bootstrap aggregation techniques such as bagging can be applied (Breiman 1996). In bagging, one takes a large number of bootstrap samples from the data set and fits a single tree to each bootstrap sample. To receive predictions for new data each of the fitted trees is used and their predictions are averaged (Prasad *et al.*, 2006). Predic-

tive performance is evaluated on those parts of the data that are not considered in the bootstrap samples (out-of-bag data, OOB). Usually, aggregated trees outperform single trees.

Random forests (RF, Breiman 2001) are a modified version of bagged trees (De'ath 2007). They employ an ensemble prediction of regression trees, i.e. a "forest" of trees is grown on the bootstrap samples. In contrast to bagging, a random subset of the predictors is used for each tree and at each node (Meinshausen 2006). This procedure results in a robust model that also yields internal error estimates and measures variable importance (Breiman, 2001). RFs include effective methods to handle missing values when training the model.

These ideas have been extended by Meinshausen (2006): Quantile Regression Forests (QRF) are a generalisation of RFs. For each node in each tree, RFs keep only the mean of the observations that fall into this node and neglect all other information. In contrast, QRFs keep the value of all observations in this node, not just their mean (Meinshausen, 2006). Thus, QRFs consider the spread of the response variable. This allows the construction of prediction intervals which cover new observations with high probability.

Regression trees, RF and QRF-models do not allow easy interpretation of the effects of single predictors although there are some methods regarding the relative variable influence and partial dependency plots (cf. De'ath 2007). They are generally far more demanding in computational power than linear regression models. Because predictions are made from a weighted average of the training data, the model predictions will always be within the range of the observations: this precludes implausible values but inhibits extrapolation.

Our study compares the capability of traditional SRCs (i.e. simple linear regression models), GLMs, RF and QRF-models for SSC prediction using data from a flood season of four catchments of different size. Ancillary data (e.g. precipitation) is used to increase the predictive power. All models are tested using a bootstrapping approach. For each catchment, the best model is applied to the entire flood season which allows the calculation of flood-based sediment yields. Eventually, the advantages and problems associated with the different models are discussed.

2. Study area, instrumentation and database

This study uses data collected during a three-month observation period (September – December 2006) in the Isábena catchment (445 km²) and two of its subbasins located in the Central Spanish Pyrenees (cf. Fig. 2). The catchment is characterised by strong heterogeneity in relief, vegetation and soil characteristics, with elevation ranging from 450 m to 2,720 m asl in the northern parts (*Axial Pyrenees*, Valero-Garcés *et al.*, 1999). The climate is a typical Mediterranean mountainous type with mean annual precipitation rates of 450 to 1600 mm, showing a strong south–north gradient due to topography (Verdú *et al.*, 2006a). Miocene continental sediments dominate the lower parts of the catchment with easily erodible materials (marls, sandstones, carbonates), leading to the formation of badlands and making them the major source of sediment within the catchment (Fargas *et al.*, 1997).

Tab. 1. Summary of measured discharge and SSC data.

	Discharge [m^3/s]			SSC [g/l]		
Sub-catchment	min	mean	max	min	median	max
Torrelaribera (n=122)	0	0.002	0.68	0.001	2.8	240.6
Villacarli (n=104)	0.10	0.65	21.2	0.001	1.3	277.9
Cabecera (n=66)	0.91	3.77	43.4	0.002	0.1	30.5
Capella (n=331)	0.5	5.6	64.3	0.0005	1.2	99.6

Tab. 2: Ancillary data used for regression (abbreviations explained in Tab. 3).

presumably approximated process				
Sediment production on slopes	Sediment production / re-mobilisation in riverbed	Exhaustion of sediment supply on slopes	Exhaustion of sediment supply within riverbed	Dilution
(discharge) *rain_x15* *rain_x60* *rain_x1d* *r_x60* *r_x1d*	*discharge* *rain1d* *cum_q_1h* *cum_q_5h*	*julian_day* *rain_x1d* *cum_q_1h* *cum_q_5h* *r_x1d*	*julian_day* *limb_dec* *cum_q_1h* *cum_q_5h*	*discharge* *rain_x15* *rain_x60* *rain_x1d* *cum_q_1h* *cum_q_5h*

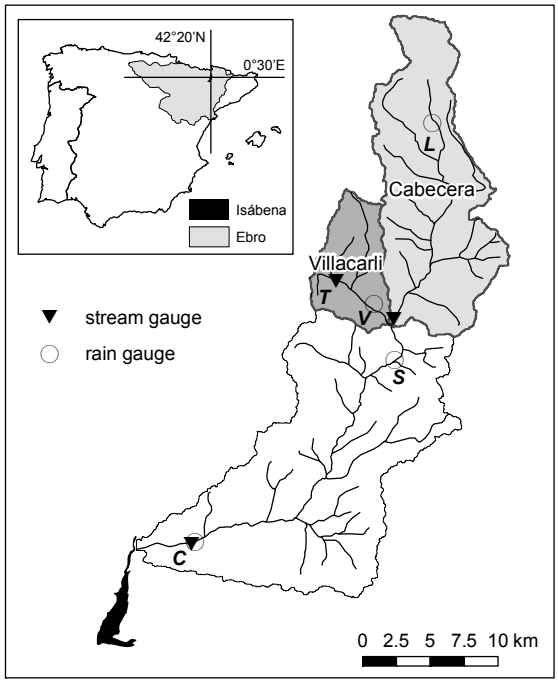

Fig. 1: Isábena catchment with monitored sub-catchments and rain gauges (C: Capella; L: Laspaules; S: Serraduy, T: Torrelaribera, V: Villacarli).

Discharge and SSC were monitored (Tab. 1) in the Isábena catchment (Fig. 1) at time intervals of 2 minutes at Torrelaribera, 5 minutes at Villacarli and Cabecera gauge and 15 minutes at Capella. SSC was measured within a flood-based sampling scheme by means of manual samples in Torrelaribera, Cabecera and Villacarli. Because of the shallow river and the highly turbulent flow, vertical mixing could be assumed complete at these locations. For Capella, automatic (ISCO 3700 automatic sampler) and manual sampling (i.e. DH-59 depth integrated sampler) was employed. In addition, turbidity was recorded every 15 minutes up to 3000 NTU (nephelometric turbidity units, i.e. 3 g/l) in Capella. The total number of SSC measurements was 122 for Torrelaribera, 104 for Villacarli, 66 for Cabecera and 319 for Capella (for more details on instrumentation, see Chapter III). The measured SSCs show great variability within up to five orders of magnitude (Tab. 1). 15-min rainfall data for three close-by rain gauges were included into the dataset.

3. Method

3.1. Model generation

Multiple models aimed at predicting SSC (our response variable) from ancillary data were set up. Ancillary datasets were selected according to the perceived capability of representing relevant processes (Tab. 2) and their continuous availability (cf. Schnabel and Maneta, 2005). Discharge data were included directly and log-transformed (*log_disch*), following common practice in sediment rating curve estimation. Further predictors are the Julian day, the sum of rainfall for 15 minutes, 60 minutes and 1 day registered at the three gauges Villacarli, Laspaules and Capella (denoted e.g. as *rain_capella15*), the respective USLE erosivity factors (Wischmeier & Smith, 1978) for 60 minutes and 1 day (denoted e.g. as *r_capella1d*), the cumulated discharge of

the previous one, five hours and the entire observation period (denoted as e.g. *cum_q_5h*) and the rate of change in discharge (*limb_dec*).

Tab. 3: Abbreviations used in the text and their meaning.

Abbreviation	Meaning
rain_x15	Cumulated rainfall of 15 min recorded in x
rain_x60	Cumulated rainfall of 60 min recorded in x
rain_x1d	Cumulated rainfall of 1 day recorded in x
r_x60	Hourly rainfall recorded in x
r_x1d	Daily rainfall erosivity recorded in x
cum_q_1h	Cumulated discharge during 1 hour
cum_q_5h	Cumulated discharge during 5 hours
cum_q_all	Cumulated discharge for entire observation period
log_disch	Log-transformed discharge data
limb_dec	Rate of change in discharge

3.1.1. Set up of traditional sediment rating curves (SRCs)

Traditional sediment rating curves resulted from fitting a linear relationship between SSC and *discharge* or *log(SSC)* and log(discharge), respectively. The extent of the Capella data set additionally also allowed performing the latter process separately for single floods (denoted *sSRC* hereafter).

3.1.2. Set up of generalised linear models (GLMs)

GLM-regression was performed using the Box-Cox-transformation (Box and Cox, 1964, Eq. 2) and logit-transformation (Eq. 3) as link functions. The Box-Cox-parameter λ was selected by maximum-likelihood estimation (Fox, 2002). The logit-transformation was performed on SSC/*maxval*, where the value for *maxval* was manually adjusted to achieve normality in the response variable. Both link functions were chosen because of their potential to reduce heteroscedasticity and their effect of constraining model predictions to positive values.

$$Y^* = \begin{cases} \dfrac{Y^{\lambda} - 1}{\lambda} \; for\; \lambda \neq 0 \\ \ln(Y) \quad for\; \lambda = 0 \end{cases} \qquad \textit{Eq. 2}$$

$$Y^* = \ln\left(\frac{Y/maxval}{1 - Y/maxval}\right) \qquad \textit{Eq. 3}$$

Y^*	transformed variable
Y	untransformed variable (SSC)
λ, *maxval*	transformation parameters

We performed predictor variable selection to find the minimum adequate model and obtain concise robust models by preventing overfitting and eliminate collinearity in the predictors (e.g. Harrell, 2001). Since most of the predictors included are related to rainfall-runoff processes, many of them are correlated. Collinearity in the predictors can be problematic when interpreting coefficients or for prediction if the correlation structure is not constant (Fox, 2002). For all locations, the predictors could be grouped into roughly three independent classes. Therefore, in the reduced models, only three not strongly correlated predictors (i.e. |Spearman correlation coefficient|<0.6) were included. Because there is no established "standard" procedure for variable selection (Crawley, 2002), three different methods were used:

Best subset regression (e.g. Chatterjee and Price, 1991) performs an exhaustive search of all combinations of (in our case up to 3) predictors. We then selected the best model (according to Mallow's *Cp* criteria) with uncorrelated predictors.

In *hierarchical partitioning* (Mac Nally, 1996), the independent predictive power of each predictor is computed. We selected the three predictors with the highest percentage of independent effects, making sure they are uncorrelated.

The *stepwise procedure on bootstrapped dataset* (Harrell, 2001) generates a bootstrap sample of the full dataset, select the minimum adequate GLM by a „stepwise"-algorithm employing Bayes Information Criterion (BIC) as a selection criterion

(which is stricter than the commonly used Akaike Information Criterion, AIC, cf. e.g. Reineking and Schröder, 2006). This procedure was repeated 1000 times. We chose the predictors that had been selected most often in the 1000 repetitions, making sure they are uncorrelated.

3.1.3. Set up of Random forests (RF) and Quantile Regression Forests (QRF) models

Starting with the full set of predictors, the optimum number of selected predictors used for splitting at each node (parameter *mtry*) was selected according to the lowest out-of-bag error E_{OOB} for the RF model: For each tree *i*, the mean squared error $E_{OOB,i}$ for the OOB-data is computed. E_{OOB} is calculated from the average error of all $E_{OOB,I}$ (Breiman, 2001). For QRF, the same *mtry* was used. The minimum size of terminal nodes (*nodesize*) was set to five in both approaches.

3.2. Model comparison and selection

To assess the reliability and robustness of the employed models, validation was performed using a bootstrapping approach (n=1000), where bootstrapped training data sets were generated and model performance was assessed on the remaining test data. We then used the Spearman correlation coefficient R_{Sp} between modelled and observed SSC, averaged over all bootstrap runs, as a measure of goodness-of-fit. $R_{Sp,full}$ for the full dataset is calculated as

$$\overline{R_{Sp,full}} = mean[cor_{Sp}(SSC_{mod}, SSC_{obs})] \quad \text{Eq. 4}$$

$R_{Sp,test}$ for the test dataset is computed as

$$\overline{R_{Sp,test}} = mean[cor_{Sp}(SSC_{mod}^{test}, SSC_{obs}^{test})] \quad \text{Eq. 5}$$

Optimism in R_{Sp} (Harrell (2001), p. 94):

$$O_{R_{Sp}} = \overline{R_{Sp,train}} - \overline{R_{Sp,test}} \quad \text{Eq. 6}$$

with

$$\overline{R_{Sp,train}} = mean[cor_{Sp}(SSC_{mod}^{train}, SSC_{obs}^{train})]$$

where *SSC* denotes suspended sediment concentration, subscripts "*obs*" and "*mod*" meaning "observed" or "modelled" values, respectively. Superscripts "*full*", "*train*" and "*test*" refer to the entire, training or test dataset, respectively.

R_{Sp} is more suited to deal with nonlinear models and the range of the data over several orders of magnitude than the traditionally used coefficient of determination R^2. The "optimism" in R_{Sp} gives information on the dependency of the model structure on the subset of the training data and thus its robustness.

3.3. Sedigraph prediction and calculation of sediment yield

For each of the datasets, the most appropriate model was applied to data of the complete monitoring period, i.e. September, 10 – December, 12. The obtained sedigraph data contained three values for each time step: a „best estimate", being the value predicted by the model, and a lower and upper value comprising the 95 % confidence interval for prediction.

Sediment yields for flood and inter-flood periods were computed using a Monte-Carlo-approach: For each time step, we randomly drew a SSC-value from the 95 % confidence interval, according to its probability. Subsequently, the sediment yield for the current time span (flood or inter-flood period) was obtained by multiplying with the discharge data. Repeating the previous two steps n times yielded a distribution of sediment yield estimates, from which we computed the 95 % confidence interval for the population (see examples in Fig. 2 and Fig. 3).

Model building and statistical analyses were conducted using R (R-Team Development Core, 2006) with the packages *car* (Fox, 2006), *leaps* (Miller and Lumley, 2006), *MASS* (Venables and Ripley, 2002), *randomForests* (Liaw and Wiener, 2002), and *quantregForest* (Meinshausen, 2007).

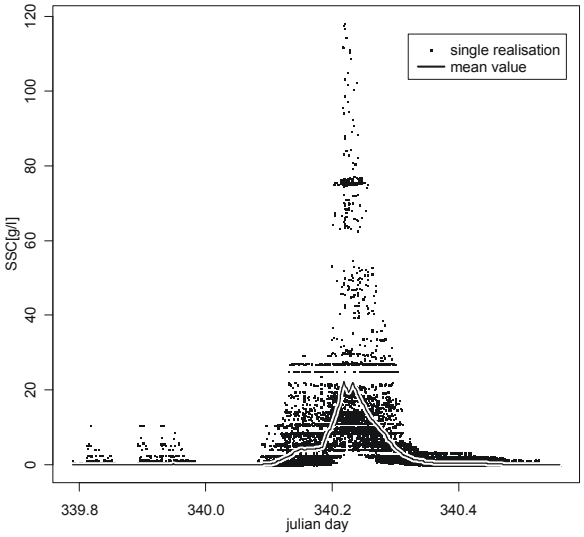

Fig. 2: Monte-Carlo-simulation of SSC. Dots represent single realizations of of the MC-simulation, the continuous line their mean SSC-value (example from Torrelaribera, flood 12).

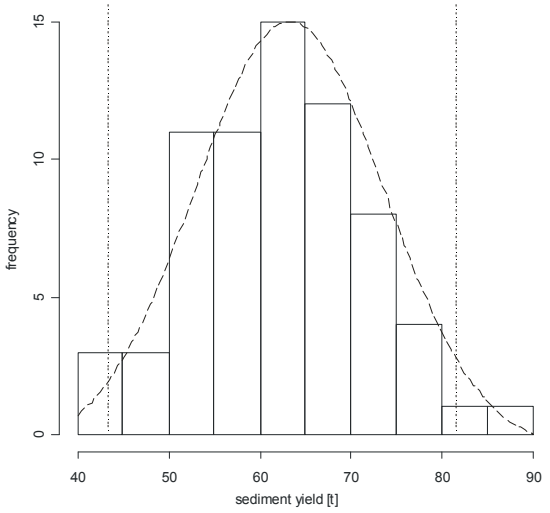

Fig. 3: Distribution of sediment yield computed by Monte-Carlo-method using 70 realisations (dashed: fitted normal distribution, dotted: 95 % confidence interval, example from Torrelaribera).

4. Results and Discussion

4.1. Model building and predictor selection

For all datasets, optimum transformations of the response variable to achieve normal distribution were obtained either by logit- or Box-Cox-transformation with parameters *maxval*=300 and λ=0, respectively.

The three methods of predictor selection propose different subsets as being most suitable for further consideration (see Tab. 4). In four cases, variable selection by bootstrapping did not show any preference, making this method the least dependable for the given datasets. For the Villacarli and Capella datasets, best subset and regression and hierarchical partitioning lead to the same subset of predictors, while the results of both methods differ when applied to the datasets of Torrelaribera and Cabecera. Moreover, for the Capella dataset, predictor selection by bootstrapping differs from the other methods only in choosing daily erosivity instead of daily rainfall values as predictor.

For Torrelaribera, log-transformed discharge is contained in all selected model structures. The predictors *julian_day*, *rain15* and *cum_q_all* have been selected twice each. For Villacarli, hierarchical partitioning and best subset search yielded the same combination of predictors for both transformations, which also included the log-transformed discharge.

Discharge (or log thereof) is an important predictor for all locations except Cabecera where it has only been selected twice. Instead, julian_day and rainfall-related predictors are included, indicating that discharge apparently plays a minor role for SSC here. In all but two predictor sets, julian_day or cum_q_all is contained. Since both are increasing monotonically, this suggests a systematic trend in SSC during the observation period.

4.2. Comparison of model performance

Tab. 5 compares the model performances in terms of Spearman rank correlations, RMSE and optimism. For the traditional SRC-approaches of relating SSC to discharge or the respective log-transformations, differences cannot be observed with regard to R_{Sp}. For Torrelaribera and Capella, the log-transformation reduces the RMSE, but for Villacarli and Cabecera the untransformed version outperforms the regression of log-transformed values in terms of RMSE. The GLMs including more variables generally show a better performance (higher R_{Sp}, lower RMSE) than the traditional SRCs, especially for Capella. Considerable differences

among the GLMs exist for Villacarli and Cabecera, which is particularly pronounced in the case of V2 with poor performance. Except for the Cp1-4, the GLMs show comparatively high values for optimism in R_{Sp}. This notion of low robustness of the GLMs is also apparent in the numerical instability: during the bootstrapping, for some GLMs in up to 95 % of the bootstrap cycles (e.g. Cp3) the model could not be fitted to the training data. RF and QRF models deliver the best performance in $R_{Sp,full}$ and $R_{Sp,train}$ except for RF of Cabecera. The RFs feature the lowest RMSE-values, those of QRF are slightly higher but generally lower than those of the GLMs. Optimism of the RFs and QRFs is also low (if not the lowest) among all investigated models. The best overall R_{Sp} values range from 0.85 to 0.95, except for Cabecera, where only 0.65 to 0.67 are achieved.

For Cabecera, additionally to the models listed in Tab. 5, a traditional SRC was fitted for each flood separately, yielding a set of SRCs specific for each event (sSRC). When applied to the full dataset, the sSRC model achieves an RSME of 10.4, making it only marginally better than the GLMs, and being clearly outperformed by the RF and QRF models with RMSEs of 5.3 and 6.9, respectively.

Because of their favourable properties, the RF and QRF-models will be used for the future analyses for all gauges.

4.3. Sedigraph prediction and calculation of sediment yield

The reconstructed sedigraphs show good agreement with the observed data (e.g. Fig. 4). However, high SSC values, especially at the beginning of the observation period, are partially underestimated, probably resulting from the low number of observations of this kind and the characteristics of conservative estimation of QRF.

Tab. 4: Results of predictor selection. Abbreviations see Tab. 3.

	Transformation	Selection Method	Predictors	Code
Torrelaribera	boxcox	best subset	log_disch, r_villacarli1d, cum_q_all	GLM_T1
		hier. part.	log_disch, julian_day, rain15	GLM_T2
		bootstrap	*no preference*	-
	logit	best subset	log_disch, rain15, cum_q_all	GLM_T3
		hier. part.	log_disch, julian_day, rain15	GLM_T4
		bootstrap	*no preference*	-
Villacarli	boxcox	best subset	log_disch, rain60, cum_q_all	GLM_V1
		hier. part.	log_disch, rain60, cum_q_all	
		bootstrap	rain15, limb_dec, rain1d	GLM_V2
	logit	best subset	log_disch, rain60, cum_q_all	
		hier. part.	log_disch, rain60, cum_q_all	GLM_V3
		bootstrap	*no preference*	-
Cabecera	boxcox	best subset	rain15, rain1d, rain_laspaules60	GLM_Cb1
		hier. part.	rain1d, julian_day, discharge	GLM_Cb2
		bootstrap	rain15, rain_laspaules1d, julian_day	GLM_Cb3
	logit	best subset	julian_day, rain1d, rain_laspaules60	GLM_Cb4
		hier. part.	rain1d, julian_day, discharge	GLM_Cb5
		bootstrap	*no preference*	-
Capella	boxcox	best subset	log_disch, rain1d, cum_q_all	GLM_Cp1
		hier. part.	log_disch, rain1d, cum_q_all	
		bootstrap	log_disch, r_villacarli1d, cum_q_all	GLM_Cp2
	logit	best subset	log_disch, rain1d, cum_q_all	GLM_Cp3
		hier. part.	log_disch, rain1d, cum_q_all	
		bootstrap	log_disch, r_villacarli1d, cum_q_all	Cp4

Tab. 5: Performance of models used for SSC prediction.

	Model	Full dataset	OOB data		
		$R_{Sp,full}$	$R_{Sp,test}$	RMSE	Optimism R_{Sp}
Torrelaribera	SSC~discharge	0.75	0.74	29.98	0.25
	log(SSC)~log(log_disch)	0.75	0.74	27.02	**0.18**
	GLM_T1	0.79	0.71	28.61	0.80
	GLM_T2	0.77	0.72	**26.95**	0.55
	GLM_T3	0.77	0.71	33.21	0.95
	GLM_T4	0.68	0.69	33.23	0.90
	Random Forests	**0.88**	**0.83**	**26.46**	0.46
	Quantile Regression Forests	**0.91**	**0.87**	27.48	**0.22**
Villacarli	SSC~discharge	0.64	0.64	25.85	**0.24**
	log(SSC)~log(log_disch)	0.64	0.63	25.98	0.25
	GLM_V1	0.68	0.65	**25.65**	0.93
	GLM_V2	0.42	0.04	30.57	0.89
	GLM_V3	0.69	0.63	33.33	1.19
	Random Forests	**0.85**	**0.76**	**24.24**	0.24
	Quantile Regression Forests	**0.89**	**0.83**	27.09	**0.09**
Cabecera	SSC~discharge	0.40	0.39	5.73	0.24
	log(SSC)~log(log_disch)	0.40	0.39	6.06	0.29
	GLM_Cb1	0.38	0.62	4.28	0.64
	GLM_Cb2	0.63	**0.65**	3.56	0.55
	GLM_Cb3	0.59	0.62	4.23	1.03
	GLM_Cb4	0.58	0.59	**4.18**	0.96
	GLM_Cb5	0.63	0.59	3.95	0.76
	Random Forests	**0.65**	0.58	**3.89**	**0.23**
	Quantile Regression Forests	**0.67**	**0.67**	5.09	**0.09**
Capella	SSC~discharge	0.14	0.13	17.15	**0.02**
	log(SSC)~log(log_disch)	0.14	0.14	14.08	**0.00**
	GLM_Cp1	0.75	0.73	**11.73**	0.07
	GLM_Cp2	0.76	0.75	12.04	0.06
	GLM_Cp3	0.75	0.75	12.76	0.27
	GLM_Cp4	0.76	0.75	13.05	0.24
	Random Forests	**0.94**	**0.84**	**8.30**	0.07
	Quantile Regression Forests	**0.93**	**0.88**	12.21	0.07

The confidence bounds are quite narrow shortly after the event and during low flows but widen considerably during periods of high dynamics, reflecting a higher level of uncertainty in these estimates. For Torrelaribera, Villacarli and Capella, SSC-values tend to be somewhat overestimated during the low-flow periods at the beginning of the observation. For Villacarli and Capella with continuous runoff, this effect may lead to a slight overestimation of the early inter-flood sediment yields, while it is irrelevant for Torrelaribera because of the ephemeral runoff regimen.

The Monte Carlo simulation for calculating sediment yield has been performed on a flood-basis to analyze the effect of individual floods. Fig. 5 shows the respective results for Villacarli. The greatest absolute uncertainties are related to the large flood events in September, where the confidence interval increases to 20 % of the value of best estimate. For later floods, the absolute range of the confidence intervals decreases. During low-flows, they are relatively narrow due to the low variability of SSC during these periods.

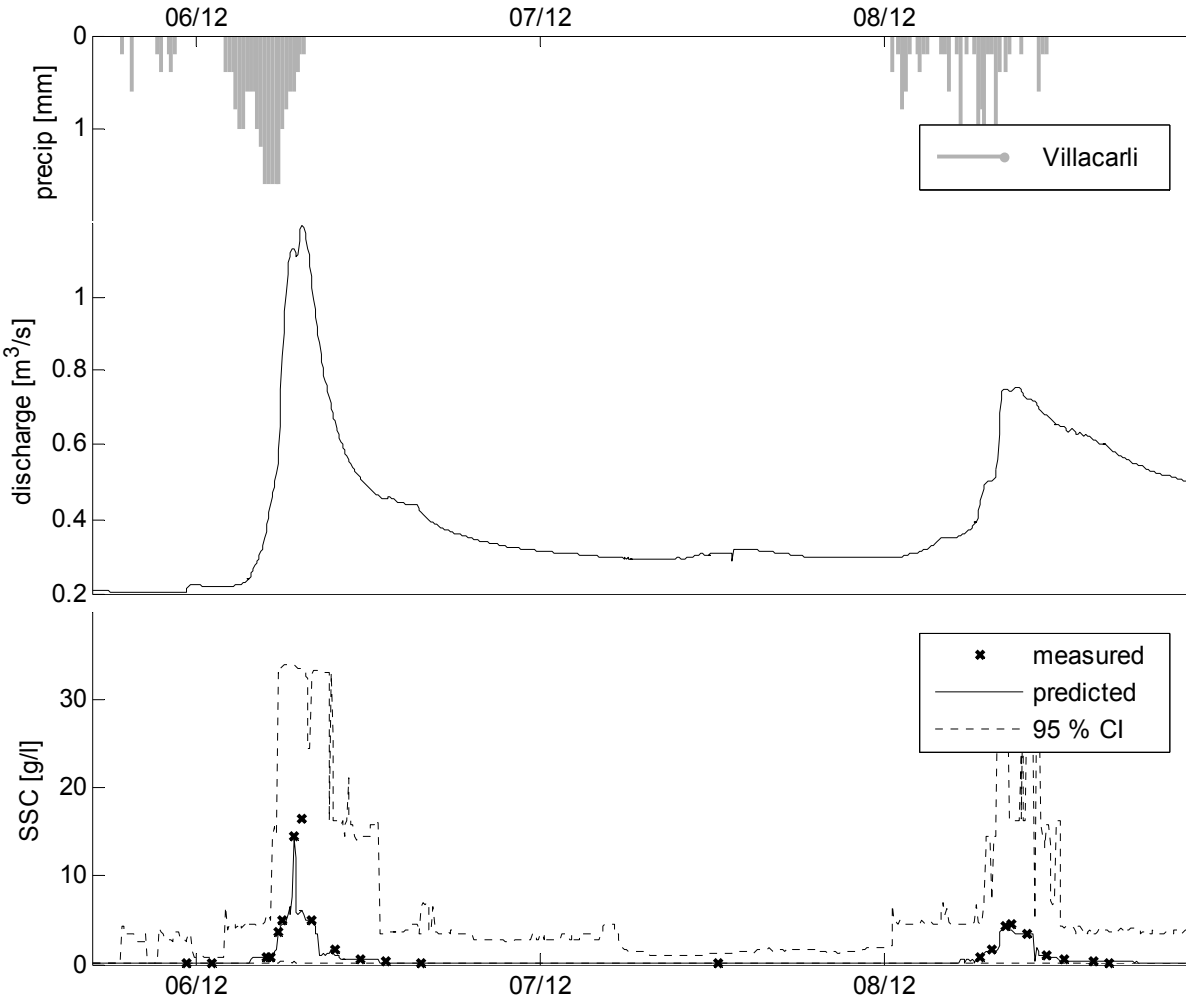

Fig. 4: Close-up-view of rainfall, discharge and SSC (measured and modelled) for two floods at Villacarli.

Tab. 6: Total sediment yield with 95 % confidence interval for the different gauges within the observation period as calculated with the QRF-model.

gauge	Total sediment yield [t]	CI-95% [t]	Coefficient of variation [%]
Torrelaribera	509	419-599	8.9
Villacarli	74,103	63,971-84,235	6.9
Cabecera	20,087	18,340-21,832	4.4
Capella	173,706	149,100-197,702	7.1

For the sediment yield of the entire observation period, the relative size of the confidence interval ranges from 9 to 18 % of the mean value. Apparently, the large relative confidence intervals are associated with large RMSE-value of the underlying model (cf. Tab. 6).

4.4. Analysis of effects of predictors, reproduction of hysteresis loops

Fig. 6 depicts the variable importance of the 12 most important predictors for the RF-models. For each predictor, the loss of model performance (expressed as increase in Mean Squared Error, IncMSE) is quantified when it is omitted from the model. Thus, the explanatory power of each predictor can be assessed. For Torrelaribera, SSC is mainly explained by the predictors *discharge*, rate-of-change in discharge *limb_dec* and daily rainfall *rain1d*. Whereas *discharge* (or *log_disch*, respectively) has also been identified as an important predictor for the GLMs (see Tab. 4), this is not the case for the latter two predictors favoured by RF.

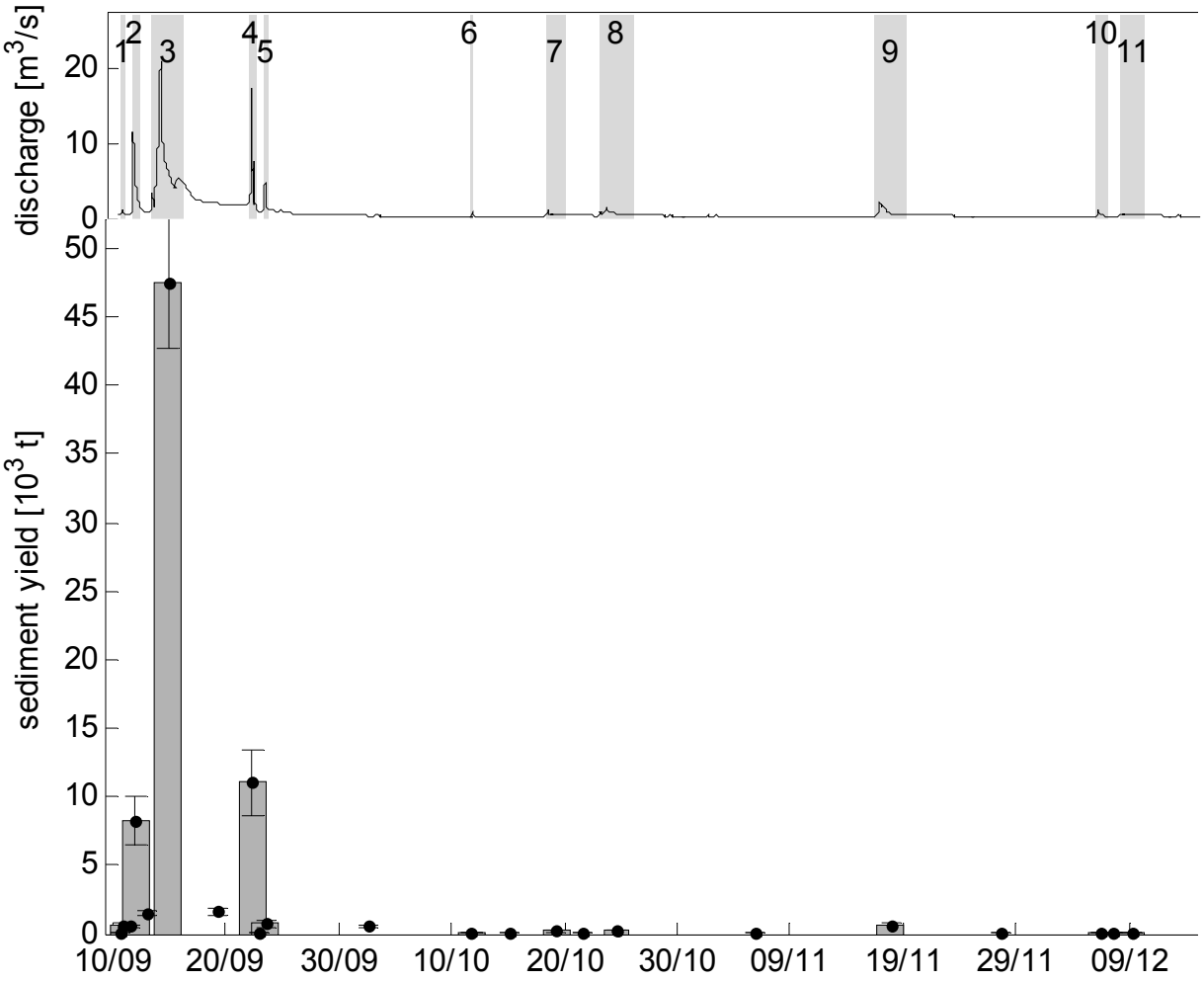

Fig. 5: Hydrograph (top), sediment yield of flood (bars and whiskers) and interflood (whiskers only) periods at Villacarli. The whiskers comprise the 95 % confidence interval. The grey bars underlying the hydrograph depict the numbering of the floods.

For Villacarli, *discharge*, *julian_day* and *limb_dec* have the highest explanatory power. The former two are also included in four of the five GLMs as *log_disch* and *cum_q_all*; the latter appears only in one GLM (see Tab. 4). For Cabecera and Capella, the predictive explanatory power is more concentrated in few predictors: the Cabecera-model relies mostly on *rain1d*, *julian_day* and *r_laspaules60*. The predictive power of the former two has also been identified by the variable selection methods for the GLMs, resulting in their inclusion in four of five GLMs.

At Capella, SSC dynamics are mostly reflected in the predictor *julian_day* which could be a result of the high number of temporally close samples of the automatic sampler and their relative similarity in SSC. Thus, RF shows its capability of taking advantage of higher sampling frequency when combined with a rather steady evolution of the response variable. Apart from this effect which essentially builds on interpolation in time, the predictors *discharge* and its cumulative sums over one and five hours hold some explanatory power for the RF-model, although not very distinct. The latter two are not included in any of the GLMs, whereas *rain1d*, favoured by four of the six GLMs, only ranks among the least important predictors for RF.

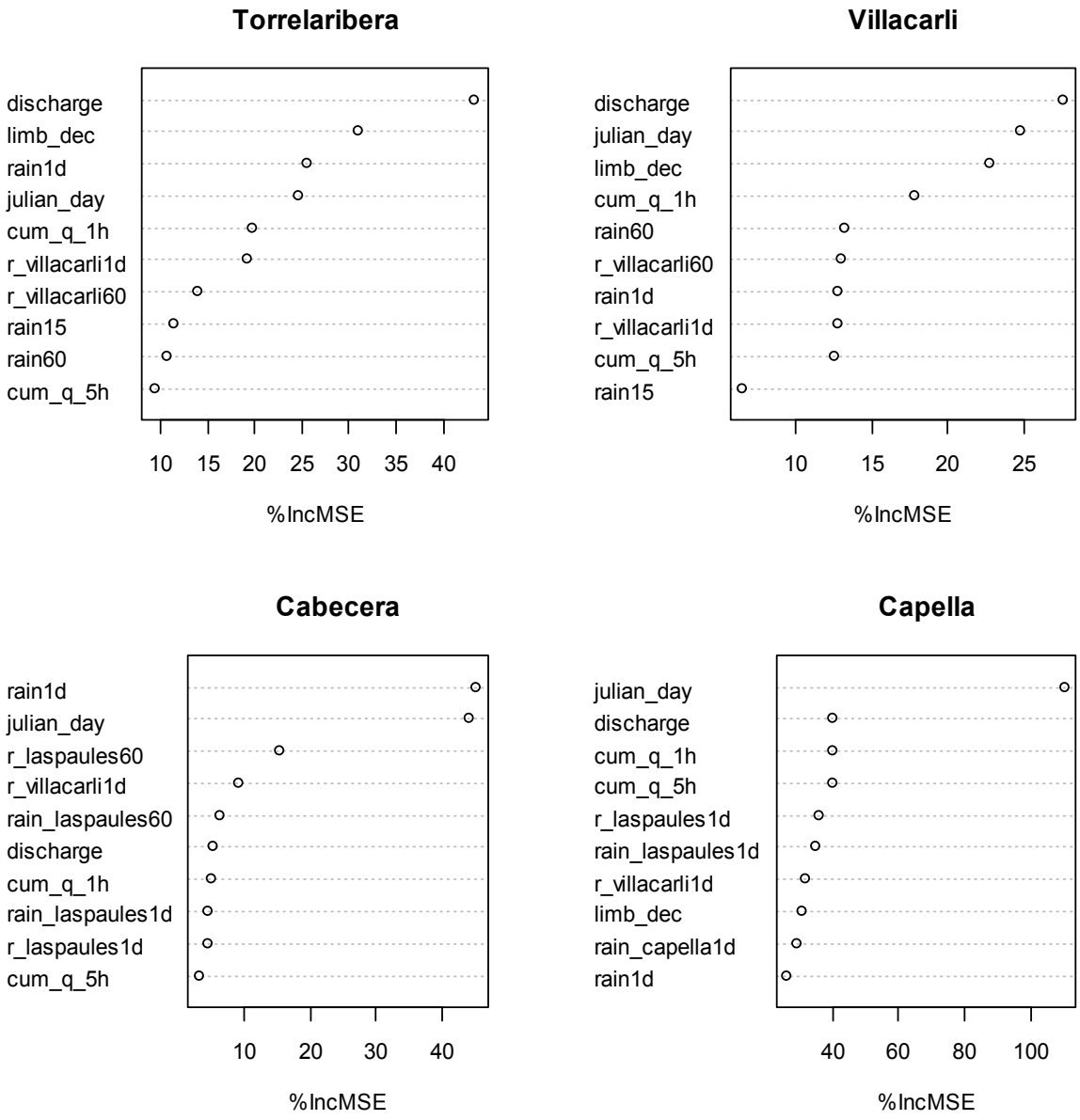

Fig. 6: Variable importance for application of RF-model. Predictors equivalent in the RF-model (log_disch~discharge, cum_q_all~julian_day) have been omitted. For abbreviations, see Tab. 3.

In contrast to GLMs, regression trees and Fuzzy Logic, where the influence of each predictor can be interpreted from coefficients, tree structure or rules respectively, RF and QRF do not provide easy insight. Nevertheless, where interactions are not too complex, the qualitative effect of important predictors can still be revealed by suitable plots.

In a simple traditional SRC ($SSC \sim Q$), the slope S of the Q-SSC-relation ($S = dSSC/dQ$) is a constant, usually positive, value. When using log-transformed data ($log(SSC) \sim log(Q)$), S is a function of Q itself. We analysed S for the RF model. In Fig. 7 each dot represents S for one record in the dataset, with one of the predictors (plotted along the x-axis) varied throughout its entire range. As with traditional SRCs, S is positive regardless of daily rainfall and the Julian day, but may vary considerably (from almost zero to 2.5), reflecting the effects of other predictors. On average (Fig. 7a, black line), however, S decreases gradually for very high amounts of daily rainfall (>40 mm). This suggests that changes in discharge have progressively less effect under conditions of much prior rainfall. Analogously, Fig. 7b depicts a similar effect for the advancing season.

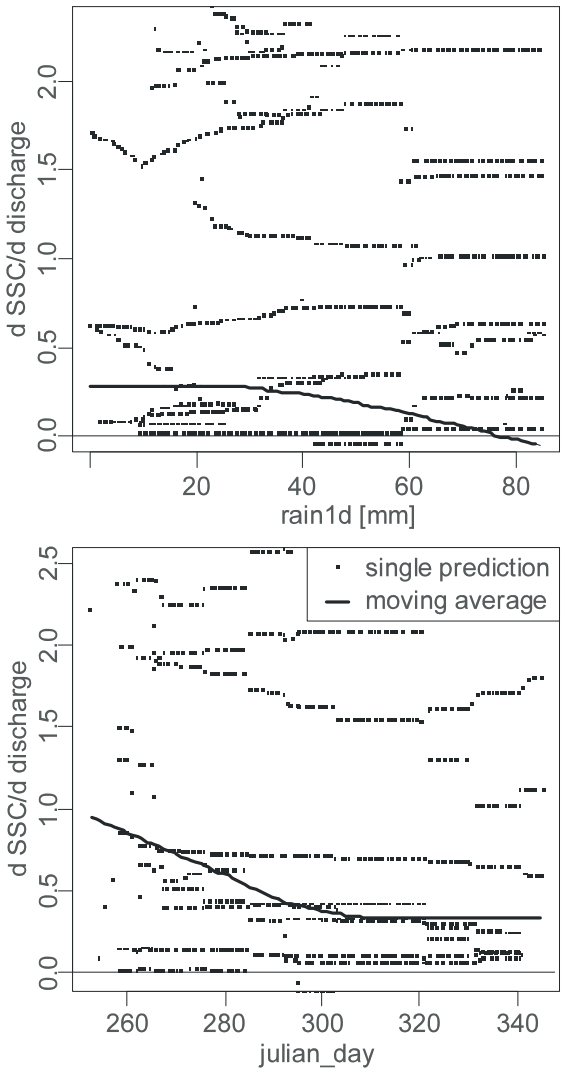

Fig. 7a, b: Effect of changes in SSC per change in discharge for different conditions of daily rainfall (a, top) and season (b, bottom). The continuous line marks the moving average (example from Torrelaribera).

Hysteresis

Hysteresis is a common feature of the discharge-SSC relationship during a flood (Williams, 1989). This effect cannot be reproduced by traditional SRCs and most other univariate approaches, but requires advanced methods (e.g. fuzzy logic, artificial neural networks, Lohani *et al.*, 2007). RF and QRF also provide this capability. For a monitored flood, the observed values with clockwise hysteresis are closely reproduced (Fig. 8a). For a completely unmonitored event, a plausible characteristic with a clockwise hysteresis is also predicted, although somewhat spiky in some parts (Fig. 8b).

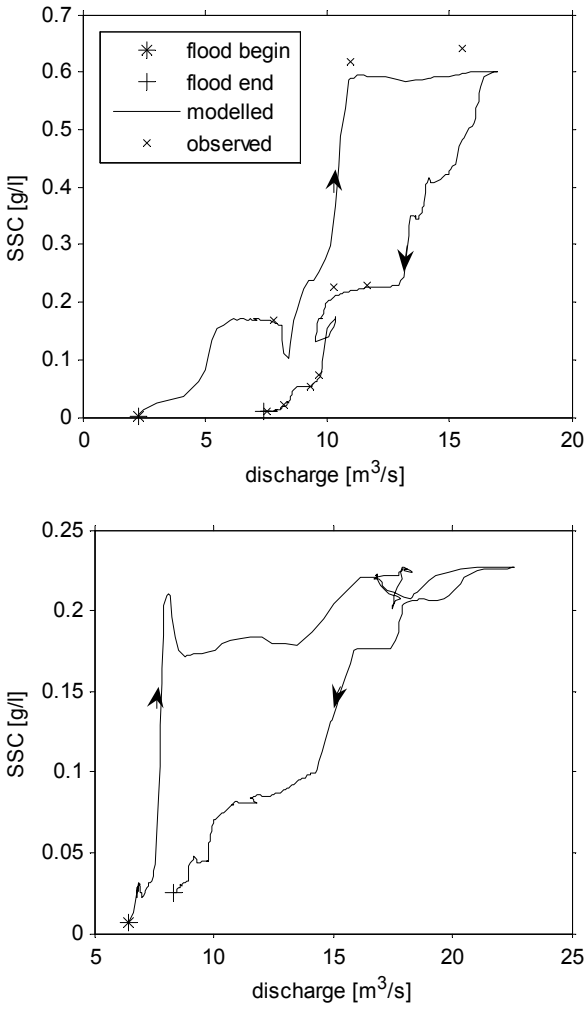

Fig. 8a,b: Hysteresis loops for a monitored (a, top) and an unmonitored flood (b, bottom); floods 5 and 4 at Cabecera.

4.5. Discussion of model properties, shortcomings

For the given datasets, the tested models showed pronounced differences in their performance in predicting SSC. Traditional SRCs performed poorly in reproducing SSC-variability. Since discharge as the only predictor is insufficient, the application of multivariate models is indicated. In the case of GLMs, this requires the choice of the appropriate link functions, and the best set of predictors to prevent overfitting. The three different methods for predictor selection yielded inconclusive results, which only converged slightly for the data set with the largest sample size (Cabecera, see Tab. 4). The performance of the analysed GLMs deteriorated strongly on the test data set. This suggests that, despite all

efforts, an apparently good fit on the training data was partially caused by overfitting the models using more degrees of freedom. The investigated GLMs do not include any interactions between predictors and no predictor can have a non-linear effect, which also contributes to their inferiority when compared to RF and QRF that can implicitly account for these effects.

The good performance of RF / QRF and their favourable properties make them a promising technique for SSC prediction. Moreover, the results illustrated in Fig. 7 allow plausible conclusions for the underlying processes: Fig. 7a suggests that changes in discharge have progressively less effect under conditions of much prior rainfall, which is presumably a result of the exhaustion of sediment supplies due to depletion. Analogously, Fig. 7b can be interpreted as a similar effect for the advancing season, probably also because of sediment exhaustion or, implicitly, decreasing rainfall intensity as the season progresses. These findings confirm the perception based on field-observation of a relatively intricate system of sediment delivery, where various processes of sediment production, temporal storage and conveyance interact.

Beside the errors that are related to instrumentation and monitoring setup (discussed in Chapter III), the following limitations of the proposed methods must be pointed out:

Regression analysis as performed here assumes independent observations. Due to the time-series characteristics of the matter, however, a certain degree of serial correlation must be expected. The limited number of temporally-close samples suggests that short term variability on the scale of 30 min is considerable for the headwater catchments, but autocorrelation at Capella is apparently an issue.

The applied QRF-method can be seen as an adaptive neighbourhood regression procedure: Each prediction is computed from a weighted mean of all observations, restricting the range of the predictions to the range of the observations. The resulting effect of underestimating peak concentrations on one hand and the overestimation of low SSC on the other hand has also been observed with linear regression and ANN models (Schnabel and Maneta, 2005; Lohani *et al.*, 2007) and may eventually lead to an underestimation of SSC variability.

The regression was performed using samples of an observation period of only three months. This restricts the applicability of the derived models to this time span. For temporal extrapolation, sampling of longer time period is mandatory. Regarding the high inter-annual variability rainfall and, thus, of sediment transport processes, temporal extrapolation is especially problematic as annual yields may be subject to major variability of up to an order of magnitude (Regüés *et al.*, 2000). Therefore, the training data must contain a wide range of observations. Furthermore, for longer time spans, the definitions of the supplementary variables such as Julian day and cumulated runoff have to be replaced by cyclic predictors such as the seasonality indices used by Holtschlag (2001).

The Monte Carlo method for assessing the confidence intervals of the sediment yield calculation assumes uncorrelated data in time, otherwise the prediction interval is likely to be underestimated (Meinshausen, pers. comm.). As mentioned before, this point could not be properly investigated.

In spite of these limitations, the presented methodology clearly performs better than traditionally used SRCs, because additional influential processes can be accounted for. The use of GLMs was problematic because the choice of the optimum set of predictor variables turned out to be strongly dependent on the variable selection method and thus not robust. Only for the largest dataset (Capella) did the variable selection methods produce comparable results, while in general the selected variables differed. Predictor selection by bootstrapping proved to be the least robust method because it was not able to designate important predictors for some cases or returned combinations of relative poor performance.

5. Conclusion

Predicting suspended sediment concentrations from auxiliary data is often performed using models of different complexity. Especially in small catchments with high SSC dynamics and a multitude of involved processes, the traditional sediment rating curve-approach of relating SSC to discharge is unsatisfactory. We employed traditional sediment rating curves (SRC), generalised linear models (GLM), Random Forests (RF) and Quantile Regression Forests (QRF) techniques and included ancillary predictor data to improve the predictive power. While GLMs could generally reproduce observed SSC better than traditional SRCs, the choice of the most suitable predictors remains problematic because of the different results produced by the variable-selection methods employed. Furthermore, some GLMs tended to be numerically unstable and all of them showed a considerable drop in performance when used on independent test data not included in the training. In contrast to the GLMs, the non-parametric RF and QRF models provided the best performance and, in the case of QRF, allowed the calculation of confidence intervals for the predictions, which enabled the computation of sediment yields and the associated uncertainties. The proposed method identifies predictors with high explanatory power. Multiple interactions of predictors can be accounted for without prior knowledge, and in the case of simple interactions, these can be interpreted. These advantages, which cannot be found combined in any of the established methods, provide potential for tackling questions of suspended sediment transport in rivers in a qualitative and quantitative way, especially when based on a limited number of samples.

6. Acknowledgements

This research was carried out within the SESAM-project (Sediment Export from Semi-Arid catchments: Measurement and Modelling) funded by the German Science Foundation (Deutsche Forschungsgemeinschaft, DFG, Grant No. BR 1731/3-1). The second author has a research grant from the Catalan Government and the European Social Fund. Rainfall data were obtained from the Spanish National Institute of Meteorology (INM) and the Ebro Water Authorities (SAIH). Hydrological data were supplied by the Ebro Water Authorities (SAIH). The Ebro Water Authorities also provided logistic support for using the Capella gauging station. We would like to thank Ramon J. Batalla and Damià Vericat for the installation of the sampling equipment in Capella and to the students of the University of Potsdam assisting in the field and in the laboratory.

Chapter III:

Flood-Based Analysis of High-Magnitude Sediment Transport Using a Non-Parametric Method

Abstract

Upland erosion and the resulting reservoir siltation is a serious issue in the Isábena catchment (445 km², Central Spanish Pyrenees). During a three-month period, water and sediment fluxes have been monitored at the catchment outlet (Capella), two adjacent sub-catchments (Villacarli, 41 km²; Cabecera, 145 km²) and the elementary badland catchment Torrelaribera (8 ha). This paper presents the results of the monitoring, a method for the calculation of a sedigraph from intermittent measurements and the derived sediment yields at the monitored locations. The observed suspended sediment concentrations (SSC) demonstrate the role of badlands as sediment sources: SSC of up to 280 g/l were encountered for Villacarli, which includes large badland areas. SSC at the Cabecera catchment, with great areas of woodland, barely exceeded 30 g/l. SSCs directly at the sediment source (Torrelaribera) were comparable to those at Villacarli, suggesting a close connection within this sub-catchment. At Capella, SSCs of up to 99 g/l were observed. For all sites, SSC displayed only a loose correlation with discharge, inhibiting the application of a simple sediment rating curve. Instead, ancillary variables acting as driving forces or proxies for the processes (rainfall energy, cumulative discharge, rising/falling limb data) were included in a quantile regression forest model to explain the variability in SSC. The variables with most predictive power vary between the sites, suggesting the predominance of different processes. The subsequent flood-based calculation of sediment yields attests high specific sediment yields for Torrelaribera and Villacarli (6,277 and 1,971 t km^{-2}) and medium to high yields for Cabecera and Capella (139 and 410 t km^{-2}) during the observation period. In all catchments, most of sediment was exported during intense storms of late summer. Later flood events yield successively less sediment. Relating upland sediment production to yield at the outlet suggests considerable effects of sediment storage within the river channel.

Key words: suspended sediment, sediment yield, sediment rating curve, quantile regression forests, Isábena

Published as
Francke, T., López-Tarazón, J. A., Vericat, D., Bronstert, A., Batalla, R. J. 2008. Flood-Based Analysis of High-Magnitude Sediment Transport Using a Non-Parametric Method. *Earth Surface Processes and Landforms* **33**: 2064 – 2077, DOI: 10.1002/esp.1654

1. Introduction

Reservoirs face siltation worldwide. However, siltation is accelerated in areas where runoff occurs over highly erodible unconsolidated sediments on bare slopes (i.e. badlands on marls, mudstones or shales) under severe climatic conditions, such as in the Mediterranean mountains, with long dry periods and storms of high rainfall intensity. There, most sediment is detached and eroded during short high magnitude rainfall events. Under such circumstances erosion rates are very high, creating high-density flows in the river network that reach the lowlands, even in large catchments. Quite often sediments are deposited in reservoirs located at the basin outlet. Sedimentation in reservoirs is not only an environmental issue but also a socio-economic problem, since it causes water quality problems and, especially, a progressive reduction in dam impoundment capacity, which creates serious problems for water management, especially near dam outlets.

Badlands are considered to be characteristic of arid regions but they also occur in wetter climates with high intensity storm events such as in the Mediterranean (Gallart *et al.*, 2002). The so-called humid badlands are found in mountainous areas such as the Southern Alps (e.g. Mathys *et al.*, 2005) and the Pyrenees (e.g. Clotet *et al.*, 1988). There, mean annual precipitation is around 700 mm or higher. Rainfall mostly occurs in the form of high intensity storm events. Vegetation growth is no longer limited by water availability but by the high erosion rates and freezing on north exposed slopes (Regüés *et al.*, 2002). This is the case for the Isábena River basin, a 445 km² catchment located in the Central Pyrenees that drains extensive areas of badlands that have been identified as the main source of the sediment deposited in the downstream Barasona Reservoir (Valero-Garcés *et al.*, 1999). Instantaneous concentrations of suspended sediment of up to 300 g/l have been measured at the basin outlet (López-Tarazón, 2006). The Barasona Reservoir supplies the region with water for drinking and irrigation. The large amount of sediment input coming from the badlands leads to a severe reduction in the storage capacity of the reservoir. Therefore, intense monitoring and specific modelling are needed to gain a better understanding of the magnitude and frequency of erosion and sediment transport in these particular fluvial environments which will help with informing management decisions in relation to the long-term availability and quality of water resources.

Within this context, this study aims to quantify flood-based sediment yields in two highly active headwater catchments in the upper Isábena River. The results are compared with the sediment delivery from a zero-order badland catchment and the sediment yield at the outlet of the basin, upstream of the reservoir. The findings provide insights into the magnitude and temporal dynamics of sediment delivery and its driving forces. For this purpose, a novel regression approach is applied that allows the interpolation of intermittent measurements of suspended sediment concentrations, computes confidence intervals for these estimates and enables the calculation of sediment loads. Sediment fluxes are quantified at a range of spatial scales and catchments units (i.e. badland, headwater tributaries, river mainstem, lowland). Sediment yields and improved process understanding aid calibration and contribute to improvements in a numerical hydrological and sediment transport model (Bronstert *et al.*, 2007) as well as the development of a 1D-model of reservoir sedimentation (Mamede *et al.* 2006). The paper develops a comprehensive conceptual framework to couple river channel with wider catchment processes; specifically, it links particle detachment and soil erosion to in-channel sediment transport and downstream sedimentation. Thus, it provides new data and methods relevant to studies of sediment transport in highly erodible montane catchments, many of which are experiencing increasing frequency of extreme flows and high rates of

sediment loss as a result of environmental change.

2. Study Area

This study was carried out in the Isábena catchment (Central Spanish Pyrenees) and two of its main sub-basins Villacarli and Cabecera (Fig. 1). The catchment has an area of 445 km² and is part of the Ebro Basin. It is characterised by heterogeneous relief, vegetation and soil characteristics. Elevation increases from 450 m a.s.l. in the southern and central parts of the catchment (i.e. Intermediate Depression and Internal Ranges) to up to 2,720 m a.s.l. in the northern part (i.e. Axial Pyrenees). The climate is typical of Mediterranean mountainous areas, with mean annual precipitation of 767 mm (from 450 to 1600 mm) and an average potential evaporation rate of 550 to 750 mm, both rates showing a strong south–north gradient due to topography (Verdú et al, 2006a). Vegetative cover includes deciduous woodland, agriculture, pasture and *matorral* in the valley bottoms, evergreen oaks, pines and *matorral* in the higher areas. The Northern parts are composed of Paleogene and Cretaceous sediments and the southern lowlands are mainly dominated by Miocene continental sediments. These areas consist of easily erodible materials (marls, sandstones), leading to the formation of badlands and making them the major source of sediment within the catchment (Fargas *et al.*, 1997). Badlands can mainly be found in the Villacarli sub-basin (6 % of total area), while they are almost absent in the adjacent Cabacera sub-basin (<0.1 % of total area). Within the former, the areal fraction of badlands may be as high as 30 %, as it is the case for the zero-order badland catchment Torrelaribera.

The Isábena River drains into the Barasona Reservoir (Fig. 1). The dam was constructed in the early 1930s for an original capacity of 71 hm^3 and it was enlarged in 1972 reaching a total capacity of 92 hm^3. The reservoir supplies water mainly to the Aragón and Catalunya canal that irrigates an area of ca. 70,000 ha. For almost 75 years the reservoir has been progressively silting up at a rate of between 0.3 and 0.5 hm^3 of sediment deposited per year. Engineering works during the 1990s released sediment through the dam bottom outlets resulting in around 5 hm^3 of sediment being sluiced through the dam. Nowadays the reservoir capacity equals that of 1993 (76 hm^3).

3. Methodology

3.1. Instrumentation

During a three-month observation period (September – December 2006), discharge (hereafter Q) and suspended sediment concentration (hereafter SSC) were monitored at four sites in the Isábena catchment (Tab. 1, Fig. 1). Late summer and autumn is when most thunderstorms and rainfall events take place, therefore this study focussed on this time of the year. The discharge was measured using a capacitive water stage sensors/loggers (Trutrack WT-HR) installed at suitable cross sections at the Torrelaribera, Villacarli and Cabecera sub-catchments (Fig. 1). Flow stage was recorded at a 2 to 5 minute interval. At Torrelaribera, a sharp-crested V-notch weir provided a constant cross section, while at Villacarli and Cabecera the river constriction below bridges were employed. Repeated discharge measurements were made using the volumetric technique, current meter (OTT C2) transects and tracer dilution (NaCl) completed with cross section surveys (Geodimeter total station). During high water stages and for safety reasons, flow velocity was measured at the water surface only (Villacarli) and at a wider section (Cabecera). Water stage-discharge rating curves were derived by combining the stage-mean velocity and stage-area methods as being more robust for extrapolation (Mosley and McKerchar *et al.*, 1993). Water depth was recorded at a 15 minute time interval at the Capella gauging station at the basin outlet. This station is operated by the Ebro Water Authorities whose stage-discharge rating curve was used for discharge calculation.

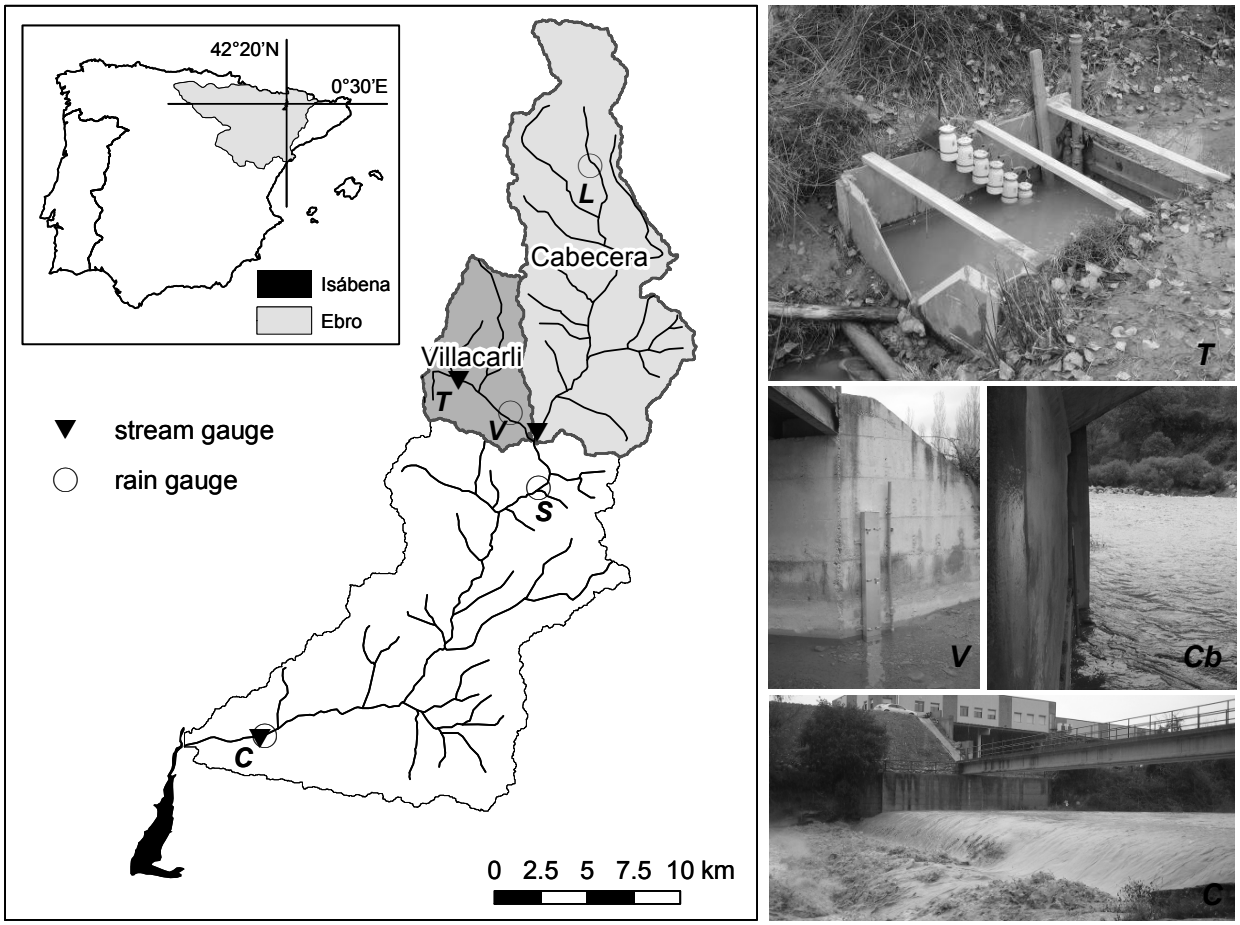

Fig. 1: Isábena catchment and monitored sub-catchments Villacarli and Cabecera (C: Capella; Cb: Cabecera; L: Las Paules; S: Serraduy, T: Torrelaribera, V: Villacarli).

Tab. 1: Summary of sub-catchment characteristics.

Sub-catchment	Area (km^2)	Lithology	Dominant land-use
Torrelaribera	0.08	Mesozoic marls	Matorral Badlands (30 %)
Villacarli	41	Mesozoic marls, limestone, sandstone	Forest Matorral Pasture Badlands (6 %)
Cabecera	145	Conglomerates, Limestone	Forest Pasture [Badlands (<0.1 %)]
Isábena (Capella gauging station)	445	as in Villacarli and Cabacera plus quaternary deposits	Forest Matorral Pasture Agriculture [Badlands (<0.02 %)]

Suspended sediment was manually sampled and stored in 1-litre-bottles at a frequency of 20 to 90 minutes during flood events and routinely during low flows. Due to highly turbulent flow conditions, mixing was assumed complete. Additionally, a total of six samples originate from rising stage sediment samplers at Torrelaribera and Villacarli (Fig. 1). At the Capella station, samples were obtained by means of an ISCO automatic sampler and manual sampling; in addition, turbidity is recorded

every 15 minutes up to 3000 NTU (i.e. 3 g/l). A calibration equation was developed to convert turbidity to SSC using 490 pairs of values gained from water samples (*SSC [g/l]=0.0012 NTU+0.0605; r^2=0.82*). Out of the data set obtained from the turbidimeter, twelve measurements (weekly interval) were used in the analysis to represent the otherwise undersampled low-flow periods, complementing the measurements obtained from the automatic sampler. The data collection resulted in 611 values of SSC over the four study sites (Torrelaribera:122; Villacarli:104; Cabecera: 66; Capella: 331). Samples were vacuum filtered (Millipore, 0.045 mm pore size) or decanted when concentrations were (approximately) above 4 g/l, oven-dried and weighed to determine SSC.
Precipitation was measured using a tipping-bucket rain gauge installed in Villacarli. In addition, 15-minute rainfall data for the Cabecera and the Isábena catchments were obtained from the rain gauges at Las Paules and Capella (Ebro Water Authorities P030 and P047, respectively, see Fig. 1).

3.2. Interpolation of SSC measurements

Discharge and SSC show poor statistical relationships in all the study sites, impeding the use of the traditional Flow Duration Curve method (Walling, 1984) to calculate the sediment yield. A continuous sedigraph was produced allowing the calculation of sediment yields from ancillary data using a Quantile Regression Forests model (hereafter QRF). QRF (Meinshausen, 2006) are a non-parametric multivariate regression technique that builds on Random Forests (RF) regression tree ensembles (Breiman., 2001). Regression trees (a.k.a. CARTs, Breiman *et al.*, 1984) are constructed by recursive data partitioning, which can include both categorical and continuous data from ancillary datasets. RF and QRF employ an ensemble of these trees, each one grown on a random subset of the training data. Model predictions are obtained from the mean of the prediction of each single tree (RF) or based on the distribution of these single-tree predictions (QRF). RF and QRF perform favourably when dealing with nonlinearity, imply no assumptions about the distribution of the data and are robust and capable of handling non-additive behaviour, which makes them particularly attractive for the problem at hand. Furthermore, measures of variable importance are calculated: For each predictor, the loss of model performance (expressed as increase in Mean Squared Error, IncMSE) is quantified when it is omitted from the model. Thus, the explanatory power of each predictor can be assessed (see Fig. 2 for example).

Tab. 2: Ancillary data used for regression analysis (abbreviations explained in the text).

presumably approximated process				
Sediment production on slopes	Sediment production / re-mobilisation in riverbed	Exhaustion of sediment supply on slopes	Exhaustion of sediment supply within riverbed	Dilution
(discharge) rain_x15 rain_x60 rain_x1d r_x60 r_x1d	discharge rain1d cum_q_1h cum_q_5h	julian_day rain_x1d cum_q_1h cum_q_5h r_x1d	julian_day limb_dec cum_q_1h cum_q_5h	discharge rain_x15 rain_x60 rain_x1d cum_q_1h cum_q_5h

For the use as additional predictors, ancillary datasets (Tab. 2) were selected according to the perceived capability of representing relevant processes (cf. Schnabel and Maneta, 2005) and their continuous availability. These predictors include the Julian day, the sum of rainfall for 15 minutes, 60 minutes and 1 d registered at the three gauges Villacarli, Laspaules and Capella (denoted e.g. as *rain_capella15*), the respective USLE erosivity factors for 60 minutes and 1 day (denoted e.g. as *r_capella1d*), the cumulative discharge of the previous one and five hours (denoted as e.g. *cum_q_5h*) and the rate of change in discharge (*limb_dec*).

To assess the reliability and robustness of the employed models, validation was performed using a bootstrapping approach (n=1000), where bootstrapped training data sets were generated and model performance on the remaining test data assessed. The Spearman correlation coefficient R_{Sp} between modelled and observed SSC, averaged over all bootstrap runs, was used as a measure of goodness-of-fit. $R_{Sp,full}$ for the full dataset is calculated as

$$\overline{R_{Sp,full}} = mean[cor_{Sp}(SSC_{mod}, SSC_{obs})] \quad \textit{Eq. 1}$$

$R_{Sp,test}$ for the test dataset is computed as

$$\overline{R_{Sp,test}} = mean[cor_{Sp}(SSC_{mod}^{test}, SSC_{obs}^{test})] \quad \textit{Eq. 2}$$

Optimism in R_{Sp} (Harrell, 2001) is estimated as

$$O_{R_{Sp}} = \overline{R_{Sp,train}} - \overline{R_{Sp,test}} \quad \textbf{\textit{Eq. 3}}$$

with

$$\overline{R_{Sp,train}} = mean[cor_{Sp}(SSC_{mod}^{train}, SSC_{obs}^{train})]$$

where subscripts "*obs*" and "*mod*" mean "observed" or "modelled" values, respectively. Superscripts "*full*", "*train*" and "*test*" refer to the entire, training or test dataset, respectively. R_{Sp} is more suited to deal with nonlinear models and the range of the data over several orders of magnitude than the traditionally used coefficient of determination R^2. The "optimism" in R_{Sp} gives information on the dependency of the model structure on the subset of the training data and thus for the models robustness.

3.3. Sedigraph prediction and calculation of sediment yield

By applying the calibrated models to data of the complete monitoring period (September 10 to December 15, 2006) in the temporal resolution of the discharge dataset, SSC data for each timestep was estimated (i.e. values for best estimate, lower and upper limit of the 95 % Confidence Interval for prediction, hereafter CI). Subsequently, flood-based sediment yields and their confidence intervals were computed using a Monte-Carlo-approach:

Tab. 3: Mean, upper and lower quartile (q25 %, q75 %) of monthly rainfall and maximum daily rainfall recorded at INM-station Serraduy 1988-2005 compared to data measured during observation period (2006).

Month	Monthly rainfall [mm]		Max daily rainfall [mm]	
	Mean 1988-2005 (q25 %-q75 %)	*Year 2006 (percentile)*	*Mean 1988-2005 (q25 %-q75 %)*	*Year 2006 (percentile)*
September	87 (67-94)	252 (>94)	32 (25-36)	57 (94)
October	80 (24-117)	42 (39)	24 (12-34)	13 (33)
November	61 (21-84)	26 (37)	21 (10-26)	22 (74)
December	55 (23-72)	40 (63)	23 (11-30)	22 (63)

For each time-step, random SSC-value was randomly drawn from the 95 % CI, according to its probability. From these values, the flood-based sediment yields were computed. Repeating this process 70 times allowed the calculation of the CI for the sediment yield of each flood.
Model building and statistical analyses were conducted using the statistic software R (R-Team Development Core, 2006) with the randomForest (Liaw and Wiener, 2002) and quantreg-Forest (Meinshausen, 2007) packages.

4. Results

4.1. Primary data

Rainfall was unusually strong in September 2006 (Tab. 3). The monthly total of 252 mm is almost three times the 20-year average value at the station of Serraduy that is located 2 km downstream from the confluence of the Villacarli and Cabecera torrents (Fig. 1). The September precipitation surpassed the previous maximum recorded September rainfall by more than 70 mm. The maximum daily rainfall of 57 mm also ranks among the highest within the record. From October to December 2006, rainfall characteristics were close to average (within the interquartile range). At Capella rain gauge station (Fig. 1), the September precipitation of 2006 was 202 mm compared to a mean of 92 mm and a previous maximum of 149 mm (10 years of data). Similar conditions were encountered at the rain gauge located in Las Paules (10 years of data), with percentile values of 100 and 90 for monthly rainfall and maximum daily rainfall in September, respectively, confirming that September 2006 was unusually wet over the entire catchment.

4.2. Discharge and suspended sediment concentration

Tab. 4 summarizes Q and SSC measurements at the four monitored sections. The continuity of discharge increases with increasing catchment size. The smaller catchment, Torrelaribera (Fig. 1), shows an ephemeral character with relatively high discharges of up to 0.68 m^3/s quickly following summer thunderstorms and drying up within hours thereafter. Late in the season, discharge becomes more persistent with baseflows of less than 1 l/s. The surrounding Villacarli valley (Fig. 1) still showed flashy behaviour with a response time of one to two hours after heavy rainfall, resulting in peak discharges as high as 21 m^3/s, with recessions usually lasting one day. Discharge reached values as low as 0.1 m^3/s but never ceased completely. Cabecera, as the largest of the headwater subcatchments, experienced the highest discharges. The maximum recorded Q of 44 m^3/s equals ten times the mean discharge over the study period, evidence of less variability than in the smaller subcatchments. The onset of floods was on average seven hours later than at Villacarli while water stage would also rise abruptly within a very short time. This delay and the much flatter recession limb testify to a considerably less flashy runoff regime than that at Villacarli. Discharge at Capella (i.e. the catchment outlet) is quantitatively mainly controlled by the behaviour of Cabecera, which, on average, yielded two-thirds of the runoff of the entire catchment, while Villacarli only represents one fifth (Verdú *et al.*, 2006b). The delay of the onset of the floods at Capella when compared to Villacarli varied greatly and even preceded the latter for some cases, showing the effect of small downstream flashy tributaries and heterogeneous rainfall distribution. Approximately, this delay is 10 hours between Torrelaribera and Capella, 7 hours between Villacarli and Capella and 5 hours between Cabecera and Capella. The different runoff response characteristics are also reflected in the occurrence of floods in the sub-catchments. Whereas 13 and 11 flood events were identified in Torrelaribera and Villacarli, respectively, only 8 flood events occurred in Cabecera. Moreover, the latter floods are considerably delayed with regard to Villacarli and in one case are not related to a corresponding

flood at all. Further downstream at the Capella station, only 10 floods were observed.

Suspended sediment concentration follows a pattern similar to the discharge. In Torrelaribera, the observed concentrations range from a few milligrams to 240 g/l, covering six orders of magnitude. The recession of SSC to pre-flood level is usually quicker than the recession of the hydrograph but can be interrupted by rainbursts. This behaviour could also be observed in Villacarli, where the measured range of SSC is even larger (for more details see Tab. 4). Maximum SSC at Cabecera station reached 30 g/l registered during September floods. However, after this month the maximum observed SSC decreased to less than 2 g/l. Thus, SSC is generally one order of magnitude lower than those measured in Torrelaribera and Villacarli. Dynamics appear mainly influenced by local rainbursts, which often produce SSC peaks long before maximum discharge is reached. At the Capella section, SSC during September floods frequently exceeded 50 g/l, decreasing to peak values of approximately 8 g/l during late autumn floods. At all observation sites, the magnitude of discharge and SSC decreased from the end of the summer throughout the autumn: the onset of heavy storm events after the summer dry period (September) caused the most extreme values of both discharge and SSC. As rainfall as the driving force decreased (Tab. 3), so did the magnitude of the flood events and the related sediment concentrations.

Tab. 4: Summary of measured discharge(Q) and suspended sediment concentration (SSC) data.

Sub-catchment	Q						SSC		
	$[m^3 s^{-1}]$			$[l/s^{-1} ha^{-1}]$			$[g l^{-1}]$		
	min	mean	max	min	mean	max	min	median	max
Torrelaribera (n=122)	0	0.002	0.68	0	0.25	85	0.001	2.8	240.6
Villacarli (n=104)	0.1	0.65	21.2	0.02	0.16	5.17	0.001	1.3	277.9
Cabecera (n=66)	0.91	3.77	43.4	0.06	0.26	2.99	0.002	0.1	30.5
Capella (n=331)	0.5	5.6	64.3	0.01	0.13	1.46	0.0005	1.2	99.6

Tab. 5: Performance of SSC-prediction using QRF in comparison with traditional SRCs.

	model	R_{Sp}		Optimism in R_{Sp}
		full dataset	test data	
Torrelaribera	SSC ~ Q	0.75	0.74	0.25
	log(SSC) ~ log(Q)	0.75	0.74	0.18
	QRF	0.91	0.87	0.22
Villacarli	SSC ~ Q	0.64	0.64	0.24
	log(SSC) ~ log(Q)	0.64	0.63	0.25
	QRF	0.89	0.83	0.09
Cabecera	SSC ~ Q	0.40	0.39	0.24
	log(SSC) ~ log(Q)	0.40	0.39	0.29
	QRF	0.67	0.67	0.09
Capella	SSC ~ Q	0.16	0.16	0.02
	log(SSC) ~ log(Q)	0.16	0.16	0.00
	QRF	0.95	0.88	0.05

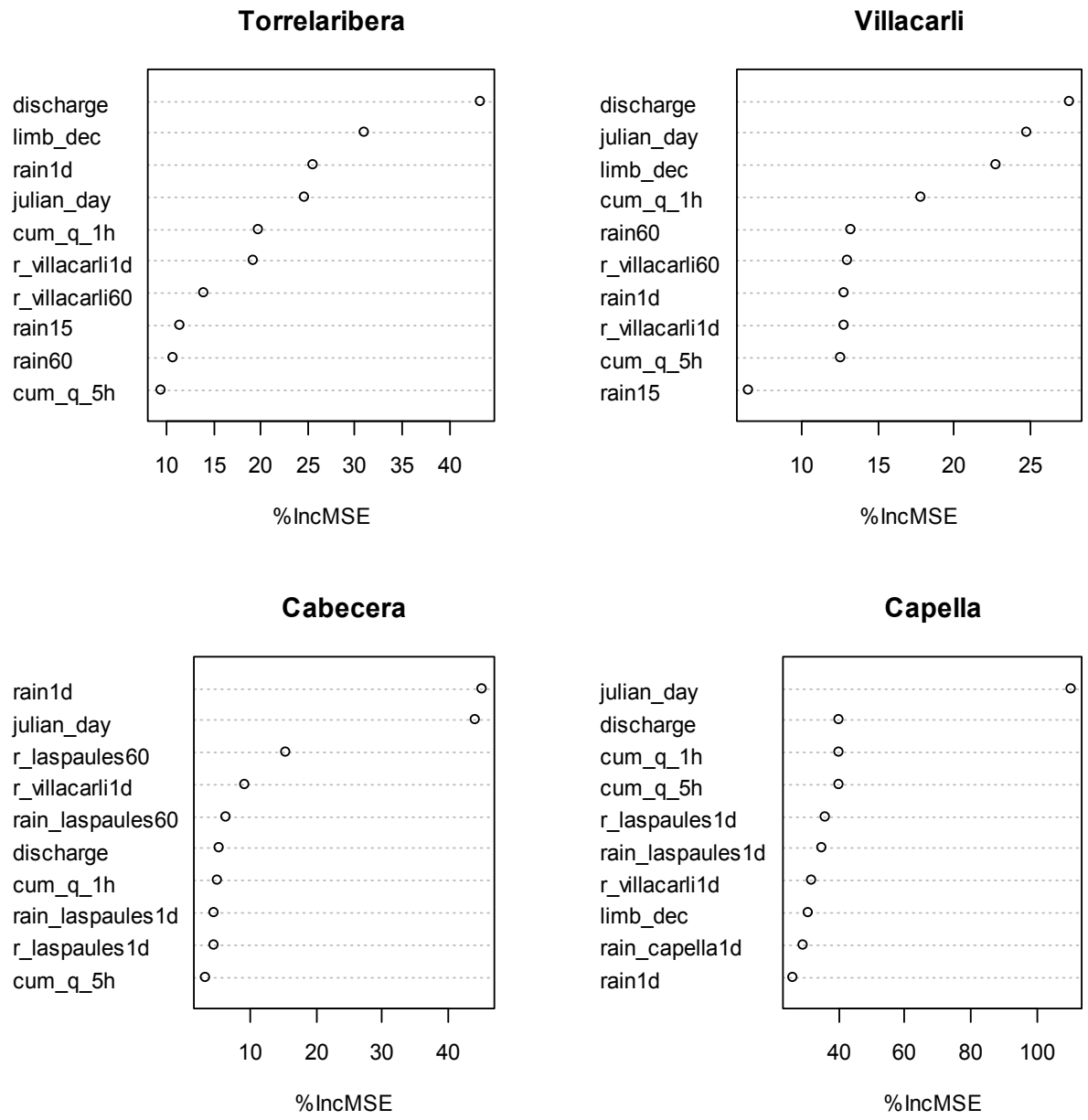

Fig. 2: Variable importance for application of QRF-model (for details cf. section 3.2).

4.3. Interpolation of SSC measurements

For the four headwater monitoring sections, the traditional application of a rating curve model (hereafter SRC) in the form of log(SSC)~log(Q) performs unsatisfactorily (Tab. 5), especially with regard to the temporal dynamics and general trend of seasonal decline in SSCs. For all observation sites, the QRF model provides a better goodness of fit, especially for Cabecera and Capella. For Villacarli and Cabecera, the QRF furthermore shows lower values for optimism in R_{Sp}, making the model more robust and less dependent on single measurements.

Fig. 2 plots the variable importance of the 12 most important predictors for the QRF-models. The results confirm that discharge is insufficient for SSC prediction if not supplemented by other ancillary predictors. The important role of the Julian day underlines the strong seasonal dependence of sediment dynamics. For Cabecera, discharge is not even among the most appropriate predictors, suggesting that areas of major discharge generation do not coincide with the major sediment sources.

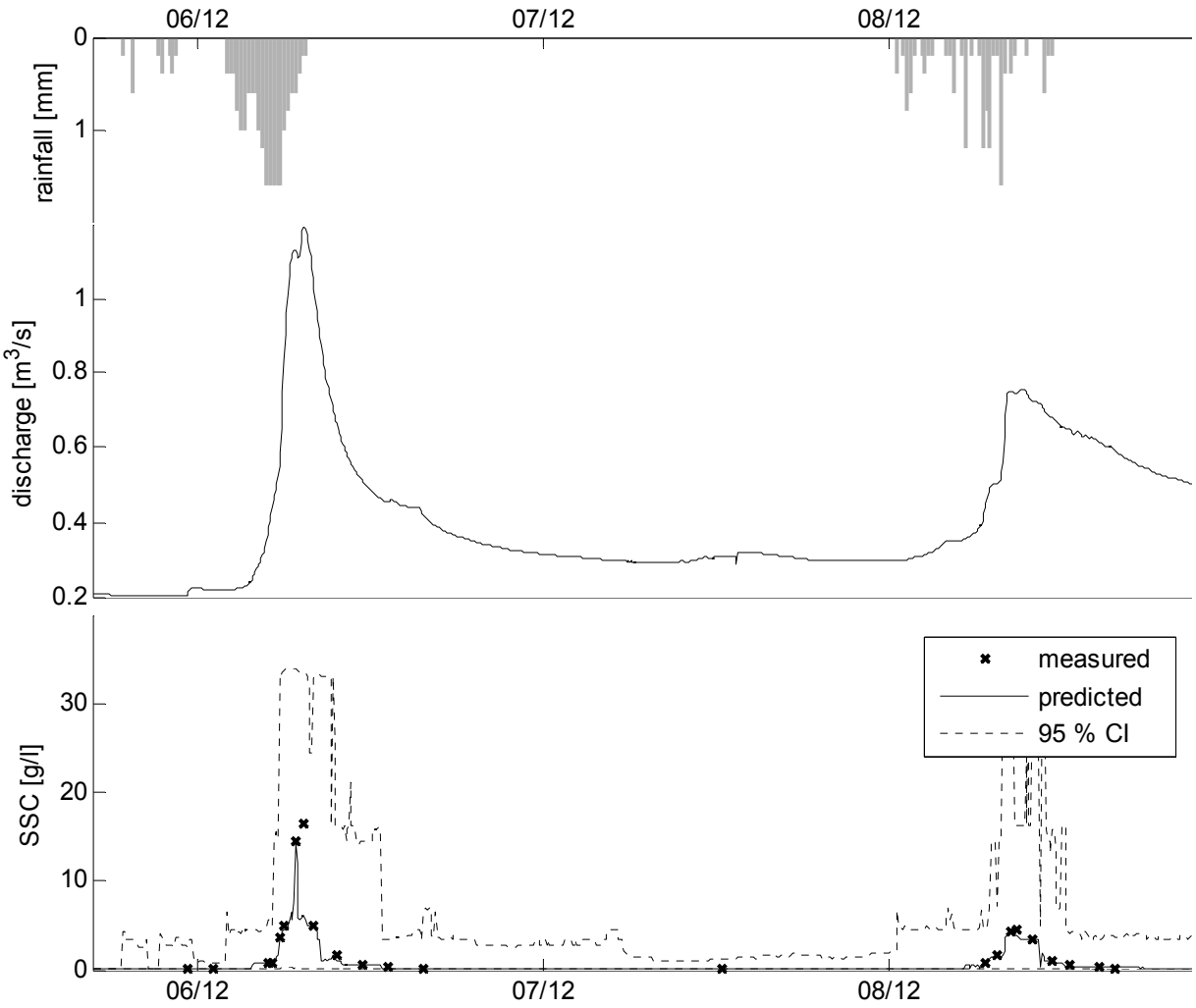

Fig. 3: Close-up-view of rainfall, discharge and SSC (measured and modelled) for two floods at Villacarli (CI: 95 % confidence interval).

4.4. Sedigraph prediction

The reconstructed sedigraphs show moderate to good agreement with the observed data (Tab. 5, Fig. 3). However, high SSC values, especially at the beginning of the observation period, are partially underestimated, probably resulting from the low number of observations of this kind and the characteristics of conservative estimation of QRF. The confidence bounds are quite narrow shortly after the peak of the event and during low flows, but widen considerably during periods of high dynamics, reflecting a higher level of uncertainty in these estimates. At the Torrelaribera and Villacarli stations SSC values tend to be somewhat overestimated during low-flow periods at the beginning of the observation period. For Villacarli with continuous runoff, this effect may lead to a slight overestimation of the early inter-flood sediment yields, while it is irrelevant for Torrelaribera because of the ephemeral runoff regimen.

4.5. Sediment yield

Mean flood-based sediment yields for Torrelaribera (see Fig. 4 and Tab. 6) range from 0.2 to 161 t, with CI 95 % ranging from 6 % (flood 4) to 39 % (flood 7) of the estimated value. Interflood periods are generally negligible in terms of sediment yield, with the low-flow period between flood 4 and 5 being the exception with an export budget of 2.1 t. During the entire observation period, 99.5 % of the sediment export occurred during floods.

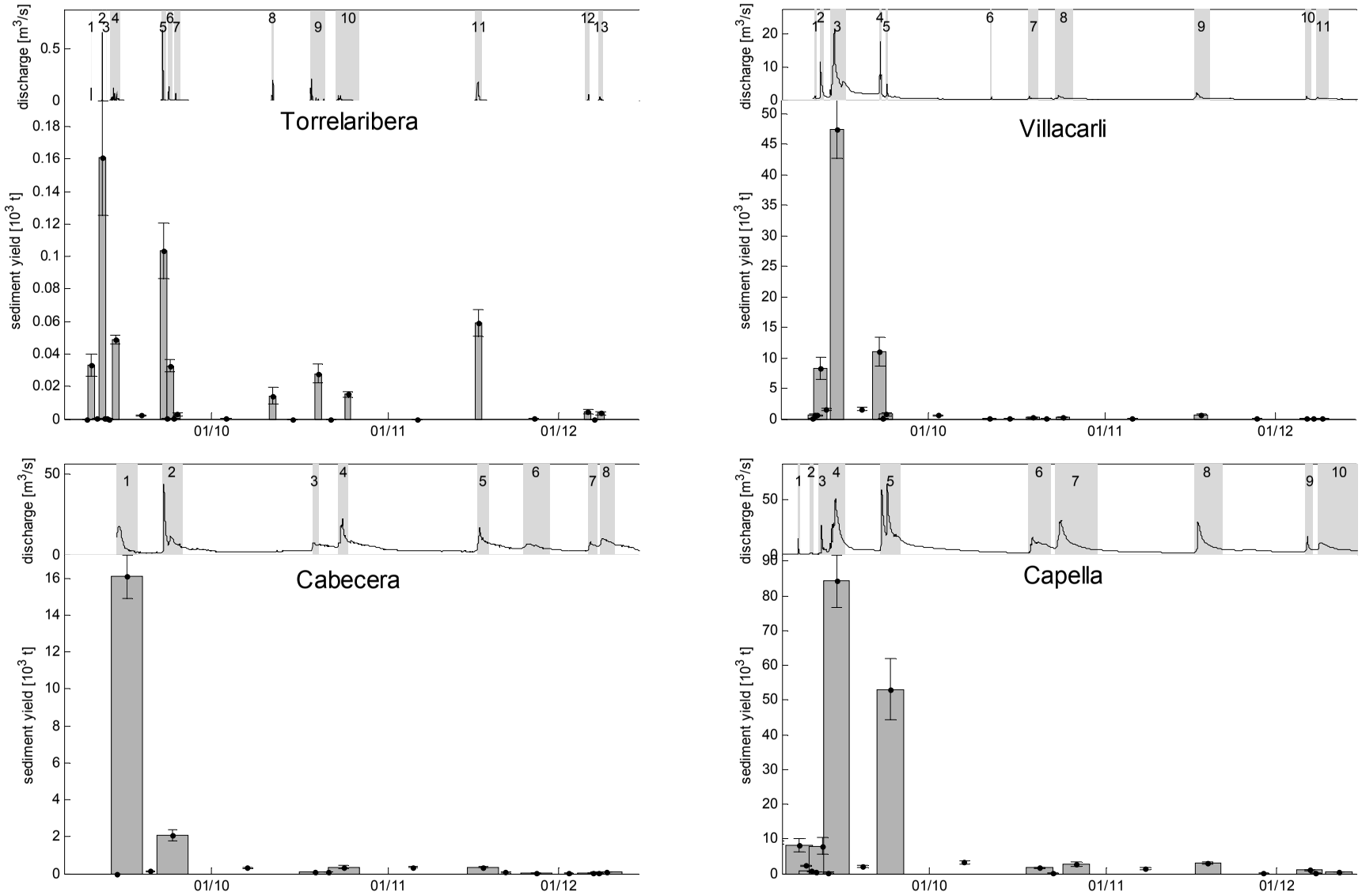

Fig. 4: Sediment yield of flood (bars and whiskers) and interflood (whiskers only) periods. The whiskers comprise the 95 % CI. The grey bars underlying the hydrograph depict the numbering of the floods.

Tab. 6: Flood based sediment yields. Note that the flood numbers are not related between locations.

Location	Flood number	Begin	Duration [h]	Rainfall [mm]	Total runoff [m^3]	Sediment yield [t]	CI sediment yields [t]
Torrelaribera	1	09.09.	3	9	478	33.1	26.2 - 40.0
	2	11.09.	2	13	2,170	160.8	125.5 - 196.1
	3	12.09.	2	6	8	0.2	0.1 - 0.2
	4	13.09.	39	107	1,771	48.7	45.9 - 51.4
	5	22.09.	17	53	3,391	103.4	86.2 - 120.6
	6	23.09.	22	28	1,590	32.6	29.0 - 36.3
	7	24.09.	19	9	392	2.8	1.7 - 3.9
	8	11.10.	8	11	331	14.3	9.4 - 19.2
	9	18.10.	62	34	1,082	28.0	22.3 - 33.7
	10	22.10.	96	32	1,182	15.1	13.3 - 17.0
	11	16.11.	30	49	2,235	58.9	50.9 - 67.0
	12	05.12.	19	22	295	4.5	3.2 - 5.7
	13	08.12.	18	14	350	3.5	2.5 - 4.6
Villacarli	1	10.09.	10	4	27,039	683	582 - 784
	2	11.09.	17	21	268,505	8,263	6,445 – 10,081
	3	13.09.	68	99	1,696,951	47,447	42,665 – 52,230
	4	22.09.	12	54	281,243	11,019	8,669 – 13,369
	5	23.09.	9	27	77,422	743	457 – 1,029
	6	11.10.	8	12	12,064	57	41 - 74
	7	18.10.	42	31	78,311	194	157 - 232
	8	23.10.	74	31	176,044	301	254 - 347
	9	16.11.	67	43	201,012	643	553 - 733
	10	06.12.	23	20	39,905	111	79 - 143
	11	08.12.	52	14	89,263	65	53 - 76
Cabecera	1	14.09.	88	49	2,041,727	16,073	14,874 – 17,272
	2	22.09.	83	96	3,220,319	2,081	1,787 – 2,376
	3	18.10.	23	39	539,922	70	62 - 78
	4	23.10.	40	31	1,703,302	359	265 - 453
	5	16.11.	45	50	1,561,124	359	302 - 417
	6	24.11.	110	12	2,007,849	43	40 - 47
	7	06.12.	38	16	807,548	34	30 - 38
	8	08.12.	60	13	1,799,918	77	70 - 84
Capella	2	10.09.	13	8	65,475	653	6,306 – 10,104
	3	11.09.	43	30	778,536	9,244	504 - 783
	4	13.09.	66	107	5,392,881	84,066	5,669 – 10,283
	5	22.09.	82	85	7,650,513	49,979	76,492 – 91,848
	6	11.10.	11	8	302,157	299	44,336 – 61,906
	7	18.10.	92	41	3,179,673	1671	1,400 – 1,879
	8	23.10.	176	27	6,783,747	2783	2,222 – 3,270
	9	16.11.	119	43	4,395,069	3053	2,718 – 3,384
	10	06.12.	35	21	815,382	1052	932 – 1,154
	11	08.12.	182	12	3,845,718	399	443 - 560

At Villacarli station (see Fig. 4 and Tab. 6), mean flood-based sediment yields varied from 57 to 47,500 t, with CI 95 % ranging from 10 % (flood 3) to 38 % (flood 5). Even between floods, significant amounts of sediment (i.e. 6 % of the total sediment yield of the study period) were exported from the catchment, especially at the beginning of the observation period. Interflood periods preceding floods 2 and 6 yielded several hundred tons, exceeding greatly the yield of the late autumn periods. The concentration of sediment export in late summer and early autumn is much more pronounced than for Torrelaribera, which hints at the importance of flushing effects and depletion of temporary sediment storage.

Mean flood-based sediment yields at Cabecera (see Fig. 4 and Tab. 6) varied from 33 to 16,073 t, with CI 95 % ranging from 7 % (flood 1) to 26 % (flood 4) of the estimated value. Apparently, sediment concentration is less variable at Cabecera, enabling better predictability and narrower CI, in comparison with Torrelaribera and Villacarli. Interflood periods yielded several hundred tons in the early observation period and thus exceeded those of the late autumn floods. The total contribution of interflood periods is 5 % of the overall sediment yield. The seasonal trend of decreasing sediment yield is even more pronounced than for Villacarli: sediment transport (flood and interflood periods) mainly took place during the first floods after summer, later floods contribute only very little to the overall yield. Overall export rates are considerably lower than those at Villacarli, despite the larger catchment area (see discussion below).

At the catchment outlet in Capella the highest sediment yield could be observed during the September floods, which exported up to 84,000 t from the catchment (see Fig. 4 and Tab. 6). Thus, the two strong September floods 4 and 5 accounted for nearly 77 % of the total suspended load for the whole study period. Later floods of similar water yield produced only a fraction of this amount, producing yields in the order of the interflood periods only. However, looking at the entire observation period, low flows contributed to 6 % of the overall sediment transport. Only one SSC sample is available for the low flow period in early September. This seemed to lead to an implausibly high estimate of SSC and yield during that period. Therefore, that period has been excluded from analysis.

For all locations, the highest sediment export rates from the catchment could be observed during the first floods of late summer and early autumn. During that period, the overall amount of rainfall was highest and the most intense storms occurred, which generated much runoff. For Torrelaribera and Villacarli, the sediment yield is closely related to the overall runoff of the floods. This effect could not be observed for Cabecera and Capella where sediment is exported virtually completely during the first two major floods (i.e. 98 and 77 % of the total yield, respectively); successive floods contribute only with minor yields.

5. Discussion and Final Remarks

The length of the observation period confined to 3 months and the unusual wet September greatly limit the long-term representativity of the obtained values. Thus, even though late summer/autumn is presumably the season of highest sediment export rates of more than 70 % of the annual yield (Gallart *et al.*, 2005; López-Tarazón, 2006) and are therefore responsible for a major part of the annual sediment yield, the given values may not be representative of the long term average. This temporal extrapolation is especially problematic as annual yields may be subject to major variability of up to an order of magnitude (Regüés *et al.*, 2000a).

During the observation period, approximately 74,100 t of suspended sediment were exported from the Villacarli catchment (41 km^2). The Cabecera catchment (145 km^2) yielded around 20,000 t in the same period (Tab. 7). Relating these numbers to the catchment area results in specific sediment yields (hereafter SSY) for

the monitoring period of 1971 and 139 t km^{-2}, respectively. The above-mentioned limitations notwithstanding, the former value suggests a very high sediment activity and compares with mean annual sediment yields of similar catchments such as those in the Vallcebre area with badlands (2800 t km^{-2}a^{-1}, Regüés *et al.*, 2000a, 5 year of monitoring), despite being 40 times larger in area. The SSY obtained for the entire Isábena catchment at Capella is 410 t km^{-2}. This number is slightly above the 350 t km^{-2}a^{-1} yield for the entire Ésera catchment by Sanz Montero *et al.* (1996) and ranks as moderate to high in relation to data for 44 Mediterranean catchments given by de Vente *et al.* (2006), both being long-term estimates derived from reservoir siltation. The great difference in SSY between the adjacent catchments of Villacarli and Cabecera underlines the influence of different hydrological response and, especially, the predominant role of badlands (covering 6 % of the Villacarli sub-catchment) as the primary sediment source for the Villacarli torrent, a geological formation that is almost absent in the Cabecera catchment (<0.1 % of area).

Tab. 7: Total and specific sediment yield for observation period (95 % CI in brackets).

gauge	Total sediment yield [t]	Specific sediment yield [t km^{-2}]
Torre-laribera	509 (419-599)	6,277 (5,166-7,388)
Villacarli	74103 (63,971-84,235)	1,970 (1,701-2,240)
Cabecera	20,087 (18,341-21,832)	139 (127-151)
Capella	173,705 (149,710-197,702)	409 (353-466)

The elementary catchment of Torrelaribera has the highest SSY of the three monitored areas. The value of 6,277 t km^{-2} falls somewhat short of the 30,200 t km^{-2}a^{-1} reported by Martínez-Casasnovas and Poch (1997) and 60,000 t km^{-2}a^{-1} reported by Regüés *et al.* (2000a) for badland plots in the Vallcebre catchment (5 years of monitoring). This may be attributed to the fact that only 30 % of the Torrelaribera catchment is composed of bare badland slopes. Its special settings result in a sediment delivery ratio of ~70 %, based on the survey of a dateable sediment trap and erosion pin measurements. Thus, using the portion of the basin occupied by such slopes instead of the whole catchment, the SSY value is close to the above mentioned values.

As shown in the previous section, most of the sediment load is transported during flood periods, underlining the importance of the temporal distribution of water and sediment fluxes between flood and inter-flood periods. This temporal concentration is especially pronounced in Torrelaribera, where less than 1 % of the sediment load is transported during low flow, due to the ephemeral behaviour of the catchment. The pronounced flashiness of Torrelaribera is expressed in the fact that 90 % of water and sediment fluxes occur in only 4 % of the time (Fig. 5). For Villacarli and Cabecera, the fraction of sediment transported during low flows is 6.1 and 4.9 %, respectively. The water fluxes from Villacarli, Cabecera and their combined outflow (C+V, i.e. calculated as the sum of the values of each) become successively more balanced with time. In contrast, sediment flux is highly concentrated in time. For C+V, 90 % of the sediment is transported in approximately 1 % of the time (i.e. 2.2 % for Villacarli). Further downstream at Capella, sediment flux is somewhat more evenly distributed in time (90 % of sediment in 9 % of the time), although the catchment keeps its flashy behaviour with regard to runoff.

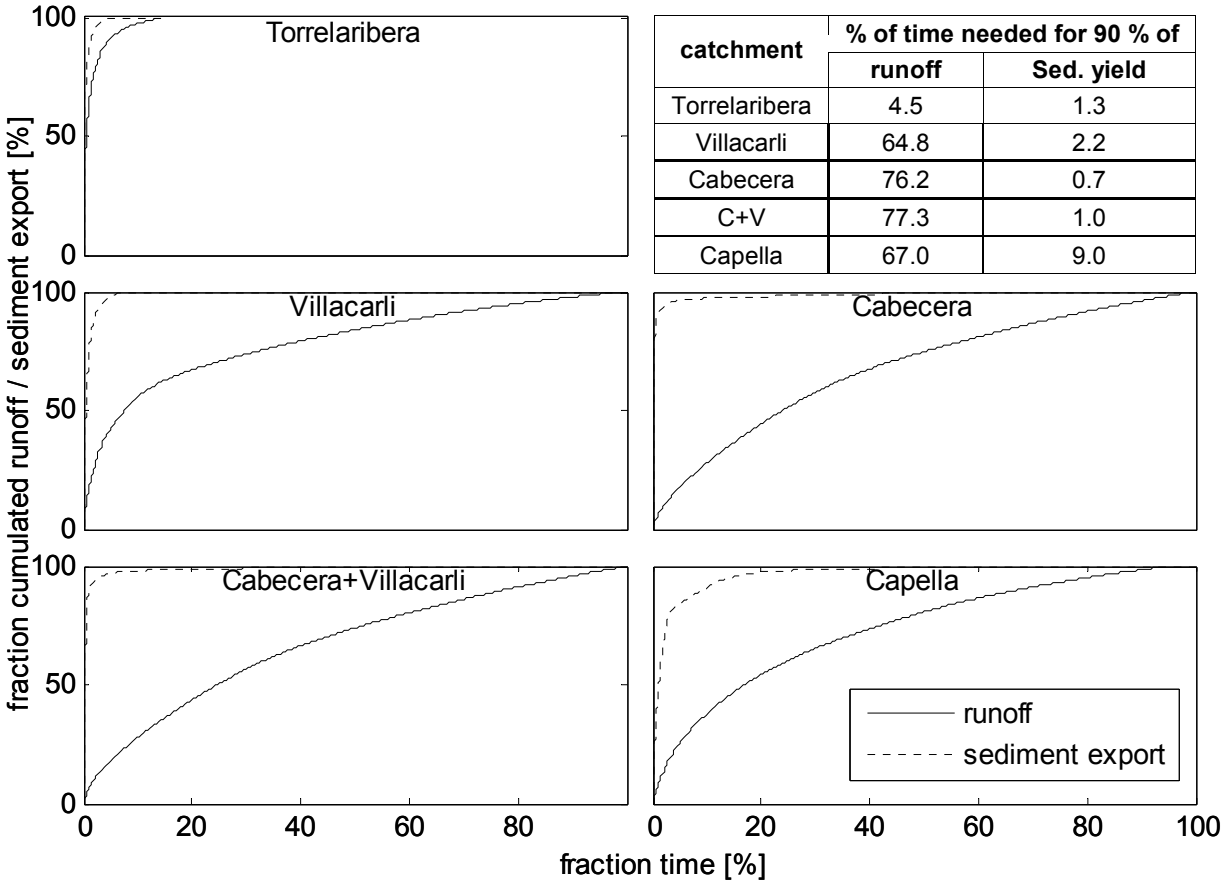

catchment	% of time needed for 90 % of	
	runoff	Sed. yield
Torrelaribera	4.5	1.3
Villacarli	64.8	2.2
Cabecera	76.2	0.7
C+V	77.3	1.0
Capella	67.0	9.0

Fig. 5: Duration curves of water and sediment fluxes. Cabecera+Villacarli (C+V) denotes the simulated properties of the confluence of sub-catchments Villacarli and Cabecera.

Relatively high sediment fluxes even during low flows have also been observed by López-Tarazón (2006) in the lower Isábena. In the relatively dry year of 2005, up to 70 % of the time was required to transport 90 % of the sediment. Although Fargas *et al.* (1997) also identified further sediment sources downstream of the Villacarli-Cabecera confluence, it is unlikely that these provide an asynchronous sediment input to cause a more continuous sediment flux downstream at Capella. This phenomenon is presumably a result of the effect of sediment storage in the river channel, which is supported by field observations, although no quantitative data are available to support this hypothesis yet.

Fig. 6 compares the sediment yield calculated for the headwater catchments and the catchment outlet. During the early floods (floods 1 and 2), the headwater catchments, namely Villacarli, release 67–100 % of the sediment yield observed at the outlet, suggesting a high degree of sediment connectivity within the river network. During the smaller successive flood in late autumn, the headwater catchments provide only 9-27 % of the sediment loads measured at the outlet. This could be explained by the increasing role of the downstream tributaries as the flood season progresses or the riverbed with temporary sediment deposits as a source for the sediments leaving the catchment.

The results of this paper are a synthesis of numerous working steps, some of which are subject to simplifying assumptions and/or a certain degree of error that cannot always be quantified. The major source of error during measurements is related to the water stage–discharge conversion in non-regular cross sections that suffer scour and fill processes during floods. In addition, the higher discharge values are more uncertain because of the extrapolation of the rating curve (i.e. Q measurements were increasingly difficult during high flow). Since high sediment fluxes usually coin-

cide with high discharge, errors in the upper part of the rating curve can certainly influence the subsequent calculation of the sediment yield. However, due to the time-series characteristics of the measurements, a certain degree of serial correlation in the data must be expected, which could not be investigated due to the limited number of temporally-close SSC-samples.

Effectively, the QRF-method computes each prediction from a weighted mean of all observations, restricting the range of the predictions to the range of the observations. Although we are confident of having captured virtually the entire range of SSC-conditions, we cannot exclude the possibility of having missed the absolute maximum in SSC. The resulting effect of underestimation of peak concentrations and overestimation of low SSC has also been observed with linear regression and ANN models (Schnabel and Maneta, 2005) and may lead to an underestimation of SSC variability. Due to the limited time-span of monitoring and the employed predictor Julian Day, the method cannot be applied. With regard to the inter-annual variability of sediment transport processes and the unusually wet month of September, the obtained results cannot be extrapolated.

The findings of this study reveal the magnitude of the sediment transport processes and their temporal and spatial complexity that require methods of analysis beyond the simple use of traditional rating curves. Further instrumentation is planned to elucidate the role of temporary sediment storage in the river and the contribution of downstream tributaries. The results will be used to validate whether the current process-based modelling approach in the river is appropriate. Alternatively, the use of a more empirical approach using the shape of the sediment duration curves as a function of the catchment size is to be considered.

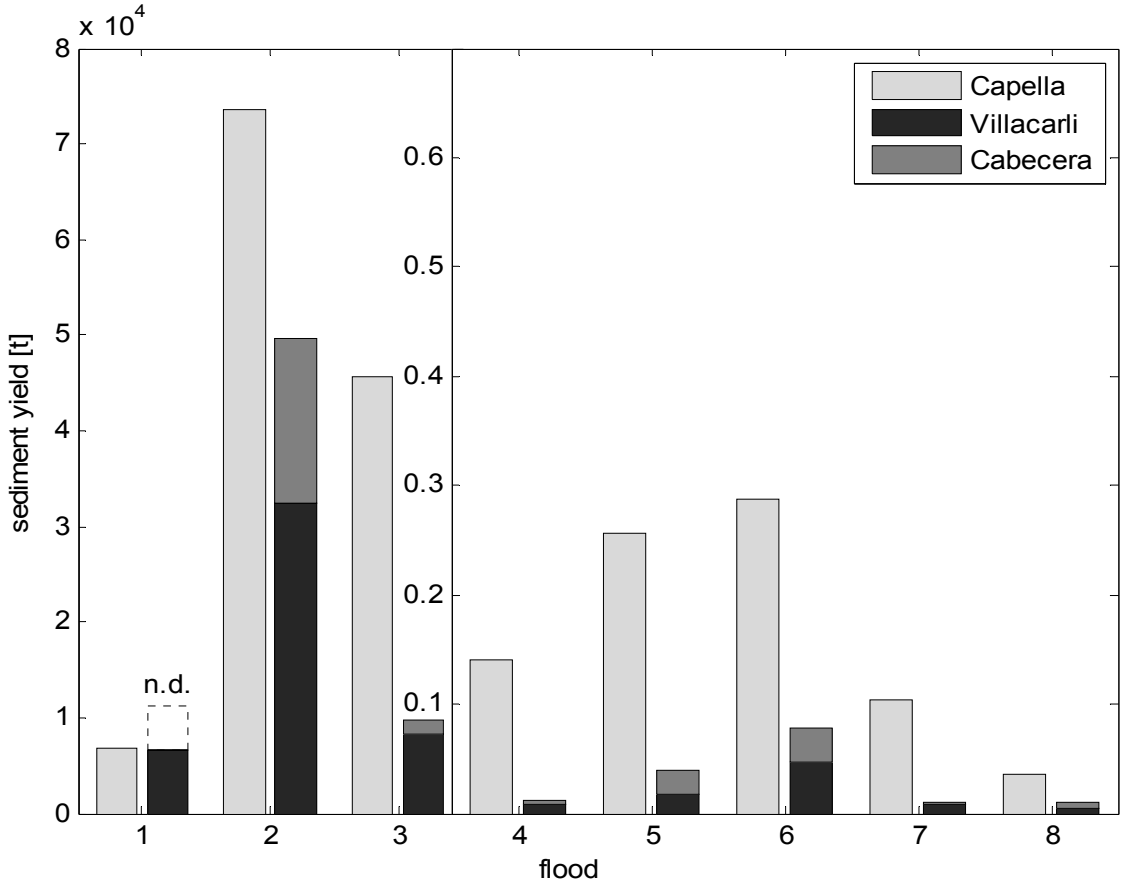

Fig. 6: Combined sediment yield of Villacarli and Cabecera compared to sediment yield at Capella. Note the different scale for flood 1-3; "n.d." denotes "no data".

6. Acknowledgements

This research was carried out within the SESAM-project (Sediment Export from Semi-Arid catchments: Measurement and Modelling) funded by the German Science Foundation (Deutsche Forschungsgemeinschaft, DFG). The second author has a research grant funded by the Catalan Government and the European Social Fund. Rainfall data were obtained from the Spanish National Institute of Meteorology and the Ebro Water Authorities (SAIH). Hydrological data were supplied by the Ebro Water Authorities (SAIH). The Ebro Water Authorities also provided logistic support for using the Capella gauging station. Thanks are due to the students of the University of Potsdam assisting in the field and in the laboratory.

Chapter IV:

Automated catena-based discretization of landscapes for the derivation of hydrological modelling units

Abstract

In hydrological and soil erosion modelling at large spatial scales, semi-distributed approaches may use representative hillslope profiles to reproduce landscape variability. Until now, the process of delineating landscape units as homogeneous parts of the landscape with regard to their terrain, vegetation and soil properties required expert knowledge and familiarity with the study area. In addition, the delineation procedure was often highly time-consuming and included a high degree of subjectivity. This paper presents a novel, semi-automated approach for the delineation of landscape units, the derivation of representative toposequences and their partitioning into terrain components. It incorporates an algorithm to retrieve representative catenas and their attributes for elementary hillslope areas based on elevation and other key spatial data frequently required as environmental model input, e.g. vegetation and soil data. An example application for the Ésera catchment in Spain illustrates that with the presented approach upscaling of hillslope properties becomes feasible for environmental modelling at large scales while ensuring reproducible results.

Keywords: Automated discretisation, catena, landscape unit, semi-distributed modelling, terrain classification

Published as
Francke, T., Güntner, A., Mamede, G., Müller., E., Bronstert, A., 2008. Automated catena-based discretization of landscapes for the derivation of hydrological modelling units. *International Journal of Geographical Information Science* 22: 111-132.

1. Introduction

In hydrological and erosion modelling, spatial discretisation of the landscape into modelling units is usually accomplished using a fully-distributed, semi-distributed or lumped scheme. While the fully distributed approach is relatively straightforward by often using raster-based input data as derived from, e.g., remote-sensing, the data volume and computational demand increase strongly with extent of the domain and finer grid resolution. This is a limiting factor for practical applications (e.g. Bathurst, 2002, Garbrecht and Martz, 2000). Moreover, raster cells of fixed resolution and non-adjustable shape impose an artificial discretisation of fluxes (e.g. overland flow) in the process representation.

Models that are not based on a raster representation require pre-processing steps in Geomorphometric Regionalisation (Schmidt and Dikau, 1999) to describe the spatial domain in the model. At small scales, 'hillslope-based' models like WEPP (Flanagan and Nearing, 1995) or KINEROS (Woolhiser *et al.*, 1990) delineate the stream network and parameterise the surrounding runoff contributing areas (hillslopes) with a detailed and georeferenced representation of their longitudinal profiles. Models designed for larger river basins like WASA (Güntner and Bronstert, 2004), SWAT (Neitsch *et al.*, 2002) and SWIM (Krysanova *et al.*, 2000) apply semi-distributed schemes. Conceptually, hillslopes undergo an object aggregation into functional units of a higher order (e.g. in Hydrological Response Units in SWIM, landscape units in WASA), which are represented by characteristic parameters. Georeference of the elementary object is only partially preserved by assigning areal fractions to higher-order objects (e.g. sub-basins) with known location.

Although GIS can greatly facilitate the retrieval of hillslope information, deriving the exact location of hillslope profiles is often performed manually (e.g. Maurer, 1997) and introduces a certain degree of subjectivity (Cochrane and Flanagan, 2003). Moreover, the process is labour-intensive or even unfeasible for larger catchments, because available GIS-tools allow further object-aggregation in crude ways only (Schmidt and Dikau, 1999). Thus, for use in large-scale models like SWAT and SWIM, hydrological response units are usually derived by mere intersection of GIS-map layers such as land-use, management and soil data. For each entity a mean value for slope is computed. This method naturally cannot preserve the intra-slope distribution of properties nor topological information.

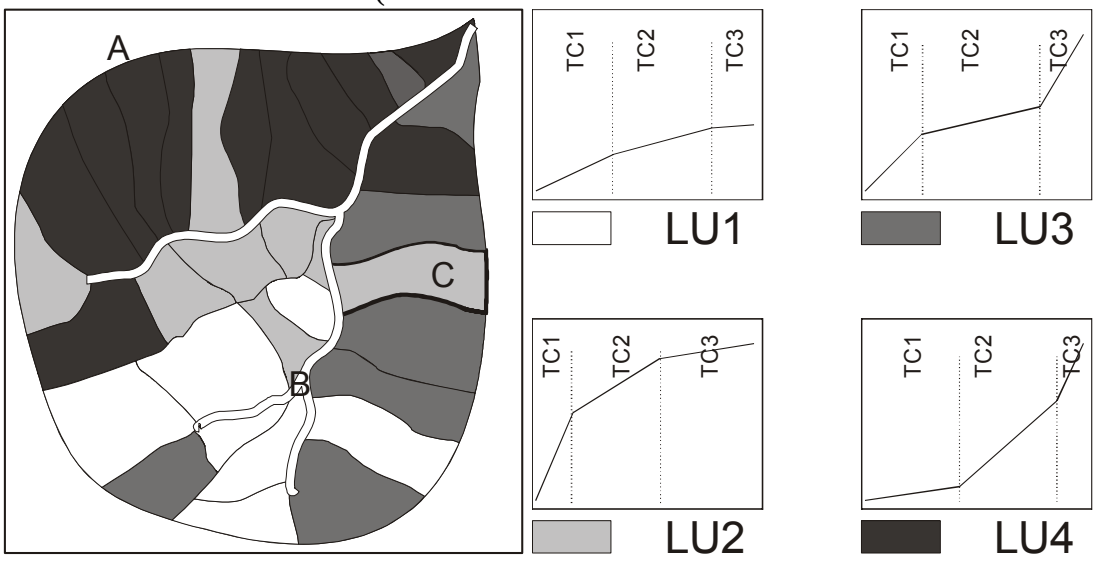

Fig. 1: Explanation of terminology: landscape units (LUs) are homogenous parts of the catchment, represented by toposequences that consist of terrain components (TCs).
[A: catchment boundary; B: river; C: example of an EHA].

Garbrecht and Martz (2000) presented object analysis methods ('Data Reduction methods') for deriving representative values for the length and slope of subcatchments. However, depending on the definition of these parameters, significant differences may result from the different Data Reduction methods. For deriving basic morphometric hillslope parameters, Cochrane and Flanagan (2003) used a sophisticated weighted mean technique to compute the average slope values and the average length from all flowpaths for a given hillslope area. By this way, more details of the hillslope geometry are preserved and a complete profile instead of a single value for slope is produced. The results can be used in models that represent hillslopes as flowstrips of constant width (e.g. WEPP, KINEROS). Information on variable hillslope width as supported in models such as CATFLOW (Maurer, 1997) is not generated, nor can additional attributes such as soil and vegetation be considered.

For semi-distributed models like WASA or SWAT, the derived hillslope properties must be upscaled by performing a further object aggregation. Hillslopes are grouped into classes that comprise profiles with similar distribution of topography, soil and vegetation properties along the hillslope. The resulting objects may be represented by a considerably reduced set of parameters, but the upscaling produces biased results when done manually, especially if multiple attributes are to be considered in the classification process.

Güntner and Bronstert (2004) used the SOTER concept (FAO 1993), transformed by Gaiser *et al.* (2003), to parameterise the sub-areas of river basins with similar hillslope characteristics. The SOTER concept was introduced to provide a consistent method for the worldwide delineation of the so-called SOil-TERrain-units, focussing on the properties mentioned above (topography, soils, etc.). However, this concept was not specifically designed with application to hydrological and erosion modelling in mind. Its implementation depends to a large degree on expert knowledge and thorough familiarity with the area of interest. Moreover, representing large spatially contiguous areas with a single hillslope profile is necessarily a rather strong simplification of reality, especially for relatively heterogeneous landscapes with different hillslopes types in close proximity.

To address the challenges in the parameterisation of 'hillslope-based' models described above, a novel, semi-automated algorithm for the delineation of landscape units is presented in this paper. Although tailored for use with the WASA model, the algorithm can potentially be applied for other models that require the derivation of representative hillslopes in the catchment. Nevertheless, the WASA terminology is used in this paper as illustrated in Fig. 1: landscape units (LU) are parts of the catchment that can be characterised by a typical toposequence. Toposequences are idealised hillslope profiles representing the upscaled properties of the hillslopes they represent. Toposequences always start at a local divide and end at the channel. They are composed of terrain components (3 TCs in Fig. 1). Each TC has a distinct slope gradient and soil- and vegetation-association. The term catena is used for a hillslope profile of a particular hillslope area with a concrete spatial reference. The meaning of both toposequence and catena is not limited to morphometrical attributes, but is used more generally as a set of attributes (including soil properties, for example) along the length of a hillslope.

The presented algorithm called 'LUMP' (Landscape Unit Mapping Program) was designed to fulfil the following demands:

(1) The delineation of landscape units (LU) is to be automated. The algorithm should reduce subjective decisions on spatial discretisation to a minimum but at the same time allow for including prior knowledge.

(2) For each LU, a representative toposequence must be computed. The toposequences have to be decomposed into terrain components (TCs).

(3) The properties of the resulting LUs and TCs (area, slope,

length, soil and vegetation properties, etc.) must be derived as input data for the hydrological model. (4) Besides a silent 'default' mode, a more sophisticated 'expert' mode is necessary to check and modify intermediate results, if desired. (5) For the purpose of visualisation and easy data import/export, the close interaction with a GIS is mandatory.

This paper describes how these functions are implemented in LUMP (Section 2). The quality of the algorithm and its limitations are discussed for an example application in Section 3.

2. Methods

LUMP assesses various representative properties of elementary hillslope areas, assigns similar areas to the same LU class and, finally, produces a spatially continuous map displaying the extension of the LUs within the area of interest. The partitioning of the representative toposequences of the LUs into TCs and computing the resulting TC parameters conclude the tasks of LUMP. The steps of the entire algorithm are illustrated in Fig. 2, detailed explanations are given below. LUMP consists of a set of interacting scripts for GRASS-GIS (GRASS Development Team, 2005) and Matlab™ (Mathworks, 2002). The scripts and a technical documentation are freely available (SESAM, 2006).

2.1. Delineation of elementary hillslope areas (EHA)

2.1.1. Concept

An elementary hillslope area (EHA) is the basic unit that is used for the calculation of a representative catena. It comprises a contiguous slope area that can be characterised by a representative catena. All EHAs with a similar catena form a LU (see Fig. 1). This means that an EHA must be large enough to cover the range from the channel to the local divide but small enough to contain only one characteristic hillslope type. Thus, its size depends on the spatial scale of the hillslopes to be expected and the resolution of the digital elevation model (DEM) used. Consequently, the minimum size of the EHA also determines the resolution at which the spatial extent of the LUs will be generated.

2.1.2. Data used

The delineation of the EHAs requires a digital map of the stream network, provided directly or computed from a DEM. The DEM is also needed to derive flow accumulation with common GIS-operations that are used in later steps.

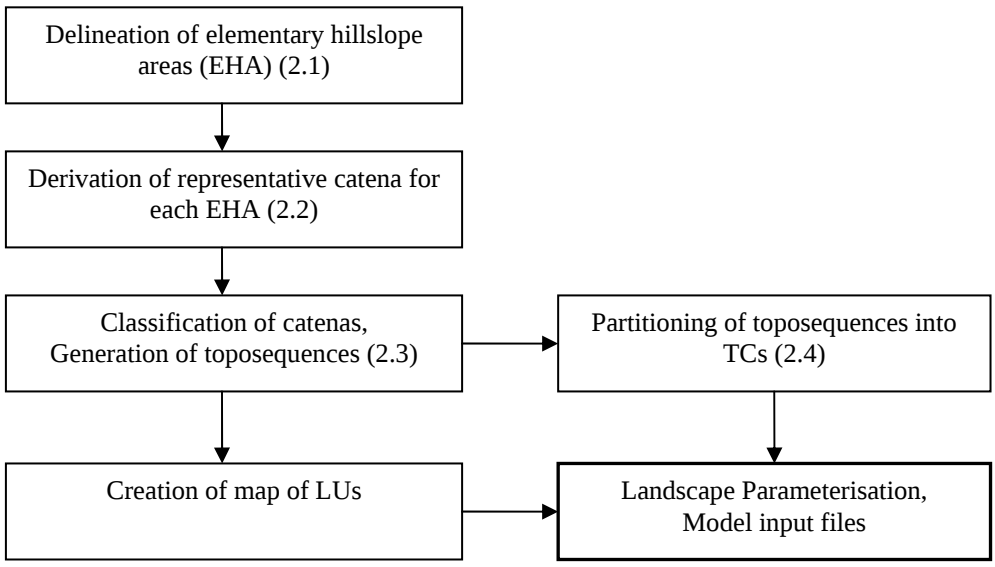

Fig. 2: Steps performed in the LUMP process with reference to the respective section in this paper in brackets.

2.1.3. Algorithm

All flow-related GIS-operations described use a hydrologically corrected, i.e. filled DEM, according to common practice (Garbrecht and Martz, 2000).

EHAs are equivalent to small sub-catchments, which are hillslope areas that drain into the first adjacent downslope channel (Garbrecht and Martz, 2000). Thus, their delineation (Fig. 3) can be done with standard GIS-algorithms (e.g. *r.watershed* with GRASS). By applying an appropriate threshold value for flow accumulation area, the catchment can be subdivided into areas that cover the extent of EHAs (Fig. 4). The resulting delineation can be modified manually by the user, if required.

Fig. 3: Example of a delineation of a catchment into 660 elementary hillslope areas (Ésera basin, North-Eastern Spain, basin area: 1231 km²).

2.1.4. Limitations

Especially with ephemeral rivers, the delineation of the river network – and thus the separation between hillslope and river cells – is not always straightforward. The user has to ensure that the distinction made corresponds to distinct dominating flow regimes (i.e. flow on hillslopes and river flow) and their representation in the model. Each EHA must have a minimum number of cells to be able to be processed in the next step. When using lower resolution DEMs (cell-size > 50 m), this may lead to EHAs that cover larger areas, which increases the probability of lumping different hillslope types within this EHA. Thus, low resolution DEMs will finally result in coarser and more generalised maps of LUs.

2.2. Derivation of representative catena for each EHA

2.2.1. Concept

The calculation of representative catenas is based on the created EHAs. Preliminary studies indicated that the concept of calculating representative catenas based on a 2D-domain (areal data) perform far better than methods based on randomly sampled hillslope profiles (linear data). The results of the latter are very sensitive to DEM-noise and to variations in the algorithm (Francke, 2005, Francke *et al.*, 2006). Instead, by calculating representative catenas from the EHAs, each single cell is included in the computation. The calculations are based on the approach given by Cochrane and Flanagan (2003), extended by additional attributes (e.g. soil, vegetation; further termed 'supplemental data'). Moreover, hillslope width as a function of the distance to the river is also computed.

2.2.2. Data used

This step requires two more grid maps that are generated from the DEM and the river network. The raster map 'relative elevation' contains difference between the elevation of a cell and the elevation of the rivercell it drains to. The map 'flowpath length' is generated from the travel distance of the waterflow from a cell to the river.

Additional spatial data relevant for hydrological and sediment modelling can be included as maps containing either quantitative data (e.g. aspect, LAI, erodibility, groundwater levels, etc) or categorical, i.e. nominal or classified data (soils, land-use, aggregated prior knowledge like hydrological response units or connectivity classes, etc). All data are used at the same resolution as in the DEM.

2.2.3. Algorithm

Cochrane and Flanagan (2003) proposed methods for the computation of a representative catena profile for a given hillslope, which comprise equations for calculating the representative catena length and the representative catena profile. The representative catena length is the length to be used when representing a hillslope as a series of rectangles with constant width (as in the WEPP model). The representative catena profile describes the gradient along the respective hillslope.

Representative catena length

Cochrane and Flanagan (2003) present the 'Chanleng"- and 'Calcleng"-method for the computation of the representative catena length. The Chanleng-method (calculation of catena length based on area and length of adjacent channel) is restricted to hillslopes draining to the sides of channels (i.e. no headwater slopes). It also requires the determination of the length of the adjacent channel reach, is consequently very sensitive to the resolution of the used raster map. Therefore, the Calcleng-method (calculation of catena length based on flowpath lengths) was chosen, which is independent of the calculation of the channel length. The original Calcleng-method is based on the processing of all flowpaths in the hillslope. For the easier-to-perform cell-based calculation, this translates to:

$$L = \frac{\sum_{c=1}^{m} (l_c \times a_c)}{\sum_{c=1}^{m} a_c} \qquad \text{Eq. 1}$$

where

L : representative catena length [m]

m : number of cells which have no upslope contributing area [-]

l_c : flowpath length from current cell to river as contained in map 'flowpath length" [m]

a_c : area of flowpath [m^2]

with

$$a_c \cong l_c \qquad \text{Eq. 2}$$

which allows the calculation of L for each EHA. L determines the distance from the bottom of the hillslope at which the representative profile (computed below) is truncated. Fig. 4 illustrates the results of the calculation of the representative length for an example EHA.

Representative catena profile

For the calculation of the representative morphometric profile, the 'Linear Average Representative Slope Profile" method is used. According to Cochrane and Flanagan (2003), this method produces results which are not significantly different from more elaborate methods such as the 'Exponentially Transformed Average Representative Slope" and 'Weighted Average Representative Slope Profile".

When generalising this concept, a representative value not only for slope but for any other attribute can be computed for each point along the representative catena. Again, the original calculation is based on the flowpaths within the hillslope. It implies that each single cell within the hillslope is considered as many times as it is a member of a flowpath. This is equal to weighting a cell's value by the flowpath density at this cell:

$$A_i = \frac{\sum_{c=1}^{n} a_c * fd_c}{\sum_{c=1}^{n} fd_c} \qquad \text{Eq. 3}$$

where

A_i : value of attribute of mean catena at the distance i from the channel

n : number of cells in hillslope with distance i from the channel [-]

a : value of attribute at given cell

fd_c : flowpath density at given cell [-]

Flowpath density at each cell c is approximated as:

$$fd_c \cong \sqrt{fa_c} \qquad \text{Eq. 4}$$

where fa is the flow accumulation (upslope contributing area) derived before.

The above calculation of the longitudinal profile uses relative elevation rather than slope as used by Cochrane and Flanagan (2003), because the former is independent of the choice of slope calculation methods and thus more robust than the derivative slope (Evans, 1990).

For quantitative attributes, Eq. 3 can be applied directly. For each categorical attribute with *r* classes, Eq. 3 is processed *r* times for each class separately. Thus, a mean probability or fraction for each class is computed for every distance *i* from the channel (see section 'Classification of catenas" for details).
Fig. 4 depicts the results of the calculation of the mean catena profile for an EHA.

Additionally derived hillslope properties

For each EHA, the cumulative density of the number of cells $dens_{cum}$ is calculated as:

$$dens_{cum}(i) = k = |\{c_1, c_2, ...c_k\}| \qquad \text{Eq. 5}$$

where c_{index} are all cells with

$$flowpath\_length(c_{index}) \leq i \qquad \text{Eq. 6}$$

$dens_{cum}$ is a measure of the distribution of hillslope area as a function of its distance from the river. The gradient of this function describes hillslope width. Thus, the areal convergence of EHAs, i.e. the change in width along the length, can be captured (see Fig. 4). This attribute can be used in the classification process and for hillslope parameterisation if required by the model.

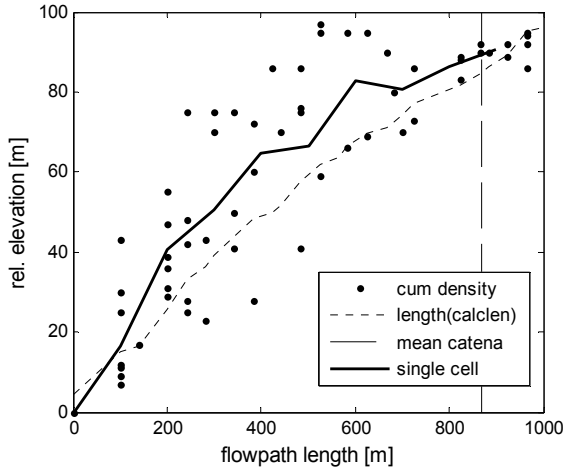

Fig. 4: Example of a representative catena computed from an EHA. Black dots mark individual cells within the EHA. The coarsely dashed vertical line denotes the representative length, which determines the top end of the mean catena profile (bold line).

For each EHA, the representative catena and its attributes is finally resampled to the resolution of the DEM and passed to the classification process.

2.2.4. Limitations

The concept of describing a three-dimensional landscape by using two-dimensional catenas is necessarily a simplification. Although the calculation of hillslope width along the length of the catena preserves some characteristics of the three-dimensional reality, this will hardly reflect the true process of flow concentration downhill, especially because the calculated hillslope width generally increases downslope. This 'convergence paradox" (Bogaart and Troch, 2006) can explicitly only be dealt with if the resolution of the DEM allows the identification of individual flow concentrating features at the hillslope. Alternatively, flow concentration may be treated implicitly within the model (e.g. Güntner and Bronstert, 2004).
The number of cells within an EHA decreases with its size. Therefore, the calculation of the representative catena becomes more sensitive to the value of a single (possible erroneous) cell. On the other hand, very large EHAs may average over distinct hillslope types as described in section 'Delineation of EHAs", which will lead to averaged and probably not very representative catenas.

2.3. Classification of catenas, generation of toposequences

2.3.1. Concept

The previous step produced a representative catena for each EHA. The length and relative elevation gain (difference in elevation between top and foot) of these catenas varies, as does the number of their respective catena points from discrete sampling, depending on the output resolution of the previous step. Beside the morphometrical data, a set of various supplemental attributes (quantitative and/or categorical) can optionally be associated to each point of a catena (as with 'LAI' and 'soils' in Tab. 1).

Tab. 1: Example properties of three (hypothetical) catenas, as returned by the derivation of representative catenas.

Catena-ID	point-ID	Elevation	LAI	Soils – areal fractions				
				Soil A	Soil B	Soil C	Soil D	Soil E
1	1	2025	9.1	0	0	0	0.5	0.5
1	2	2026	6.2	0.4	0	0	0.2	0.4
1	3	2108	3.0	0.4	0	0	0.2	0.4
1	4	2145	2.0	0	0.2	0	0.2	0.6
1	5	2211	3.0	0	0	0	0.6	0.4
2	1	2163	4.6	0.5	0	0.25	0	0.25
2	2	2229	2.5	0.25	0	0.5	0	0.25
2	3	2281	6.5	0.6	0	0.2	0	0.2
2	4	2352	2.7	0.2	0	0	0.6	0.2
2	5	2394	4.5	0.2	0	0	0.2	0.6
2	6	2470	3.3	0.4	0	0	0.4	0.2
2	7	2556	1.5	0.2	0	0	0.6	0.2
2	8	2637	1.5	0.2	0	0	0.2	0.6
3	1	1528	10.2	0	0	0	0.2	0.8
3	2	1592	6.5	0	0	0	0.4	0.6
3	3	1816	5.5	0	0	0.2	0.6	0.2
...								

LUMP classifies all catenas into a given number of classes using cluster analysis. The attributes used in the clustering process are:

- horizontal and vertical length (elevation gain relative to foot of catena, expressed as single values for each catena)
- shape of hillslope profile, and
- sets of supplemental attributes, stored for each point along the catena, that further characterise hillslope properties.

The classification is not limited to a single value for each catena but regards attribute characteristics along the hillslope. LUMP enables the classification considering multiple attributes with different physical units or categorical data: The successive classification runs perform the classification for each single attribute separately, with the final class assignment resulting from the intersection of the single classification steps.

2.3.2. Algorithm

In cluster analysis, 'similarity" of two objects is measured with the help of their distance in a multi-dimensional vector-space. Therefore, as a first step all catenas are resampled to a unit-resolution by converting all catenas to the same number of catena-points using linear interpolation which allows their representation as vectors with the same number of elements. The median of the number of sampling points of the catenas is used for determining the number of points *u_res* in the unit-resolution.

For categorical (i.e. classified) supplemental data, the class-ID merely reflects the membership of a certain class but is numerically meaningless as a quantitative measure. Therefore, any categorical attribute with *n* classes is internally converted to a vector $\boldsymbol{v}$ of the length *n*. The relatedness to class m is expressed as a fraction stored at the *m*'th component of $\boldsymbol{v}$. This concept allows for incorporating the occurrence of multiple classes at one point (e.g. at catena point 1 soil classes D and E were encountered, see Fig. 5). It also enables the resampling described above by interpolation fractions and allows including the supplemental data in the clustering process. Tab. 1 and Tab. 2 illustrate this concept.

Tab. 2: Internal representation of catena 1 (see Tab. 1) after resampling.

Catena point, resampled	Horizontal length	Shape	LAI	Fraction				
				Soil A	Soil B	Soil C	Soil D	Soil E
1	482.80	0.00	9.10	0.00	0.00	0.00	0.50	0.50
2		0.00	7.10	0.28	0.00	0.00	0.32	0.40
3		0.12	5.34	0.40	0.00	0.00	0.20	0.40
4		0.34	3.78	0.40	0.00	0.00	0.20	0.40
5		0.38	3.55	0.35	0.00	0.00	0.15	0.50
6		0.45	3.38	0.35	0.00	0.00	0.15	0.50
7		0.49	2.76	0.30	0.05	0.00	0.20	0.45
8	Elev. gain	0.59	2.27	0.11	0.15	0.00	0.20	0.55
9		0.76	2.31	0.00	0.14	0.00	0.32	0.54
10	186.00	1.00	3	0.00	0.00	0.00	0.60	0.40

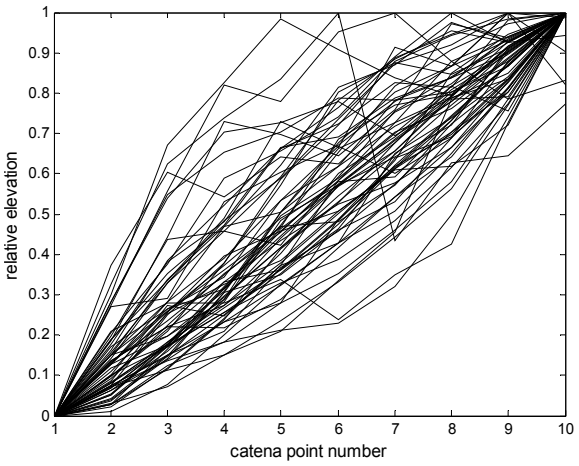

Fig. 5: 60 catenas, resampled to a unit resolution of 10 catena points and normalized (example from Ésera catchment).

The elevation profiles of the resampled catenas is then normalised to a vertical extension of unity. This conversion results in an attribute vector which holds the normalised 'shape" of the hillslope profile and will further be referred to as the shape-attribute. The true horizontal length and the elevation gain are stored as separate attributes of the catena. Tab. 2 gives an example of the internal representation of all attributes of the resampled catena 1.

For each attribute included, LUMP classifies the set of catenas into the specified number of classes. Increasing the number of classes for an attribute considered predominant allows the user to force the algorithm to produce a more detailed classification with regard to that attribute. On the other hand, attributes which are, e.g., set to produce one class only, will not contribute to a further partitioning of the dataset (e.g. attribute 'LAI' in the example given in Tab. 3 is not used to further partition the dataset). The catena attributes 'Horizontal length' and 'Elevation gain' are treated together as a composite attribute (further referred to as xy-extent) as a measure of catena extent and mean slope. An adjustable weighting factor fac_y multiplying 'Elevation gain' allows emphasizing this element of the two-element vector c_{xy}. All other attributes are represented in c_a containing the attribute values along the entire catena:

$$c_{xy} = \{ L_x ; \quad fac_y \cdot L_y \} \qquad \text{Eq. 7}$$

$$c_a = \{ a(1,1); \quad a(1,2) \quad \ldots \quad a(u\_res, nclasses[na]) \}$$

where *nclasses(a)* is the number of classes of the attribute, which is 1 for all quantitative data.

The final class membership of a catena results from the unique combination of the successive classification assignment according to each attribute (Tab. 3). Thus, all catenas with an identical classification assignment throughout all attributes are finally to the same class.

LUMP uses either an unsupervised k-means clustering algorithm to produce the number of classes specified by the user or a supervised cluster algorithm based on pre-defined end members. Both options use squared Euclidean distances.

Tab. 3: Example of successive classification of 4 catenas with 4 attributes.

	Attribute				
Catena ID	horizontal length, elevation gain (2 classes)	shape (3 classes)	LAI (1 class)	soil (2 classes)	final classification (<= 2x3x1x2 classes)
1	1	1	1	1	1
2	2	2	1	2	2
3	1	3	1	2	3
4	1	1	1	1	1
…					

A dendrogram, the silhouette coefficient and a silhouette plot (Kaufman and Rousseeuw, 1990) can give a visualisation of the quality of the separation and the distinctiveness of the classes. Since each node in the dendrogram represents a split of the respective subgroup, this figure can be a guide in selecting an appropriate number of classes for the given task and attribute. The vertical distance of the nodes usually decrease, indicating that increasing the number of classes yields progressively less improvements in the classification of the dataset.

A representative toposequence for each resulting class is computed by averaging the catena attributes of the members of the respective class:

$$a\_ts(k)_j = mean[a(h_k)_j] \qquad Eq.\ 8$$

where $a\_ts(k)_j$ refers to the jth attribute of the toposequence representing class k. h_k is an index to all catenas belonging to class k. The toposequences are then passed for further processing to the partitioning module (see following section) and stored for inclusion in input files of the model.

The classification results are re-imported into the GIS by re-classifying each EHA according to the membership of its representative catena (Fig. 7).

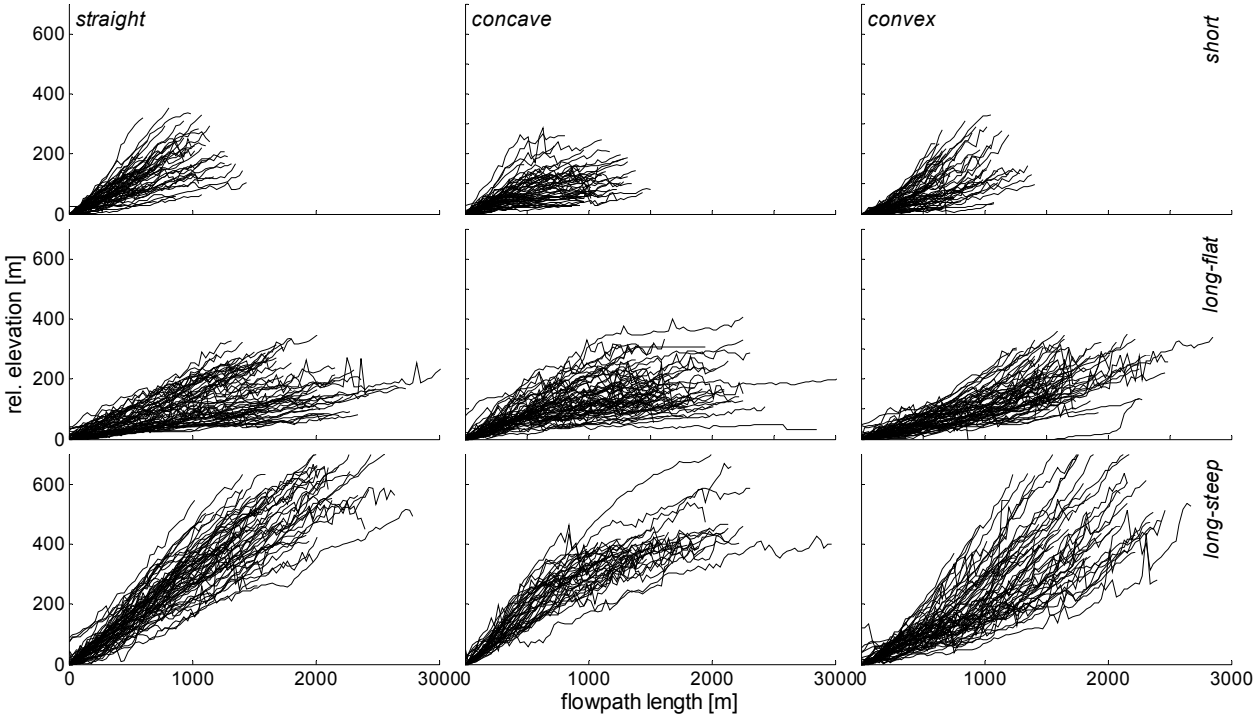

Fig. 6: 518 catenas classified into 9 classes (3 classes in attribute shape, 3 classes in attribute xy-extent.

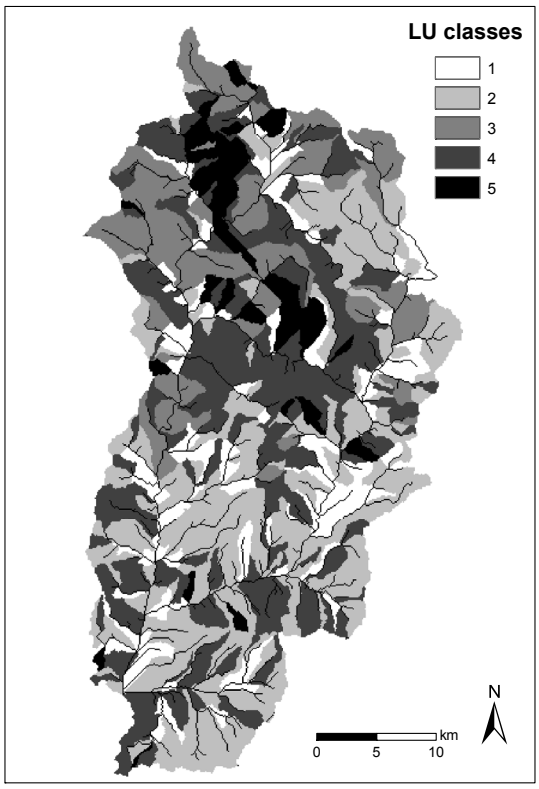

Fig. 7: Example of delineated LUs as a result of a classification.

2.3.3. Limitations

Resampling the catenas implies a loss of information for catenas of which the number of catena points is reduced. On the other hand, catenas with few points are internally resampled to a higher resolution. Thus, their number of catena points is increased, although the actual information is not that detailed.

Currently, the user has to specify the number of classes to be produced for each attribute. A silhouette plot and the dendrogram can help with choosing this number appropriately. An automatic selection of the number of classes will be added to future versions of LUMP.

An advantage of the applied method is the optional inclusion of multiple layers of supplemental information into the classification process. This option, however, also requires a certain amount of expert knowledge to adjust the respective number of classes accordingly. It is the responsibility of the user to choose appropriate numbers to produce LUs that are meaningful with regard to the intended modelling purpose.

2.4. Partitioning of the toposequences of the LUs into terrain components (TCs)

2.4.1. Concept

The classification step produces one representative toposequence for each LU. To describe different segments within the hillslope, the toposequences can further be partitioned into terrain components (TCs). A TC is an idealised representation of a continuous part of the toposequence having uniform slope and distinct characteristics of supplemental attributes. The algorithm sub-divides each toposequence into a user-specified number of TCs by delineating parts according to the definition above (Fig. 8). Besides slope gradients, each available supplemental attribute can be included into the partitioning process. For each attribute a the respective weighting factor facTCa has to be specified. This weighting scheme allows including multiple attribute of different physical units.

2.4.2. Algorithm

Each toposequence is converted into a matrix m (*u_res* x *nrows*) so that each column contains the entire set of attributes for one point of the toposequence. *nrows* is a function of the number of attributes *na'* at each point of the toposequence:

$$nrows = \sum_{a=1}^{na} nclasses_a \qquad Eq.\ 9$$

The user-specified weighting factor fac_a of each attribute *a* is adjusted according to Eq. 10 to ensure consistent weighting independent of the number of classes used in categorical attributes:

$$facTC_a* = facTC_a \frac{1}{ncomp_a \cdot nclasses_a} \qquad Eq.\ 10$$

where $ncomp_a$ denotes the number of components the attribute uses and $nclasses_a$ is the number of classes of the attribute, which is 1 for all quantitative data. Attribute weighting is performed by multiplying each row of m with the resulting weighting factor $facTC_a^*$.

Tab. 1: Internal representation of a toposequence for TC-partitioning, all weighting factors set to 1.

toposequence point	1	2	3	4	5	6	7	8	9	10
Slope	0.00	0.10	0.18	0.13	0.08	0.14	0.20	0.20	0.18	0.13
LAI	9.1	7.1	5.3	3.8	3.6	3.4	2.8	2.3	2.3	3.0
Soil A	0	0.28	0.4	0.4	0.35	0.35	0.3	0.11	0	0
Soil B	0	0	0	0	0	0	0.05	0.15	0.14	0
Soil C	0	0	0	0	0	0	0	0	0	0
Soil D	0.5	0.32	0.2	0.2	0.15	0.15	0.2	0.2	0.32	0.6
Soil E	0.5	0.4	0.4	0.4	0.5	0.5	0.45	0.55	0.54	0.4

LUMP employs an optimisation towards minimum variance for delineating similar parts within a toposequence. This method partitions the toposequence in a way that the overall variance $\boldsymbol{v_{o,p}}$ within the n_{TC} TCs is minimised throughout all possible permutations of partitionings p:

$$v_{o,p} = \sum_{j=1}^{n_{rc}} l_j \cdot \mathrm{var}(TC_j) \qquad \textit{Eq. 11}$$

$$|v_{o,p}| \rightarrow Min$$

The factor l_i is a weighting term that equals the length of the respective TC.

The overall variance $\boldsymbol{v_o}$ of a given partition p is a vector of *nrows* elements. Each element contains a single variance value, computed from weighted sum of variances of one attribute.To compare the $\boldsymbol{v_{o,p}}$ of different partitionings p the vector-norm of $\boldsymbol{v_{o,p}}$ is used.

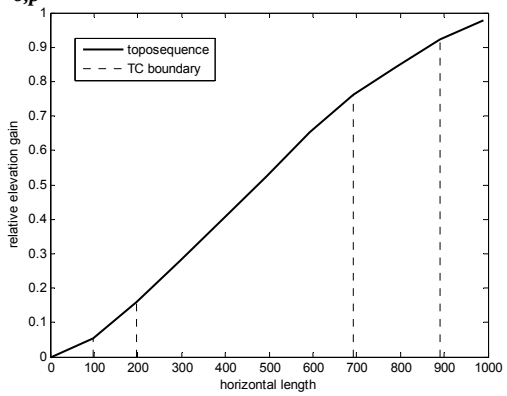

Fig. 8: Example toposequence of a LU, partitioned to 5 TCs based on minimisation of variance.

2.4.3. Limitations

The choice of an adequate number of TCs has to be made by the user, pondering the contradicting demands of an appropriate representation and a reasonable generalisation. Thus, it is a function of the landscape characteristics and the requirements and capabilities of the target model and has to be adjusted accordingly.

For sub-dividing the toposequence into TCs, the slope data are incorporated into the algorithm. The slope at each point of the toposequence is calculated from the horizontal spacing and the elevation gain to the next uphill point. At the most uphill point of the toposequence, however, the previous downhill point must be used, because no uphill point is available.

The TC-concept allows the occurrence of several soil and vegetation classes within a TC. In theory, a hillslope segment with constant slope and soils A and B alternating exactly at each point of the toposequence is conceptually a TC with uniform soil characteristics. This hypothetical example, however, has a rather high variance component for the soil attribute which might spuriously force the described algorithm to split this hillslope segment into several TCs.

3. Example application and discussion

3.1. Study area

An example run of LUMP was performed for the Ésera catchment (Central Spanish Pyrenees), which is located at about 42°20'N and 0°30'E. The catchment, with an area of 1231 km², is part of the Ebro Basin and is characterised by heterogeneous relief, vegetation and soil characteristics. Elevation increases from 430 m in the southern and central parts of the catchment (*Intermediate Depression* and *Internal Ranges*) to up to 3000 m asl in the northern parts (*Axial Pyrenees*, Valero-Garcés *et al.*, 1999, see Fig. 9, left).

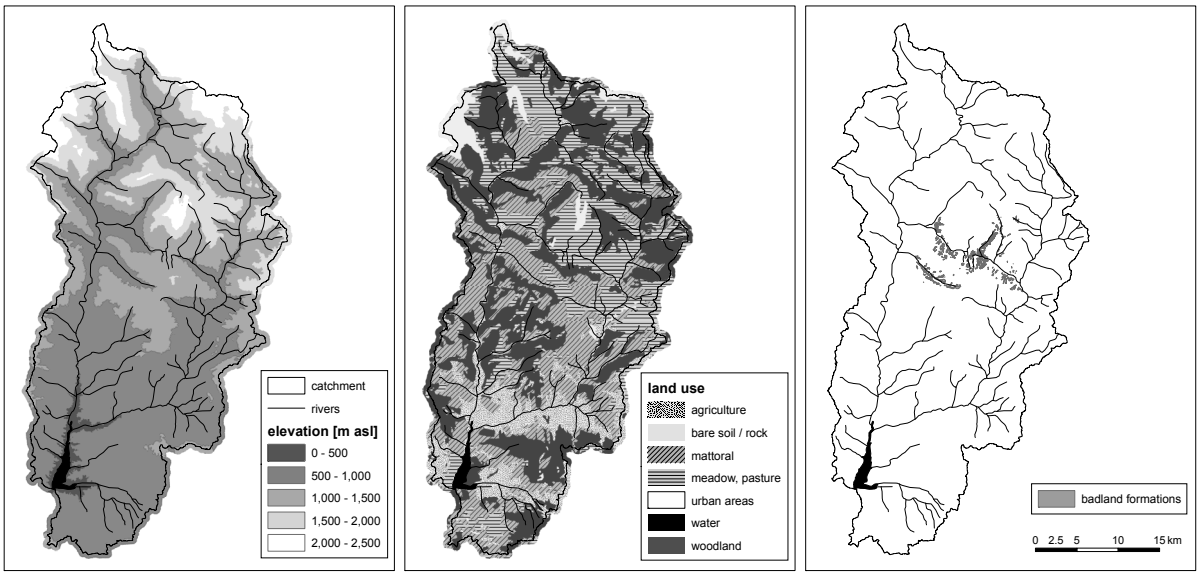

Fig. 9: relief (left), land-use (center) and occurrence of badlands (right) in the Ésera catchment, NE-Spain.

The climate is a typical Mediterranean mountainous type with mean annual precipitation rates of 600 to 1200 mm and an average potential evaporation rate of 550 to 750 mm, both rates showing a strong south-north gradient due to topography. The vegetation includes deciduous oaks, agriculture, pastures and mattoral in the valley bottoms, evergreen oaks, pines and mattoral in the higher areas (see Fig. 9, center). While the northern parts are composed of Paloeozoic rocks, Paloegene and Cretaceous sediments, the lower parts are mainly dominated by Miocene continental sediments. These areas consist of easily erodible materials (marls, sandstones, carbonates), leading to the formation of badlands (Fig. 9, right) and making them the major source of sediment within the catchment (Fargas *et al.*, 1997).

3.2. Application of LUMP, results

Aiming at the parameterisation of a hydrological and sediment transport model, the geospatial data of elevation (30-m-DEM derived from ASTER imagery), the mean LAI (derived from the land-use map, C.H.E, 1998) and the occurrence of badlands (derived from orthophotos) were assumed important proxies for runoff and sediment dynamics and processed with the LUMP algorithm. Based on the delineation of the catchment into 930 EHAs, representative catenas were derived as described in the methods section. LUMP was configured to classify the catenas into three classes regarding the attributes hillslope-shape, xy-extent, LAI and into two classes with regard to badland-occurrence.

Of the 54 (3x3x3x2) possible LU-classes, 42 classes resulted. The final LU-delineation is the intersection of the four maps below (Fig. 10a-d), but for legibility, the map is displayed for each of the attributes with classes of similar properties grouped within the same shade.

The LU-delineation viewed according to the attributes xy-extent, LAI and badland-occurrence (Fig. 10b-d) show clear correlations with the input maps of the respective attribute (Fig. 9). The central to southern parts of the catchment are covered by LUs with flat hillslope profiles, steeper and longer catenas are only found in the northern parts. This distribution matches the actual properties of the catchment. The LAI-aggregated map of the LUs (Fig. 10c) resembles the land-use map with LUs of high LAI mainly located in woodland areas and low-LAI LUs to be found in the valley bottoms where agriculture and pastures prevail.

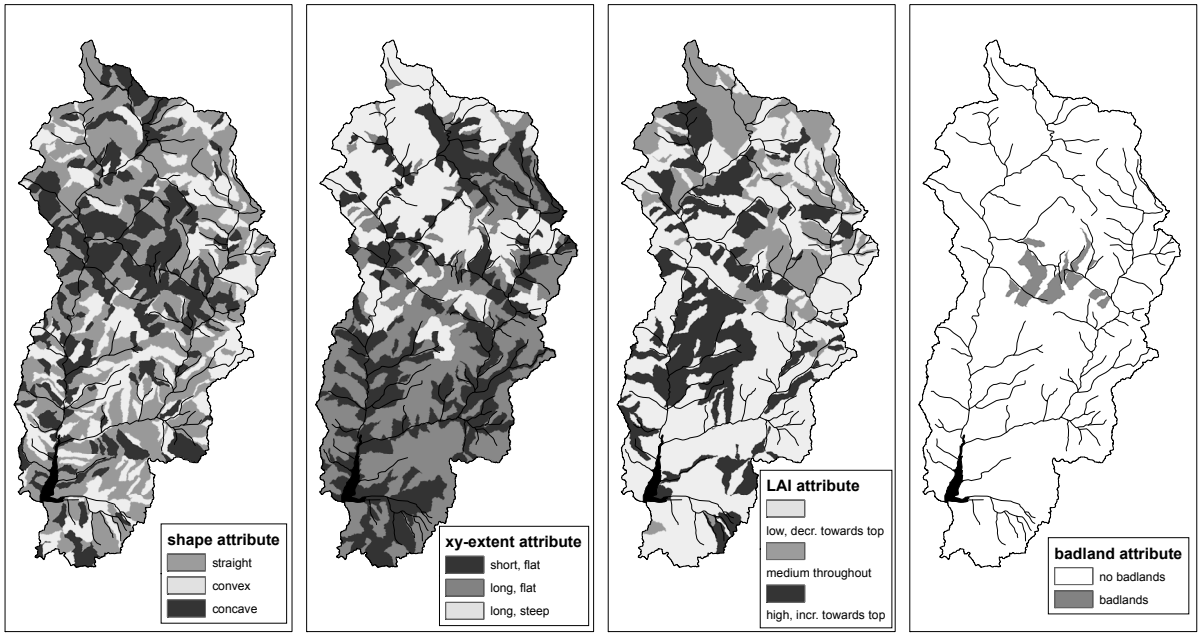

Fig. 10: LUs delineated by LUMP, grouped by similar classes within the attributes shape (a), xy-extension (b), LAI (c) and badland occurrence (d).

The spatial resolution of the LU-map is considerably coarser than the land-use map as an effect of the minimum size of the EHAs, the low number of three classes used for this attribute and the resulting averaging effects. This also explains the characteristics of the LU-map with regard to badland occurrence (Fig. 10d). The general location of the badland areas and their distribution is reproduced adequately by the LU-map, but the level of detail is reduced during the upscaling process.

The quality of the representation of the shape-attribute is difficult to assess from Fig. 10a. Therefore, the LUs were aggregated by shape and xy-extension class, resulting in nine classes. The respective areas were re-analysed as described in the section 2.2. This procedure allows a visual validation of the distribution of hillslope properties within the delineated LUs, which are supposed to be similar in shape and xy-extent within a class. Furthermore, the consistency of the algorithm can be assessed by comparing the properties of the toposequences (generated by LUMP) and the representative catenas (derived directly from the assigned area of each LU using Eq. 1 and Eq. 3).

In Fig. 11, the 3 classes of the shape-attribute (straight, concave, convex) are arranged column-wise, the xy-extent-attribute (short-flat, long-flat, long-steep) is ordered in rows. Comparing the different scatter-characteristics of all the cells in each of the nine LU-aggregations, it can be concluded that LUMP partitioned the catchment into distinctive classes. There however, remains a large variation in the hillslope morphometry within each LU, especially in the case of the combination concave/long-steep. This fact indicates that the low number of 3-by-3 classes for hillslope-morphometry (chosen for illustrative purposes) results in LU-classes that still comprise a considerable variety of morphometrical hillslope types. In order to represent the wide range of hillslope types in the catchment, more LU-classes are recommended to decrease the variance within the LUs.

Fig. 11 shows that the toposequences of the LUs closely resemble the representative catenas derived from the re-analysis of the respective areas. Slight deviations are only evident at the upper parts of some LUs. Thus, the algorithm proves to be consistent because it delineates LUs and produces respective toposequences that are equivalent to representative catenas that are derived directly from these areas.

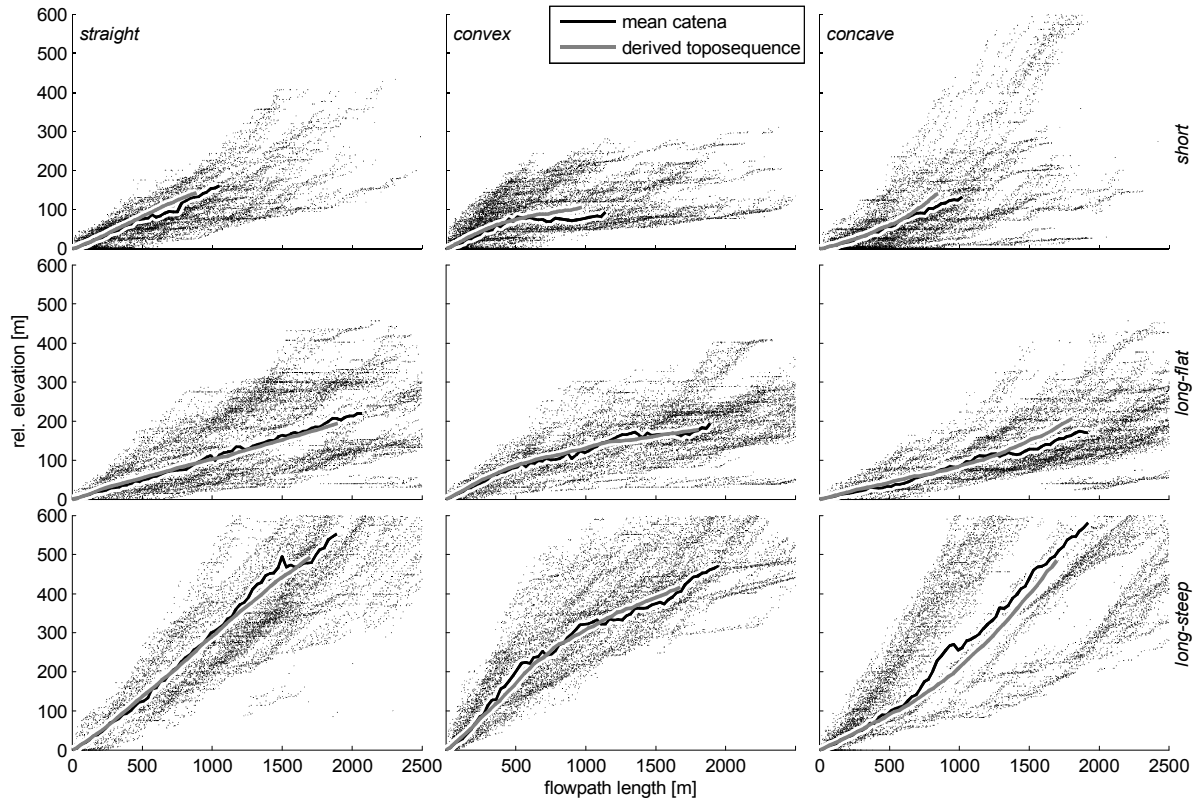

Fig. 11: Mean toposequences of aggregated LUs (LUMP output) and representative catenas derived directly from the LU-areas.

3.3. Discussion

Although the delineation of LUs and the derivation of toposequences produced plausible and consistent results, their appropriateness is ultimately to be judged by the performance of model applications. The performance of the LUMP results as model input will strongly depend on the selected landscape attributes and the number of classes into which each attribute is classified. Test runs with the hydrological model WASA for the Ésera catchment suggest that simulation results in terms of river runoff are sensitive to shifts in the classification focus between attributes and to the resulting modelling units and parameters at the sub-basin scale (in average 75 km² in size), while this was not the case at the basin scale (1231 km²) (Francke *et al.*, 2006).

Little experience yet exists for selecting the appropriate number of classes into which a specific landscape attribute should be classified. For hillslope erosion, some authors tried to quantify the relative importance of multiple process factors (e.g. Curtis *et al.*, 2005; Schoorl *et al.*, 2004). Scherrer and Naef (2003) classified various soil and terrain attributes according to their role for runoff generation processes. These findings may give an indication as to which attributes are to be included in the classification in great detail, i.e., in many classes. The transferability to other catchments, however, remains uncertain.

Moreover, the optimal set of class numbers will depend on the model used and its particular process representation. A model that does not consider a certain attribute in its process parameterisation is unlikely to improve performance when this attribute is resolved in great detail in the delineation process. Furthermore, the target variable (e.g. runoff coefficient, sediment yield) for which the simulation is to be optimised will likely affect the choice of attributes to be included and their number of classes in the classification. The investigation of the relations between model performance and the number of classes for different attributes for a given model and target variable

is a future task and is beyond the scope of this study.
An unresolved problem remains the definition of the hillslope extent and the length of its representative catena. Saying that the hillslope should reach from the watershed divide down to the river, the determination of its length encompasses a scale problem, i.e., it depends on the resolution of the available river network information. This, in turn, depends either on the scale of an existing river network map or on the user-defined threshold to indicate at which flow accumulation value the river network starts when generating by means of GIS analysis. The lack of an unbiased definition for the initiation point of a river is an inherent problem when deriving parameters like hillslope length (Schmidt and Dikau, 1999). Conceptually, the threshold should aim at separating the 'hillslope" and 'river" domain according to the prevailing transport processes and how they are most suitably represented by the respective model equations.

4. Conclusions

LUMP is a tool for the semi-automated delineation of landscape units and their partitioning into terrain components. It facilitates the preparation of spatial data for the application of semi-distributed, hillslope-based models and ensures reproducible results. LUMP allows for including expert knowledge by incorporating various landscape attributes and by 'weighing' them by a large number of classes according to the perceptual understanding of their impact on catchment processes. Thus, it overcomes several shortcomings of the discretisation strategies currently used in semi-distributed modelling: the hillslope-based parameterisation becomes feasible for larger spatial domains due to the automated algorithm while ensuring reproducible results by reducing subjective decisions.
The LUMP algorithm derives representative hillslope parameters and upscales the hillslope properties with the help of landscape units. In this way, the delineation of modelling units and their parameterisation can be performed automatically for meso- to large scale catchments where a manual procedure is unfeasible and upscaling is mandatory. In contrast with methods based on mere intersection of multiple layers, LUMP preserves information on the distribution of landscape parameters in relation to the river network and their topographic position and thus allows for addressing connectivity issues in model applications.
In the presented application example, LUMP showed a satisfying capability of delineating LUs. Depending on the chosen attributes and respective number of classes, different spatial discretisation schemes of the same study area may result. The optimum number of classes and the selection of attributes depend on the choice of the model used and the target variable for which the calculation is to be optimised. LUMP provides new opportunities for further research on this subject because it allows the efficient and reproducible investigation of the effects of spatial discretisation in semi-distributed modelling. The implications of applying the LUMP-derived results in meso-scale hydrological and sediment modelling are currently being investigated.

5. Acknowledgement

This research was carried out within the SESAM-project (Sediment Export from large semi-arid catchments: Measurement and Modelling) funded by the Deutsche Forschungsgemeinschaft (DFG). The valuable comments of the two anonymous reviewers are gratefully acknowledged.

Chapter V:

Modelling water availability, sediment export and reservoir sedimentation in drylands with the WASA-SED Model

Abstract

The process-based, spatially semi-distributed modelling framework WASA-SED for water and sediment transport in large dryland catchments is presented. The WASA-SED model simulates the runoff and erosion processes at the hillslope scale, the transport processes of suspended and bedload fluxes in the river reaches and the retention and remobilisation processes of sediments in reservoirs. The modelling tool enables the evaluation of management options both for sustainable land-use change scenarios to reduce erosion in the headwater catchments as well as adequate reservoir management options to lessen sedimentation in large reservoirs and reservoir networks. The model concept, its spatial discretisation and the numerical components of the hillslope, river and reservoir processes are summarised and current model applications are reviewed to demonstrate the capabilities, strengths and limits of the model framework.

Keywords: sediment transport, erosion, reservoir sedimentation, modelling, drylands

Published as
Mueller, E. N., Güntner, A., Francke, T., Mamede, G., 2008. Modelling water availability, sediment export and reservoir sedimentation in drylands with the WASA-SED Model. *Geosci. Model Dev. Discuss.* 1 (1) 285-314

[author's note: The manuscript underwent modifications during the review process after this document was compiled. Please check the journal for the final version.]

1. Introduction

In drylands, water availability often relies on the retention of river runoff in artificial lakes and reservoirs. Such regions are exposed to the hazard that the available freshwater resources fail to meet the water demand in the domestic, agricultural and industrial sectors. Erosion in the headwater catchments and deposition of the eroded sediments in reservoirs frequently threatens the reliability of reservoirs as a source of water supply. Erosion and sedimentation issues have to be taken into account when analysing and implementing long-term, sustainable strategies of land-use planning (e.g. management of agricultural land) and water management (e.g. reservoir construction and management).

The typical scale relevant for the implementation of regional land and water management is often that of large basins with a size of several hundreds or thousands of square kilometres. To take into account the effects of changing climatic or physiographic boundary conditions on water availability and reservoir sedimentation, quantitative and deterministic descriptions are required for the water and sediment dynamics of large river basins. For this purpose, the structure, functioning and application of the WASA-SED model has been developed and is presented here. The WASA-SED model is an integrated, spatially semi-distributed, process-based modelling framework for water and sediment transport adapted to the specific environmental characteristics of dryland catchments. It enables the modelling of erosion processes at the hillslope scale, the transport processes of suspended and bedload fluxes at the river scale and the retention and re-mobilisation processes and management options of sediments at the reservoir scale.

The WASA-SED model falls into the category of meso-scale, process-based erosion models that simulate runoff generation, soil detachment and sediment transport in a spatially semi-distributed manner. The complexity of such models increases with the detail of process representation, ranging from models representing a single process of sheet erosion (e.g., EROSION-2D (Schmidt, 1991) and EROSION-3D (von Werner, 1995)), to models which differentiate between processes in rills and inter-rill areas (e.g., the MEDALUS model (Kirkby, 1997), LISEM (De Roo *et al.*, 1996; Jetten, 2002), EUROSEM (Morgan *et al.*, 1998), up to specialised gully erosion models (EGEM (USDA-SCS, 1992), STABGUL, DIMGUL (Sidorchuk, 1998, Sidorchuk and Sidorchuk 1998)). Due to their extensive and detailed data and parameter requirements, these physically-based models are not applicable to large river basins for which usually only coarse input data sets exist. Only few models are described in the literature that deal with the quantification of erosion and sediment yield relevant for water availability and reservoir management in large river basins. The erosion component in these models usually is based on modifications of the USLE or MUSLE approach (e.g., in SWRRB (Arnold *et al.*, 1989), SWIM (Krysanova *et al.*, 2000), LASCAM (Sivapalan *et al.*, 1996) and SWAT (Neitsch *et al.*, 2002). The advantage of the new WASA-SED model in comparison to existing models is its spatial representation of hillslope processes that are described for individual terrain components along the catena and its integrated treatment of large reservoirs and reservoir networks, including reservoir management options.

The paper consists of three main parts: numerical descriptions of the erosion and sediment transport processes in the hillslope, river and reservoir modules of WASA-SED; review of current model applications at the hillslope, river and reservoir scale; and a critical discussion on its capability to develop and improve water and land management in dryland regions as well as its limitations of its availability.

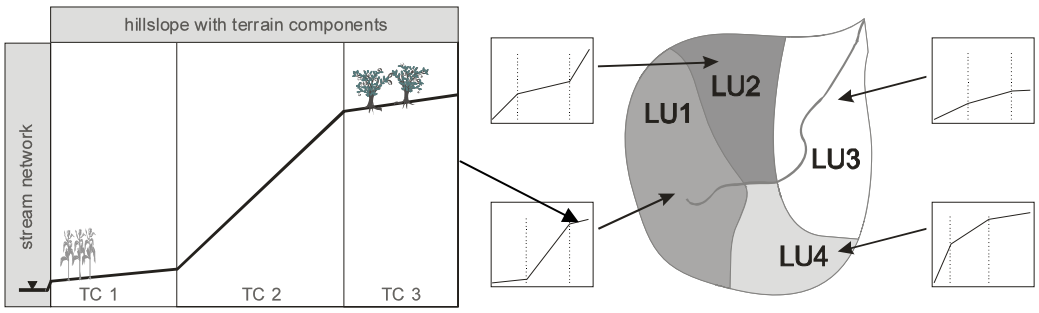

(a) (b)

Fig. 1: Spatial discretisation of the WASA-SED model (adapted after Güntner 2002): a) representative catena defined by three terrain components (TC), b) sub-basin defined by five landscape units (LU) with corresponding catenas.

2. Numerical description of the WASA-SED Model

2.1. Spatial representation of landscape characteristics

The WASA-SED model uses a hierarchical top-down disaggregation scheme developed by Güntner (2002) and Güntner and Bronstert (2004) that takes into account the lateral surface and sub-surface flow processes at the hillslope scale in a semi-distributed manner (Fig. 1). Each sub-basin of the model domain is divided into landscape units that have similar characteristics regarding lateral processes and resemblance in major landform, lithology, catena profile, soil and vegetation associations. Each landscape unit is represented by a characteristic catena that is described with multiple terrain components (lowlands, slope sections and highlands) where each terrain component is defined by slope gradients, soil and vegetation associations (soil-vegetation components) and its length. Within and between each terrain component, the lateral redistribution of surface runoff and the vertical fluxes for typical soil profiles consisting of several soil horizons is taken into account.

For a semi-automated discretisation of the model domain into landscape units and terrain components, the software tool LUMP (Landscape Unit Mapping Program) is available (Chapter IV). LUMP incorporates an algorithm that delineates areas with similar hillslope characteristics by retrieving homogeneous catenas with regard to e.g. hillslope shape, flow length and slope (provided by a digital elevation model), and additional properties such as for soil and land-use and optionally for specific model parameters such as leaf area index, albedo or the occurrence of special geomorphological features (bare rocks, badland formations, etc.). In contrast to methods based on mere intersection of multiple input layers, LUMP preserves information on the distribution of input properties in relation to the river network and their topographic position and, at the same time, allows an upscaling of small-scale hillslope properties into regional landscape units. The LUMP tool is linked with the WASA-SED parameterisation procedure through a databank management tool, which allows to process and store digital soil, vegetation and topographical data in a coherent way and facilitates the generation of the required input files for the model.

2.2. Sediment generation and transport processes in the hillslope module

The hydrological model part of WASA-SED at the hillslope scale is fully described by Güntner (2002) and Güntner and Bronstert (2004) and are not repeated here. For daily or hourly time steps, the model calculates the interception losses, evaporation and transpiration using the modified Penman-Monteith approach (Shuttleworth and Wallace, 1985), infiltration with the Green-Ampt approach (Green and Ampt, 1911),

surface and subsurface runoff and ground water recharge with a multi-layer storage approach for each soil-vegetation component in each terrain component.

The sediment module in WASA-SED provides four erosion equations of sediment generation by using derivatives of the USLE equation (Wischmeier and Smith, 1978), which can be generalised as (Williams, 1995):

$$E = \chi\, K\, LS\, C\, P\, ROKF\, A \qquad \text{Eq. 12}$$

where E is erosion (t), K the soil erodibility factor (t.ha.h.ha^{-1}.MJ^{-1}.mm^{-1}), LS the length-slope factor (-), C the vegetation and crop management factor (-), P the erosion control practice factor (-), $ROKF$ the coarse fragment factor (-) as used in the USLE and A the area of the scope (ha). χ is the energy term that differs between the USLE-derivatives. It computes as (Williams, 1995):

USLE

$$\chi = EI \qquad \text{Eq. 13}$$

Onstad-Foster

$$\chi = 0.646\, EI + 0.45\, (Q_{surf}\, q_p)^{0.33} \qquad \text{Eq. 14}$$

MUSLE

$$\chi = 1.586\, (Q_{surf}\, q_p)^{0.56}\, A^{0.12} \qquad \text{Eq. 15}$$

MUST

$$\chi = 2.5\, (Q_{surf}\, q_p)^{0.5} \qquad \text{Eq. 16}$$

where EI is the rainfall energy factor (MJ.mm.ha^{-1}.h^{-1}), Q_{surf} is the surface runoff volume (mm) and q_{peak} is the peak runoff rate (mm/h). In contrast to the original USLE, the approaches (3)-(5) incorporate the surface runoff Q_{surf} (calculated by the hydrological routines) in the computation of the energy component. This improves the sediment modelling performance by eliminating the need for a sediment delivery ratio (SDR) and implicitly accounts for antecedent soil moisture (Neitsch *et al.*, 2002). E is distributed among the user-specified number of particle size classes, according to the mean composition of the eroded horizons in the area.

Any of the mentioned approaches can be applied on the sub-basin or terrain component scale. In the former case, the USLE factors result from area-weighted means throughout the sub-basin and cumulatively for the LS-factor as proposed by Foster and Wischmeier (1974 in Haan *et al.*, 1994). If applied at the terrain component scale, the specific factors of each terrain component are used and sediment routing between terrain components is performed: any sediment mass SED_{in} (t) coming from upslope areas is added to the generated sediment mass E to obtain the sediment yield SY (t) of a terrain component. SY is limited by the transport capacity q_s (t) of the flow leaving the terrain component:

$$SY = \text{minimum}\,(E + SED_{in},\, q_s) \qquad \text{Eq. 17}$$

Two options are available to calculate the transport capacity q_s:

(a) With the sediment transport capacity according to Everaert (1991):

- if $D_{50} \le 150$ µm:
  $q_s = 1.50 \cdot 10^{-5}\, \Omega^{1.07}\, D_{50}^{0.47}\, W$
- if $D_{50} > 150$ µm:
  $q_s = 3.97 \cdot 10^{-6}\, \Omega^{1.75}\, D_{50}^{-0.56}\, W$,

$$\text{with } \Omega = \left(\rho g q S\right)^{1.5} / R^{2/3} \qquad \text{Eq. 18}$$

where Ω is the effective stream power (g$^{1.5}$.s$^{-4.5}$cm$^{-2/3}$) computed within the hydrological routines of WASA-SED, D_{50} is the median particle diameter (µm) estimated from the mean particle size distribution of the eroded soils and W is the width of the terrain component (m), ρ is the density of the particles (g.m^{-3}), g is the gravitational acceleration (m.s^{-2}), q is the overland flow rate on a 1-m strip (m^3.s^{-1}.m^{-1}) and R is the flow depth (cm).

(b) With the maximum value that is predicted by MUSLE assuming unrestricted erodibility with K set to 0.5:

$$q_s = E_{MUSLE,K=0.5} \text{ using Eq. 4} \qquad \text{Eq. 19}$$

Similar to the downslope partitioning scheme for surface runoff described by Güntner and Bronstert (2004), sediment that leaves a terrain component i is partitioned into a fraction that is routed to the next terrain component downslope ($SED_{in,TC\ i+1}$) and a fraction that reaches the river directly ($SED_{river,i}$), representing the soil particles carried through preferential flow paths, such as rills and gullies. $SED_{river,i}$ is a function of the areal fraction α_i

of the current terrain *i* component within each landscape unit according to:

$$SED_{river,i} = SY_i \left(\alpha_i \Big/ \sum_{n=i}^{nTC} \alpha_n \right) \qquad Eq.\ 20$$

where *i* and *i+1* are the indices of the current and the next downslope terrain component respectively, α is the areal fraction of a terrain component and *nTC* is the number of terrain components in the current landscape unit.

2.3. Transport processes in the river module

The river network consists of individual river stretches with pre-defined river cross-sections and where each stretch is associated with one sub-basin. Each stretch receives the water and sediment fluxes from one sub-basin and the fluxes from the upstream river network. The water routing is based on the kinematic wave approximation after Muskingum (e.g. as described in Chow *et al.*, 1988). Flow rate, velocity and flow depth are calculated for each river stretch and each time step using the Manning equation. A trapezoidal channel dimension with width *w* (m), depth *d* (m) and channel side ratio *r* (m/m) is used to approximate the river cross-sections. If water level exceeds bankful depth, the flow is simulated across a pre-defined floodplain using a composite trapezoid with an upper width of $w_{floodpl}$ (m) and floodplain side ratio $r_{floodpl}$ (m/m). The WASA-SED river module contains routines for suspended and bedload transport using the transport capacity concept. The maximum suspended sediment concentration that can be transported in the flow is calculated using a power function of the peak flow velocity similar to the SWIM (Krysanova *et al.*, 2000) and the SWAT model (Neitsch *et al.*, 2002; Arnold *et al.*, 1995):

$$C_{s,\max} = a \cdot v_{peak}^{\ b} \qquad Eq.\ 21$$

where $v_{peak}(t)$ is the peak channel velocity (m/s), $C_{s,max}$ is the maximum sediment concentration for each river stretch in (t/m^3), and *a* and *b* are user-defined coefficients. If the actual sediment concentration C_{actual} exceeds the maximum concentration, deposition occurs; otherwise degradation of the riverbed is calculated using an empirical function of a channel erodibility factor (Neitsch *et al.*, 2002):

$$SED_{dep} = (C_{s,max} - C_{actual}) \cdot V \qquad Eq.\ 22$$

$$SED_{ero} = (C_{s,max} - C_{actual}) \cdot V \cdot K \cdot C \qquad Eq.\ 23$$

where SED_{dep} (t) is the amount of sediment deposited, SED_{ero} (t) the amount of sediment re-entrained in the reach segment (t), *V* is the Volume of water in the reach (m^3), *K* is the channel erodibility factor (cm/h/Pa) and *C* is the channel cover factor (-).

For bedload transport, five transport formulae (Meyer-Peter and Müller, 1948; Schoklitsch, 1950; Bagnold, 1956; Smart and Jaeggi, 1983 and Rickenmann, 2001) are implemented for boundary conditions commonly found in upland meso-scale dryland catchments with small, gravel-bed streams as summarised in Tab. 2. For the calculation of bedload transport, near-equilibrium conditions are assumed, i.e. water and bedload discharge were thought to be steady at one time step. It was furthermore assumed that no supply limitations occurred, i.e. bedload transport was at capacity, which appears feasible for short-duration, low-magnitude flood events, where a large amount of sediments is thought to have been previously accumulated from upstream, unregulated watersheds. The bedload formulae consider both uniform and non-uniform sediments, grain sizes ranging from 0.4 to 29 mm or D_{50} values larger 6 mm and river slopes ranging between 0.003 to 0.2 m/m (Tab. 2).

2.4. Retention processes in the reservoir module

WASA-SED comprises a reservoir sedimentation module developed by Mamede (2008). It enables the calculation of reservoir life expectancy, the trapping efficiency of the reservoir, sediment deposition patterns and the simulation of several reservoir sediment management options. The water balance and the bed elevation changes due to sediment deposition or entrainment are calculated for individual

cross-sections along the longitudinal profile of the reservoir. Mamede (2008) subdivided the reservoir body (Figure 2) in a river sub-reach component, where hydraulic calculations are based on the standard step method for a gradually varied flow (Graf and Altinakar, 1998) and a reservoir sub-reach component that uses a volume-based weighting factor approach adapted from the GSTARS model (Yang and Simoes, 2002). The transitional cross-section between the two spatial components is defined as where the maximum water depth for uniform river flow, computed with the Manning equation, is exceeded by the actual water depth of the cross-section due to the impoundment of the reservoir. Consequently, the length of the river sub-reach becomes longer for lower reservoir levels and vice versa. For the reservoir routing, the water discharge Q_j of each cross-section j is calculated as:

$$Q_j = Q_{in} - (Q_{in} - Q_{out}) \sum_{k=m}^{j} v_k \qquad \text{Eq. 24}$$

with $v_k = V_k / V_{res}$

where Q_{in} and Q_{out} are the inflow and outflow discharge of the reservoir, v_k is the fraction of reservoir volume represented by the cross-section, V_k is the volume represented by cross-section k, m is the index for the first cross-section belonging to the reservoir sub-reach. The inflow discharge considers the direct river runoff from the tributary rivers, direct rainfall and evaporation from the reservoir surface.

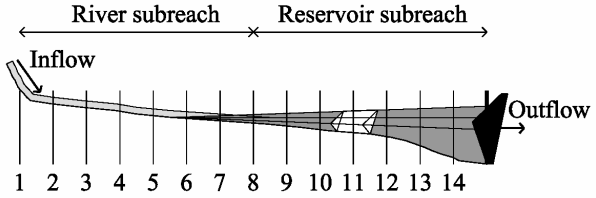

Fig. 2: Spatial discretisation of the reservoir along the longitudinal profile.

Tab. 2: Bedload transport formulae in the river module of the WASA-SED Model.

Formula	**Range of conditions**
1. Meyer-Peter and Müller (1948) $q_s = \frac{8(\tau - \tau_{crit})^{1.5}}{g\rho^{0.5}} 1000$ with: $\tau = \rho g d S$ and $\tau_{crit} = 0.047(\rho_s - \rho) g D_m$	for both uniform and non-uniform sediment, grain sizes ranging from 0.4 to 29 mm and river slopes of up to 0.02 m/m.
2. Schoklitsch (1950) $q_s = 2500 S^{1.5}(q - q_{crit}) 1000 \frac{\rho_s - \rho}{\rho_s}$ with: $q_{crit} = 0.26(\frac{\rho_s - \rho}{\rho})^{\frac{5}{3}} \frac{D_{50}^{\frac{3}{2}}}{S^{\frac{7}{6}}}$	for non-uniform sediment mixtures with D_{50} values larger than 6 mm and riverbed slopes varying between 0.003 and 0.1 m/m
3. Smart and Jaeggi (1983) $q_s = 4.2 q S^{1.6}(1 - \frac{\tau^*_{crit}}{\tau^*}) / (\frac{\rho_s}{\rho} - 1) 1000(\rho_s - \rho)$ with $\tau^* = \frac{dS}{(\frac{\rho_s}{\rho} - 1) D_{50}}$ and $\tau^*_{crit} = \frac{d_{crit} S}{(\frac{\rho_s}{\rho} - 1) D_{50}}$	for riverbed slopes varying between 0.03 – 0.2 m/m and D_{50} values comparable to the ones of the Meyer-Peter and Müller equation.
4. Bagnold (1956) $q_s = 4.25 \tau^{*0.5}(\tau^* - \tau^*_{crit})((\frac{\rho_s}{\rho} - 1) g {D_{50}}^3)^{0.5} 1000(\rho_s - \rho)$	reshaped by Yalin (1977), applicable for sand and fine gravel and moderate riverbed slopes
5. Rickenmann (2001) $q_s = 3.1 (\frac{D_{90}}{D30})^{0.2} \tau^{*0.5}(\tau^* - \tau^*_{crit}) \cdot Fr^{1.1} (\frac{\rho_s}{\rho} - 1)^{-0.5} ((\frac{\rho_s}{\rho} - 1) g {D_{50}}^3)^{0.5} 1000(\rho_s - \rho)$ with: $Fr = (\frac{v}{g \cdot d})^{0.5}$	for gravel-bed rivers and torrents with bed slopes between 0.03 and 0.2 m/m and for D_{50} values comparable to the ones of the Meyer-Peter and Müller equation in the lower slope range with an average D_{50} of 10 mm in the higher slope ranges

d: mean water flow depth (m), d_{crit}: critical flow depth for initiation of motion (m), D_{50}: median sediment particle size (m), D_{30}: grain-sizes at which 30 % by weight of the sediment is finer (m), D_{90}: grain-sizes at which 90 % by weight of the sediment is finer (m), D_m: mean sediment particle size (m), Fr: Froude number of the flow (-), g: acceleration due to gravity (m/s^2), q: unit water discharge (m^2/s), q_{crit}: unit critical water discharge (m^2/s), q_s: sediment discharge in submerged weight (g/ms), S: slope (m/m), v: water flow velocity (m/s), ρ: fluid density (1000 kg/m^3), ρ_s: sediment density (2650 kg/m^3), τ: local boundary shear stress (kg/ms^2), τ_{crit}: critical local boundary shear stress (kg/ms^2), τ^*: dimensionless local shear stress (-), τ^*_{crit}: dimensionless critical shear stress (-)

The sediment transport is computed using a one-dimensional equation of non-equilibrium transport of non-uniform sediment, adapted from Han and He (1990):

$$\frac{dS}{dx} = \frac{\alpha\omega}{q}(S^* - S) \qquad \text{Eq. 25}$$

where S is the sediment concentration; S^* is the sediment carrying capacity; q is the discharge per unit width; ω is the settling velocity; and α is the coefficient of saturation recovery. According to Han and He (1990), the parameter α can be taken as *0.25* for reservoir sedimentation and *1.0* for scouring during flushing of a reservoir and in river channel with fine bed material. Mamede (2008) adapted four sediment transport equations (Wu *et al.*, 2000; Ashida and Michiue, 1973; IRTCES, 1985; and Ackers and White, 1973) for the calculation of the fractional sediment carrying capacity of both suspended sediments and bedload for different ranges of sediment particle sizes as given in Table 2.

The bed elevation changes of the reservoir are computed for each cross-section taking into account three conceptual layers above the original bed material: a storage layer, where sediment is compacted and protected against erosion; an intermediate layer, where sediment can be deposited or re-suspended; and the top layer, where sediment-laden flow occurs. The time-dependent mobile bed variation is calculated using the sediment balance equation proposed by Han (1980):

$$\frac{\partial(QS)}{\partial x} + \frac{\partial M}{\partial t} + \frac{\partial(\rho_d A_d)}{\partial t} = 0 \qquad \text{Eq. 26}$$

where Q is the water discharge; S is the sediment concentration; M is the sediment mass in water column with unit length in longitudinal direction; A_d is the total area of deposition; and ρ_d is density of deposited material.

For each time step, the sediment balance is performed for each size fraction and cross-section, downstream along the longitudinal profile. The total amount of sediment deposited at each cross-section corresponds to the amount of sediment inflow exceeding the sediment transport capacity. On the other hand, the total amount of sediment eroded corresponds to the total amount of sediment that can still be transported by the water flux. Erosion is constrained by sediment availability at the bed of the reach. The geometry of the cross-section is updated whenever deposition or entrainment occurs at the intermediate layer. For each cross-section, the volume of sediments to be deposited is distributed over a stretch with a width of half the distance to the next upstream and downstream cross-section, respectively (Fig. 3a). Suspended sediment is assumed to be uniformly distributed across the cross-section and settles vertically, hence the bed elevation e_m at a point m along the cross-section changes proportionally to water depth:

$$e_m = e_{dep} \cdot f_{d,m} \qquad \text{Eq. 27}$$

where e_{dep} is the maximum bed elevation change at the deepest point of the cross-section caused by deposition and $f_{d,m}$ is a weighting factor which is computed as the ratio between water depth h_m at the point m and the maximum water depth h_{max} of the cross-section:

$$f_{d,m} = h_m / h_{\max} \qquad \text{Eq. 28}$$

Fig. 3b shows schematically, how the sediment is distributed trapezoidal along the cross-section as a function of water depth h_{max}, where A_m' and A_m'' are the sub-areas limited by the mean distances to the neighbour points (d_m' and d_m'', respectively, starting from the deepest point of the cross-section profile), with m running from 1 to n_w as the total number of demarcation points of the cross-section below water level.

Tab. 3: Sediment transport formulae in reservoir module.

Authors, range of sediments	Transport formula	Auxiliary equations
Wu *et al.* (2000): 0.004 to 100 mm	$q_{b,k} = P_k \phi_{b,k} \sqrt{\Delta g d^3}$	$\phi_{b,k} = 0.0053 \cdot \left[\left(\frac{n'}{n} \right)^{3/2} \frac{\tau_b}{\tau_{c,k}} \right]^{2.2}$, $n = R_h^{2/3} S_f^{1/2} / v$, $n' = \sqrt[6]{d_{50}} / 20$, $\tau_{c,k} = (\gamma_s - \gamma) d_k \theta_k \xi_k$, $\zeta_k = (P_{e,k} / P_{h,k})^{-0.6}$, $P_{e,k} = \sum_{j=1}^{q} P_{b,j} \cdot (d_k / d_k + d_j)$, $P_{h,k} = \sum_{j=1}^{q} P_{b,j} \cdot (d_j / d_k + d_j)$, $\tau_b = \gamma R_h S_f$
	$q_{s,k} = P_k \phi_{s,k} \sqrt{\Delta g d^3}$	$\phi_{s,k} = 0.0000262 \cdot \left[\left(\frac{\tau}{\tau_{c,k}} - 1 \right) \cdot \frac{V}{\omega_k} \right]^{1.74}$, $\omega = \sqrt{13.95 \cdot (\frac{v}{d})^2 + 1.09 \Delta g d} - 13.95 \cdot (\frac{v}{d})$
Ashida and Michiue (1973): 0.040 to 100 mm	$q_{b,k} = 17 \cdot P_k u_{c,k} d_k \tau_{c,k} (1 - \frac{\tau_{c,k}}{\tau_k})(1 - \sqrt{\frac{\tau_{c,k}}{\tau_k}})$	$\tau_k = \frac{u^{*2}}{\Delta g d_k}$, $u^* = \sqrt{g R_h S_f}$, $\tau_{e,k} = \frac{u_{e,k}^2}{\Delta g d_k}$, $u_{e,k} = \frac{V}{5.75 \log \left(\frac{R_h / d_{50}}{1 + 2\tau_k} \right)}$, $\tau_{c,k} = \frac{u_{c,k}^2}{\Delta g d_k}$
		$d_k / d_{50} < 0.4$: $u_{c,k} = \sqrt{0.85 \cdot u_{c,50}}$; $d_k / d_{50} > 0.4$: $u_{c,k} = \log 19 / \log(19 \cdot d_k / d_{50}) \cdot u_{c,50}$, $u_{c,50} = 0.05 \cdot \Delta g d_{50}$
	$q_{s,k} = C \cdot V (e^{-p \cdot a} - e^{-p \cdot h}) \cdot \frac{e^{p \cdot a}}{p}$	$p = \frac{6 \cdot \omega_k}{0.412 \cdot u^* h}$, $C = 0.025 \cdot p_k \left(\frac{f(\varepsilon_0)}{\varepsilon_0} - F(\varepsilon_0) \right)$, $f(\varepsilon_0) = \frac{1}{\sqrt{2\pi}} e^{(-0.5 \cdot \varepsilon_0^2)}$, $F(\varepsilon_0) = \frac{1}{\sqrt{2\pi}} \int_{\varepsilon_0}^{\infty} e^{(-0.5 \cdot \varepsilon_0^2)} d\varepsilon$, $\varepsilon_0 = \frac{\omega_k}{0.75 \cdot u^*}$
IRTCES, (1985): 0.001 to 100 mm	$q_t = \Omega \frac{Q^{1.6} S^{1.2}}{B^{0.6}}$	Ω=1600 for loess sediment Ω=650 for $d_{50} < 0.1$ mm Ω=300 for $d_{50} > 0.1$ mm
Ackers and White (1973): 0.040 to 100 mm	$q_t = P_k \psi V d_k \left(\frac{V}{u^*} \right)^{n0} \left(\frac{F_{gr}}{F_{gr,cr} \xi_k} - 1 \right)^{m_o}$	$d_k^* = d_k (\Delta g / v^2)^{1/3}$ $1 < d_k^* < 60$: $n_o = 1 - 0.56 \cdot \log(d^*)$, $m_o = \frac{9.66}{d^*} + 1.34$, $\psi = 10^{-3.53 + 2.86 \cdot \log(d^*) - \log^2(d^*)}$, $F_{gr,cr} = \frac{0.23}{\sqrt{d^*}} - 0.14$ for $d_k^* > 60$: n_o=0, m_o=1.5, ψ=0.025, $F_{gr,cr}$=0.17

$q_{b,k}$: transport rate of the k-th fraction of bedload per unit width, $q_{s,k}$: fractional transport rate of non-uniform suspended load, k: grain size class, P_k: ratio of material of size fraction k available in the bed, Δ: relative density (γs/ γ−1), γ and γ_s: specific weights of fluid and sediment, respectively; g: gravitational acceleration; d_k: diameter of the particles in size class k, $\varphi_{b,k}$: dimensionless transport parameter for fractional bed load yields, v: kinematic viscosity, τ: shear stress of entire cross-section $\tau_{c,k}$: critical shear stress, θ_c: critical Shields parameter, ξ_k: hiding and exposure factor, $P_{e,k}$ and $P_{h,k}$: total exposed and hidden probabilities of the particles in size class k, $P_{b,j}$: probability of particles in size class j staying in the front of particles in size class k, τ_b: average bed shear stress; n: Manning's roughness, and n': Manning's roughness related to grains, R_h: hydraulic radius, S_f: the energy slope, V: average flow velocity, $d50$: median diameter, ω: settling velocity, q_t: total sediment transport capacity at current cross-section ($q_t = q_s + q_b$, for the equations after Wu *et al.* (2000) and Ashida e Michiue (1973)), S: bed slope, B: channel width, Ω: constant as a function of grain size, u^*: shear velocity, $u_{c,k}$: effective shear velocity, F_{gr}: sediment mobility number, n_o, m_o, ψ, $F_{gr,cr}$ are dimensionless coefficients depending on the dimensionless particle size d_k^*, C: concentration at a reference level a

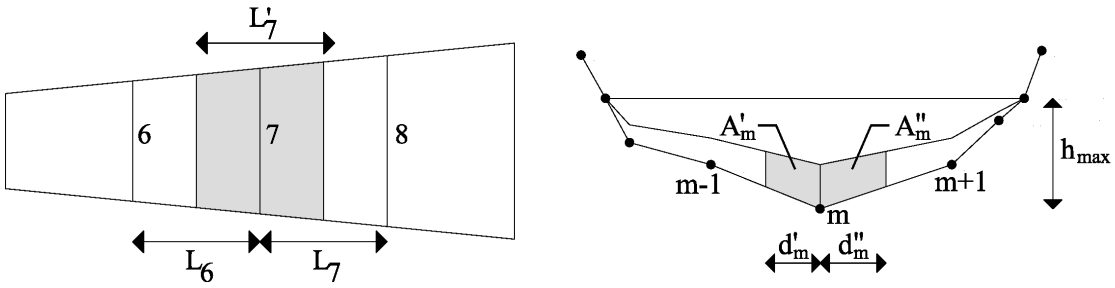

(a) (b)

Fig. 3: Bed elevation change: a) plan view along longitudinal profile, b) deposition along an individual cross-section of the reservoir.

Bed entrainment is distributed in an equivalent way by assuming a symmetrical distribution of bed thickness adapted from Foster and Lane (1983). The bed elevation change due to erosion is constrained by the maximum thickness of the intermediate layer. The bed elevation change e_m is given by:

$$e_m = e_{ero} \cdot f_{e,m} \qquad \textit{Eq. 29}$$

where e_{ero} is the maximum bed elevation change at the deepest point of the cross-section caused by erosion and $f_{e,m}$ is a weighting factor given by Forster and Lane (1983):

$$f_{e,m} = 1 - (1 - X_m)^{2.9} \qquad \textit{Eq. 30}$$

where X_m is a normalised distance along the submerged half perimeter given by:

$$X_m = X / X_{\max} \qquad \textit{Eq. 31}$$

where X is the actual distance along the submerged half perimeter of the cross-section and X_{max} is the total wetted half perimeter between the cross-section point at the water surface and the deepest point of the cross-section.

The implemented reservoir sedimentation routines allow the simulation of reservoir management options for the reduction or prevention of sedimentation (Mamede, 2008) such as annual flushing operation or partial drawdown of the reservoir water level. Both management operations result in a remobilisation of previously deposited sediments and the release of sediments out of the reservoir. The management options can then be used to calculate the life expectancy of the reservoir by taking into account potential scenarios of water and land management for different land-uses and erosion prevention schemes in the upslope catchments. Besides the above sediment routine for individual large reservoirs, WASA-SED optionally provides a module to represent water and sediment retention processes within networks of farm dams and small reservoirs that often exist in large numbers in dryland areas. These mini-reservoirs cannot be represented explicitly each of them in a large-scale model. Instead, WASA-SED applies a cascade structure that groups the reservoirs into different size classes according to their storage capacity, defines water and sediment routing rules between the classes and calculates water and sediment balances for each reservoirs class. Details of the approach are presented with regard to the water balance in Güntner *et al.* (2004) and for related sedimentation processes in Mamede (2008).

2.5. Summary of model input and output data

The model runs as a Fortran Windows Application for catchment sizes of about 50 to 5,000 km^2 on daily or hourly time steps. Climatic drivers are hourly or daily time series for precipitation, humidity, short-wave radiation and temperature. For model parameterisation, regional digital maps on soil associations, land-use and vegetation cover, a digital elevation model with a cell size of 100 metres (or smaller) and, optional, bathymetric surveys of the reservoirs are required. The soil, vegetation and

terrain maps are processed with the LUMP tool (see above) to derive the spatial dis-
Tab. 4 summarises the input parameters for the climatic drivers and the hillslope, river and reservoir modules. The vegetation parameters may be derived with the comprehensive study of, for example, Breuer *et al.* (2003), the soil and erosion parameters with the data compilations of, e.g., FAO (1993, 2001), Morgan (1995), Maidment (1993) and Schaap *et al.* (2001), or from area-specific data sources.
The model output data are time series with daily time steps for lateral and vertical water fluxes and sediment production from the sub-basins, the water and sediment discharge in the river network and the bed elevation change due to sedimentation in the reservoir as summarised in Tab. 5. A manual for model parameterisation and a trail version plus the latest updates of the model, LUMP and auxiliary tools can be found on the WASA-SED internet page at http://brandenburg.geoecology.uni-potsdam.de/projekte/sesam.

3. Review, uncertainty and limits of WASA-SED model applications

The model has been employed in several recent research studies to evaluate the effects of land and reservoir management on the water and sediment export of large dryland catchments. Güntner and Bronstert (2004) and Güntner *et al.* (2004) applied the hydrological part of the model to assess water availability in large river basins (up to several 10000 km²) in the semi-arid northeast of Brazil. By comparing simulation results to observed time series of river discharge and reservoir water storage they showed that the model could reasonably represent the pronounced seasonal and inter-annual hydrological variations in this environment.
Mueller *et al.* (2008 and *submitted*) yielded good results when testing the model against measured daily water and sediment discharge (suspended and bedload) data for a 2.5 km^2, a 65 km^2 and a 222 km^2 catchment in the Pre-Pyrenees of Spain. No model calibration was required which suggests a sufficient reproduction of the underlying generation and transport processes. The temporal dynamics of individual flood events that trigger soil erosion at the mountainous hillslope and sediment transport in the river reaches was reproduced in most cases. The simulated values of suspended sediment concentration and bedload compared well to measured ones obtained from ISCO 3700 automatic samplers and manual sampling over a time period of three years (Batalla *et al.* 2005). The tested model was then used to develop an effective, erosion-prevention scheme through a selected afforestation of steep hillslopes for the region that was previously heavily used for agricultural production. The spatial model representation of hillslopes into individual, subdivided terrain components with separate terrain, soil and vegetation characteristics (Fig. 1) made the WASA-SED model particularly functional for the detection and management of erosion-prone hotspots. Other large-scale models do not provide such a suitable spatial structure of the landscape. The spatially semi-distributed SWAT model (Neitsch *et al.*, 2002), for example, uses hydrologic response units to group input information in regard to land-use, soil and management combinations, thus averaging out spatial variations along the hillslope essential for sediment generation and transport. In comparison, grid-based models such as the LISEM model (Jetten, 2002) may incorporate a higher degree of spatial information, but are often limited in their applicableness due to computing time (for small grid sizes) and lack of exhaustive spatial data. The advantage of the terrain component concept in the WASA-SED model is that it captures the structured variability along the hillslope essential for overland flow generation and erosion, but at the same time does not require the parameterisation and calculation of otherwise micro-scale processes.

Tab. 4: Model input parameters.

Type	Model input parameter
Climate	Daily or hourly time series on rainfall (mm/day, mm/h) Daily time series for average short-wave radiation (W/m^2) Daily time series for humidity (%) Daily time series for temperature (°C)
Vegetation	Stomata resistance (s/m) Minimum suction (hPa) Maximum suction (hPa) Height (m) Root depth (m) LAI (-) Albedo (-) USLE C (-)
Soil	No. of horizons* Residual water content (Vol. %) Water content at permanent wilting point (Vol. %) Usable field capacity (Vol. %) Saturated water content (Vol. %) Saturated hydraulic conductivity (mm/h) Thickness (mm) Suction at wetting front(mm) Pore size index (-) Bubble pressure (cm) USLE K ($t.ha.h.ha^{-1}.MJ^{-1}.mm^{-1}$) Particle size distribution**
Soil vegetation component	Manning's n (-) USLE P (-)
Terrain and river	Hydraulic conductivity of bedrock (mm/d) Mean maximum depth of soil zone (mm) Depth of river bed below terrain component (mm) Storage coefficient for groundwater outflow (day) Bankful depth of river (m) Bankful width of river (m) Run to rise ratio of river (-) Bottom width of floodplain (m) Run to rise ratio of floodplain side slopes (-) River length (km) River slope (m/m) D_{50} (median sediment particle size) of riverbed (m) Manning's n for riverbed and floodplains (-)
Reservoir	Longitudinal profile of reservoir (m) Cross-section profiles of reservoir (m) Stage-volume curves Initial water storage and storage capacity volumes (m^3) Initial area of the reservoir (ha) Maximal outflow through the bottom outlets (m^3/s) Manning's roughness for reservoir bed Depth of active layer (m) Spillway coefficients Dry bulk densities of deposits

* for each soil horizon, all following parameters in the column are required

** of topmost horizon

Medeiros *et al.* (*submitted*) evaluated the spatial and temporal patterns of connectivity in regard to sediment generation and transport for a 933 km^2 dryland basin in the semi-arid northeast of Brazil in the State of Ceara. The dryland region is exposed to prolonged droughts and runoff frequently occurs only during high-intensity rainstorm events on a few days per year, resulting in high erosion rates on degraded fields. Using the landscape unit approach, Medeiros *et al.* (*submitted*) evaluated the effects of slope and position of terrain components on the lateral redistribution and re-infiltration of overland flow and consequent deposition patterns of suspended sediments. Erosion rates and sediment export out of the catchment could be assessed in a spatially distributed way in a relation to how well individual hillslopes and sub-catchments of the basin were connected to the river network and to the catchment outlet. It could be shown how catchment connectivity and thus basin response in terms of water and sediment export varied as a function of rainfall event characteristics.

Tab. 5: Model output files.

Spatial unit	Output (daily time series)
Sub-basins	potential evapotranspiration (mm/day) actual evapotranspiration (mm/day) overland flow (m^3/day) sub-surface flow (m^3/day) groundwater discharge (m^3/day) sediment production (t/day) water content in the soil profile (mm)
River	water discharge (m^3/s) suspended sediment concentration (g/l) bedload rate as submerged weight (kg/s)
Reservoir	sediment outflow from the reservoir (t/day) bed elevation change due to deposition or erosion (m) storage capacity and sediment volume changes (hm^3) life expectancy (years) effluent size distribution of sediment (-)

Reservoir sedimentation triggered by erosion from badland areas was modelled by Appel (2006) and Mamede (2008) for a 1,340 km^2 catchment in the north-east of Spain. The high erosion rates from badlands, which are a typical landform of that region consisting of unvegetated unconsolidated marl sediments, leads to significant sedimentation and hence reduction of storage capacity for downstream reservoirs, which are intensively used for water supply and power generation. Appel (2006) showed that the erosion module of WASA-SED is able to reproduce the extreme erosion rates of badlands that reach up to 550 t/ha per year, equivalent to circa 3 centimetres per year. Mamede (2008) then applied the reservoir module to the Barasona Reservoir with a maximal storage capacity of 92 hm^3 and a length of ca. 10 km using a total number of 53 cross-sections. Mamede was able to reproduce annual bed elevation changes due to sedimentation of badland sediments along individual cross-sections of the reservoir. The testing data for bed elevation change along those cross-sections were available from repeated, annual bathymetric surveys that were repeatedly taken over the last 20 years. In addition, the WASA-SED model was applied to predict the development of the storage capacity and the expected life time of the Barasona Reservoir as a function of badland erosion and implemented management options such as frequent flushing or partial draw-down of the reservoir to release sediment through the bottom outlets. Model results showed the significance of the management options: if no management options are applied, the entire reservoir is filled with sediments after 47 years; with different draw-down scenarios the life expectancy is calculated to vary between 64 and 80 years, whereas with frequent flushing operations, sedimentation occurs at much lower rates, thus preserving the original storage capacity perpetually.

The modelling studies demonstrated the wide range of environmental problems at the meso-scale where the WASA-SED model may be employed to comprehend the underlying sediment transfer processes and to develop sustainable management strategies for land and water resources. Nevertheless, the success and, hence, the uncertainty of process-based erosion mod-

elling at large scales have always been influenced by two major shortcomings (Quinton, 2004; Boardman and Favis-Mortlock, 1995; Beven, 2001): the lack of spatial input data at that scale and the knowledge gap on how to integrate over small-scale processes. The above review of model applications showed several shortcomings of WASA-SED. Uncertainties towards process descriptions existed in regard to processes that occur in the interstorm period such as the soil moisture dynamics under different vegetation and the erosion processes that are governed by the weathering, freezing and thawing cycles of the upper soil layer. In addition, the model contains only limited descriptions of processes which are commonly not regarded to be relevant for dryland settings, but may influence the hydrological regime under certain conditions, such as snow melt and groundwater movement. Uncertainties existed towards model input data on the spatial variability of rainfall data for high-intensity storm events that tend to be often highly localised and are highly influential on runoff and sediment generation. Other frequent input uncertainties were soil maps at the meso-scale that normally include only a few soil profiles, which are often insufficient to describe the complex interflow and overland flow dynamics at steep, heterogeneous hillslopes.

4. Conclusions

The WASA-SED model is a new tool for the qualitative and quantitative assessment of sediment transfer in dryland environments. The model currently focuses on research applications of process-based studies on the hillslope, river and reservoir scale. However, its capabilities to evaluate land-use change scenarios and reservoir management options may as well make it a valuable decision-making tool for regional water authorities. The model's assets are threefold: Firstly, the spatially detailed representation of catena characteristics using the landscape unit approach enables an effective way of parameterising large areas without averaging out topographic details that are particularly relevant for sediment transport. Crucial spatial information on for example the slope angle is preserved for the various sections of the catena. The information on overland flow dynamics allows at the same time a realistic calculation of transport capacities and deposition patterns along the catena. The semi-distributed approach of WASA-SED model thus provides a more feasible hillslope representation than raster-based erosion models, which normally lack satisfactory aggregation methods for topographic information when large cell sizes are employed to represent the often highly heterogeneous catenas of dryland catchments.
Secondly, the WASA-SED framework allows a coherent handling of spatial input data in combination with the semi-automated discretisation tool LUMP (Chapter IV). The tool provides an objective and easily reproducible delineation of homogeneous terrain components along a catena and consequently an upscaling rationale of small-scale hillslope properties into the regional landscape units. At the river scale, representative river stretches and for reservoirs, the concept of non-localised small reservoirs provide efficient ways for regionalised parameterisation strategies. And thirdly, the WASA-SED model enables an integrative assessment of hillslope, river and reservoir processes, thus including the very different sediment transport and storage behaviour and potential management options of landscape compartments of large catchments.
Nevertheless, the uncertainties in regard to both the process descriptions and the model input of WASA-SED in combination with the potential error propagation of the hydrological modules on sediment export calculations recommend caution as with any modelling exercise at large scales.

5. Acknowledgements

This research was carried out within the SESAM (Sediment Export from Semi-Arid Catchments: Measurement and Modelling) project and was funded by the Deutsche Forschungsgemeinschaft.

Chapter VI:

Modelling the effects of land-use change on runoff and sediment yield for a meso-scale catchment in the Southern Pyrenees

Abstract

The Southern Pre-Pyrenees experienced a substantial land-use change over the second half of the 20th century owing to the reduction of agricultural activities towards the formation of a more natural forest landscape. The land-use change over the last 50 years with subsequent effects on water and sediment export was modelled with the process-based, spatially semi-distributed WASA-SED model for the meso-scale Canalda catchment in Catalonia, Spain. It was forwarded that the model yielded acceptable results for runoff and sediment yield dynamics without the need of calibration, although the simulation capabilities may not yet be sufficient for decision-making purposes for land management. Modelling the effects of the past land-use change, the model scenarios resulted in a decrease of up to 75 % of the annual sediment yield, whereas modelled runoff remained almost constant over the last 50 years. The relative importance of environmental change was evaluated by comparing the impact on sediment export of land-use change, that are driven by socio-economic factors, with climate change projections for changes in the rainfall regime. The modelling results suggest that a 20 % decrease in annual rainfall results in a decrease in runoff and sediment yield, thus an ecosystem stabilisation in regard to sediment export, which can only be achieved by a substantial land-use change equivalent to a complete afforestation. At the same time, a 20 % increase in rainfall causes a large export of water and sediment resources out of the catchment, equivalent to an intensive agricultural use of 100 % of the catchment area. For wet years, the effects of agricultural intensification are more pronounced, so that in this case the intensive land-use change has a significantly larger impact on sediment generation than climate change. The WASA-SED model proved capable in quantifying the impacts of actual and potential environmental change, but the reliability of the simulation results is still circumscribed by parameterisation and model uncertainties.

Keywords: land-use change, afforestation, land abandonment, hydrological modelling, sediment yield

submitted as
Mueller, E. N., Francke, T., Batalla, R., Bronstert, A., 2008. Modelling the effects of land-use change on runoff and sediment yield for a meso-scale catchment in the Southern Pyrenees. *Catena.*

In revision (March 2009)
[author's note: The manuscript underwent modifications during the review process after this document was compiled. Please check the journal for the final version.]

1. Introduction

Substantial parts of the Pre-Pyrenees in the north-eastern part of Spain have experienced an extensive land-use change over the second half of the 20th century owing to the reduction of agricultural activities towards the formation of a more natural landscape (Lasanta-Martinez *et al.*, 2005, Garcia-Ruiz *et al.*, 1996). Traditionally, the area was characterised by intensive agricultural use even on very steep hillslopes that led to severe soil erosion. Due to a demographic change and socio-economic change, the migration of the rural population and consequent depopulation of the region (Ortigosa *et al*., 1990, Garcia-Ruiz and Valero-Garces, 1998), many cultivated fields were abandoned, especially the terraced fields on the slopes while in the valley bottoms agriculture has been intensified. Abandoned fields have either been affected by a natural process of plant recolonisation by mostly shrubs, or have been reforested with conifers.

The fast abandonment of traditional agricultural practices and the large extent of the areas affected by vegetation recovery make the Pyrenees a good example for assessing the impact of land-use change on the hydrological response and sediment delivery dynamics (Gallart and Llorens, 2004, Lopez-Moreno, *et al.* 2006). Afforestation is reported to have changed the hydrological behaviour of headwater catchments of the Ebro basin by modifying surface runoff and by reducing the peak flow, soil erosion and sediment export. According to Garcia-Ruiz *et al.* (1996) and Ortigosa and Garcia-Ruiz (2000), some of the most important rivers in the region and their alluvial fans have recently stabilised their sedimentary structures, caused by plant re-establishment in the channels and on the riverbanks. Lopez-Moreno *et al.* (2006) analysed the evolution of floods in the central Spanish Pyrenees during the period 1955-1995 and detected a general negative trend in flood intensity, an increase in the importance of low flows in the total annual contribution against a stable frequency distribution of precipitation events. They linked a decrease in the siltation rates in the Pyrenean reservoirs (with a consequential increase in their expected life-span) with a decrease in the torrentiality of Pyrenean rivers. Land-use and plant-cover changes were estimated to be responsible for the loss of up to 30 % of the average annual discharge from the 1950s until present (Begueria *et al.*, 2003).

During the so-called traditional land-use system, soil erosion was probably the most important environmental problem in the region (Garcia-Ruiz *et al.*, 1996). At present, at least one third of the former agricultural areas remain bare, i.e. without dense shrub or forest cover, hence the observed negative trend of water and sediment fluxes may continue in the near future if vegetation recovery continues. On the other hand, the region may experience a renewed increase of agricultural production as, for example, vineyard plantations are forced to move up from the Ebro plains to the foothills of the Pyrenees because conditions in their traditional vineyards become increasingly dry due to the regional effects of global warming (Nash, 2007).

Only a limited amount of quantitative data on the hydrological response and sediment delivery is available for the Pyrenean region to assess the effects of past and future land-use changes related to land abandonment, intensification and/or afforestation. Therefore, in order to evaluate the impacts of environmental change on a meso-scale dryland basin, a modelling study was carried out for the Canalda catchment of the Ribera Salada River in the Southern Pyrenees using a process-based water and sediment transport model (the WASA-SED model). Specific focus was placed on the evaluation and discussion of model capabilities to reproduce flux generation for current land-use without the need of calibration, thus reducing the adverse effects of error propagation from the simulated hydrological fluxes on the calculation of sediment budgets.

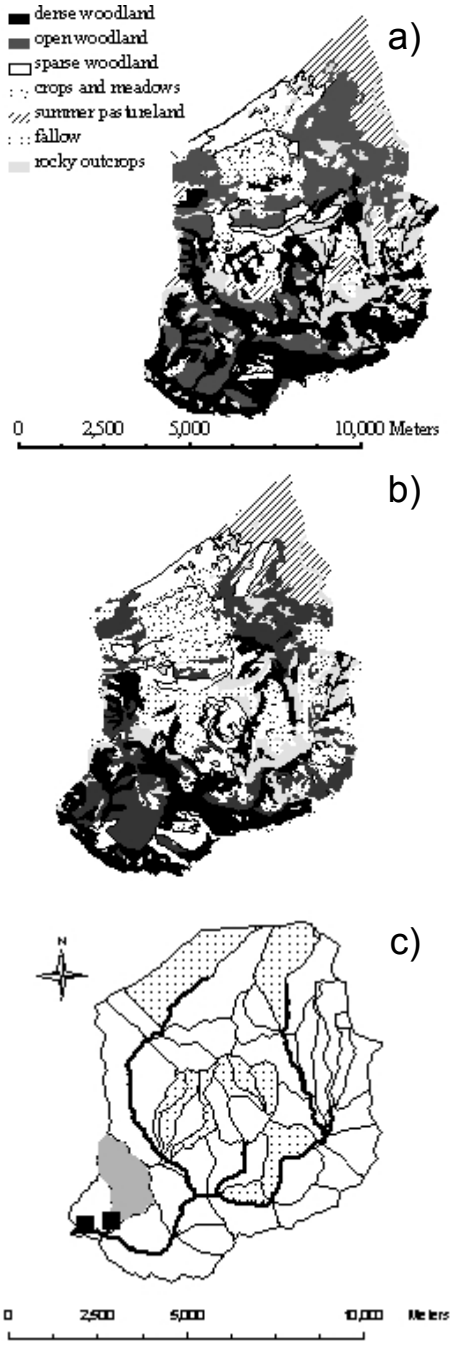

Fig. 1: Canalda Catchment characterisation: a) past (1957) and b) current (1993) land-use maps, derived after Ubalde et al. (1999), c) Canalda model domain with the river network, location of the nested catchment Cogulers (shaded grey), the sampling stations (■), landscape units derived with the LUMP algorithm (dotted units refer to hillslopes with large gradient).

The tested model was then used to simulate the effects of land abandonment and afforestation between 1957 and 1993 on runoff and sediment export out of the meso-scale catchment. To get an insight in the relative importance of environmental change on sediment export, the model was furthermore applied to evaluate the relative importance of land-use change scenarios in comparison with the potential effects of climate change scenarios on sediment budgets.

2. Materials and methods

2.1. Study area

Land-use change from agricultural use (mostly crop cultivation) to afforestation is examined in a headwater catchment of the Ribera Salada, a typical Pre-Pyrenean, mountainous river, tributary of the Segre River, in turn the major tributary of the Ebro. The area has a typical Mediterranean mountainous climate, where rivers never dry up, although flows are very low during the summer. Mean annual precipitation and evaporation varies between 500-800 mm and 700-750 mm respectively. Snowmelt plays only a secondary role and most floods are due to autumn and winter thunderstorms. The altitude ranges between 460 m a.s.l. in the southwest and 2400 m a.s.l. in the northeast of the entire Ribera Salada Catchment. The geology in the headwaters of the catchment is dominated by folded Triassic to Ecocene limestones, marls and some evaporites (gypsum and salts), whereas the central and lower parts of the basin are comprised by an extensive deformed Eocene-Oligocene molassic sequence at the bottom of a folded thrust. The catchment is mostly on conglomerate supporting, sandy-loamy soils; the erosion processes being rather limited under normal precipitation.

The current vegetation includes evergreen oaks and pines in the valley bottoms and deciduous oaks in the upper areas. Ubalde *et al.* (1999) evaluated the land-use change between 1957 and 1993 for the Canalda catchment (with at total area of 65 km^2) in regard to reduction of agriculture accompanied by land abandonment and subsequent afforestation. They reported a decrease of crop and meadowland from 9.1 to 3.7 km^2, a decrease of fallow land from 7.5 to 3.9 km^2 and an increase of forested areas from 26 to 40 km^2 (equivalent to 62 % of

the catchment area; from now on referred to as *past* and *current land-use*, Fig. 1a and b). The effect of this land-use change on water and sediment generation was evaluated here with the WASA-SED model (Güntner, 2002).

Daily model testing data are available for the Ribera Salada River at the outlet of the Canalda catchment (65 km^2, 42°5'45N, 1°27'26E) and the nested Cogulers catchment (2.4 km^2, 42°5'38N, 1°26'45E)**.** Flow discharge was measured daily with level sensors and suspended sediment concentrations were collected during storm events with ISCO 3700 automatic samplers covering the time period 1999-2000 (Batalla *et al.* 2005, Rius *et al.* 2001). A nearby climate station located in the centre of the Ribera Salada provides daily values for rainfall, temperature, humidity and radiation.

2.2. Model description

The process-based, spatially semi-distributed WASA-SED model (Güntner 2002, Güntner and Bronstert 2004, Mamede 2008) was employed to model the effects of land-use change on the generation of water and sediment fluxes. The WASA-SED model uses a multi-scale, hierarchical approach for landscape discretisation allowing the reproduction of small-scale influence in landscape variability on runoff generation and erosion along the catena, even if the model is applied to meso-scale catchments. The model runs with daily time steps and can be used for individual storm events and for long-term simulations. The model domain is spatially discretisised into *landscape units* that are homogeneous in regard to their major landform, lithology and soil associations and each landscape unit is composed of a number of *terrain components along representative catenas* that are homogeneous in regard to their slope gradients, soil associations and vegetation. Each terrain component is described by *representative profiles* of soil-vegetation components (see Güntner 2002 for a detailed description). The hydrological components contain process descriptions for interception, evapotranspiration, infiltration, soil water balance, overland flow (saturation and infiltration excess), interflow, groundwater discharge and a Muskingum river routing scheme. Sediment generation on the hillslopes in the form of soil erosion by water is modelled using the MUSLE-approach (Williams, 1995). Sediment routing is performed along the catena between the individual terrain components, i.e. any sediment mass coming from upslope areas is added to the generated sediment mass of each downslope terrain component to obtain the sediment yield. The sediment yield of a terrain component is limited by the transport capacity of the water flow leaving the terrain component, which is in turn a function of effective stream power of the overland flow. The sediment module thus takes explicitly into account the influence of the spatial variability of slope, vegetation and overland flow generation on the sediment transferral down individual catenas. Suspended sediment transport in the river network is modelled using the transport capacity concept, where the maximum sediment concentration that can be transported in the flow is calculated using a power function of the peak flow velocity (e.g. as in Neitsch *et al.* 2002). A full description of the WASA-SED model is given in Mueller *et al.* (2008), Güntner (2002) and Mamede (2008).

2.3. Parameterisation of the model

Appendix 1 summarises the necessary input parameters related to vegetation dynamics, soil properties and river hydraulics for the WASA-SED model. Model testing was conducted for the years 1999 and 2000 (with annual rainfall of 675 and 702 mm), where testing data were available. For the evaluation of the effects of land-use change in the Canalda Catchment, the land-use maps by Ubalde *et al.* (1999) from 1957 and 1993 were used (Fig. 1a, b). Spatial soil information was available from Ubalde *et al.* (1999), with dominant soil classes being Lithic Leptosol and Eutric Cambisol.

The relevant modelling elements for the WASA-SED model, i.e. landscape units, terrain components and soil profiles with soil-vegetation components were delineated using the semi-automated LUMP algorithm (Fig. 1c; for LUMP, see Chapter IV).

3. Results and Discussion

3.1. Testing of modelling results at Cogulers and Canalda

Sediment-transport models are particularly prone to propagation errors, as their performance depends to a great extent on the correct partition of overland flow and subsurface flow of the hydrological model (Wainwright and Parsons, 1998). Calibrating a process-based transport model may be regarded as distorting underlying process descriptions, and it was therefore decided not to employ model calibration, but rather to parameterise the model with measured soil, vegetation and hydrological parameters.

The simulated hydrographs in Fig. 2 depicted for both the smaller hillslope catchment Cogulers (2.5 km^2) and the mesoscale Canalda catchment (65 km^2) show that the temporal dynamics of the floods, i.e. the occurrence and timing of peak discharge of small-magnitude and larger flood events are reasonably well reproduced in most cases for the two years 1999-2000 and both spatial scales. As sediment transport occurs mainly during flood events, model testing was focused on the analysis of storm rather than interstorm periods (i.e. performance of the model to reproduce periods with low flow or baseflow was disregarded). The Nash-Sutcliffe (1970) coefficient of efficiency E was computed for individual flood events, where a rain storm normally occurred on the first day, and high flow continued for three to seven days afterwards, with E given by:

$$E = 1.0 - \sum_{i=1}^{N}(O_i - P_i)^2 / \sum_{i=1}^{N}\left(O_i - \tilde{O}\right)^2 \qquad \textit{Eq. 1}$$

where P_i are the simulated daily and O_i are the observed daily water discharges and N denoting the number of days a flood event last until water discharge is down to baseflow level (for the Ribera Salada: ca. three to seven days) and $\tilde{O}$ denoting the mean observed discharge over the entire period of an individual flood event.

The Nash-Sutcliffe index for the major storm events on Julian Day 138, 262 and 317 (1999) varies between 0.4 and 0.7 for the hillslope catchment Cogulers, and between 0.2 and 0.7 for the Canalda catchment. For the other storm events, negative values were obtained. For the rainfall event on Julian Day 293 (1999), the model apparently overpredicts runoff by a considerable amount (0.37 m^3/s versus simulated 2.93 m^3 for a rainfall amount of 23 mm at Canalda). No rainfall had occurred previously for one month. It appears that the model did not represent the dry upper soil layer and groundwater storage correctly, as it does not store and temporarily withhold infiltrated water in the sub-surface soil layers, but rather transfer it directly through groundwater recharge and interflow into the river. The model discrepancy for this storm event might have arisen due to a misrepresentation of the complex groundwater interactions of mountainous catchments. Considering that the WASA-SED model was originally designed for erosion processes in drylands, it includes only a simplistic description of groundwater processes, which overstates the direct contributions of interflow and groundwater recharge into the river (without considering any time delays).

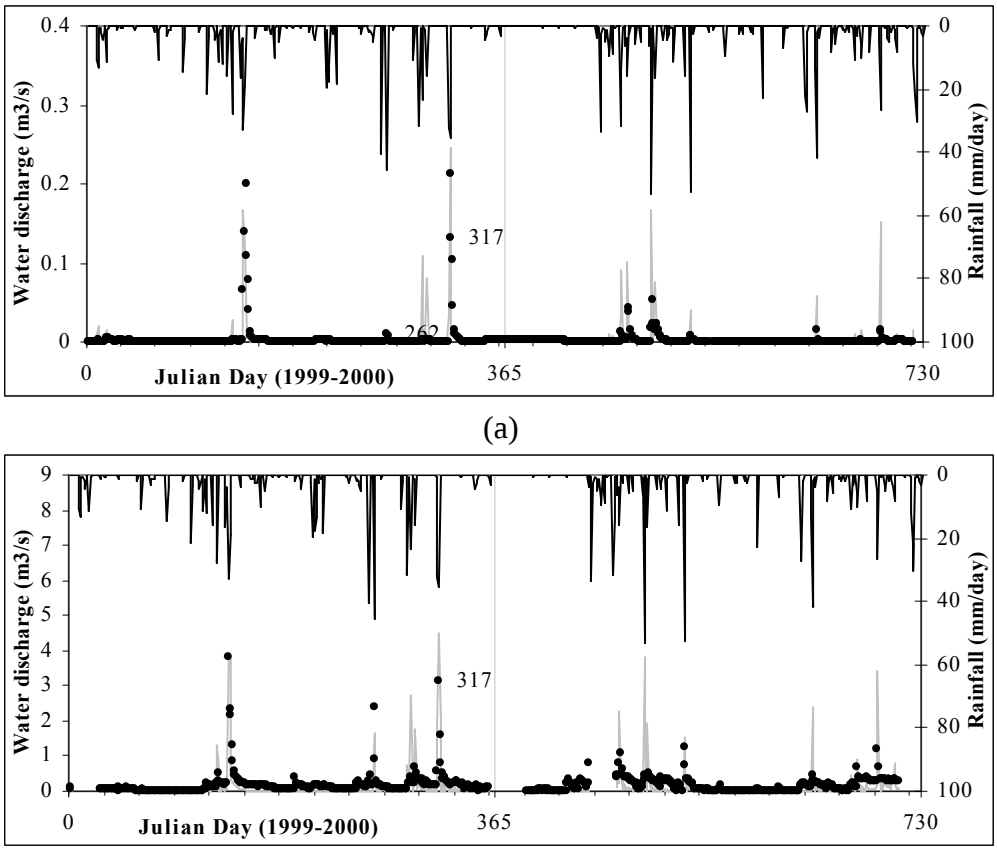

Fig. 2: Measured and simulated hydrographs at the outlet of Cogulers (a) and Canalda (b) for the years 1999-2000 (dots: measured, grey line: simulated, black line: rainfall, gaps in hydrographs are due to gaps in the measured time series).

On days 128 and 273 (year 2000), large amounts of rainfall occurred (53 and 44 mm), however, only comparatively small discharges were measured at Canalda (Tab. 1) with low runoff coefficients (8 and 5 %) compared to the yearly averaged runoff coefficient of 15 %. At the same time, at the smaller, nested Cogulers catchment, substantial runoff was measured on day 128 (year 200), which makes it unlikely that only little runoff occurs at the downslope Canalda outlet, unless the storm event was very localised.. The measuring device at Canalda failed to record several periods in the year 2000, so uncertainty towards the observed discharge data have to be taken into account when using these data for model validation.

The Nash-Sutcliffe coefficient is known to cause at times an underestimation of model performance due to time shifts or systematic differences between measurement and simulation (Jachner *et al.*, 2007). For the application of such a complex model, it may be considered more important to reproduce essential patterns instead of seemingly exact numerical values. Tab. 1 gives as two alternative measures for quality assessment the coefficients of determination (R^2) and a comparison of measured and observed total runoff and runoff coefficients per event. All three measures suggest strong similarities between measured and simulated flux values for the events on Julian Days 128, 297 (1999) and 107, 128, 273, 311 and 329 (2000) (Tab. 1). Considering all applied qualitative measures, one can summarise that the model shows poor performance for the small storm events (Days 293 in 1999, 273 and 311 in 2000), a good performance for the two large storm events (Day 162 in 2000 and 138 in 1999) and a mixed performance for medium storm events.

Tab. 1: Testing criteria for simulations runs of water fluxes at the outlets of Cogulers and Canalda catchments.

a) Cogulers (2.4 km^2)

Year	Julian Day	NS*	R^{2*}	Rain (mm)	Total runoff (m^3/day)		Runoff coefficient	
					measured	simulated	measured	simulated
1999	138	**0.4**	**0.64**	52	**57,216**	**30,154**	0.45	0.24
1999	262	**0.7**	**0.74**	45	**1,718**	**1,642**	**0.02**	**0.02**
1999	293	-2224.0	0.00	24	1,448	20,995	0.03	0.37
1999	317	**0.6**	**0.70**	68	**45,977**	**29,722**	**0.28**	**0.18**
2000	107	-1.1	0.52	16	**10,081**	**12,787**	**0.27**	**0.34**
2000	128	-6.9	**0.73**	53	**16,067**	**24,278**	**0.13**	**0.19**
2000	162	-15.5	0.56	53	2,070	5,702	0.02	0.05
2000	273	-10.0	**0.99**	44	1,717	5,789	**0.02**	**0.05**
2000	329	-99.0	0.46	27	3,432	14,774	0.05	0.23

b) Canalda (65 km^2)

Year	Julian Day	NS*	R^{2*}	Rain (mm)	Total runoff (m^3/day)		Runoff coefficient	
					measured	simulated	measured	simulated
1999	128	-10.0	**0.91**	28	**142,103**	**210,643**	**0.08**	**0.12**
1999	138	**0.2**	0.58	52	**941,472**	**742,694**	**0.29**	**0.23**
1999	262	**0.7**	**0.98**	45	**322,423**	**181,872**	**0.11**	**0.06**
1999	293	-87.0	0.30	24	109,177	385,085	0.07	0.26
1999	297	-10.0	**0.86**	16	**182,210**	**236,650**	**0.19**	**0.24**
1999	317	**0.5**	**0.82**	68	**703,984**	**696,730**	**0.17**	**0.17**
2000	107	-10.0	0.11	16	**295,718**	**289,354**	**0.30**	**0.29**
2000	128	-281.0	0.00	53	265,205	676,339	0.08	0.21
2000	162	**0.5**	**0.86**	53	**233,809**	**180,576**	**0.07**	**0.06**
2000	273	-118.0	**0.85**	44	129,348	305,338	0.05	0.11
2000	311	-0.3	**0.73**	10	**140,368**	**132,538**	**0.22**	**0.21**
2000	329	-9.9	**0.92**	27	219,175	385,258	0.13	0.23

* NS: Nash Sutcliffe index (1970)

** R^2: coefficient of determination

Bold: simulated storm events that show strong similarity to measured ones in regard to hydrograph shape, total runoff and runoff coefficient

As the significant part of soil erosion and sediment-transport occurs during large storm events, hydrological model performance was considered acceptable enough to examine the results of the erosion module. The testing of the simulated sediment fluxes is problematic as only a limited number of suspended sediment samples (6 to 24 samples) were collected for individual rainstorm events. However and despite of this limitation, sampling covers a wide range of flow conditions providing concentrations over the period of several hours. The derivation of the total sediment yield for a storm event from measured concentrations is not trivial, as the interpolation of concentrations between sampling times might considerably falsify actual sediment loads (Holtschlag, 2001). To get an insight into model performance, the simulated sediment concentrations were therefore compared with the range of measured minimum, mean and maximum concentrations where comparable values were obtained for Julian Days 317 (1999) and 108, 128, 131 and 272 (2000) (Tab. 2). The measurement in the beginning of April 2000 (day 107) with a mean value of 0.269 g/l and runoff of 1.1 m^3/s at Canalda was not reproduced by the model. Interestingly, only a small rainfall amount occurred that day (16 mm) and the previous rainfall event was 6 days before, with an amount of 31 mm. One potential explanation of the model discrepancy is that runoff generated by snowmelt in the upper parts of the catchment had led to a flushing of sediments that had accumulated in the river during the winter season – a process, which the model was unable to reproduce.

Tab. 2: Comparison between measured (mean, minimum and maximum values) and simulated sediment concentrations (SS) at the outlets of the Cogulers and Canalda catchments.

a) Cogulers (2.6 km^2)

Year	Julian Day	Measured SS (g/l)			Simulated SS (g/l)
		Mean	Min	Max	
1999	138	-	-	-	0.046
1999	290	0.062	0.005	0.130	0.000
1999	317	0.032	0.004	0.101	**0.098**
2000	102	0.039	0.005	0.080	**0.041**
2000	128	0.650	0.007	4.716	**4.796**
2000	131	0.016	0.000	0.077	**0.000**
2000	272	0.253	0.045	0.764	0.025

b) Canalda (65 km^2)

Year	Julian Day	Measured SS (g/l)			Simulated SS (g/l)
		Mean	Min	Max	
1999	138	-	-	-	1.730
1999	297	0.123	0.024	0.123	0.007
1999	317	0.161	0.040	0.606	**0.215**
2000	102	0.062	0.013	0.125	**0.030**
2000	107	0.269	0.063	0.932	0.020
2000	128	1.795	1.480	2.109	**1.131**
2000	272	1.442	1.261	1.622	**0.918**

Bold: simulated suspended sediment concentrations that fall within the range of minimum-mean-maximum values of measured concentrations

The model also simulated a considerable sediment concentration of 1.7 g/l at the outlet of Canalda on Day 138 (1999), when apparently no concentrations were measured. On the same day, a large runoff of 3.8 m^3/s was measured for a rainfall amount of 49 mm. It is unlikely that for a storm event of that size no sediment transport had occurred, which might suggest that the measuring device for suspended sediment failed to work on that day.

In terms of total annual sediment yield, the WASA-SED model calculated 2,045 tons for 1999 and 2,449 tons for 2000 for the Canalda Catchment. The values are of the same order of magnitude as annual suspended loads estimated by Batalla *et al.* (2005) who derived a mean load of 13,600 tons/year for the Canalda Catchment using the flow duration curve method proposed by Walling (1984) for the time period 1942-1995. However, as their estimated annual sediment yields exhibited a wide range varying between 16 t/year and 41,800 t/year, thus covering four orders of magnitude, a comparison of Batalla *et al.*'s results with the WASA-SED results appears impractical. At this point, it is difficult to say which estimating method produces more reliable results: the spatially explicit sediment-transport simulations of the WASA-SED model or the Flow Duration Curve method where measured discharge time series of a neighbouring catchment and a statistical relation in form of a power function between runoff and suspended sediment load were used.

3.2. Discussion of model performance and applicability

Overall, the testing of the simulated water and sediment fluxes shows that the WASA-SED model is able to reproduce the general dynamics such as occurrence and timing of flood events and the occurrence of sediment export in a reasonable manner. The hydrological module exhibits problems in reproducing some of the medium-sized flood events for the two testing years. The performance of the hydrological model could have been improved by employing calibration techniques, but it was refrained from doing so as the study did not focus on fitting curves to measured hydrographs, but to bridge the gap between

existing land-use and sediment flux data and both past and future changes in ecosystem structure. It is well known, that by using calibration it is possible to fit simulated hydrographs to measured hydrographs resulting in high Nash Sutcliffe coefficients; however, this often comes along with an utterly unrealistic pattern of source and sink areas and on the expense of process descriptions (Thapa and Bardossy, 2008, Mueller *et al.*, 2007). In a nutshell, major drawbacks of calibrating a spatially distributed, process-based model include drastically limited portability of the model parameterisation (e.g. in regard to different land-use parameterisation), significant deviation of calibrated model parameters to measured parameters in the field and inadequate integration over spatial variability of the model input parameters. It was decided that an uncalibrated model that reproduces large storms, where most of the sediment-transport occur, in an appropriate manner would give a more reliable picture of the interlinked land-use and sediment budget dynamics than a calibrated (and potentially overfitted) model with distorted process description and corresponding error propagation. The model performance is considered at this point not adequate enough to simulate land management scenarios, e.g. for the identification of those hillslopes which are particularly prone to sediment export and thus should be afforested to reduce sediment export. However, as no calibration was employed, the model is thought to be portable allowing calculations with altered boundary conditions, i.e. for different past and future land-use and climate change scenarios.

Keeping in mind that currently hardly any information are available on sediment budgets for past and future land-use for that region (Valero-Garces *et al.*, 1999), the following model scenarios will give some first quantitative figures and thus an important baseline for hypothesis building and future discussion on the evolution of sediment budgets in such a dryland setting. For the analysis of the subsequent model scenarios, it has to be kept in mind that while the testing study showed that the overall results are plausible, the model did show limitations in its performance. Uncertainties towards for example the consistency of the testing data set of monitored water and sediment fluxes, the spatial variability of rainfall data for high-intensity storm events and potentially the insufficient process descriptions of groundwater movement, snowmelt and interstorm periods in combination with the potential error propagation of the hydrological modules on sediment export calculations recommend caution as with any modelling exercise at the meso-scale (Mulligan and Wainwright, 2004, Quinton, 2004).

3.3. Comparison of simulated runoff and sediment export for past and current land-use change scenarios

Scenario simulations were carried out to compare the generation of simulated runoff and sediment export from the Canalda catchment between current land-use and the land-use of the 1950s. The two land-use maps by Ubalde *et al.* (1999) were used as described in section 2.3 (Fig. 1). In addition, two extreme land-use scenarios were evaluated: a complete afforestation and an intensification of agriculture of the entire catchment. Current water and sediment budgets were compared with the ones for the past, forest and agriculture scenarios for a representative dry, medium and wet year (496, 675 [test year of section 3.1] and 772 mm/year, respectively, time series as measured in Canalda over the last ten years) and for an individual, previously tested, large storm event on day 317 of 1999 (runoff discharge of 3.5 m^3/s, which is equalled or exceeded 2 % of the time) that performed well in the testing study (Table 3). That budgets of the individual storm event, in which a substantial amount of the annual sediment yield was produced and the yearly budgets show the same trends, should build some confidence for the application of the model for the calculation of annual budgets for different land-uses. The annual budgets suggest that the

past land-use generated almost the same runoff volume, but 35-76 % more sediment fluxes in comparison to current land-use. A complete afforestation potentially leads to a considerable decrease of runoff (14 to 40 %) and a nearly 100 % reduction of sediment export out of the catchment. In contrast, the intensification of agriculture may result in a substantial increase in both runoff (4 to 19 %) and sediment export (279 to 514 %).

No quantitative data are available for the Ribera Salada region on the alteration of runoff volume and sediment export due to the land abandonment and afforestation over the last 50 years. However, the comparison of past and current land-use is in line with quantitative studies that were conducted in the Pre-Pyrenean region, as described in the introduction. Lopez-Moreno *et al.* (2006), for example, detected a negative trend in flood intensity and a decrease in the siltation rates of reservoirs due to a decrease of sediment export from headwater catchments of the Ebro. However, the simulated reduction of runoff is much less than the one reported by Begueria *et al.* (2003), who obtained a runoff reduction of around 30 % for the past 50 years through time series analysis of data from gauging stations in the Pre-Pyrenean region. The reduction of Begueria *et al.* is more similar to the one simulated for the scenario of complete afforestation (runoff reduction from current land-use between 14-40 %). This suggests that the land-use change in the Canalda catchment over the last 50 years might not have happened in an efficient manner: most of the afforestation occurred in the central band of the catchment and the change might have had a larger effect on runoff and sediment budgets if it would have been carried out on the steeper slopes in the upper parts of the catchment, where large amounts of runoff are generated (see shaded areas in Fig. 1c).

Although the fourth scenario - the renewed intensification of agriculture -appears unlikely at the moment, it might become a more attractive option in the light of climate change over the next new decades. According to Leipprand *et al.* (2008), temperatures for the inland of the Iberian Peninsula are projected to increase by between 1.8–2°C every 30 years in the summer months and are projected to have increased in total up to 5-7 °C for the time after 2070. If temperature increase forces farmers from the Ebro lowlands to use fields in the higher parts of the Pre-Pyrenees, as is already starting to happen with vineyards (Nash, 2007), then stringent land management practices are required to avoid a potential modelled increase of sediment export of up to 400 %.

Tab. 3: Percentage change of annual water and sediment budgets for current land-use in comparison to past land-use, complete afforestation and intensification of agriculture for the Canalda Catchment.

	Land-use	Unit	Dry year	Medium year	Wet year	Single event
Water	Current	m^3	1631837	3518813	6214579	827971
	Past	% change	2 %	0.3 %	-0.5 %	0.5 %
	Complete afforestation	% change	-40 %	-33 %	-18 %	-14 %
	Intensive agriculture	% change	19 %	15 %	4 %	13 %
Sediment	Current	tons	10	2045	9297	1919
	Past	% change	40 %	76 %	35 %	50 %
	Complete afforestation	% change	-97 %	-99.8 %	-99.4 %	-99.9 %
	Intensive agriculture	% change	279 %	421 %	514 %	333 %

3.4. Comparison of the impact of land-use changes with potential effects of climate change

The WASA-SED model can now be utilised to get an insight into the relative importance of environmental change: what has a larger impact on a dryland setting as the Canalda Catchment in regard to runoff and sediment export - land-use change or the potential effects of climate change (e.g. changes in the precipitation regime)?
The land-use change scenarios were implemented to cover the wide range of potential land-use varying from an intensification of agriculture (100 % of catchment area used for agriculture) over an extensification (mixed used) to an extreme scenario of complete afforestation. For the mixed scenarios, a sustainable land-use was assumed where afforestation occurs first on the steeper hillslope, and extends further downslope as the forest area increases. As stated before, the intensification of agriculture appears unlikely at the moment, but its occurrence is possible if current lowland agriculture in the Ebro Depression is forced uphill by increasing temperatures (see section 3.3, Nash, 2007). Although land-use changes may be driven by the indirect consequences of climate change, the two drivers were evaluated here independently.
Leipprand *et al.* (2008) and Moreno *et al.* (2005) derived climate change projections for Spain using several general circulation models and a regional climate model. They predict, within their reported boundaries of uncertainty, in regard to precipitation: 1) for the autumn season, a slight increase of rainfall for the north-eastern part of Spain (15-45 mm); 2) in spring and summer seasons, a decrease of precipitation across the Spanish peninsula with pronounced reductions in the northern coastal and mountainous regions during the summer (45-180 mm); and 3) a reduction in the number of events by the 2080s, but at the same time an increase in the intensity of storms in the Mediterranean basins (i.e. there might be a smaller number of storm events, but the few storms will generate floods of higher intensity than normally occur today). Current climate change scenarios are highly uncertain and contradictory for the Southern Pyrenean region (with uncertainty of predictions up to ± 50 %), suggesting both an increase and a decrease of rainfall rates, which makes the derivation of time series of future rainfall difficult. The substantial part of sediment export is caused during a small number of large-magnitude floods and no export is typically generated during low-flow conditions. Therefore, the climate change scenarios were implemented by altering the rainfall intensities of storm events through varying the daily rainfall amount in percentages (using the current land-use after Ubalde, 1999). Variations of storm frequencies were not considered in this study.
Figures 3 and 4 display the variation of annual runoff and sediment yield for the Canalda Catchment for a representative dry, medium and wet year (see Section 3.3, note that the numbering of the x-axis for the climate change scenario is in inverse order to match the increase of runoff and sediment yield corresponding to an increase in agricultural fields or precipitation). For the medium year, more runoff and at the same time a comparatively similar amount of sediment yield is produced for changes of annual rainfall varying between ± 20 % and catchment area covered with forest varying between 0 and 100 %. For example, a decrease of rainfall by 10 % is equivalent to an increase of catchment area by 25 %. For the dry year, no sediment production occurred for any of the scenarios.
Simulated sediment budgets resulting from the land-use change towards intensive agriculture equates with the change in total sediment budgets from an *in*crease of rainfall by around 20 % for the medium year. At the same time, annual runoff increases by factor 1.5 when the catchment is simulated with a 20 % increase of annual rainfall in comparison to the intensive agriculture scenario for the medium year.

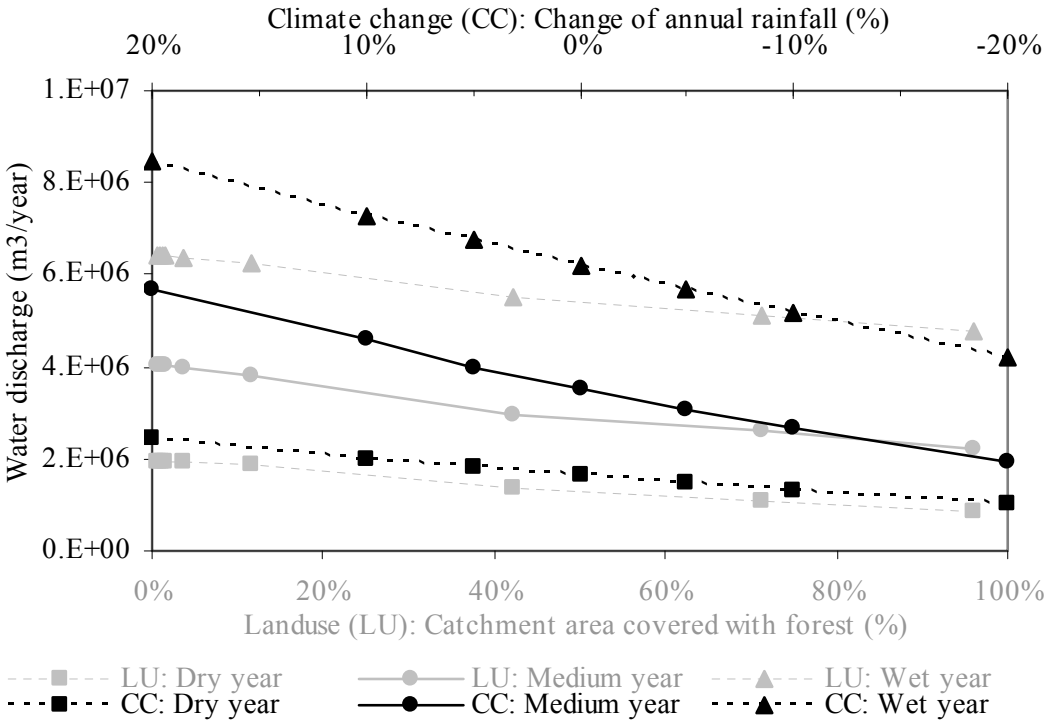

Fig. 3: Comparison of the relative importance of climate change (CC: annual rainfall varying between ± 20 %) and land-use change (LU: catchment area covered with forest, reminding area used for agriculture) on annual runoff at the outlet of the Canalda Catchment (for a representative dry, medium and wet year). Note: the budgets for the climate change scenarios with 0 % rainfall change correspond to the present land-use and climatic settings.

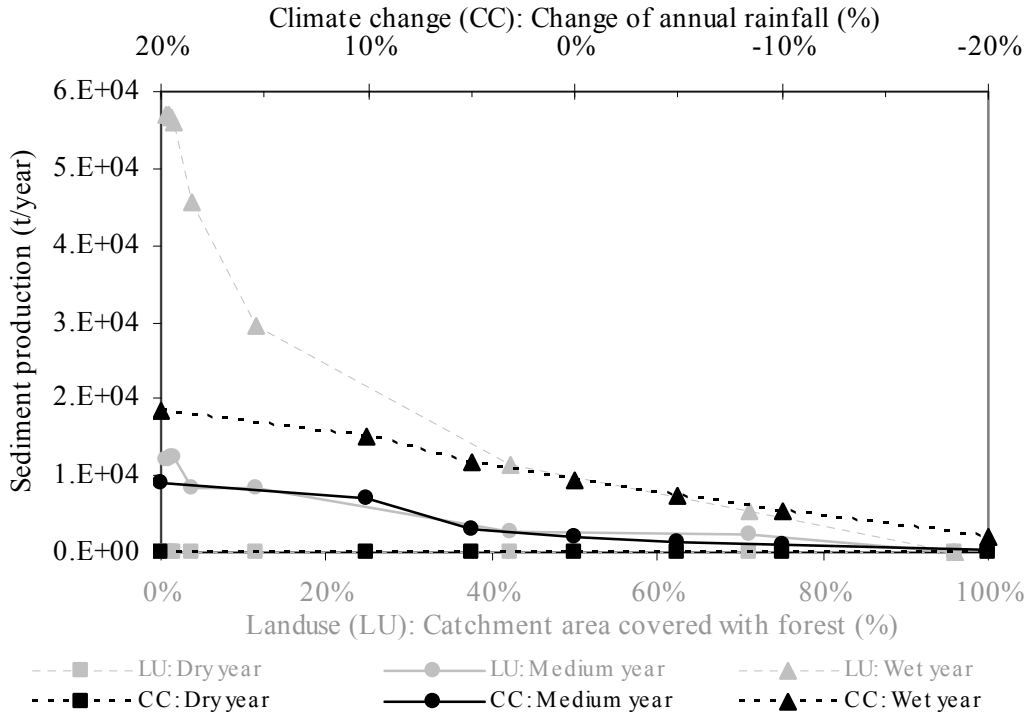

Fig. 4: Comparison of the relative importance of climate change (CC: annual rainfall varying between ± 20 %) and land-use change (LU: catchment area covered with forest, reminding area used for agriculture) on annual sediment yield at the outlet of the Canalda catchment (for a representative dry, medium and wet year).

For the wet year, an increase of rainfall by 20 % generates an equivalent increase in runoff amount, but a substantial smaller sediment yield (31 %) in comparison to the intense agriculture scenario.
The scenario for a complete afforestation equates to the climate change scenario with a reduction of rainfall by 20 %, resulting in small annual runoff rates and no sediment production for both scenarios. For this climate scenario, already a relatively small reduction in annual rainfall rates decreases the power of the large storm events to such an extent that they are not able to produce enough overland flow and thus no erosion on the steeper hillslopes.
The relative importance of environmental change can now be rated for the land-use and climate change scenario simulations. The modelling simulations suggest that a 20 % decrease in annual rainfall results in a decrease in runoff and sediment yield, thus an ecosystem stabilisation in regard to sediment export, which can only be achieved by a substantial land-use change towards complete afforestation. At the same time, a 20 % increase in rainfall causes a large export of water and sediment resources out of the catchment, equivalent to an intensive agricultural use of 100 % of the catchment area. For wet years, the effects of agricultural intensification are more pronounced, so that in this case the intensive land-use change has a significantly larger impact on sediment generation than climate change. The plots in Figure 3 and 4 on the rating of environmental change can only be interpreted within the stated limits of parameterisation and model uncertainties; however they give some first quantitative figures and an important baseline for future discussions on how such a dryland setting might undergo future ecosystem stabilisation or alteration.

4. Conclusions

Socio-economic reasons have led to an environmental change in the form of land abandonment and afforestation of formerly agricultural land for substantial parts of the Southern Pyrenees since the 1950s, resulting in a decrease of sediment export towards the Ebro Depression. The WASA-SED model proved capable of reproducing the general dynamics of water and sediment budgets of current land-use and provided some quantitative measures on runoff and sediment export for past and extreme land-uses (renewed intensification and complete afforestation) for the meso-scale Canalda catchment. The Canalda area is an interesting example of how a previously intensively used ecosystem was stabilised in regard to water and sediment generation and this ecosystem stabilisation can be taken as being representative for the mountainous regions of the north-eastern part of the Iberian Peninsula (i.e. Southern Pyrenees). However, the region might experience future destabilisation due to the possible effects of climate change. Although future climate projections for the region are highly uncertain, the model gave some answers on the relative importance of land-use versus potential climate change scenarios. It enabled a direct comparison of annual water and sediment budgets for land-uses ranging from intensive agriculture to complete afforestation with equivalent budgets for altered annual rainfall regimes.
The presented results are based on an uncalibrated but tested model that enabled a simplified reproduction of the underlying erosion and transport dynamics. It was decided that an uncalibrated, process-based model that reproduces large storms, where most of the sediment-transport occur, in an appropriate manner would give a more reliable picture of the interlinked land-use and sediment budget dynamics than a calibrated model with distorted process descriptions. Current soil erosion models at the meso-scale are thought not advanced and user-friendly enough to be employed for land management applications (de Vente *et al.*, 2008). However, although the modelling results may not yet provide firm grounds for land management and deci-

sion-making purposes, they provide a sufficient degree of confidence that at least the order of magnitude of simulated budgets for the future and past environmental change scenarios are plausible. At the same time, they give a first quantitative baseline on how to compare and discuss the impacts of land-use and climate change in an organised manner, which may prove valuable for hypothesis building and for setting up new monitoring schemes and modelling efforts for sediment budgeting along dryland catenas.

5. Acknowledgements

This research was carried out within the SESAM (Sediment Export from Semi-Arid Catchments: Measurement and Modelling) project, funded by the Deutsche Forschungsgemeinschaft. Authors gratefully acknowledge the work done by two anonymous reviewers whose comments greatly improved the original version of the manuscript.

Appendix: Model input parameters

Specification of vegetation parameters

Vegetation	Stomata resist. [s/m][4]	Min suction [hPa][4]	Max suction [hPa][4]	Ksat [mm/h][1]	Height [m][4]	Root depth [m][4]	LAI [-][4]	Albedo [-][4]	Manning's n [-][2]	MUSLE C [-][3]
Agriculture, annual crops	195	2756	22000	75	0.6	1.71	3.16	0.24	0.2	0.25
Meadows and pastures	30.2	250	8000	75	0.3	0.14	0.4	0.2-0.27	0.045	0.1515
Deciduous woodland	119	650	8000	500	5.13	2.05	0-5.64	0.2-0.26	0.2	0.00158
Coniferous woodland	119	650	8000	500	10	2.75	4.54	0.1-0.16	0.2	0.00058
Sparse woodland	119	650	8000	500	7.57	2.16	2.27-4.88	0.15-0.19	0.2	0.05
Shrubs	400.6	650	8000	140	1.5	1	2-3.35	0.16-0.29	0.15	0.031
Rock	770	613	8000	0	0.09	0.1	0.1	0.3	0.02	0

[1] Verdu *et al.* (2000); [2] Morgan (1995) ; [3] Antronico *et al.* (2005) ; [4] Breuer *et al.* (2003)

Specification of soil parameters (de la Rosa *et al.*, 2004)

Soil	No. of horizons	Residual w.c. [Vol %]	W.c. at PWP [Vol %]	Usable field capacity [Vol %]	Saturated w.c. [Vol %]	Thick ness [mm]	Suction at wetting front [mm]	Pore size index [-]	Bubble pressure [cm]
Ustochrept/Ustorthent (Ustifluvent)	3	0.056	0.239	0.117	0.388	300	163	0.332	40
Ustorthent/Ustochrep (Haplustalf, Haplustoll)	2	0.062	0.239	0.133	0.438	300	31	0.340	175
Cryorthent/Cryochrept (Cryoboralf, Rendoll)	2	0.069	0.239	0.126	0.409	233	48	0.295	71
Ustorthent/Ustochrept (Rhodustalf)	2	0.062	0.239	0.133	0.438	300	31	0.340	175
Rock	1	0.056	0.082	0.346	0.439	300	70	0.500	150

values given for uppermost horizon, w.c.: water content, PWP: permanent wilting point

MUSLE K: computed from particle-size distribution and OM-content of topmost horizon based on Williams (1995)

Specification of terrain and river parameters

Parameter	Value
Hydraulic conductivity of bedrock	5 mm/h
Mean maximum depth of soil zone	500 mm (Batalla *et al.* 2005)
Depth of river bed below terrain component	500 mm
Initial depth of groundwater below surface	1500 mm
Storage coefficient for groundwater outflow	5 days
Bankful depth of river	0.5-2 m
Bankful width of river	4-12 m
Run to rise ratio of river	2 m/m
Bottom width of floodplain	20-100 m
Run to rise ratio of floodplain side slopes	4 m/m
Manning's n for riverbed	0.02

Slope, hillslope length and portions of terrain components were derived from a 30-m resolution digital elevation model

Chapter VII:

Modelling water and sediment yield in the highly erodible Isábena catchment, NE Spain

Abstract

This study explores the performance of the numerical model WASA-SED in terms of hydrology and sediment yield prediction for the Isábena (450 km²) and its sub-catchments. The approach outlined for calibrating five key parameters performed reasonably robustlybut several parameter optima exist. The sensitivity of the model to different parameter optima, variation in rainfall data and different configuration of the hillslope erosion-routine is analyzed.
The model yields an adequate reproduction of the measured water and sediment fluxes for the considered periods of 4 months and 3 years, respectively. The hydrological model, despite the daily resolution and partially inadequate input data situation, achieves Nash-Sutcliffe efficiency values of 0.32 to 0.84 (calibration period) and 0.52 to 0.61 for the validation period (3 years).
Comparing different approaches suggests that the performance of the sediment model is highest when a combination of MUSLE or MUST, applied at the scale of landscape units, combined with a transport capacity limitation is used. Sediment yield is predicted with as little as 11 % error for the Villacarli catchment, but with an overestimation ranging from 48 to 96 % for the catchment outlet during the validation period (3 years). This is mainly caused by an overestimation of erosion in the Lower Isábena. Further limitations of the model comprise the correct representation of transmission losses of water and temporary sediment storage in the main channel.

Keywords: badlands, erosion modelling, hydrological modelling, sediment yield

In preparation for submission to *Catena*

.

1. Introduction

In many catchments and rivers worldwide, erosion causes a variety of challenges. On-site effects like soil degradation and the loss of fertility of agricultural areas affect the areas of sediment generation. On the other hand, detached sediments that are conveyed to the river network can pose a multitude of problems related to channel navigability, habitat of riverine species, irrigation water supply, power generation and reservoir siltation (Walling, 1977; Williams, 1989). While many relevant processes take place on the scale of hillslopes and first order catchments, the usual management scale comprises entire river basins and is thus situated at the meso-scale. The complexity of the interacting processes (e.g. sediment detachment, transport to the river, deposition and remobilisation in the river channel) require an approach that can integrate these processes and accommodate the heterogeneity of the study area. Numerical modelling is a suitable approach to fulfil these demands. The WASA-SED model (see Chapter V) has been developed to represent the relevant hydrological and sediment-related processes. Its discretisation scheme allows integrating characteristic features of the catchment while maintaining reasonable input data, storage and computational demands. Parameterizing and validating the model for a meso-scale catchment allows the assessment of the model's capabilities and limitations, and in future steps opens up the possibility of predicting the catchment behaviour under changing environmental conditions, such as land-use and climate change. An improved prior knowledge of the catchment's response enables the development of adaptation strategies that can mitigate possibly negative impacts induced by the changing environment.

This study presents the application of WASA-SED to the Isábena catchment. The parameterisation and derivation of input, calibration and validation time series (section 3.2), and a calibration strategy (section 3.3) is described. The two major components of the WASA-SED, hydrological (section 4.1) and sediment model (section 4.2), are analysed with regard to their performance and sensitivity to uncertainties in the model input. The subsequent validation comprises the comparison of model results to measurement at three different levels. Finally, four land-management scenarios are analysed (section 4.4).

2. Study area

The study area covers the catchment of the Isábena river. It comprises 445 km² in the Central Spanish Pyrenees and drains to the Ebro. The area experiences a typical Mediterranean-mountainous climate with a strong north-south gradient due to topography in precipitation (450-1600 mm) and potential evaporation (550-750 mm/a) (Verdú *et al.*, 2006a).

Land-use is dominated by agriculture, pasture and mattoral in the lower parts and higher fractions of woodlands of evergreen oaks and pines in the upper parts. The very heterogeneous lithology includes Paleogene and Cretacious sediments in the north and Miocene continental deposits in the southern lowlands. The latter comprise easily erodible Marls that lead to the formation of badlands. In spite of their low areal fraction in the catchment (<0.02 %, see Chapter III), the extremely high erosion rates of the unvegetated surfaces make them a major sediment source for the catchment (Fargas *et al.*, 1997). Badlands are concentrated almost exclusively in the sub-catchment Villacarli (see Fig. 24a), which causes strong contrasts in terms of specific sediment yield within the catchment (Chapter III). The silty sediments generated by the badlands can be efficiently transported by the river to the Barasona reservoir at the catchment outlet at large quantities (> 200,000 t a^{-1} ≅ 440 t km^{-1} a^{-1}, López-Tarazón *et al.* 2009). This reservoir supplies water for ca. 70,000 ha of irrigated land in the Ebro depression. The reservoir's initial capacity of 92 hm³ (Valero-Garcés *et al.*, 1999, Navas *et al.*, 2004) has been progressively re-

duced by siltation, with only minor relief due to engineering works during the 1990s. The current reservoir capacity of just 76 hm^3, the high sediment input from its tributaries and the continuing water demand demonstrate the need for a thorough assessment of water and sediment dynamics in the basin (Mamede, 2008).
The catchment was instrumented to measure discharge and suspended sediment concentration close to its outlet (gauge Capella) and the two major headwater catchments Villacarli and Cabecera (Fig. 1). Chapter III provides details on instrumentation and measurements.

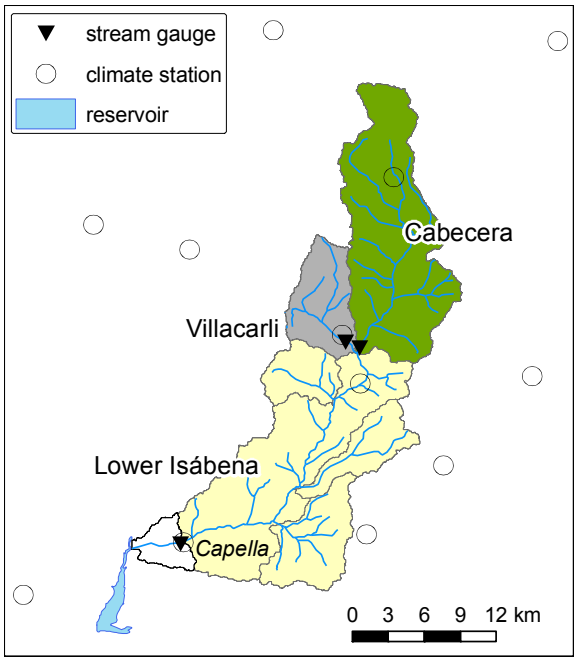

Fig. 1: Isábena catchment: instrumentation and sub-catchments.

3. Methods

This section summarizes the methods applied during this study. Due to the complexity of many of them, the descriptions have been condensed (but for futher details see Müller & Francke, 2009). In the first section (3.1), the WASA-SED model is introduced, followed by a description of the parameterisation procedure (3.2). The sections on calibration (3.3) and validation (3.5) give information on the adjustment of the model and performance assessment, while model sensitivity is analyzed in section 3.4. The last section describes the generation of scenarios (3.6). The respective results are presented separately for the hydrological model (section 4.1) and the sediment model (section 4.2).

3.1. The WASA-SED model

In this study, the WASA-SED model was used for water and sediment modelling. This processed-based, spatially semi-distributed model is based on the hydrological model WASA (Güntner, 2002; Güntner & Bronstert, 2004) which uses a multi-scale, hierarchical approach for landscape discretisation. This allows reproducing the influence of small-scale landscape variability on runoff generation along the catena and within the catchment, even if the model is applied to meso-scale catchments. The model's discretisation scheme consists of

a) sub-basins
b) landscape units (LUs; areas that are homogeneous in terms of geology, soil and vegetation associations, landform along the toposequence)
c) terrain components (parts of the landscape unit with homogeneous slope)
d) soil-vegetation components (combination of land-use and soil with characteristic sequence of soil horizons).

The hydrological model contains process descriptions for interception, evapotranspiration, infiltration, soil water balance, overland flow (saturation and infiltration excess), interflow and groundwater discharge at the hillslope scale. With WASA-SED, a Muskingum river routing scheme, an advanced reservoir module (Mamede, 2008) and sediment related routines have been added. The model provides four erosion equations for sediment generation based on derivatives of the USLE equation (Wischmeier and Smith, 1978): USLE, Onstad-Foster, MUSLE and MUST (Williams, 1995), which can be applied at the sub-basin or landscape unit scale and are optionally combined with a transport-capacity limitation by Everaert (1991). Suspended sediment transport in the river network is modelled using the transport capacity concept where the maximum sediment concentration that can be trans-

ported in the flow is calculated using a power function of the peak flow velocity (e.g. as in Neitsch *et al.* 2002). For a full description of the WASA-SED model see Chapter V.

3.2. Parameterisation

3.2.1. Geospatial data for model parameterisation

A variety of geospatial data is required for the parameterisation of WASA-SED. Tab. 4 summarizes the data sources used in this study.

3.2.2. Semantical data sources

The geographical data on the distribution of soils and land-use classes had to be complemented by respective properties of the mapped classes. The soil properties (soil hydraulics and particle size distributions) were parameterized based on the soil data base derived from the SEISnet-soil data base MicroLEIS (de la Rosa *et al.*, 2004). The properties of badland surfaces were obtained from own measurements (35 samples); "bare rock" surfaces were considered completely impermeable. This procedure resulted in 34 soils featuring 17 distinct horizon associations. The plant-physiological parameters were extracted from the Plant Parameter Database (PlaPaDa, Breuer & Frede, 2003, and Breuer *et al.*, 2003). Seasonal dynamics of the vegetation parameters were not included.

Manning's n values for land-use classes are based on Morgan (2005). The USLE soil erodibility factor K and coarse fraction factor were computed from particle-size distribution and OM-content of topmost horizon (Williams, 1995). Values for the USLE cover factor C resulted from data for Mediterranean areas published by Antronico *et al.* (2005), Pistocchi *et al.* (2002), ARSSA (2005), Morgan (1995) and López-Vicente *et al.* (2008); the protection factor P for cropland was assigned according to ICONA (1987); for all other land-use classes P was set to 1. The river properties were determined using field-work data and by DEM analysis.

3.2.3. Catchment discretisation, delineation of landscape units

The catchment was subdivided into six sub-catchments as proposed by Verdú (2003). The delineation of landscape units and the derivation of their respective parameters were performed using the LUMP-algorithm (Chapter IV), using the map layers soils, land-use and the abundance of badlands as ancillary information. This procedure resulted in 82 landscape units with 5 terrain components each. The ground water delay *gw_delay* of a LU was assumed to be a function of its length *length_lu*, mean slope *slope_lu* and fraction of bare rock surface *frac_rocky*:

$$gw\_delay = k \cdot length\_lu \cdot (1-frac\_rocky)/slope\_lu \quad \text{Eq. 1}$$

The factor *k* was used in the calibration (see below).

Tab. 4: Geospatial data sources.

Layer	Source	Author	Resolution / scale
topography	DEM generated from ASTER and SRTM data using stereo-correlation	SESAM, unpublished	30 m
soils	Mapa de suelos (Clasificacion USDA, 1987)	CSIC/IRNAS, 2000	1:1 000 000
Lithology	Geología Dominio SINCLINAL DE TREMP; mapa "Fondos Aluviales"	CHEBRO, 1993	1:50 000 / 200 000
Land-use	Usos de Suelos (1984/1991/1995) de la cuenca hidrográfica del Ebro	CHEBRO, 1998	1:100.000
Badlands	Digitized from high-resolution airphotos	SESAM, unpublished	1:5000
River stretches	Field survey	SESAM, unpublished	-

3.2.4. Input time series, meteorological parameters, test data

Climate data used in this studies originate from measurements at the stations of the Instituto Nacional de Meteorología (INM), the stations of the Sistema Automático de Información Hidrológica (SAIH) and own measurements. For the time span of the modelling, data from 11, 5 and 1 station(s) were available for rainfall, temperature and humidity/radiation, respectively. Where necessary, data were aggregated to daily resolution. Separate time series for each sub basin resulted from inverse-distance interpolation to the centroids of the sub-catchments.

Sub-daily rainfall variability is considered in WASA-SED for the mean rainfall intensity correction (*kfcorr*) and the maximum 30-minutes rainfall intensity (*I30*). Both were admitted time-variant to account for varying intra-daily rainpeaks. They were implemented by regression with the daily rainfall amount in the form of

$$kfcorr = kfcorr\_a \cdot daily\_precip^{-1} + 1 \quad \text{Eq. 2}$$

and

$$I30 = a \cdot daily\_precip^{b}, \quad \text{Eq. 3}$$

respectively (Fig. 2), where *daily_precip* is daily rainfall [mm] and *kfcorr_a*, *a* and *b* are regression coefficients.

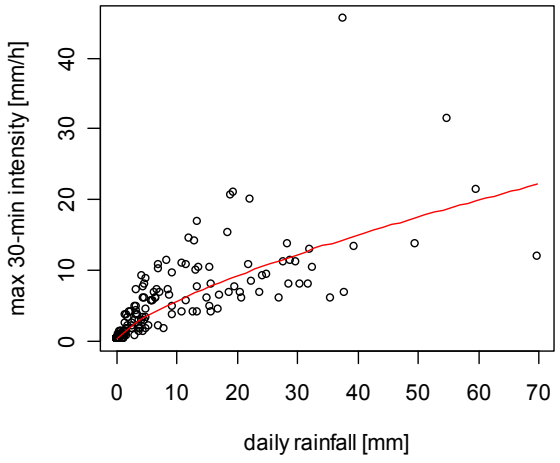

Fig. 2: Estimation of maximum 30-min rainfall intensity from daily rainfall (example from the raingauge Villacarli, R2log= 0.89).

Discharge data used in the calibration and validation process was obtained by own measurements (Cabecera, Villacarli) or from the water authorities (Capella). Suspended sediment concentration was determined using a flood-based sampling scheme or automatically in the case of Capella. Details on instrumentation can be found in Chapter II. Nonparametric multivariate regression using Quantile Regression Forests allowed the reconstruction of continuous sedigraphs and flood-based sediment yields (details in Chapter III).

3.3. Calibration

Despite its process-oriented concept, several parameters for the WASA-SED remain immeasurable and have to be calibrated. Calibration also serves to compensate for the parameter inaccuracy that arose from the regionalisation of sparse data and their incommensurability, caused by their scale- and model-structure dependent interpretation as compared to real measurements.

From the findings of Güntner (2002) and manual testing, five parameters were identified as crucial. These are the ground water recession constant (*gw_delay*), the soil depth of soil profiles that are not terminated by bedrock (*soildepth*), the hydraulic conductivity of the bedrock (*kf_bedrock*), the depth of the river bed below the land surface (*riverdepth*) and a correction factor for the hydraulic conductivity of the soil horizons (*kfscale*). Each parameter was initialized with a plausible value according to field observations, literature or set to 1 (*kfscale*). Calibration was then performed by applying factors to these default values (denoted as *_f*). Constraining the interval of these factors ensured that the respective parameters remained within a physically plausible range.

To achieve optimum results, the calibration was performed automatically for the three gauges where measured discharges were available (see Tab. 5). The Lower Isábena was calibrated with pre-specified (i.e. measured) inflow of the two headwater catchments Cabecera and Villacarli, the temporal extent of which determined the calibration period.

Tab. 5: Calibration, spatial and temporal extent.

Gauge	Included sub-catchments	Discharge data / calibration period	Sediment data
Cabecera	1	15/09/2006 - 27/04/2008	15/09/2006 - 04/01/2007
Villacarli	1	11/09/2006 - 30/04/2007	11/09/2006 - 04/01/2007
Capella (Lower Isábena)	4 (+2 pre-specified)	15/09/2006 - 29/01/2007	complete

A compound weighted expression served as the objective function *o*:

$$o = RMSE_{all} + 2 \cdot RMSE_{hiflow} \qquad Eq.\ 4$$

where RMSE stands for the root mean squared error for the entire series ($RMSE_{all}$) and that of high flows only ($RMSE_{hiflow}$). The latter served to emphasize the optimization on the good representation of floods.

Parameter optimization was first attempted using the gradient-based optimization software PEST (Doherty, 2004). The results, however, suggested that the algorithm only produced minor improvements on the parameter set, presumably due to many local minima of the objective function and/or poor initial estimates. Consequently, better initial estimates had to be found, using Latin Hypercube-based sampling of the parameter space (McKay *et al.*, 1979). However, the pronounced parameter interaction and the resulting equifinality (e.g. Beven, 2000) inhibited the detection of parameter optima and did not produce well-performing and plausible parameter sets. Therefore, this concept was enhanced by classifying the discharge data into four phases: low-flow, rise, peak and recession. Now each parameter's perceived influence as implemented in the model concept was evaluated by assigning values of 0 (no influence) to 2 (very influential) as listed in Tab. 6.

Tab. 6: Perceived parameter influence for phases of the hydrograph expressed as weighting factors f_*.

	$f_{lowflow}$	f_{rise}	f_{peak}	$f_{recession}$
gw_delay	2	0	0	1
soildepth	1	1	1	2
kf_bedrock	2	1	1	2
riverdepth	1	1	1	2
kf_scale	1	2	2	2

Each parameter's performance was evaluated for each phase by using a compound objective function *o**:

$$o^* = f_{lowflow} \cdot o_{lowflow} + f_{rise} \cdot o_{rise} + f_{peak} \cdot o_{peak} + f_{recession} \cdot o_{recession} \qquad Eq.\ 5$$

where o_{phase} is a measure-of-goodness (i.e. RMSE, bias, Nash-Sutcliffe index) for the respective phase. This scheme was applied iteratively by successively narrowing the parameter ranges to intervals that produce behavioural simulations (see Fig. 3). This process revealed (local) parameter optima for most parameters and ensured parameter combinations that were physically plausible and thus consistent with the model's process description. The 30 best parameter sets (in terms of RMSE, Nash-Sutcliffe coefficient and bias) served as initial parameter estimates for runs using PEST. The resulting optimum parameter sets produced by PEST often differed considerably in their values despite providing very similar performance of the hydrological model, underlining the equifinality of the problem. Of these, the best performing parameter sets in terms of RMSE were used for further analysis. The overall best set was used as a reference scenario. The uncertainty introduced by this somewhat arbitrary choice is addressed in the sensitivity analysis (section 3.4).

The calibration was restricted to the hydrological model only. For sediment modelling, the performance of 12 settings of the sediment model was assessed for each subcatchment. These 12 combinations resulted from the four erosion equations USLE (Wischmeier and Smith, 1978), OF (Onstad and Foster, 1975), MUSLE, MUST (Williams, 1995) and 3 application options (application on sub basin scale, LU-scale with and without transport capacity limit according to Everaert (1991); for details,

see description of erosion module in Chapter V). The relative error e_{SY} in total sediment yield served as a measure of model performance:

$$e_{SY}=(Y_{sim}-Y_{obs})/Y_{obs} \qquad \text{Eq. 6}$$

where Y_{sim} and Y_{obs} denote simulated and measured sediment yield, respectively. Additionally, observations and model results are compared on an event-basis with regard to manually assigned flood event and the periods between these ("interfloods").

3.4. Sensitivity analysis

Güntner (2002) extensively analysed the sensitivity of WASA's hydrological output to various model input data, such as precipitation, model structure and parameters for his study area in Ceará, Brazil. His settings differ in several aspects from this study: the considerably larger spatial scale (the typical sub basin size for Ceará is comparable to the area of the entire Isábena catchment), rainfall seasonality (much more pronounced in Ceará) and the higher number of climate stations (which allowed the comparison of different interpolation techniques for Ceará). Thus, his results are not directly transferable to the situation for the Isábena. Furthermore, Güntner focussed on long-term water balance, while this study needs to aim for an adequate representation of flood events and sediment yields. With regard to these aspects, for this study two key issues (precipitation and model parameters) are investigated. The analysis is limited to the uncertainty due to (1) the hydrological parameterisation and the calibration strategy and (2) those that is related to the inaccuracy of rainfall data, conducted for the Villacarli catchment because of its outstanding importance for sediment generation.

The sensitivity to the choice of parameter set (1) was evaluated by comparing the best five sets of the hydrological parameterisations resulting from the 30 PEST runs (see 3.3). The sensitivity to rainfall (2) was assessed by running the model with modified rainfall time series, which were generated by simple scaling of the daily data by -20 to +20 %.

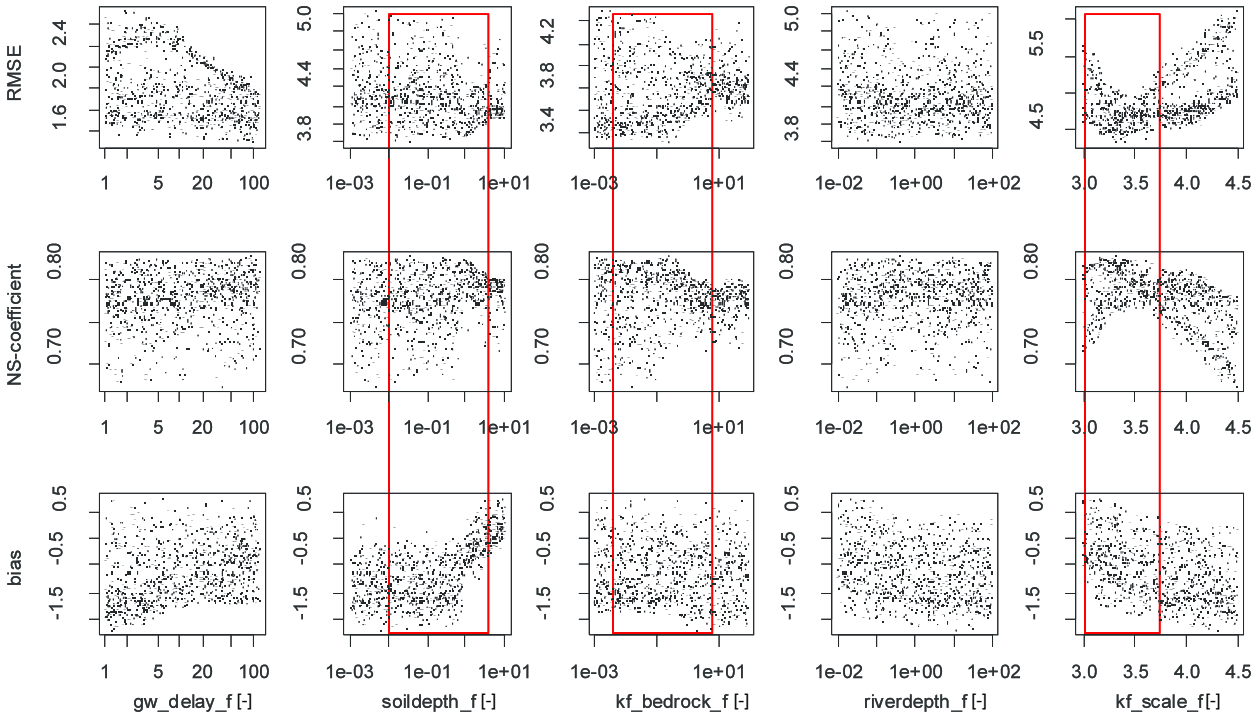

Fig. 3: successive narrowing of parameter ranges using phase-specific goodness-measures (example from lower Isábena, 3. iteration. For the subsequent iteration, the ranges of parameter factors soildepth_f, kf_bedrock_f and kf_scale_f can be narrowed as shown by the red boxes).

3.5. Validation

Due to the limited extent of the data for the headwater catchments (6 months), no direct validation could be performed without compromising the length of the calibration period too much. Instead, a joint validation using the long time-series at the catchment outlet (Capella, see Fig. 1) served for this purpose.

For the final assessment of model performance, validation was performed at three levels: Firstly, the measured discharge of the headwater catchments (Cabecera, Villacarli) was substituted by the model output of these two sub-catchments for the calibration period (validation 1). Secondly, a homogenous parameterisation of the entire Isábena was assembled (validation 2). For this, the best parameter set of the three sub-catchments was used to calculate a lumped parameter set by using the arithmetic mean, as opposed to the validation 1 and 3, where each sub-catchment is parameterized with a specific parameter set.

Thirdly, the overall model performance was evaluated by using the separately-modelled output of the headwater catchments for a longer simulation period (01/05/2005 to 30/04/2008), including and excluding the calibration period (validation 3).

3.6. Scenario definition

Since badland formations in the Isábena constitute a major sediment source despite their relatively low areal extent (Chapter III), these areas can be effective targets for the reductions of sediment yield (e.g. Kirkby & Bracken, 2005). Remediation measures can range from on-site solutions (revegetation, geotextiles, etc.) to off-site measures like the construction of sediment traps. These traps in their simplest form may consist of a sufficiently large plain at the footslopes of the badlands to allow the deposition of a large fraction of the eroded sediments. One such trap has inadvertently been constructed by road works at the Torrelaribera-badland (B1), which has been extensively studied during fieldwork.

The example sediment trap at Torrelaribera was subject to several fieldwork measurements and monitoring of the colluvial volume, erosion-, deposition- and sediment export rates (SESAM, 2006). Simultaneous monitoring of erosion, deposition and sediment delivery allowed the estimation of the trapping efficiency of the trap which is estimated at 6 to 18 %. The scenarios assume that sediment retention measures of similar efficiency can be implemented at all slopes that contain badlands. The model includes this by assuming a sediment delivery ratio (SDR) of 94 % (=100 %-6 %, scenario 1) and 82 % (=100 %-18 %, scenario 2) for all landscape units that contain badlands. As visible in Fig. 24a, this mainly affects the Villacarli sub-catchment.

Scenario 3 assumes that mattoral vegetation can be re-established at all badland areas. Thus, it implies an optimum success of mitigation measures, which is a rather optimistic assumption. The scenario is parameterized by assigning the respective vegetation attributes of the mattoral to badland areas and replacing the USLE K- and C-factors accordingly. Soil hydraulic properties remained unmodified.

Scenario 4 serves as a comparison of the above mentioned options to optimized agricultural practices. Renschler *et al.* (1999) compared different crop rotation cycles in Spain and computed a reduction in the C-factor from maximum (poorest option) to the minimum (best sediment management) by 43 %. This value corresponds closely to 42 % difference in C-values between “conventional” and “biologic” agriculture in Italy (Märker *et al.*, 2008) and 40–65 % reduction of erosion due to improved agricultural practice for Croatia (Basic *et al.*, 2004). Therefore, for scenario 4 we assume a reduction of 45 % in the C-factor for all agricultural areas. Lacking detailed temporal information, this reduction is superimposed on the seasonal C-factor dynamic given by López-Vicente *et al.* (2008). For all scenarios, the simulation period covered is June 2005 until April 2008.

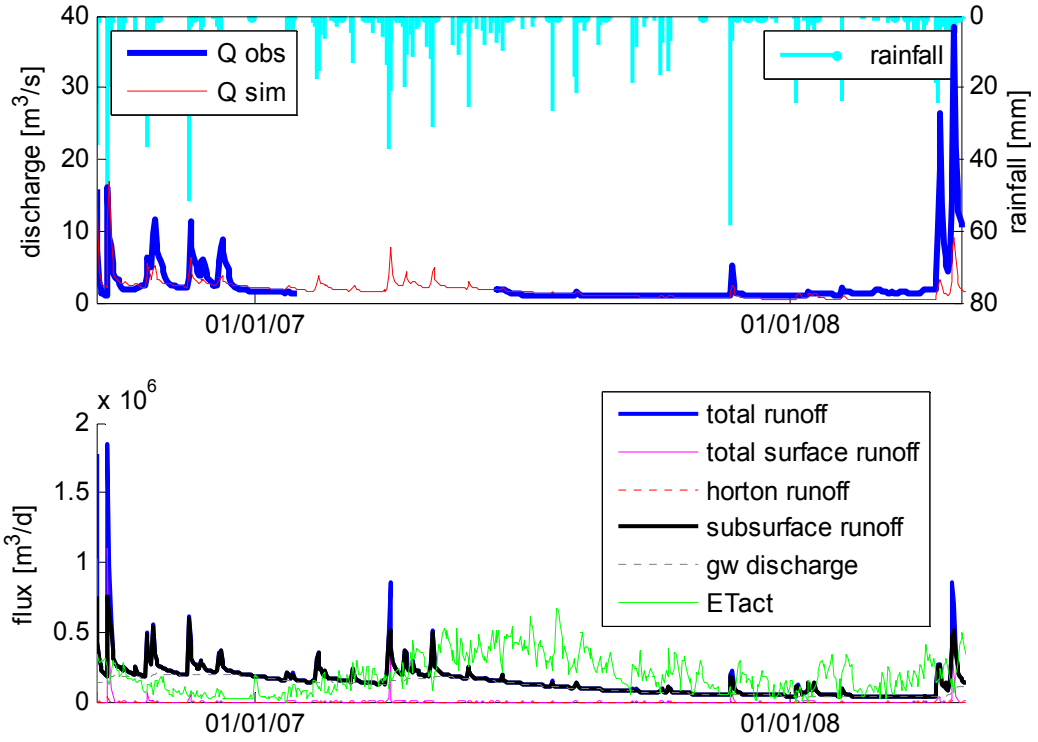

Fig. 4: Model results of best parameter set for Cabecera catchment, calibration period. Q obs: observed discharge; Q sim: simulated discharge; gw discharge: discharge from groundwater storage; ETact: actual evapotranspiration.

4. Results and discussion

4.1. Hydrological model

4.1.1. Calibration

Tab. 7 lists performance measures for the entire calibration period and a period excluding the heavy floods of September 2006 and April 2008. Apparently, WASA-SED has difficulties reproducing both these large floods and the periods of less discharge with a single parameter set for all catchments.

Tab. 7: Summary of model performance during calibration period. NS: Nash-Sutcliffe coefficient.

Gauge	NS (complete)	NS (without major floods)
Cabecera	0.32	0.50
Villacarli	0.70	0.24
Capella	0.84	0.81

For Cabecera, the model performs acceptably for the September and October 2006 period. The model performance deteriorates over the rest of the calibration period, tending to underestimate peakflow. Underestimation is especially apparent for April 2008. The detailed view of the flow components in Fig. 4 illustrates a plausible regime: surface runoff occurs only during heavy storms, subsurface runoff on the scale of days and a groundwater dynamic on the monthly scale.

The underestimation of the April 2008 floods may partially be a result of the inadequacy of the parameterisation of vegetation dynamics in the model. In reality, vegetation (and thus evapotranspiration) is at its minimum in the winter season. However, vegetation dynamics are not considered in the parameterisation, leading to relatively high evaporative fluxes even in winter. This presumably results in an underestimated antecedent soil moisture and thus less runoff for the storms of April 2008 in the model. Likewise, the mismatch may merely be a result of comparatively low rainfall at the raingauge Las Paules, which dominates the interpolation of rainfall data and thus may lead to an underestimation of mean precipitation for the Cabecera sub basin.

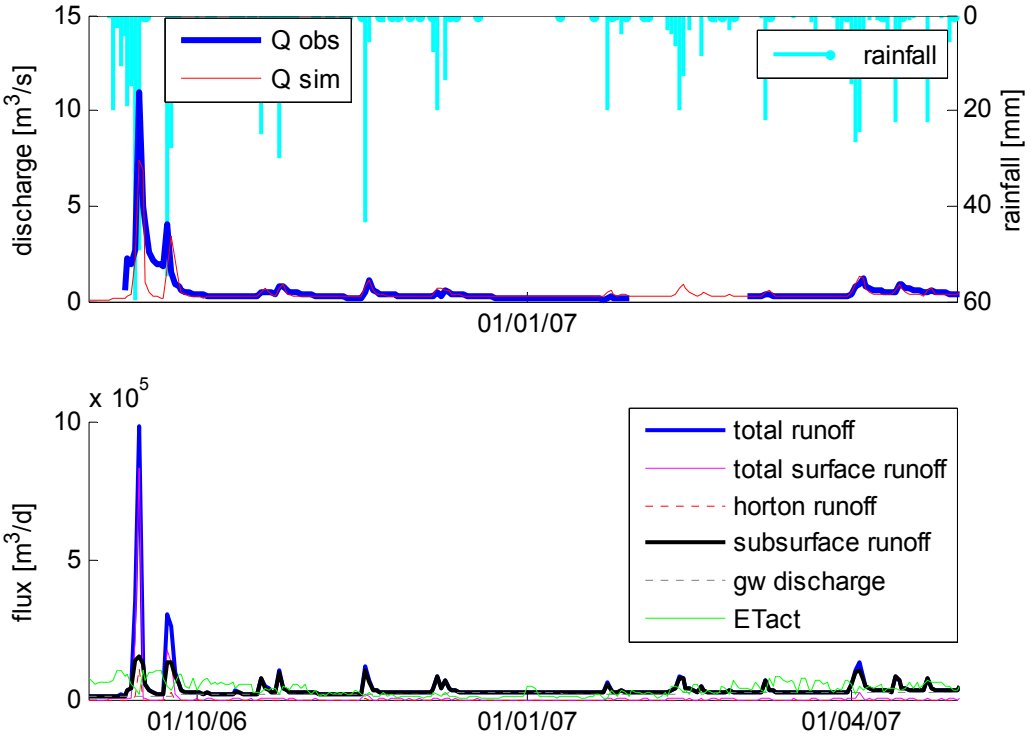

Fig. 5: Model results of best parameter set for Villacarli catchment. For abbreviations see Fig. 4.

In contrast, model performance for the Villacarli sub-catchment (see Tab. 7, Fig. 5) is much better with only some volume deficits for the September 2006 and a tendency to overestimation during low-flow periods. The flow components in Fig. 5 are plausible, except for the very slow groundwater response, which causes the unrealistically high base flow discharge.

The volume deficits for the September 2006 floods are probably a result of difficulties in establishing the stage-discharge relationship for these high discharges and an unstable river cross-section at the gauge (cf. Chapter III).

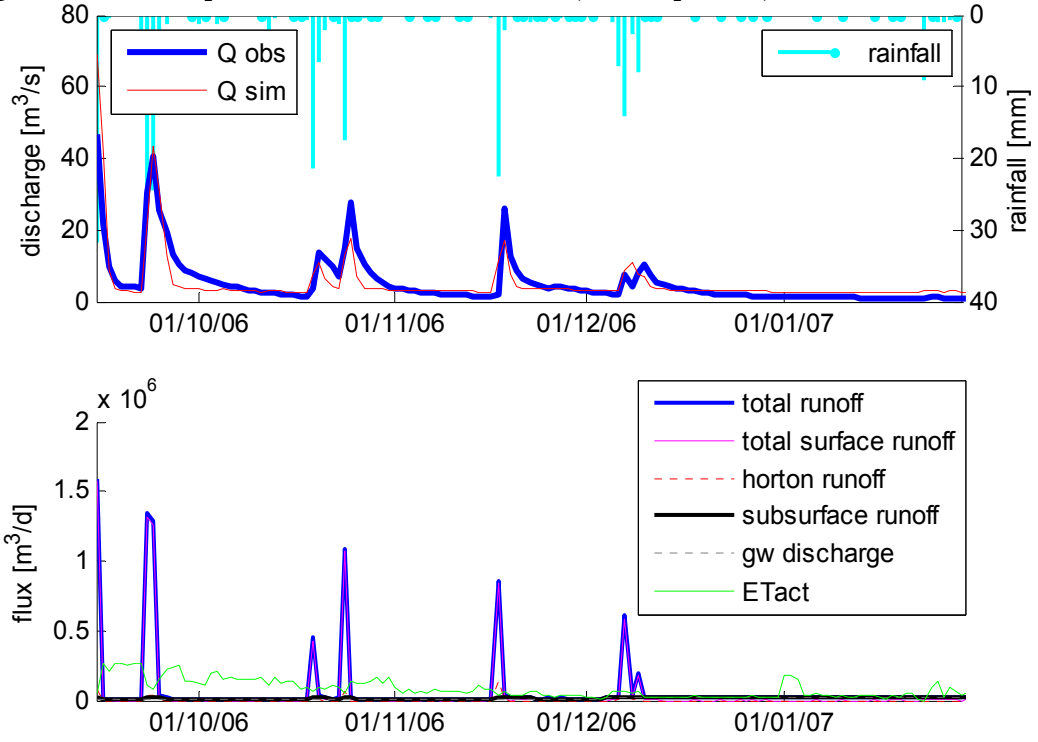

Fig. 6: Model results of best parameter set for Lower Isábena catchments. For abbreviations see Fig. 4.

Among the three modelled sub-catchments, the Lower Isábena shows the least differences between the performance for the full time span and the time span excluding the floods (Tab. 7). However, despite feeding measured discharge of the headwaters into the model, some shortcomings of the model are apparent (Fig. 6). The model tends to produce the onset of the floods too early for some floods (mid-Oct and mid-Nov 2006) although the timing of the peak discharge is correct. Consequently, the rising limb is slightly attenuated when compared to the observations.

Low flow is generally overestimated. However, during these periods, the *measured* discharge at the headwaters can exceed twice that of the outlet, which is presumably caused by transmission losses in the riverbed (details are discussed in section 4.3). Since these losses have not been parameterized, the model is bound to overestimate low flows when transmission losses are relevant.

These shortcomings suggest that the processes in the river (conveyance, transmission losses) are not adequately reflected with the simple parameterisation used in this study. Preliminary tests also point to the fact that the resolution of one day is too coarse for the processes described.

4.1.2. Sensitivity analysis

As laid out in section 3.4, the model's sensitivity to the uncertainties due to choice of parameter set and due to inaccuracy of rainfall data are assessed for the Villacarli sub-catchment, using the best five sets of the hydrological parameterisations resulting from the 30 PEST runs (see 3.3).

(1) Uncertainty due to choice of parameter set

NS-values of the 5 best hydrological parameter for the full simulation period range from 0.58 to 0.70; for the constrained period (i.e. without the major floods of Sep 2006) from 0.24 to 0.31 (Tab. 8). An increase in performance for the smaller floods seems to be correlated with reduced performance for the entire period which, again, underlines the difficulties in adequately reproducing low flows and peaks with the same parameter set.

Tab. 8: Model uncertainty due to choice of parameter set, Villacarli sub-catchment.

#Paramset	NS (complete)	NS (without major floods)
1 (reference)	0.70	0.24
2	0.69	0.25
3	0.59	0.29
4	0.61	0.36
5	0.58	0.31

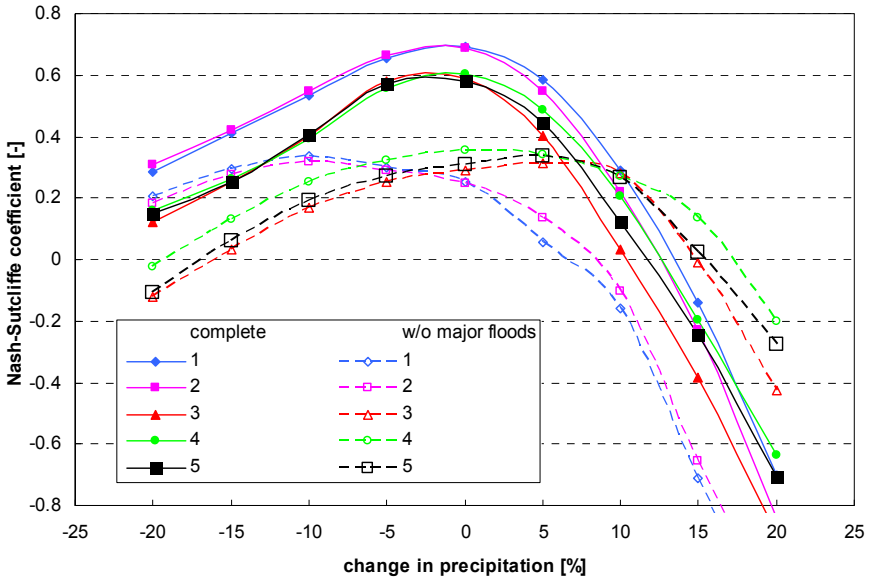

Fig. 7: Sensitivity of hydrological model to errors in rainfall input data.

(2) Uncertainty due to inaccuracy of rainfall data

Rainfall data are subject to measurement errors and effects introduced by the regionalisation (i.e. representativeness of included stations, interpolation method). Fig. 7 illustrates the effects of an assumed error in rainfall (from -20 to +20 %) on the performance of the hydrological model.
For all five parameter sets, the total model efficiency decreases when an error in the rainfall data is introduced. The magnitude of this decrease is very similar throughout the five parameter sets. However, the model efficiency for the constrained period is affected diversely: The two parameter sets of superior overall performance (1 and 2) reach a maximum efficiency of 0.31 to 0.33 when rainfall is reduced by 10 %. In contrast, the remaining parameter sets show a slight improvement if rainfall is increased by 5 %.
Conclusion: Absolute differences in overall model performance between the five best parameter sets in terms of the NS-coefficient are about 0.12 and are thus comparable to a change in rainfall amount of -7 or +5 %, respectively. Considering the current density of rain gauges in the catchment (~1 raingauge/100 km²), the large spatial variability of the rainfall (Verdú *et al.*, 2006a) and the simplistic interpolation method used, an error of at least the magnitude of 10 % must be expected. Therefore, the uncertainties in rainfall data appear to outweigh the uncertainties related to the hydrological parameterisation.

4.1.3. Validation

As explained in detail in section 3.5, the model validation was performed for the catchment outlet (gauge Capella) at three levels: semi-distributed parameterisation of the entire Isábena catchment (Cabecera, Villacarli and the Lower Isábena, validation 1), modelling the Isábena catchment with a lumped parameter set (validation 2) and extending the simulation period to three years (validation 3).

Validation 1: Semi-distributed parameterisation of entire catchment

With a NS-coefficient of 0.71 (Tab. 9) discharge is still adequately reproduced by the model when using the modelled output of the headwater catchments instead of the measured data (as used in the calibration). Deviations are apparent, especially during recessions and low flow conditions (Fig. 8), reflected in a NS-coefficient decreased to 0.65 when the major floods are excluded. The relatively low contribution of the Lower Isábena sub-catchment to total runoff (cmp. *Q simsubbas* vs. *Q sim*, Fig. 8), despite its large area, is consistent with observations (Verdú *et al.*, 2006b).

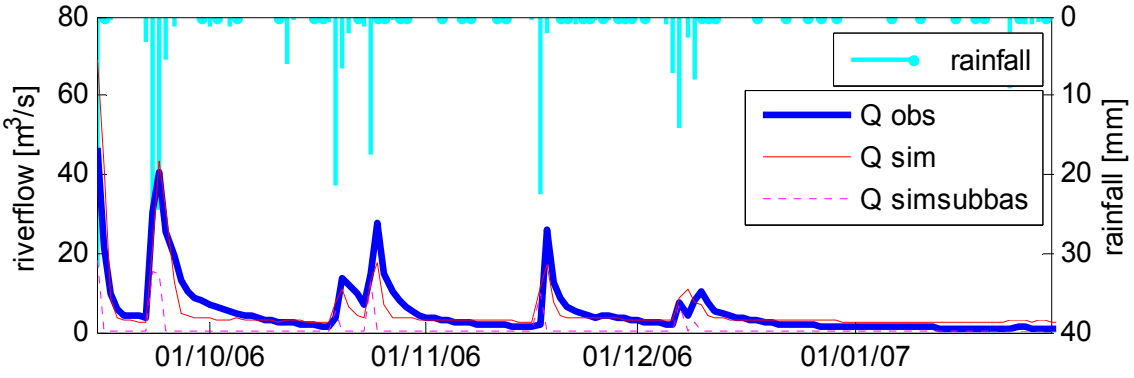

Fig. 8: Model validation at gauge Capella (Lower Isábena) using modelled headwater discharge (validation 1). Q simsubbas: runoff generated in the Lower Isábena.

Tab. 9: Performance of hydrological model at the catchment outlet (Capella) at three validation levels compared to performance of calibration.

	NS (complete)	NS (without major floods)
calibration	0.83	0.81
validation 1	0.71	0.65
validation 2	0.55	0.38
	01/05/2005 – 30/04/2008	**without calibration period**
validation 3	0.61	0.52

Validation 2: Lumped parameterisation of entire catchment

Aggregating the sub basin-specific parameter sets obtained from the calibration to a homogenous parameterisation reproduces the discharge at the catchment outlet with significantly lower performance than the distributed version in validation 1 (Tab. 9).

Discharge is underestimated almost all of the time (Fig. 9). The poor performance suggests that the calibrated parameter sets for the single sub basins are very specific and cannot be substituted by a homogenous parameter set. The reasons for this may be the undue aggregation of spatial heterogeneity (soils, bedrock, etc.) when using a lumped set, the heterogeneity of rainfall characteristics (aggregated into a single value of *kfcorr* for all sub basins) and/or simply the choice of different local optima during the calibration, the arithmetic mean of which is far from any optimum. Consequently, the tested lumped parameterisation is currently unfeasible. Evidently, the model needs to accommodate sub basin-specific values of the calibrated parameters. Alternatively, calibrating a lumped parameter set could result in a single set with better performance. However, given the computation times of running the model at the catchment scale, its implementation will be time consuming and the performance at the basin scale will presumably be lower.

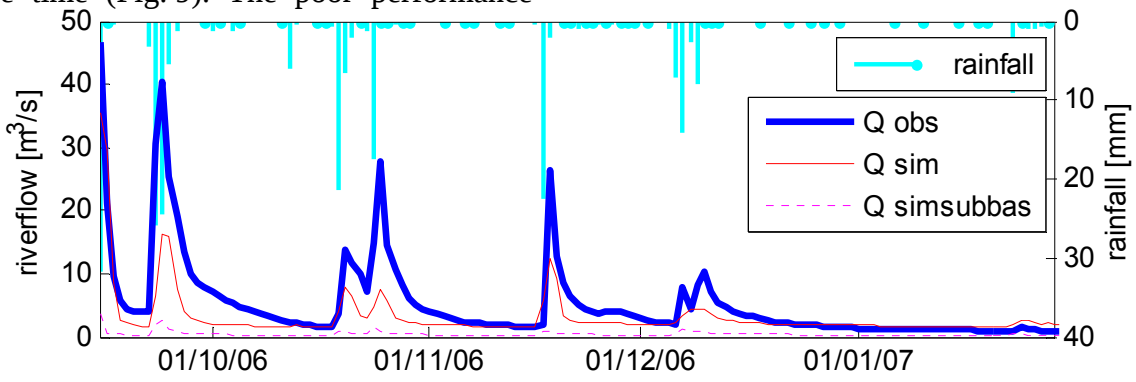

Fig. 9: Model validation at gauge Capella (Lower Isábena) using a lumped parameterisation.

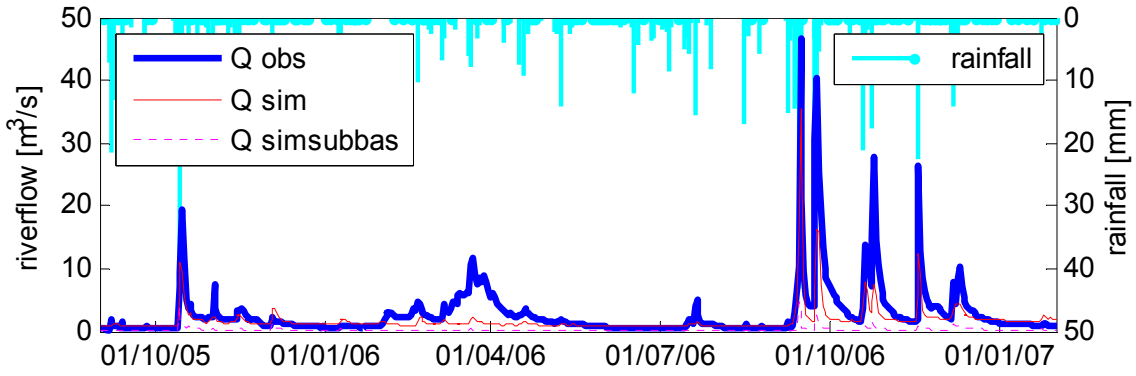

Fig. 10: Validation of entire Isábena catchment for an extended time span (01/05/2005 – 30/04/2008).

Validation 3: Semi-distributed parameterisation for extended time span

For this part of the validation, the model runs were performed separately for each sub basin as in validation 1. Simulation period was 01/05/2005 to 30/04/2008, which corresponds to the record of SSC-measurements.

The model's efficiency for the full period reaches 0.61. Excluding the calibration period, this value declines to 0.52 (Tab. 9). The model tends to overestimate the peaks of the large floods (Fig. 10). This may be an artefact of rainfall interpolation method: while inverse-distance interpolation usually tends to lower rainfall intensities, it may overestimate total rainfall in the catchment under certain circumstances. Due to their distribution, the three northernmost rain gauges in the catchment (see Fig. 1) dominate the interpolated values for the major part of the catchment. Hence, at any time that rainfall is recorded at these three gauges, the interpolation will effectively impose relatively high precipitation rates (orographic North-South gradient, Verdú *et al.* 2006a) onto roughly two-thirds of the catchment. This leads to the overestimation of areal rainfall, when rainfall is actually much more localized and/or restricted to the higher altitudes.

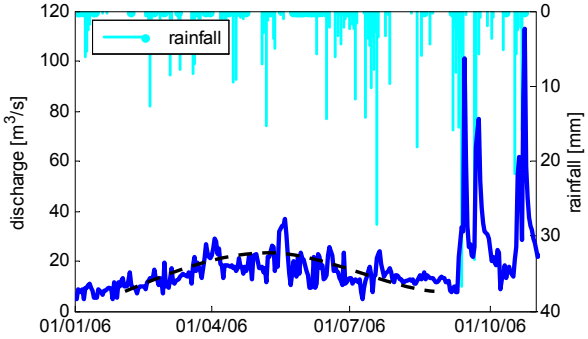

Fig. 11: Discharge of the Ésera (gauge Graus) showing the influence of snowmelt highlighted by the dashed line

The floods of spring 2006 and February 2007 are particularly poorly reproduced. During these periods, snowmelt processes are assumed to cause the somewhat atypical catchment response. This assumption is supported by a similar shape (although even more damped) of the hydrograph of the Ésera river in the neighbouring catchment (Fig. 11). Lacking a process description for snowmelt, WASA-SED necessarily reproduces discharge poorly during these periods. However, excluding these periods and the calibration period improves the model's efficiency only slightly to 0.56.

Baseflow is overestimated for the most part of the period. Especially after the strong groundwater recharge during the wet autumn of 2006, the poor reproduction of baseflow dynamics becomes apparent. This problem has already been observed for the headwater catchments (as discussed in sections 4.1.1). The representation of low flow is governed by groundwater dynamics, for which WASA-SED includes only a rather simple approach. Moreover, this problem is aggravated by the neglect of the processes of transmission losses in the lower river reach: According to observations, between the confluence of the headwaters and the outlet these losses can amount to more than 2 m³/s (Fig. 12). During low flow, this is equivalent to up to 50 % loss – probably even more if the discharge of the lower tributaries would also be considered. Since the measurements of low flow must be assumed to be rather precise (most direct discharge measurements were conducted during these conditions), transmission losses or hyporheic flow definitely play a significant role. This issue causes great uncertainties for the calibration of the Lower Isábena catchment. Moreover, the lumped treatment of the lower four sub-catchments (see Fig. 1) contributes to these difficulties.

The deterioration in model efficiency when compared to validation 1 suggests that calibrating the model to the time span of 9/2006-1/2007 did not capture the necessary range of hydrological processes sufficiently to find a universal parameter set. Seasonality in parameters and storm characteristics may be the cause of this problem (Beven, 2000). A longer calibration period could be beneficial, as soon as the necessary data are available.

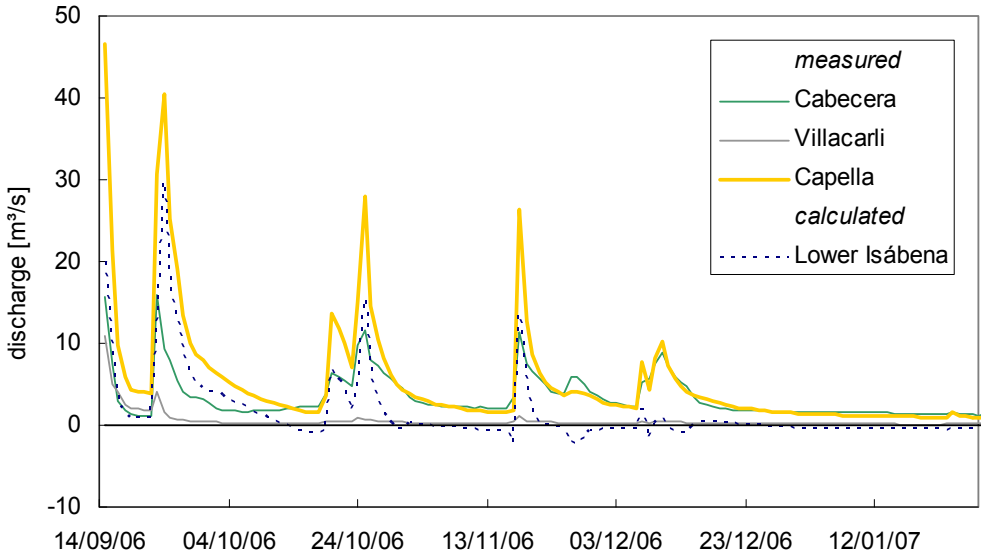

Fig. 12: Measure discharge at the headwaters (Villacarli, Cabecera) and the outlet (Capella) of the Isábena.

4.2. Sediment model

4.2.1. Evaluation of erosion-related equations

Erosion-related parameters were not calibrated; instead, different implementations of the respective equations are compared (see 3.3).

Cabecera

Tab. 10 shows the relative error for the entire observation period and excluding the first two extremely large floods. No sediment related processes in the river were considered as they are assumed to be negligible at the seasonal scale for the Cabecera catchment.

When applied at the sub basin scale, USLE and OF strongly overestimate SY, especially during the smaller floods. MUSLE and MUST, which consider modelled runoff (and thus, implicitly, the sediment delivery ratio), perform significantly better and especially well for the period of the smaller floods.

Tab. 10: Relative error of sediment model at Cabecera.

		*observation**	*yield whole period [t]*	*yield without major floods [t]*
			20089	2034
application scale	**erosion equation**	**transport capacity-equation**	e_{SY} [%] (complete)	e_{SY} [%] (without major floods)
sub-basin	USLE	-	1112	6073
sub-basin	Onstad-Foster	-	716	3946
sub-basin	MUSLE	-	245	45
sub-basin	MUST	-	69	4
LU	USLE	-	876	4493
LU	Onstad-Foster	-	571	2951
LU	MUSLE	-	327	188
LU	MUST	-	203	173
LU	USLE	Everaert	115	97
LU	Onstad-Foster	Everaert	72	105
LU	MUSLE	Everaert	136	58
LU	MUST	Everaert	64	45

obtained using QRF, see Chapters II and III

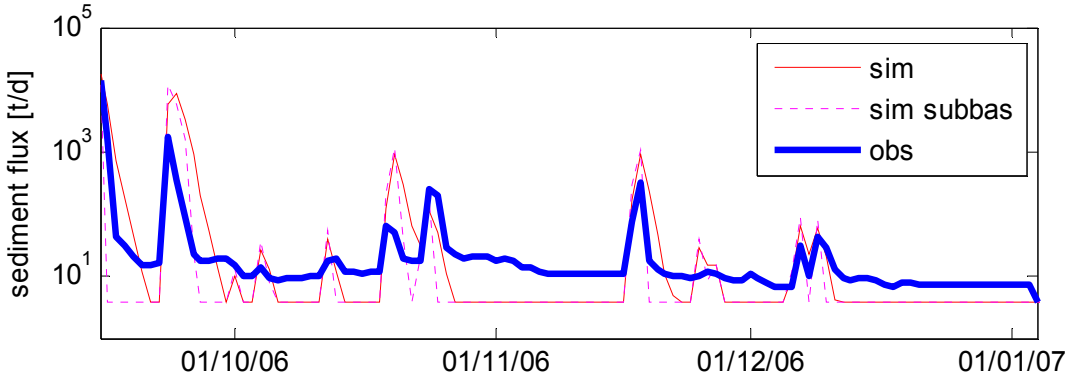

Fig. 13: Sediment fluxes of the Cabecera catchment during the calibration period (MUST+Everaert[1991]) sim: with river module; sim subbas:without river module; obs: observed values interpolated using QRF.

Applying the erosion equation at the LU-scale allows for a less averaged representation of landscape characteristics and reduces the spatial scale to the target scale of USLE and OF. Consequently, these two show somewhat improved performance while still overestimating. SY-values obtained with MUSLE and MUST increase for the smaller floods and are thus poorer estimates than those obtained from the sub-basin-scale application.

Introducing a transport capacity limit (Everaert, 1991), the performance of all erosion models increases for the major floods. Thus, USLE and OF produce acceptable predictions. MUSLE and MUST tend to overestimate the smaller floods slightly more in these settings than when applied at the sub basin scale.

MUSLE and MUST show the most robust predictive capabilities throughout all settings and the best performance for the transport-limited mode. On a sub-basin scale and LU-scale (with transport capacity limitation) MUST performs well both for major and minor floods. The latter will be used for further analysis due to its higher spatial resolution of the simulation results than its counterpart at the sub basin scale.

Peaks in sediment flux are generally strongly overestimated while low flow transport of sediment is mostly underestimated (Fig. 13). This fact suggests that some rainfall-independent sediment supply (e.g. from remobilisation of sediment storage in the riverbed) needs to be accounted for. Including the river module can remedy this shortcoming when analyzed at the resolution of flood-events (Fig. 14): the underestimation of sediment transport during the interflood periods is slightly alleviated. However, comparing modelled and measured sediment dynamics in Fig. 13 reveals that low-flow concentrations are still poorly reproduced.

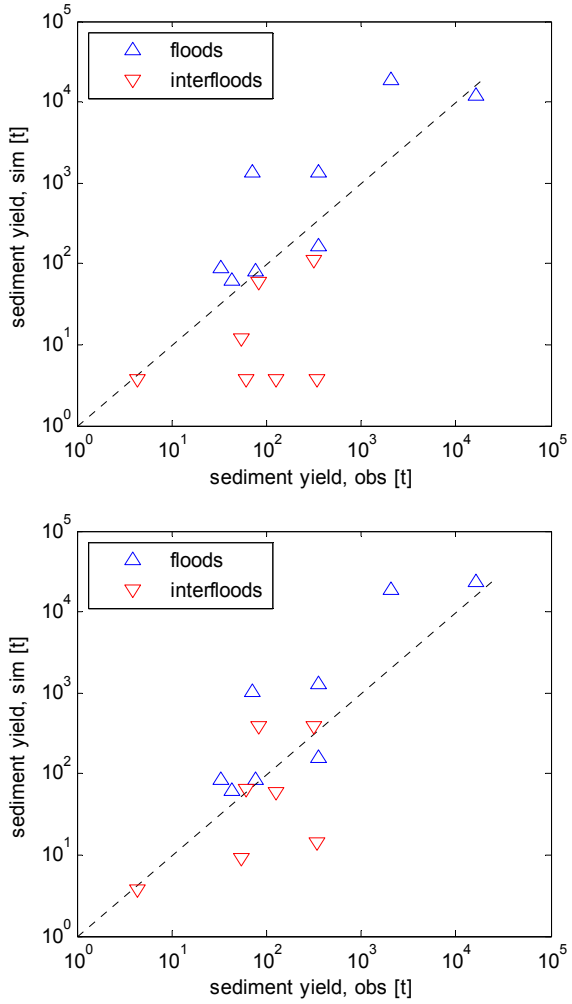

Fig. 14 a: Flood-based sediment yields without (top) and b: with the river module (bottom) at Cabecera (modelled with MUST+Everaert[1991]).

Villacarli

Tab. 11 shows that the different implementations of the erosion equations for the Villacarli catchment follow a similar pattern to that observed at Cabecera. However, overestimation is less severe and even underestimation is apparent. The latter is especially pronounced for the application including the transport limit for the smaller floods.
MUSLE and MUST show the most robust predictive capabilities throughout all settings and the best performance for the transport-limited mode. MUSLE will be used in the further steps.
While peaks in sediment flux are generally well reproduced, low flow transport of sediment is hardly represented (Fig. 15). The river module can improve the performance for some of the interflood periods only marginally (Fig. 16). This underlines the outstanding role of sediment storage in the riverbed, which is supported by field observations.

Tab. 11: Relative error of sediment model at Villacarli.

		*observation**	*yield whole period [t]*	*yield without major floods [t]*
			73909	1791
application scale	**erosion equation**	**transport capacity-equation**	e_{SY} [%] (complete)	e_{SY} [%] (without major floods)
sub-basin	USLE	-	241	4368
sub-basin	Onstad-Foster	-	131	2827
sub-basin	MUSLE	-	34	-13
sub-basin	MUST	-	-30	-28
LU	USLE	-	93	2232
LU	Onstad-Foster	-	34	1440
LU	MUSLE	-	14	14
LU	MUST	-	-18	18
LU	USLE	Everaert	-40	-58
LU	Onstad-Foster	Everaert	-52	-57
LU	MUSLE	Everaert	-11	-51
LU	MUST	Everaert	-34	-54

***obtained using QRF, see Chapters II and III**

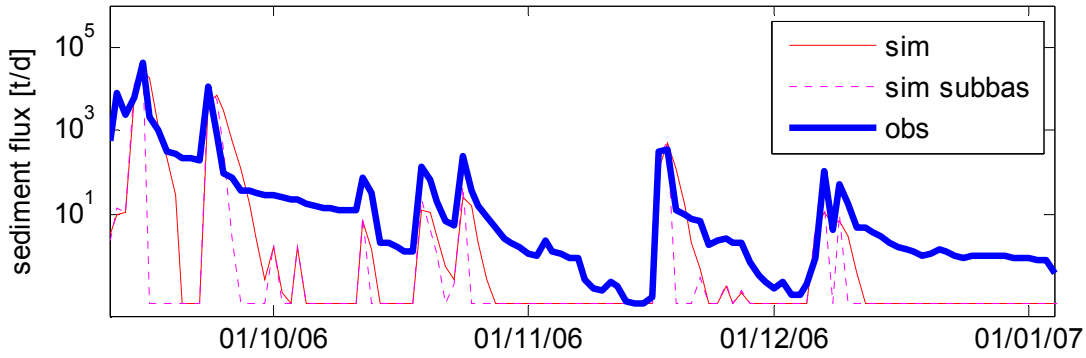

Fig. 15: Sediment fluxes of the Villacarli catchment during the calibration period (MUSLE+Everaert[1991]). For abbreviations see Fig. 13.

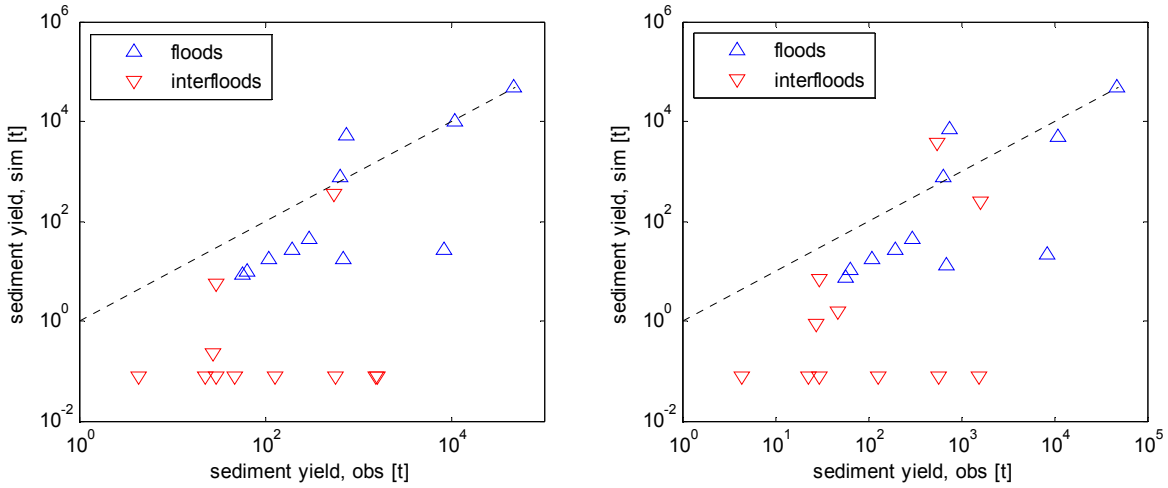

Fig. 16 a: Flood-based sediment yields without (left) and b: with the river module (right) at Villacarli (modelled with MUSLE+Everaert[1991]).

Lower Isábena

Compared to the results of Cabecera and Villacarli, the differences resulting from the settings of the sediment model are less pronounced for the Lower Isábena, which presumably is a result of the dominance of the pre-specified fluxes from the headwater catchments. However, the pattern in Tab. 12 is similar for USLE and OF. However, for MUSLE and MUST the problem of overestimation is aggravated when the application scale changes from sub basin to LU without using a transport capacity limit.

As for Cabecera, MUST shows the most robust predictive capabilities throughout all settings and the best performance for the application on the sub basin-scale. Onstad-Foster with transport capacity limitation performs comparably well.

Tab. 12: Relative error of sediment model at Capella (Lower Isábena).

		*observation**	*yield entire period [t]*	*yield w/o major floods [t]*
			119248	14654
application scale	**erosion equation**	**transport capacity-equation**	e_{SY} [%] (complete)	e_{SY} [%] (without major floods)
sub-basin	USLE	-	462	1382
sub-basin	Onstad-Foster	-	310	957
sub-basin	MUSLE	-	267	903
sub-basin	MUST	-	118	441
LU	USLE	-	394	1197
LU	Onstad-Foster	-	272	861
LU	MUSLE	-	300	1024
LU	MUST	-	210	765
LU	USLE	Everaert	147	363
LU	Onstad-Foster	Everaert	103	284
LU	MUSLE	Everaert	120	430
LU	MUST	Everaert	77	304

***obtained using QRF, see Chapters II and III**

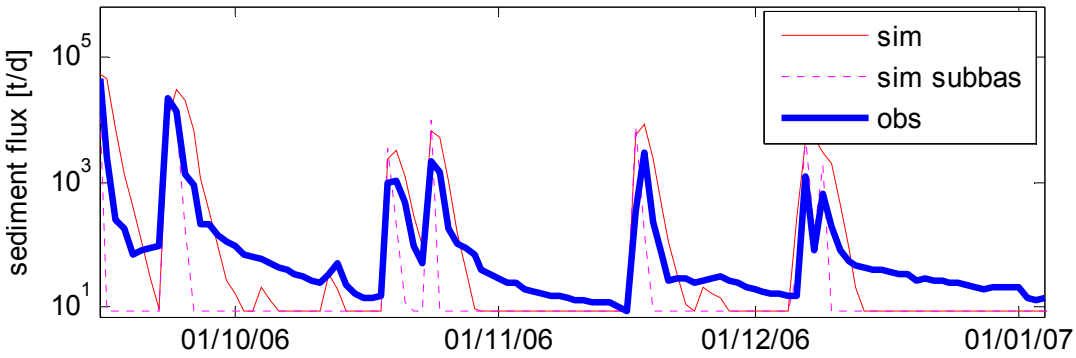

Fig. 17: Sediment fluxes of the Lower Isábena during the calibration period (MUST+Everaert[1991]). For abbreviations see Fig. 13.

In the lowermost sub-catchment itself, a significant fraction of sediment is produced only during floods (Fig. 17). In low flow periods, sediment is delivered by the headwaters or eroded from the storage of the riverbed.

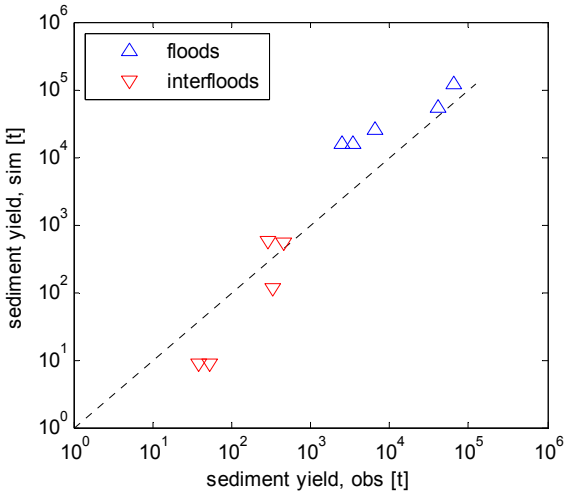

Fig. 18: Flood-based sediment yields at the Lower Isábena (modelled with MUST+Everaert[1991]).

In general, low-flow sediment budgets are well reproduced, but the flood budgets suffer a considerable overestimation (Fig. 18). Sediment dynamics are reasonably accounted for until January, 2007, when the modelled sediment flux ceases. This breakdown is caused by the complete exhaustion of sediment storage in the river bed in the model (see also Fig. 2, Chapter VIII and the related discussion), which evidently underestimates the real storage in the channel.

4.2.2. Sensitivity analysis

As laid out in section 3.4, the model's sensitivity to the uncertainties due to the choice of the parameter set and due to the inaccuracy of rainfall data are assessed for the Villacarli sub-catchment, using the best five sets of the hydrological parameterisations resulting from the 30 PEST runs (see 3.3).

(1) Uncertainty due to choice of parameter set

In order to assess the uncertainty in sediment prediction introduced by the uncertainty of the hydrological model, the best five sets of the hydrological parameterisations (see section 3.3) were run with MUSLE, applying transport capacity limit according to Everaert (1991), for the Villacarli catchment.

With the MUSLE+Everaert approach, total sediment yield varies by 24 % of the measured value between the best five parameter sets. For the smaller floods, the variation decreases to 14 %.

Tab. 13: Modelling of sediment yield (SY) using MUSLE+Everaert (1991) based on the best 5 parameter sets of the hydrological modelling (Villacarli).

*Observation**	*yield entire period* [t]	*yield w/o major floods* [t]
	73909	1791
#Paramset	e_{SY} [%]	e_{SY} [%]
1 (reference)	11	-51
2	-6	-45
3	10	-46
4	-13	-46
5	6	-37

***obtained using QRF, see Chapters II and III**

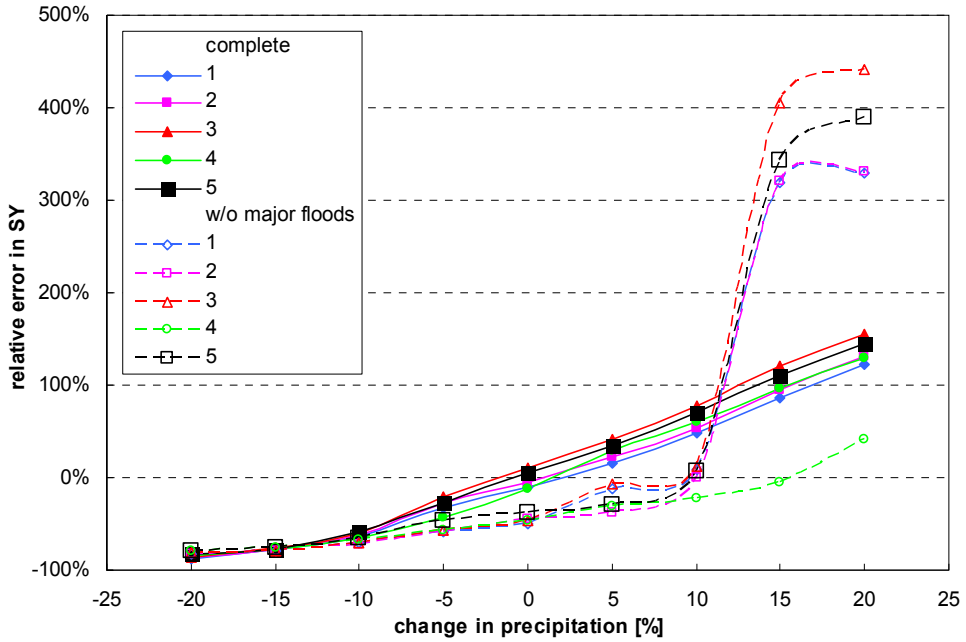

Fig. 19: Effect of modified rainfall input on performance of the sediment model for the best five parameter sets (Villacarli, modelled with MUSLE+Everaert[1991]).

(2) Uncertainty due to inaccuracy of rainfall data

Fig. 19 illustrates the effect of a modification of the rainfall series on the performance of the sediment model.

For total sediment yield, the model responds quite uniformly to changes in rainfall input, regardless of the parameter set: SY increases nearly linearly with the change in precipitation (~30 % increase in SY per 5 % increase in rainfall).

For the smaller floods, however, the model reacts far more sensitively and diversely to an increase in rainfall amount: up to an increase of 10 % in precipitation, all five parameter sets respond similarly with increasing SY. For an even larger rainfall increment, the parameter sets produce very different results. While parameter set 4 continues to show small gains in SY with increasing rainfall, the other parameter sets display an abrupt change which quadruples the sediment yield when rainfall input is changed from +10 % to +15 %. Further intensification of the rainfall does not display such a dramatic effect. Evidently, the additional rainfall input triggers some threshold process (e.g. onset of surface runoff for large areas in the catchment) that leads to this sudden rise in sediment yield.

Conclusion: The model's sensitivity to the different parameter sets is comparable to that associated with 5 % change in rainfall amount. For the smaller floods, the model shows less sensitivity as long as the rainfall increase is below 10 %, after which dramatic variations can occur. Since errors of that magnitude are very likely to occur in the rainfall data (e.g. when localized thunderstorms are not sufficiently captured by the raingauge network), this effect can explain the poorer performance of the sediment model for the smaller floods. Again, this stresses the need for an adequate monitoring of areal rainfall to ensure sound input data for the model.

4.2.3. Validation

The validation of sediment yield was carried out at three levels (see section 3.5), analogous to the validation of the hydrological model (section 4.1.3). In all cases, the respective best configuration for the sub-catchments was used (i.e. MUST + Everaert[1991] for Cabecera, MUSLE + Everaert[1991] for Villacarli, MUST + Everaert[1991] for Lower Isábena).

Validation 1: Semi-distributed parameterisation of entire catchment

The relative error in terms of sediment yield increases when the modelled fluxes of the headwaters are incorporated (see rows 2 and 3 of Tab. 14). Sediment flux is overestimated for the flood periods (see Fig. 20) in relative terms, especially for the smaller floods. Sediment transport during low flow is mostly underestimated.

Tab. 14: Performance of hydrological model at Capella with modelled headwater fluxes.

	e_{SY} [%] (complete)	e_{SY} [%] (without major floods)
Reference settings	77	304
Validation 1	96	260
Validation 2	-15	97
	01/05/2005 – 30/04/2008	**without calibration period**
Validation 3	48	48

Given the comparatively low errors in SY for Cabecera (64 %, Tab. 10) and Villacarli (-11 %, Tab. 11), the increased yield at the outlet must be caused by an overestimation of the sediment yield of the catchments of the Lower Isábena and/or an underestimation of sediment deposition in the river. The latter is supported by the observations during the calibration (section 4.2.1) and the findings in validation 3.

Furthermore, the river module reported "very high flow velocities" during almost the entire simulation period, indicating unrealistic hydraulic conditions in the river channel.

Validation 2: Lumped parameterisation of entire catchment

In the previous analyses (section 4.2.1, validation 1) the model tended to overpredict sediment yield at the catchment outlet. Evidently, the underestimation of discharge in the lumped parameterisation (section 4.1.3) compensates this overestimation (see row 4 of Tab. 14). Thus, the lumped parameterisation performs favourably in terms of sediment yield. Since this seems to be mere error compensation, it is not regarded further here. As pointed out in section 4.1.3, a lumped parameterisation is not recommended.

Validation 3: Semi-distributed parameterisation for extended time span

For this part of the validation, the model runs were performed separately for each sub basin as in validation 1 (see 4.1.3), which resulted in a relative error of 48 %, both for the entire simulation period and when excluding the calibration period.

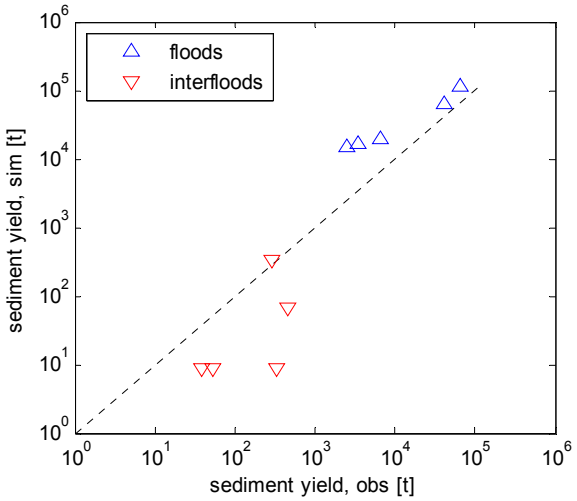

Fig. 20: Observed vs. modelled flood-based sediment yields at the Lower Isábena, based on simulated headwater fluxes of water and sediment.

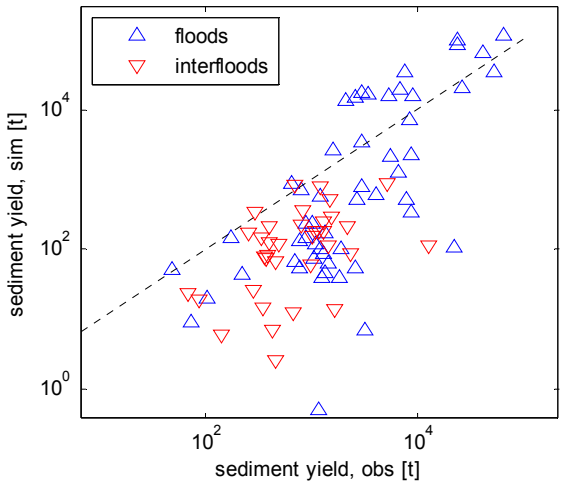

Fig. 21: Observed vs. modelled flood-based sediment yields at the Lower Isábena (5/2005-4/2008).

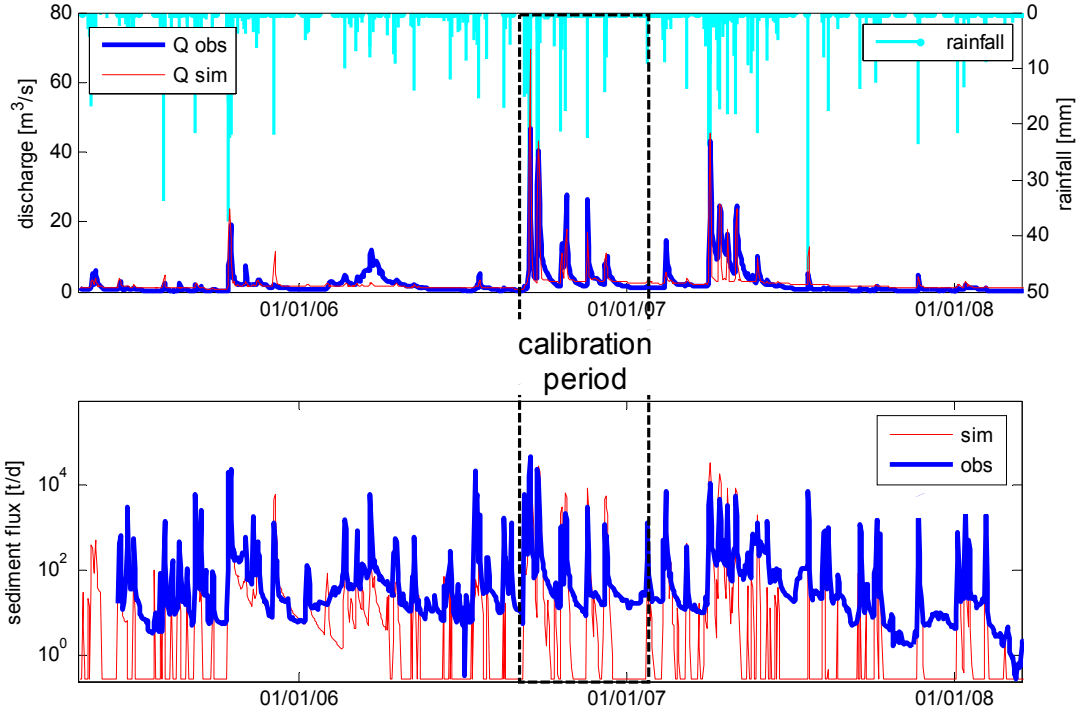

Fig. 22: Water and sediment flux at the Lower Isábena (5/2005-4/2008).

Although still overestimating, the overall relative error is lower than that obtained for the shorter time span (validation 1). Presumably, the effects of river storage average out over longer time spans, which is consistent with the absence of long-term sediment accretion in the field. In that case, the influence of the long-term erosion rates, which seem to be realistically reproduced by the model, outweigh the mismatches associated with the storage of sediments in the river at the seasonal scale. However, overestimation is apparent for the large floods, whereas the yield of small and mid-sized floods tends to be underestimated (Fig. 21).

This overestimation is much more pronounced for the 15 months after the calibration period (2/2007-4/2008, e_{SY}=200 %) than for the 16 prior to the calibration period (5/2005-8/2006, e_{SY}= -39 %). This phenomenon may be the result of the overestimation of sediment generation and delivery from the hillslopes during the major floods. While the model reflects a quite effective sediment transfer to the catchment outlet, field observations suggest that the riverbed predominantly acts as a sink for sediments during large floods (cf. López-Tarazón *et al.*, 2009), which are only exported from the catchment over a longer time span. Therefore, measured sediment flux is rather high during the pre-calibration period (Fig. 22), although sediment generation is most probably low during this relatively dry time-span. On the other hand, the intense hydrological activity in the post-calibration period presumably delivers much sediment to the river network, but a major part of it is retained in the riverbed. Apparently, these processes of river storage are not yet accounted for correctly by the river module. Fig. 23 shows the modelled sediment storage in the Lower Isábena for the calibration period. The modelled peak value of 23'690 t (15/09/2006) falls into the same order of magnitude as 53,180 t (06-16/09/2006) determined by Mueller (subm.) based on field measurements at this time. Nevertheless, the pre-run phase of the model did not adequately initialise sediment storage in the river, which is 0 prior to 12/09/2006 in the model. Considering the order of magnitude of sediment storage in the river and the uncertainty of initial value underlines the importance of an adequate representation of these processes and the initial conditions.

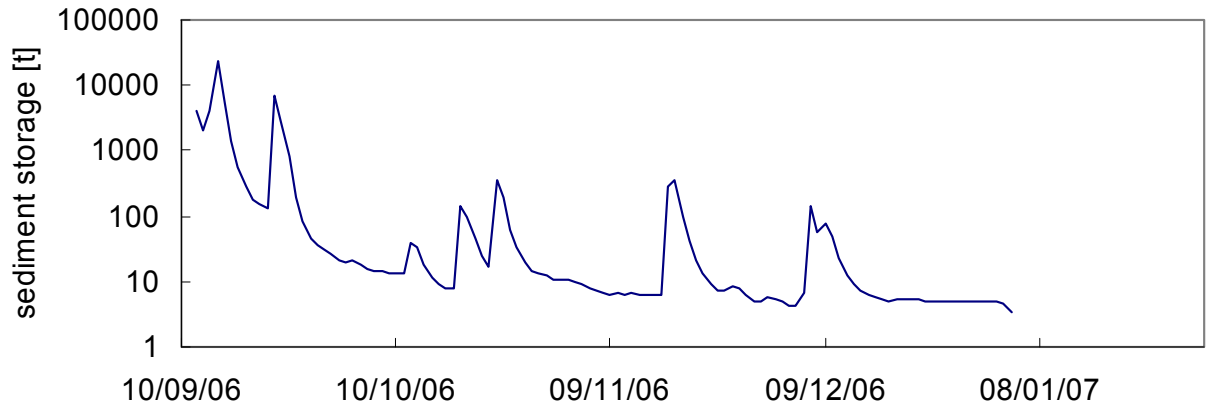

Fig. 23: Modelled sediment storage in the riverbed Lower Isábena during the calibration period. Note that the y-axis is log scale, so 0 cannot be displayed.

4.3. Conclusions on model performance

The results of the calibration and validation confirm that WASA-SED is capable of reproducing water and sediment fluxes from the Isábena, although with some limitations.

The hydrological model worked satisfactorily. Its greatest deficits concern the reproduction of some of the peaks during the validation period and the poor representation of the low flow characteristics. The former may be attributed to insufficient areal coverage of the rainfall input data (as suggested by the sensitivity analysis), unrepresented hydrological processes such as snowmelt (see validation 3) and presumably the temporal resolution of one day, which is inadequate to capture the effects of high-intensity rainfall and restricts the reliability of the hydraulic computations in the hillslope and river module. The representation of low flow is governed by groundwater dynamics, for which WASA-SED includes only a rather simple approach. The insufficient representation of transmission losses in the model (see section 4.1.3) and the lumped treatment of the lower four sub-catchment (see Fig. 1) are further limitations of the current model setup.

For the three gauges, the sediment model reproduces the measured yield with relative errors ranging from -11 to 300 % (Tab. 15) when using the optimum setting. All of these values resulted from running the model at the LU-scale, including the transport capacity limit.

Comparing the different settings for the sediment model it becomes apparent that modelled sediment generally decreases in the order “sub basin scale application”, “no transport limit”, “transport capacity limit”. This sequence is especially pronounced for USLE and OF. For these two, overestimation can exceed a relative error of 5000 % when applied at the sub basin scale (e.g. at Cabecera). Therefore, applying USLE or OF at that scale cannot be recommended; instead, the application at the LU-scale using a transport limiting concept may be preferable.

Tab. 15: Summary of best performing settings of the sediment model for the calibration period.

sub-catchment	erosion equation	transport capacity-equation	e_{SY} [%] (complete)	e_{SY} [%] (without major floods)
Cabecera	MUST	Everaert (1991)	64	45
Villacarli	MUSLE	Everaert (1991)	-11	-51
Lower Isábena	MUST	Everaert (1991)	77	304

In contrast, MUSLE and MUST are considerably more robust to the different configurations and can produce acceptable results even when applied at the sub basin scale (e.g. Cabecera). MUSLE tends to predict a higher sediment yield than MUST. Thus, it excels for Villacarli, where underestimation is still an issue. For Cabecera and the Lower Isábena, sediment yield is always overestimated, which is why MUST performs better. This imbalance between Villacarli on the one side and Cabecera and the Lower Isábena on the other is probably caused by the averaging effect of the discretisation procedure, which always levels out distinctive heterogeneities between the sub-catchments (i.e. badlands) to a certain degree (see Fig. 24a, where some badlands have also been assigned spuriously). Likewise, the extraordinary magnitude of badland erosion may simply be beyond the scope of MUSLE and MUST, which will also lead to an underestimation for Villacarli.

In summary, the presented results suggest that the application of MUST combined with a transport capacity limit performs best for predicting sediment yield in catchments with moderate erosion rates. For highly erodible (sub-)catchments or where such sub-catchments dominate the overall sediment budget, the use of MUSLE may yield better results.

Fig. 24b illustrates the erosion rates modelled for the extended validation period (see section 4.2.3). A strong contrast between the sub-catchments is evident: For the three simulation years, the Cabecera catchment features a mean specific sediment yield (SSY) of 186 t km^{-2}, while those of Villacarli and the Lower Isábena are 3732 and 2592 t km^{-22}, respectively. The low specific yield of Cabecera is consistent with field observations and a result of the predominant forest cover and resistant lithology.

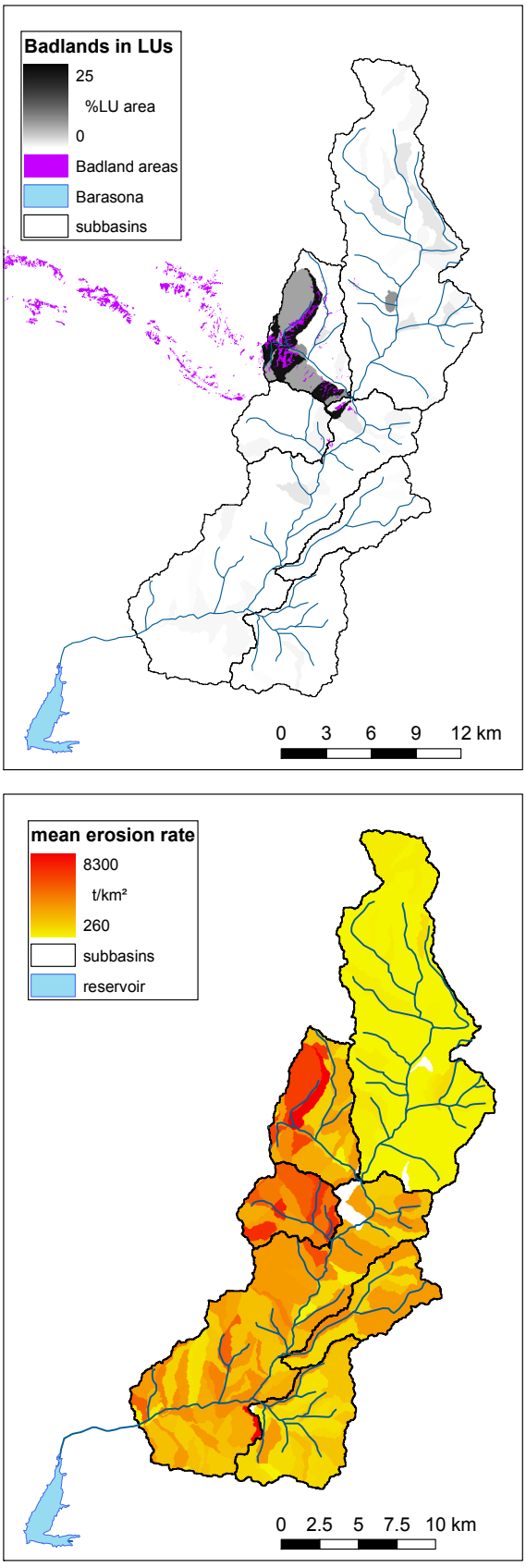

Fig. 24 a: Location of Badlands and their representation in the model (top); b: modelled erosion rates in the Isábena catchment (5/2005 – 4/2008, validation 3), visualized at the LU-scale (bottom).

For Villacarli, the SSY is closely related to the high density of badlands, which is reflected in areal percentages of more than 20 % for many LUs (Fig. 24a). Although there are also some badlands in the northern part of the Lower Isábena, the high erosion rates here show no relation to their distribution. The respective sediment yield is relatively high when compared to a value of 350 t $km^{-2}a^{-1}$ derived from reservoir siltation for the entire Ésera catchment (Sanz-Montero *et al.*, 1996), but may still be plausible when considering that the latter value is an average which also includes the northern Ésera catchment (sub-/alpine/montane, dense vegetation cover), suggesting a low SSY similar to that of Cabecera (cf. Valero-Garces *et al.* 1999). Consequently, SSY must be higher in the lower reaches, which are in turn comparable to the lower Isábena. However, although no data of the SSY for the lower Isábena are available so far, qualitative field observations and the data for the monitoring period (09/2006-01/2007, see Fig. 25) suggest that SSY for the Lower Isábena (i.e. sediment generated in the lower sub-catchments) is overestimated by a factor of approx. 4. This overestimation can be the result of the underestimated deposition in the river and in first-order channels: in the less elevated lower sub-catchments, a large fraction of the generated sediments can be deposited in the comparatively flat primary stream network. The river module in WASA-SED, however, has been parameterized with the focus on the processes in the main stem of the river, inhibiting major deposition in the first-order channels, thus leading to an overestimation of sediment delivery (cf. validation 3, section 4.1.3).

Moreover, the comparatively crude hydrological parameterisation (lumped for the lower four sub basins, plus no account being taken of the apparently important transmission losses in the lower river reach, see above) may be a reason for this overestimation. This high sensitivity to the hydrological parameterisation is apparent when running the Lower Isábena with the parameter set of Cabecera, which decreases the modelled sediment yield by a factor of 5000. Thus, the model's total performance at the catchment scale is heavily affected by the results for the Lower Isábena.

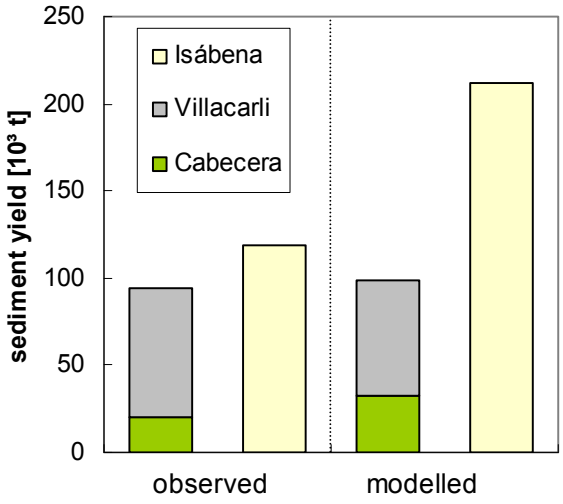

Fig. 25: Observed and modelled sediment yield for the calibration period (09/2006-01/2007).

In summary, it can be stated that erosion modelling proved most successful when approaches driven by a runoff-term (MUSLE, MUST) were applied. The additional coupling with a transport capacity limitation according to Everaert (1991) improved model performance for all approaches. Thus, the importance of an adequate representation of the runoff processes must be stressed, because of their impact to sediment generation, delivery from the hillslopes and in the channel. Where this representation of runoff is vague, as encountered in the Lower Isábena, the related modelling of sediment yield is impaired. Together with the findings of the sensitivity analysis, one may conclude that model performance can be improved primarily due to better spatial resolution of the rainfall data and the acquisition of discharge data for the downstream sub-catchments in order to allow specific calibration and the quantification of transmission losses for the lower sub-catchments.

Tab. 16: Reduction (compared to validation 3 as reference) in sediment yield for the scenarios (extended validation period, 13/06/05-30/04/08).

	reference	Sc. 1	Sc. 2	Sc. 3	Sc. 4
(sub-) basin	yield [t]	reduction [%]			
Cabecera	84932	2	5	5	4
Villacarli	145369	5	14	42	2
Isábena	640629	2	6	11	16

Scenario 1: SDR=94 % , i.e. 6 % of sediment trapped for badland LUs
Scenario 2: SDR=82 %, i.e. 18 % of sediment trapped for badland LUs
Scenario 3: conversion badlands to mattoral
Scenario 4: conservation practices in agriculture

4.4. Scenario assessment

With the model results of validation 3 (section 4.2.3) as a reference, the impact of four scenarios was assessed (see section 3.6): partial trapping of sediments from badlands (scenario 1 and 2), conversion of badlands to mattoral (scenario 3) and implementation of conservation practices in agriculture (scenario 4).

For the badland-related scenarios 1-3, the effect of the mitigation measures is most pronounced for Villacarli, followed by the entire Isábena and Cabecera (Tab. 16 and Fig. 26). This order is consistent with the order of the percentage of badlands in the sub-catchments (see Fig. 24a): In Villacarli, the mitigation measures are assigned to the majority of the LUs, while it is hardly effective in Cabecera where sediment yield is consequently less reduced.

For Villacarli, the reduction is approximately three-quarters of what would be expected if the mitigation measures affected *all* LUs (i.e. 6 and 18 %, respectively). This means that, even in Villacarli, the model generates roughly one quarter of the sediments from areas that are completely devoid of badlands. Scenario 3, with all badlands converted to mattoral, confirms that an even larger percentage of sediment originates from non-badland areas.

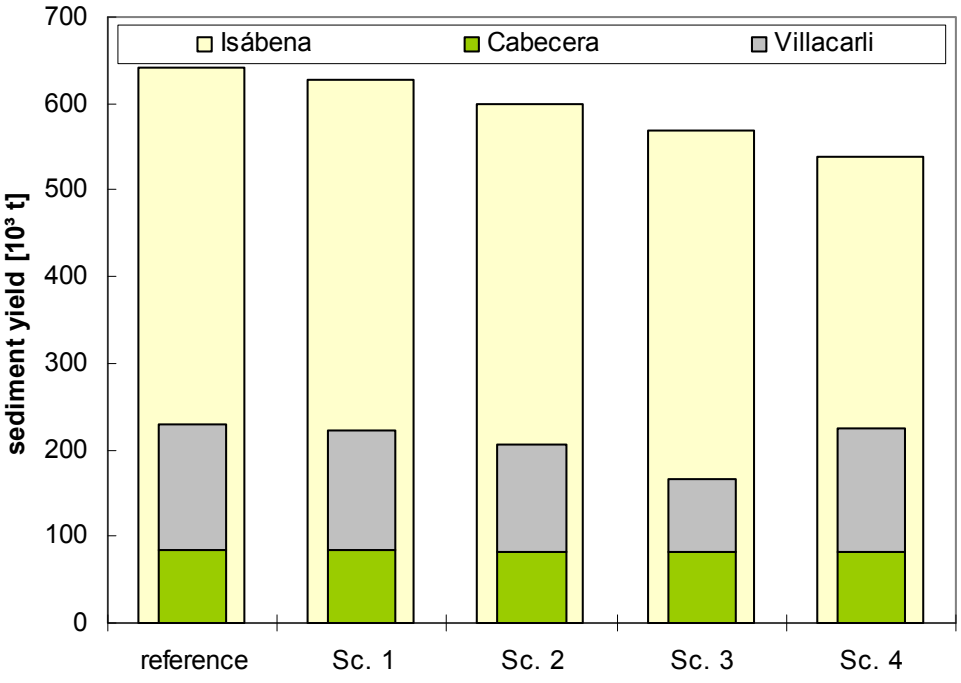

Fig. 26: Sediment yield of reference run and scenarios (extended validation period, 13/06/2005-30/04/2008).

Although erosion processes outside badlands (e.g. on agricultural land) have been observed in Villacarli, the related on-site features and the properties of the suspended sediments suggest that these only play a minor role in the overall sediment budget. Consequently, WASA-SED overestimates the contribution of non-badland areas while underestimating badland erosion. This flaw could also explain the overestimation of sediment yield in the Lower Isábena: since agricultural areas cover an increasing fraction in the four downstream catchments, their sediment yield is exaggerated in the model.

In scenario 4, the reduction of the C-factor by 45 % shows only minor effects for Cabecera and Villacarli, where agricultural areas are of little extent. For the entire Isábena, this scenario yields the greatest reduction in sediment yield of all scenarios, which contradicts the current perception of the badlands as being the major sediment source.

With regard to these issues, the overall results of the investigated scenarios must be questioned, which sheds light on the limitations of the model (see final discussion in Chapter VIII). Furthermore, the investigated scenarios contain rather strong simplifications, e.g. the assumption of a constant trapping efficiency for the badland LUs. During monitoring, the single observed trap showed large variation in TE between events. Some remobilisation of the trapped sediments was also observed. Therefore, a single value of TE as in the scenarios 1 and 2 will hardly be met in reality, where site-specific settings along the valley bottom also come into play.

Considering the large influence of runoff (see section 4.3), a change in land-use, as assumed in scenario 3, should also be accompanied by changes in the soil hydraulic properties (e.g. higher infiltration rates, deeper soils), which result in less runoff. Since this aspect has not been considered in the parameterisation, the long-term effect of badland remediation is likely to be underestimated.

Nevertheless, the order of magnitude of sediment reduction, even under the rather favourable conditions of scenario 2 and 3, suggests that the maximum possible reduction in sediment yield is quite small, especially when compared to scenario 4. When seen in context with the observed uncertainties of the model that can be as high as 20 % of sediment yield, the assumed remediation scenarios must be considered uncertain in their effect and rather inefficient, if the results are to be interpreted. Thus, other preventive measures such as an appropriate sediment management in the reservoir (drawdown and routing, flushing, see Mamede, 2008) would be indicated.

Chapter VIII:

Discussion and conclusion

1. Summary of achievements

The integrated approach of this thesis, ranging from the acquisition of fieldwork data to the final application of a catchment model, provided numerous scientific outcomes. The main findings with regard to the working tasks (see Chapter I, section 2) are summarized as follows:

1. Conceptual development and implementation of an erosion module as a component for the integrated modelling of water and sediment yield at the meso-scale

The WASA-model was extended by an erosion module. The process-based concept of WASA allowed taking advantage of the hydrological computations, which permitted the implementation of empirically (USLE and derivatives) and physically-based (transport capacity concept) descriptions of the generation and transport of sediments at the hillslope scale. The hillslope module was successfully coupled with the river and reservoir module. The resulting WASA-SED model is a hydrological and sediment transport model for the meso-scale, which is especially suited for dryland catchments and catchments affected by reservoirs.

Chapter V presented the concept and structure of the WASA-SED model. Applications to two catchments are described in Chapters VI and VII.

2. Development of appropriate upscaling and generalisation methods for the discretisation and parameterisation of the model

The developed LUMP-algorithm successfully integrates multiple geospatial layers into catena-based modelling units. Based on the spatial concept of Güntner (2002) and aggregation techniques of Cochrane & Flanagan (2003), it enables the aggregation and generalisation of landscapes and the upscaling of their parameters while preserving typical characteristics of the hillslopes. Thus, it constitutes an important component for the efficient and reproducible application of catena-based models at the meso-scale, such as WASA-SED, as described in Chapter IV.

3. Collection of adequate input parameters and time series in fieldwork and monitoring campaigns

Based on numerous fieldwork measurements, a database was assembled, which contains parameters and time series essential for modelling purposes. Focus was put on assessing sediment fluxes, which generally requires the technically-challenging continuous measurements of suspended sediment loads. We demonstrated that this goal can be achieved based on a limited number of samples. The non-parametric regression methods Random Forests and Quantile Regression Forests outperform traditional methods for the datasets collected for the River Isábena and its main sub-catchments. Besides efficiently handling the large magnitude of concentrations and complex interactions, the method allowed the identification of key predictor data, the reconstruction of sedigraphs and the computation of sediment yield with the associated uncertainties. The practical and technical experiences of this work have guided further instrumentation and monitoring in the Isábena that is being undertaken within the framework of the SESAM-project. Details are given in Chapters I, II and III.

4. Parameterisation and application of the developed model to the different study areas; identification of strengths and limitations

The WASA-SED model proved to be a robust model that can plausibly reproduce water and sediment fluxes from a meso-scale catchment even when applied without calibration (e.g. Ribera Salada), for areas with many small reservoirs (Benguê, Mamede, 2008) and for highly-erodible catchments (Isábena). Furthermore, effects of water and sediment connectivity can be reproduced plausibly (Medeiros *et al.*, subm.). WASA-SED specifically accounts for the deposition processes along the sediment conveyance path. Thus, the concept of the sediment delivery ratio, which has been criticized extensively, needs not

be employed, which distinguishes WASA-SED from many other meso-scale models.
The necessary parameterisation data for the meso-scale can be obtained from available data sources or remote sensing with a reasonable effort. With the erosion module being subject to error propagation from the hydrological module, input data quality and time series of discharge for calibration and validation are of great importance.
Model applications are presented in Chapters VI and VII.

2. Discussion and directions of further research

Besides the academic motivation of research at the river-basin scale, the understanding of the hydrological and sediment-related processes in a meso-scale catchment is an indispensable prerequisite for sound management decisions. However, the transferability of findings from other areas must be ascertained and monitoring is usually expensive, time-consuming and, characterizing the status quo, can hardly serve to assess projections into the future. Thus, modelling can be considered an attempt to integrate the current knowledge and data for a complex system. Ideally, this leads to an entirely satisfying reproduction of the system and allows subsequent predictions. Even if this ambitious goal is not met, the modelling process can still provide other information by explaining and illuminating core dynamics and uncertainties, guiding data collection, challenging prevailing perceptions and helping to discover new scientific questions (Epstein, 2008). The key results of this thesis can be found with regard to these aspects. This section will discuss how the presented strategies of data assimilation, model development and model application succeeded in achieving these goals. This aims at a reflection on the components (Chapter I, Fig. 2), their respective role in the entire modelling process, shortcomings and possible improvements.

2.1. Data assimilation

GIS data, literature data, aggregation: This study succeeded in assembling basic geospatial data such as lithology, topography and land-use. The identification of the most suitable data sources can help with efficient model application for further catchments in the studied dryland regions. However, categorical input data generally require to be supplemented by the respective parameters, which mostly raises questions of their availability, their representativeness and variability within the class. The latter is especially relevant when categories are based on other criteria than those that are of interest for the model parameterization e.g. soil maps are usually related to soil taxonomy, which does not necessarily demark soil-hydraulic and erosion-prone entities). Therefore, it is highly desirable to derive such parameters like LAI, ground cover, vegetation height, etc. more directly from remote sensing data, as proposed by e.g. Saavedra & Mannaerts (2005), Wang *et al.* (2002) and Lu *et al.* (2003). Thus derived parameters would reduce the need to use literature data for designated classes that is always limited by the transferability issue and would also allow the assessment of seasonal dynamics.
The developed LUMP algorithm (see Chapter IV) proved a valuable tool for integrating such geospatial layers and the delineation of homogeneous modelling units with respect to these parameters. Including more complex derived indicators of hydrological and sediment response, e.g. HOST-classes (“Hydrology of soil types”, Boorman *et al.* 1995) or MRZ (“morphological runoff zones”, Bracken & Kirkby, 2005), could further extend the capabilities of LUMP.

Time series data: Model input data and data for calibration/validation purposes currently pose considerable limits for the modelling. Concerning input data, rainfall measurements especially need to be improved, as they tend to be most influential for the modelling results (see Chapter VII,

section "Sensitivity analysis"). High spatial heterogeneity for the Isábena catchment has been observed by Verdú *et al.* (2006a); for the Benguê catchment, the importance of rainfall data input for modelling with WASA-SED was reported by Medeiros *et al.* (subm.). The additionally installed rain gauges alleviated the situation for the study areas. However, large-scale approaches using RADAR-imagery (e.g. Meischner, 2007) or microwave links (Messer *et al.*, 2006), or the combination thereof (Cummings *et al.*, in press), provide more effective options. Attempts to derive other climate drivers such as temperature and radiation from AVHRR/MEDOKADS data are currently in progress.

Such refined input data allow the more specific modelling at the sub-basin scale when complemented with the respective discharge (and sediment) data. The successful monitoring of the Villacarli and Cabecera sub-catchments provided this data. However, unmonitored sub-catchments had to be treated in a lumped treatment way, which does not correspond to the observed spatial heterogeneity of the parameters, input data and transmission losses (see Mamede, 2008 and Chapter VII, respectively). Extending the period and scope of the monitoring (as currently being carried out) could make the derivation of sediment yield considerably more robust, especially for dryland areas (Walling *et al.*, 2001). Where this monitoring is unfeasible, reservoir surface measurement (Liebe *et al.*, 2005) or water level detection (Berry *et al.*, 2005) by space-borne radar (ENVISAT, TerraSAR) can potentially provide proxy data for runoff generation. Other remote sensing techniques including, e.g. (IN)SAR, suspended sediment tracing across water bodies in a landscape; soil erodibility and C-factor mapping and the assessment of soil and vegetation status also hold considerable potential for deriving validation data, which is of utmost importance for modelling at the meso-scale (Vrieling, 2005).

A wealth of *Fieldwork data* regarding badland properties (Appel, 2006; SESAM, 2006), land-use characteristics (SESAM, 2006) and sediment yield from sub-catchments (see Chapter III) has successfully been collected. For any fieldwork measurement of confined spatial and temporal coverage, the question of adequate regionalisation or upscaling techniques arises. These range from simply using the average value of a large number of samples (e.g. badland soil parameters), the use of class representatives (e.g. for the land-use characteristics in Benguê; Mamede, 2008) towards more elaborate techniques like the application of non-parametric regression (see Chapter III). For the former two, the potential of an advanced regionalisation by combining the fieldwork results to remote sensing data has merely been tapped. Student projects confirmed that land-cover parameters could be related to CBERS-satellite imagery for Benguê and basic soil parameters to terrain and land-use attributes using pedometrics (McBratney *et al.*, 2000) for the Isábena. The RF/QRF method (Chapter II) was an indispensable approach that allowed the temporal upscaling of the intermittent measurement of suspended sediment concentrations. It performed favourably for the complex sediment dynamics in the Isábena and provided several advantages over alternative methods (see discussion Chapter II).

During this study, experiments with using Cs-137 for the estimation of erosion rates (e.g. He & Walling, 1997; Zapata, 2002) have been carried out. However, the necessity of appropriate upscaling technique for these "point measurements" casts doubt on the feasibility of this approach. Although Collins *et al.* (2001) and Pennock (2003) proposed methods for such upscaling, the magnitude of erosion rates and the size and heterogeneity of the Isábena catchment suggest that the current methods are unfeasible for the meso-scale (cf. Bathurst, 2002). However, the isotopic composition of sediments in the river can provide clues on the relative contribution of sediment

sources (surface and bank erosion, Walling, 2004), which could elucidate the magnitude of sediment storage in the river (see discussion, chapter VII).

2.2. Model development and application

The *WASA-SED* model proved to be a robust model that can reproduce water and sediment fluxes from a meso-scale catchment, even when applied without calibration (e.g. Ribera Salada, Chapter VI), for areas with many small reservoirs (Benguê, Mamede, 2008) and for highly-erodible catchments (Isábena, Chapter VII). Thanks to the data situation for the latter catchment, it could be shown that the concept of combining runoff-driven erosion equations and a transport capacity limitation yielded the best model performance. The most prominent limitations of the model turned out to be the representation of low flow, the reproduction of some peaks in discharge, underestimation of badland- and overestimation of lowland-erosion, and the effects of the river in terms of transmission losses and sediment storage. These model limitations arise from four sources (Liu & Gupta, 2006): parameters, observational data for driving and evaluating the model, initial conditions and model structure.

2.2.1. Parameters and observational data

Deficits in *parameters and observational data* can firstly be attributed to the problems discussed above for GIS, time series, fieldwork and literature data and the related pre-processing methods. They are thus an inherent part of the workflow shown in Chapter I, Fig. 2. Secondly, even in a physically-based model, parameters are *per se* effective parameters, reflecting the underlying assumptions of the model concept and spatiotemporal aggregation (Liu & Gupta, 2006). Hence, measured values are not strictly related to model parameters (Beven, 2002) and partially associated with issues of model structure (see below).

2.2.2. Initial conditions

Initial conditions in WASA-SED affect soil moisture, interception, groundwater, river and reservoir storage for the hydrological model, and sediment deposits in the river and reservoir(s) for the sediment model. Interception and river water constitute relatively small and volatile storages, so the initial state merely affects the first few simulation days. In contrast, soil moisture, groundwater and reservoir storage (where applicable) comprise a large potential volume and can easily affect the output for several model years, depending on the parameters and climate input. This issue is currently dealt with by repeated iterations of a pre-run phase until the relative change in the storage falls below a specified threshold. Mamede (2008) describes how completely filled/ nearly empty small reservoirs can be assumed after a prolonged rainfall/dry season in Benguê, making these periods especially suitable for the start of the modelling of these areas. For larger reservoirs of increasing volume and impoundment ratio, the initial state can be specified explicitly. In contrast, the initial conditions for the sediment model pose a more severe challenge. While the initial topography of strategic reservoirs can be derived from bathymetry, the depth of the erodible layer is rarely known and was used as a calibration parameter (Mamede, 2008). For sediment storage in rivers, the initial conditions are equally hard to define but are of similar or even greater importance, as the stored sediment is usually more prone to remobilisation (see Chapter VII, validation).

2.2.3. Model structure

Errors arising from the *model structure* are generally the most poorly understood but are potentially the most influential. They result from unknown or unrepresented processes, inappropriate approximations and simplifications, and numerical effects introduced by the mathematical implementation of the conceptual model and its spatio-temporal discretisation (Liu & Gupta, 2006).

The **hydrological model** of WASA-SED represents the processes dominating runoff-response in dryland environments (Güntner, 2002). Nevertheless, processes like crusting, macro-pore infiltration, concentration of surface runoff, routing of surface and subsurface flow, snowmelt, groundwater flow, river transmission losses and river-aquifer interaction are not or only simplistically included in the model because they were considered irrelevant for the settings the model was originally developed for. However, the results of the model applications conducted in this thesis suggest that some of these are partly responsible for model shortcomings. For the Ribera Salada catchment (Chapter VI), the need for an improved representation of groundwater movement and snowmelt became apparent. Likewise, this issue causes problems during the modelling of the Isábena, where transmission losses in the river also play a role (Chapter VII).

Besides the process-related limitations, the temporal resolution of one day affects model performance. On the one hand this means that some of the processes involved (e.g. routing of hillslope surface runoff) *need not* be considered (because it can be assumed that all surface runoff reaches the river within a day). On the other hand, phenomena like infiltration excess and hydraulic conditions in the river *cannot* be resolved adequately, and must be accounted for by, e.g. a correction of the infiltration conductivity. For the latter, the rainfall-dependent estimation of maximum 30-min rainfall intensity (Chapter VII, Fig. 2) attained some upscaling of the rainfall characteristics, but clearly incorporates some loss of detail. The former, however, eliminates the need for accurate parameters describing these processes. Thus, an increased temporal resolution might tend to augment model performance due to improved model structure but at the same time will introduce trade-offs due to the higher sensitivity of some parameters.

An extensive validation of the performance of the **sediment model** was only possible for the Isábena, where the necessary data were available. For this catchment, WASA-SED demonstrated its capability of reasonably reproducing sediment yield. The approach combining runoff-driven empirical erosion equations (MUSLE, MUST) with a transport capacity limit resulted in the best model performance, even for the two contrasting headwater catchments. This is especially remarkable considering their opposing characteristics and the high erosive activity of Villacarli (see Chapter I for more details on study areas). However, the underestimation of sediment yield for the latter and an overestimation for the sub-catchment with low erosion activity (Cabecera) is apparent. At the event scale, this tendency has also been identified by other authors (Strauss & Klaghofer, 2003; Kinnell, 2007) for USLE and its derivatives. This may be attributed to the fact that especially during large events at the catchment scale, processes like linear erosion, debris flows, mass movements and sediment dynamics in the river may completely overrule the original concepts used by the USLE. Moreover, design and application of most erosion models (namely USLE) rarely extend to non-agricultural areas such as badlands (Martínez-Carreras *et al.*, 2007), so limitations have to be expected in this context. This issue is also apparent for the Villacarli catchment (Chapter VII), with its high areal percentage of badland areas. The total modelled sediment yield of this catchment suffers only from a mild underestimation in the calibration period, suggesting that the model is capable of reflecting the high erosion rates of badlands. However, the scenario analysis suggests that the contribution of the badlands is around a mere 40 %. As discussed before, this may be attributed to the neglect of changing soil hydraulic parameters along with the land-use change, which is supported by the observed high sensitivity to the hydrological model (see discussion below). On the other hand, the obtained value may also challenge the current perception of badlands as the major sediment source (Fargas *et al.*, 1997, Valero-Garcés *et al.*, 1999). Al-

though this perception is strongly supported by qualitative observations, fingerprinting methods could help to underpin it quantitatively. For the time being, we still consider this perception as valid, which leads to the conclusion that the current sediment model of WASA-SED still holds potential for improvement for erosion hotsports like badlands.

The sediment model is heavily affected by any error produced by the hydrological model, which is common among water erosion models that are mostly "piggybacked" onto hydrological models (Rudra *et al.*, 1998). This error propagation mainly depends on the correct partition of surface- and subsurface-runoff (Wainwright and Parsons, 1998). Although errors in hydrological and sediment model can also compensate (see Chapter VII, validation 2) in some cases, the models thus obtained cannot be considered robust and transferable. The intensity of error propagation from the hydrological to the sediment model depends on the chosen erosion equations. When using MUSLE or MUST with transport capacity limit, the influence of the hydrology on sediment yield is threefold: in the energy term of the MUSLE/MUST, when computing transport capacity at the TC-scale (both being a function of surface runoff) and for the transport mechanisms in the river/reservoir (function of river/reservoir discharge). In contrast, sediment yield based on USLE applied on the sub-basin scale directly interacts with the hydrological model only in the river/reservoir. Nevertheless, the results obtained in the modelling (see Chapter "VII", section calibration) supports the contention that the additional information gained by including hydrological information outweighs errors introduced by it, which was also stated by other authors for the MUSLE (Neitsch *et al.*, 2005; Erskine *et al.*, 2002) and the USLE-M (e.g. Kinnell, 2007), whereas others object to that (Lenhart *et al.*, 2005). In fact, only by considering discontinuities of surface runoff (e.g. by reinfiltration) or sediment transport (e.g. by transport capacity limitation) along the hillslope, issues of complex water and sediment connectivity can be described. As shown in Chapter VII, coupling the erosion processes to the hydrological model in WASA-SED generally improved model performance. Nevertheless, the prediction of erosion is only improved if the model has an "adequate ability to predict runoff" (Kinnell, 2001) - a premise that is evidently satisfied to a varying degree for the different models discussed by the authors above. Apparently, this "adequate ability" is not provided for the Lower Isábena, where sediment yield is considerably overestimated because of the inadequate representation of its hydrology (Chapter VII). As mentioned above, further calibration data for the sub-catchments could alleviate this uncertainty regarding runoff. The related structural uncertainty, however, is still large in WASA-SED. The complex issues of connectivity of sediment sources to the river channel are only simplistically implemented in the model. In that context, the implementation of selective connectivity between SCVs (e.g. in the Isábena, mattoral often drains to badlands, rarely vice versa) and surface flow concentration (rill/interrill distribution, hillslope convergence) need attention. On the sub-catchment scale, open questions of transport losses or sediment storage in the river (as discussed in Chapter VII) also call for improved consideration.

2.2.4. Calibration

According to Buytaert *et al.* (2008), using other observations beyond discharge and sediment yield (e.g. fractions of flow components derived from isotope analysis, sediment origin from fingerprinting techniques, evaporative fluxes from remote sensing data) can improve model performance and reduces the problems of equifinality when used in multiobjective calibration as opposed to calibration solely by discharge. However, increasing the temporal resolution, the number of output files or the number of entities (i.e. sub-basins, LUs, TCs, etc; - catchment area has no influence due to the spatial concept of

WASA, see chapter V) leads to a higher computational demand. In that case, the presented calibration technique (Chapter VII) must be replaced by more advanced techniques (e.g. shuffled complex evolution, particle swarm optimization, cf. Zhang *et al.*, 2008).
Although applying WASA-SED is currently not yet recommended beyond the scientific level (i.e. for planning purposes), it is expected that the proposed extensions above will foster model applicability. A more detailed evaluation of scenarios (land-use, climate change) combined with an integrated assessment of options in reservoir management, opens the opportunity to address relevant questions in the presented (and potentially other) catchments. This includes problems of water yield (e.g for the Ribera Salada, as addressed in Chapter VI) economical comparison of on-/offsite sediment and water management for the Isábena and the evaluation of the effects of small versus large reservoirs in the Benguê-catchment (Mamede, 2008).

3. Conclusion

This thesis presents the results of the combined efforts in measurement and modelling of water and sediment fluxes from meso-scale catchments. It mostly provided insight into the dynamics of water and sediment yield of the Isábena (Southern Pyrenees) and its sub-catchments, and modelling efforts benefited from works done in other sub-catchments in comparable dryland environments (i.e. Benguê, NE Brasil and Ribera Salada, Southern Pyrenees). For the reconstruction of sedigraphs and sediment yield, a novel method based on non-parametric regression was developed, which excelled over traditional methods and could account for high magnitude events and complex interactions in the highly erodible catchment of the River Isábena.
The presented algorithm for automated catena-based landscape discretisation allows the integration of multiple landscape attributes for delineating homogenous landscape units. This constitutes an important aspect for the reproducible upscaling of catchment characteristics to be used in meso-scale modelling.
With WASA-SED, a model for the integrated assessment of water and sediment fluxes is available. It proved to produce plausible results without calibration; and it includes an approach that combines runoff-driven erosion equations (MUSLE, MUST) with a sediment transport limitation concept, which was successfully tested for the highly-erodible Isábena catchment. Limitations of the model have been identified as being mostly related to the resolution of input data, groundwater/low flow dynamics, transmission losses and sediment storage in the river channel.

References

Ackers, P., White, W. R., 1973. Sediment transport: new approach and analysis. *Journal of the Hydraulics Division, ASCE*, 99, 2041-2060.

Amore, E., Modica, C., Nearing, M. A., Santoro, V. C., 2004. Scale effect in USLE and WEPP application for soil erosion computation from three Sicilian basins. *Journal of Hydrology* 293 (1-4), 100 - 114.

Antronico, L., Coscarelli, R., Terranova, O., 2005. Surface erosion assessment in two Calabrian basins (southern Italy). In: Batalla, R. J., Garcia, C. (eds.): *Geomorphological Processes and Human Impacts in River Basins.* IAHS, 299: pp. 16-22.

Appel, K., 2006. Characterisation of badlands and modelling of soil erosion in the Isábena watershed, NE Spain. Unpublished MSc-thesis, Universität Potsdam, Germany.

Arnold, J. G., William, J. R., Nicks, A. D., Sammons, N. B., 1989. SWRRB (A basin scale simulation model for soil and water resources management), User's Manual, Texas A&M University Press, USA.

Arnold, J.G., Williams, J. R., Maidment, D. R., 1995. Continuous-time water and sediment-routing model for large basins. *Journal of Hydraulic Engineering* 121, 171-183.

Asselman, N. E. M., 2000. Fitting and interpretation of sediment rating curves. *Journal of Hydrology* 234 (3-4), 228 - 248.

Avendaño, C., Cobo, R., Sanz, M., Gómez, J. 1997. Capacity situation in Spanish reservoirs. In *74.* I.C.O.L.D. 19th Congress on Large Dams, Florence,.

Bagnold, R. A., 1956. The flow of cohesionless grains in fluids. *Philosophical Transactions of the Royal Society of London, Series A,* 249, 235-297.

Basic, F., Kisic, I., Mesic, M., Nestroy, O., Butorac, A., 2004. Soil Quality as an Indicator of Sustainable Tillage Practices. *Soil and Tillage Research* 78 (2), 197 - 206.

Batalla, R. J., Gómez, C. M., Kondolf, G. M., 2004. Reservoir-induced hydrological changes in the Ebro River basin (NE Spain). *Journal of Hydrology* 290 (1-2), 117 - 136.

Batalla, R., Garcia, C., Balasch, J. C., 2005. Total sediment load in a Mediterranean mountainous catchment (the Ribera Salada River, Catalan Pyrenees, NE Spain). *Zeitschrift für Geomorphologie* 49 (4), 495-514.

Bathurst, J., 2002. Physically-based erosion and sediment yield modelling: the SHETRAN concept. In: Summer, W., Walling, D. E.(eds.): *Modelling erosion, sediment transport and sediment yield.* UNESCO, 60: Paris, pp. 47-67.

Begueria S., 2006. Changes in land cover and shallow landslide activitiy: A case study in the Spanish Pyrenees. *Geomorphology* 74, 196-206.

Begueria, S., Lopez-Moreno, J. I., Morente, A., Seeger, M., Garcia-Ruiz, J. M., 2003. Assessing the effect of climate oscillations and land-use changes on streamflow in the central Spanish Pyrenees. *Ambio* 32, 283-286.

Berry, P., Garlick, J., Freeman, J., Mathers, E., 2005. Global inland water monitoring from multimission altimetry. *Geophysical Research Letters* 32, L16401.

Beven, K., 2001. Rainfall-runoff modelling. The primer. John Wiley & Sons, Chichester, UK.

Boardman, J., Favis-Mortlock, D., 1998. *Modelling soil erosion by water*. Series I: Global Environmental Change, Vol. 55, Springer, Berlin, Germany.

Bogaart, P. T. P. 2006. The convergence paradox: are catchment divergent or convergent. In Poster presented at the 2006 EGU General Assembly, Vienna,.

Boorman, D. B., Hollis, J. M., Lilly, A., 1995. Hydrology of Soil Types: a hydrologically-based classification of the soils of the United Kingdom. Report No. 126, Institute of Hydrology, National Environmental Research Council, UK.

Bracken, L., Kirkby, M., 2005. Difference in hilllsope runoff and sediment transport rates within two semi-arid catchments in southeast Spain. *Geomorphology* 68, 183-200.

Breiman, L., 1996. Bagging predictors. *Machine Learning* 24 (2), 123 - 140.

Breiman, L., 2001. Random Forests. *Machine Learning* 45 (1), 5-32.

Breiman, L. M., Friedman, J., Olshen, R., Stone, C., 1984. Classification and regression trees. Wadsworth, Belmont, CA.

Breuer, L., Eckhardt, K., Frede, H.-G., 2003. Plant parameter values for models in temperate climates. *Ecological Modelling* 169 (2-3), 237 - 293.

Breuer, L., Frede, H.-G., 2003. PlaPaDa - an online plant parameter data drill for eco-hydrological modelling approaches.

Bronstert, A., Batalla, R. J., de Araújo, J. C., Francke, T., Güntner, A., Mamede, G., Müller., E., 2007. Investigating erosion and sediment transport from head-waters to catchments to reduce reservoir siltation in drylands. In: *Reducing the Vulnerability of Societies to Water Related Risks at the Basin Scale*. IAHS-Publications, 317: Wallingford, UK, pp. 119-122.

Buytaert, W., Reusser, D., Krause, S., Renaud, J., 2008. Why can't we do better than Topmodel? *Hydrological Processes* 22 (20), 4175-4179.

Chatterjee, S., Price, B., 1991. Regression analysis by example. Wiley, New York, USA

CHEBRO, 1993. Mapa "Fondos Aluviales" 1:50000, 1993. URL: http://www.oph.chebro.es/ContenidoCartoGeologia.htm (accessed 10 Aug. 2006)

CHEBRO, 1998. Usos de Suelos (1984/1991/1995) de la cuenca hidrográfica del Ebro; 1:100.000, Consultora de M. Angel Fernández-Ruffete y Cereyo, Oficina de Planificación Hidrológica, C.H.E. URL: http://oph.chebro.es/ (accessed 1 Mar. 2006).

Chow, V. T., Maidment, D. R., Mays, L.W., 1988. Applied Hydrology. McGraw-Hill International Editions. Civil Engineering Series. Singapore

Clotet, N., Gallart, F., Balasch, C., 1988. Medium-term erosion rates in a small scarcely vegetated catchment in the Pyrenees. In: Imeson, A. C.(eds.): *Geomorphic processes in environments with strong seasonal contrasts, Vol. 2.* Catena, 13: pp. 37-47.

Cochrane, T. A., Flanagan, D. C., 2003. Representative Hillslope Methods for Applying the WEPP model with DEMs and GIS. *Transactions of the ASAE* 4 (46), 1041–1049.

Cohn, T., Caulder, D., Gilroy, E., Zynjuk, L., Summers, R., 1992. The Validity of a Simple Statistical Model for Estimating Fluvial Constituent Loads: An Empirical Study Involving Nutrient Loads Entering Chesapeake Bay. *Water Resources Research* 28, 2353-2363.

Crawford, C. G., 1991. Estimation of suspended-sediment rating curves and mean suspended-sediment loads. *Journal of Hydrology* 129 (1-4), 331 - 348.

Crawley, M. J., 2002. Statistical computing an introduction to data analysis using S-Plus. Wiley, Chichester. UK

Creutzfeldt, B., 2006. Remote sensing based characterisation of land cover and terrain properties for hydrological modelling in the semi-arid Northeast of Brazil. MSc-thesis, Universität Potsdam, Germany.

CSIC/IRNAS, 2000. Mapa de suelos (Clasificacion USDA, 1987), 1:1 Mio, Sevilla, SEISnet-website, URL: http://leu.irnase.csic.es/mimam/seisnet.htm (accessed 3 Jul. 2006)

Cummings, R. J., Upton, G. J. G., Holt, A. R., Kitchen, M., in press. Using microwave links to adjust the radar rainfall field. *Advances in Water Resources* in press

Curtis, J. A., Flint, L. E., Alpers, C. N., Yarnell, S. M., 2005. Conceptual model of sediment processes in the upper Yuba River watershed, Sierra Nevada, CA. *Geomorphology* 68, 149–166.

de Araújo, J. C., Güntner, A., Bronstert, A., 2006. Loss of reservoir volume by sediment deposition and its impact on water availability in semiarid Brazil. *Earth Surface Processes and Landforms* 51 (1), 157-170.

de la Rosa, D., Mayol, F., Diaz-Pereira, E., Fernandez, M., la, d., Rosa, D., 2004. A land evaluation decision support system (MicroLEIS DSS) for agricultural soil protection: With special reference to the Mediterranean region. *Environmental Modelling & Software* 19 (10), 929 - 942.

de Roo, A. P. J., Wesseling, C. G., Ritsema, C. J., 1996. LISEM: a single event physically-based hydrologic and soil erosion model for drainage basins. I: Theory, input and output. *Hydrological Processes* 10, 1107-1117.

de Vente, J., Poesen, J., Arabkhedri, M., Verstraeten, G., 2007. The sediment delivery problem revisited. *Progress in Physical Geography* 31 (2), 24.

de Vente, J., Poesen, J., Bazzoffi, P., Van Rompaey, A., Verstraeten, G., 2006. Predicting catchment sediment yield in Mediterranean environments: the importance of sediment sources and connectivity in Italian drainage basins. *Earth Surface Processes and Landforms* 31 (8), 1017–1034.

de Vente, J., Poesen, J., Verstraeten, G., Van Rompaey, A., Govers, G., 2008. Spatially distributed modelling of soil erosion and sediment yield at regional scales in Spain. *Global and Planetary Change* 60, 393-415.

De'ath, G., Fabricius, K., 2000. Classification and regression trees: a powerful yet simple technique for the analysis of complex ecological data. *Ecology* 81 (11), 3178–3192.

De'ath, G., 2007. Boosted Trees For Ecological Modeling And Prediction. *Ecology* 88 (1), 243-251.

Doherty, J., 2004.,*PEST - Model-independent parameter estimation. User Manual*. Watermark Numerical Computing

Eckhardt, K., Fohrer, N., Frede, H.-G., 2005. Automatic model calibration. *Hydrological Processes* 19 (3), 651-658.

Epstein, J. M., 2008. Why Model? *Journal of Artificial Societies and Social Simulation* 11 (4), 12.

Erskine, W. D., Mahmoudzadeh, A., Myers, C., 2002. Land-use effects on sediment yields and soil loss rates in small basins of Triassic sandstone near Sydney, NSW, Australia. *Catena* (49), 271– 287.

Evans, I., 1990. General geomorphometry. In: Goudie, A.(eds.): *Geomorphological techniques.* Unwin Hyman, London, UK, pp. 44-56.

Everaert, W., 1991. Empirical relations for the sediment transport capacity of interrill flow. *Earth Surface Processes and Landforms* 16, 513-532.

Everaert, W., 1991. Empirical relations for the sediment transport capacity of interrill flow. *Earth Surface Processes and Landforms* 16 (6), 513-532.

Fan, S.; Springer, F.E., 1993. Major sedimentation issues at the Federal Energy Regulatory Commission. In: Fan, S. and Morris, G. (eds.): *Notes on sediment management in reservoirs.* Water Resources Publications, Colorado, USA, 1-8.

FAO, 1993. Global and national soils and terrain digital databases (SOTER). Procedures Manual. World Soil Resources Reports, No. 74, FAO (Food and Agriculture Organization of the United Nations), Rome, Italy.

FAO, 2001. Global Soil and Terrain Database (WORLD-SOTER). FAO, AGL (Food and Agriculture Organization of the United Nations, Land and Water Development Division), URL: http://www.fao.org/ag/AGL/agll/soter.htm (accessed 12 Apr. 2007)

Fargas, D., Martínez-Casasnovas, J., Poch, R., 1997. Identification of Critical Sediment Source Areas at Regional Level. *Physics and Chemistry of the Earth* 22 (3-4), 355-359.

Flanagan, D., Nearing, M., 1995, *USDA Water Erosion Prediction Project - Hillslope profile and watershed model documentation.* , NSERL Report 10.

Foster, G. R., Wischmeier, W. H., 1974. Evaluating irregular slopes for soil loss prediction. In: *Transactions of the ASAE*. Vol. 17, 305-309.

Fox, J., 2002. An R and S-PLUS companion to applied regression. Sage, Thousand Oaks. USA

Fox, J., 2006. car: Companion to Applied Regression, R package version 1.2-1.

Francke, T., 2005. Consistency tests of the Landscape Unit Mapping Program (LUMP) for WASA. SESAM-project Working Paper, University of Potsdam. URL: http://brandenburg.geoecology.uni-potsdam.de/projekte/sesam/download/ workingpapers/ LUMP-test.pdf (accessed 5 Jun. 2006).

Francke, T., 2006. Working report of Fieldwork campaign Benguê-catchment, Brazil; Jan 2006. SESAM-project, internal working report; URL: http://brandenburg.geoecology.uni-potsdam.de/projekte/sesam/download/ workingpapers/fieldwork_brazil_07_till.pdf (accessed 19. Nov. .2008)

Francke, T., Creutzfeldt, B., Güntner, A., Maerker, M., Mamede, G., Mueller, E.N., 2006. Spatial discretisation in semi-distributed hydrological modelling using the Landscape Unit Mapping Program (LUMP). Poster presented at EGU assembly 2006, Vienna. URL: http://brandenburg.geoecology.uni-potsdam.de/projekte/sesam/download/ presentations/poster_lump.pdf (accessed 5 Jun. 2006).

Francke, T., Güntner, A., Bronstert, A., Mamede, G., Müller, E. N., 2008a. Automated catena-based discretisation of landscapes for the derivation of hydrological modelling units. *International Journal of Geographical Information Science* 22, 111-132.

Francke, T., López-Tarazón, J. A., Schröder, B., 2008b. Estimation of suspended sediment concentration and yield using linear models, Random Forests and Quantile Regression Forests. *Hydrological Processes* 22, 4892–4904.

Francke, T., López-Tarazón, J. A., Vericat, D., Bronstert, A., Batalla, R. J., 2008c. Flood-Based Analysis of High-Magnitude Sediment Transport Using a Non-Parametric Method. *Earth Surface Processes and Landforms* 33 (13), 2064 - 2077.

Gaiser, T., Graef, F., Hilger, T., Ferreira, L., Stahr, K., 2003. An information system for land resources in Piauí and Ceará. In: Gaiser, T., Krol, M., Frischkorn, H., Araú jo, J.(eds.): *Global change and regional impacts: water availability and vulnerability of ecosystems and society in the semiarid Northeast of Brazil.* Springer, Berlin, Germany, pp. 267–278.

Gallart, F., Balasch, J. C., Regüés, D., Soler, M.,

Castelltort, X., 2005. Catchment dynamics in a Mediterranean mountain environment: the Vallcebre research basins (southeastern Pyrenees) II: temporal and spatial dynamics of erosion and stream sediment transport. In: Garcia, C., Batalla, R. J.(eds.): *Catchment Dynamics and River Processes: Mediterranean and Other Climate Regions*. Elsevier, Amsterdam ; London, pp. 17-29.

Gallart, F., Latron, J., Llorens, P., Rabada, D., 1997. Hydrological functioning of mediterranean mountain basins in Vallcebre, Catalonia: Some challenges for hydrological modelling. *Hydrological Processes* 11, 1263-1272.

Gallart, F., Llorens, G., 2004. Observations on land cover changes and water resources in the headwaters of the Ebro catchment, Iberian Peninsula. *Physics and Chemistry of the Earth* 29, 769-773.

Gallart, F., Solé, A., Puigdefàbregas, J., Lázaro, R., 2002. Badland Systems in the Mediterranean. In: Bull, L. J., Kirkby, M. J.(eds.): *Dryland rivers-hydrology and geomorphology of semi-arid channels*. Wiley & Sons, Chichester, UK, pp. 299-326.

Garbrecht, J., Martz, L. W., 2000. Digital Elevation Model Issues in Water Resources Modeling. In: Maidment, D., Djokic, D.(eds.): *Hydrologic and Hydraulic Modeling Support with Geographic Information Systems*. ESRI Press, pp. 1-27.

Garcia-Ruiz, J. M., Lasanta, T., Ruiz-Flano, P., Ortigosa, L., White, S., Gonzalez, C., Marti, C., 1996. Land-use changes and sustainable development in mountain areas: a case study in the Spanish Pyrenees. *Landscape Ecology* 11, 267-277.

Garcia-Ruiz, J. M., Valoer-Garces, B. L., 1998. Historical geomorphic processes and human activities in the central Spanish Pyrenees. *Mountain Research and Development* 18, 309-320.

Graf, W. H., Altinakar, M. S., 1998. Fluvial hydraulics – flow and transport processes in channels of simple geometry. John Wiley & Sons LTDA.

GRASS Development Team, 2005. Geographic Resources Analysis Support System (GRASS GIS) Programmer's Manual. ITC-irst, Trento, Italy. URL: http://grass.itc.it (accessed 1 Mar. 2005).

Green, W. H., Ampt, G. A., 1911. Studies on soil physics I. The flow of air and water through soils. *Journal of Agricultural Science* 4, 1-24.

Güntner, A., 2002. Large-scale hydrological modelling in the semi-arid North-East of Brazil. *PIK-Report No. 77*, Potsdam Institute for Climate Research, Germany.

Güntner, A., Bronstert, A., 2004. Representation of landscape variability and lateral redistribution processes for large-scale hydrological modelling in semi-arid areas. *Journal of Hydrology* 297 (1-4), 136-161.

Güntner, A., Krol, M.S., de Araújo, J.C., Bronstert, A., 2004. Simple water balance modelling of surface reservoir systems in a large data-scarce semi-arid region. *Hydrological Sciences Journal* 49(5), 901-918.

Haan, C. T., Barfield, B. J., Hayes, J. C. 1994. Design hydrology and sedimentology for small catchments. Academic Press, San Diego, CA, USA.

Han, Q.W., 1980. A study on the non-equilibrium transportation of suspended load. *Proc. Int. Symps. on River Sedimentation*, Vol.2 (Beijing China), pp. 793-802.

Han, Q., He, M., 1990. A mathematical model for reservoir sedimentation and fluvial processes. *International Journal of Sediment Research*, 5, 43-84.

Harrell, F. E., 2001. Regression modeling strategies with applications to linear models, logistic regression, and survival analysis. Springer, New York, USA.

Hastie, T., Tibshirani, R., Friedman, J. H., 2001. The elements of statistical learning. Springer, New York, USA.

He, Q., Walling, D., 1997. The Distribution of Fallout 137Cs and 210Pb in Undisturbed and Cultivated Soils. *Applied Radiation and Isotopes* 48 (5), 677-690.

Hessel, R., 2006. Consequences of hyperconcentrated flow for process-based soil erosion modelling on the Chinese Loess Plateau. *Earth Surface Processes and Landforms* 31 (9), 1100-1114.

Holtschlag, D. J., 2001. Optimal estimation of suspended-sediment concentrations in streams. *Hydrological Processes* 15, 1133-1155.

Huisman, J., Pohlert, T., Breuer, L., Frede, H. - G., 2005. The power of multi-objective calibration: two case studies with SWAT. In Proceedings of the 3rd International SWAT Conference, Zürich, Switzerland, July 11-15, 2005.

ICONA, 1987. Mapas de estados erosivos: Cuenca hidrográfica del Ebro. Madrid: Instituto Nacional para la Conservación de la Naturaleza. Ministerio de Agricultura, Pesca y Alimentación

IRTCES, 1985. Lecture notes of the training course on reservoir sedimentation. International Research of Training Center on Erosion and Sedimentation, Sediment Research Laboratory of Tsinghua University, Beijing, China.

Jachner, S., van den Boogaart, K. G., Petzoldt, T., 2007. Statistical methods fort he qualitative assessment of dynamic models with time delay (R Package qualV). *Journal of Statistical Software* 22, 1-30.

Jetten, V., 2002. LISEM user manual, version 2.x. Draft version January 2002. Utrecht Centre for Environment and Landscape Dynamics, Utrecht University, The Netherlands.

Kaufman, L., Rousseeuw, P., 1990. Finding Groups in Data: An Introduction to Cluster Analysis. Wiley, Chichester, UK.

Kinnell, P. I. A., 2001. The USLE-M and Modeling Erosion Within Catchments. In: Stott, D. E., Mohtar, R. H., Steinhardt, G. C.(eds.): *Sustaining the global farm. Selected papers from the 10th International Soil Conservation Organization Meeting, May 24-29, 1999, West Lafayette, IN.* USDA-ARS National Soil Erosion Laboratory, West Lafayette, USA, pp. 924-928.

Kinnell, P. I. A., 2004. Sediment delivery ratios: a misaligned approach to determining sediment delivery from hillslopes. *Hydrological Processes* 18 (16), 3191-3194.

Kinnell, P. I. A., 2007. Runoff dependent erosivity and slope length factors suitable for modelling annual erosion using the Universal Soil Loss Equation. *Hydrological Processes* 21 (20), 2681-2689.

Kirkby, M. J., 1997. Physically based process model for hydrology, ecology and land degradation. In: Brandt, C.J., Thornes, J.B. (eds.): *Mediterranean Desertification and Land-use*. Wiley, Chichester, UK.

Kirkby, M., Bracken, L., 2005. Modelling hillslope connectivity and channel interactions in semiarid areas : implications for hillslope restoration following land abandonment. In: *Geomorphological processes and human impacts in river basins.* IAHS, 299: pp. 3-15.

Kirkby, M. J., Irvine, B. J., Jones, R. J. A., Govers, G. (in press) The PESERA coarse scale erosion model for Europe: I – Model rationale and implementation. *European Journal of Soil Sciences*.

Kisi, O., 2005. Suspended sediment estimation using neuro-fuzzy and neural network approaches. *Hydrological Sciences-Journal* 50 (4), 683-696.

Kisi, O., Emin Karahan, M., Sen, Z., 2006. River suspended sediment modelling using a fuzzy logic approach. *Hydrological Processes* 20 (20), 4351-4362.

Krysanova, V., Wechsung, F., Arnold, J., Srinivasan, R., Williams, J., 2000, *SWIM (Soil and Water Integrated Model), User Manual.* , PIK-Report, Vol. 77, Potsdam Institute for Climate Research, Potsdam, Germany.

Kundzewicz, Z., Mata, L., Arnell, N., Döll, P., Kabat, P., Jiménez, B., Miller, K., Oki, T., Sen, Z. S. I., 2007. Freshwater resources and their management. In: Parry, M., Canziani, O., Palutikof, J., van der Linden, P., Hanson, C.(eds.): *Climate Change 2007: Impacts, Adaptation and Vulnerability. Contribution of Working Group II to the Fourth Assessment Report of the Intergovernmental Panel on Climate Change.* Cambridge University Press, Cambridge, UK, pp. 173-210.

Lasanta-Martinez, T., Vicente-Serrano, S. M., Cuadrat-Prats, J. M., 2005. Mountain Mediterranean landscape evolution caused by the abandonment of traditional primary activities: a study of the Spanish Central Pyrenees. *Applied Geography* 25, 47-65.

Leipprand, A., Kadner, S., Dworak, T., Hattermann, F., Post, J., Krysanova, V., Benzie, M., Berglund, M., 2008. Impacts of climate change on water resources - adaptation strategies for Europe, Commissioned by the German Federal Environment Agency, Research Report 205 21 200, UBA-FB 001175.

Lenhart, T., Rompaey, A. V., Steegen, A., Fohrer, A., Frede, H.-G., Govers, G., 2005. Considering spatial distribution and deposition of sediment in lumped and semi-distributed models. *Hydrological Processes* 19, 785–794.

Liaw, A., Wiener, M., 2002. Classification and Regression by Random Forests. *R News* 2 (3), 18-22.

Liebe, J., van de Giesen, N., Andreini, M., 2005. Integrated Water Resource Assessment. *Physics and Chemistry of the Earth, Parts A/B/C* 30 (6-7), 448 - 454.

Liu, Y., Gupta, H. V., 2006. Uncertainty in hydrologic modeling: Toward an integrated data assimilation framework. *Water Resources Research* 43, W07401.

Lohani, A. K., Goel, K., Bhatia, K. K. S., 2007. Deriving stage–discharge–sediment concentration relationships using fuzzy logic. *Hydrological Sciences-Journal* 52 (4), 793-807.

Lopez-Moreno, J. I., Begueria, S., Garcia-Ruiz, J. M., 2006. Trends in high flows in the central Spanish Pyrenees: response to climatic factors or to land-use change? *Hydrological Sciences Journal* 51, 1039-1050.

López-Tarazón, J. A., 2006. Transport de sediment en suspensió al riu Isàbena (conca de l'Ebre). MSc-thesis, Universitat de Lleida, Catalonia, Spain.

López-Tarazón, J., Batalla, R. J., Vericat, D., Francke, T., 2009, in press. Suspended Sediment Transport in a Highly Erodible Catchment: The River Isabena (Central Pyrenees). *Geomorphology*.

López-Vicente, M., Navas, A., Machín, J., 2008. Identifying erosive periods by using RUSLE factors in mountain fields of the Central Spanish Pyrenees. *Hydrology and Earth System Sciences Discussions* 4 (4), 2111-2142.

Lu, H., Prosser, I. P., Gallant, J. C., Moran, C. J. P. G., Stevenson, J. G., 2003. Predicting sheet-wash and rill erosion over the Australian continent. *Australian Journal of Soil Research* (41), 1037-1062.

Mac Nally, R., 1996. Hierarchical partitioning as an interpretative tool in multivariate inference. *Australian Journal of Ecology* 21, 224-228.

Maidment, D. R., 1993. Handbook of hydrology. MGraw-Hill, New York, USA.

Mallows, C. L., 1973. Some Comments on Cp. *Technometrics* 15, 661-675.

Mamede, G., 2008. Reservoir sedimentation in dryland catchments: Modelling and management. PhD thesis, Universität Potsdam, Germany, URL: http://opus.kobv.de/ubp/volltexte/2008/1704/.

Mamede, G. L., Bronstert, A., Francke, T., Müller, E., de Araújo, J. C., Batalla, R. J., Güntner, A. 2006. 1D Process-based modelling of reservoir sedimentation: a case study for the Barasona Reservoir in Spain. In: *Conference Proceedings River Flow 2006*. International Conference on Fluvial Hydraulics, Lisbon, Portugal, September 06 - 08, 2006.

Märker, M., 2001. Regionale Erosionsmodellierung unter Verwendung des Konzepts der Erosion Response Units (ERU) am Beispiel zweier Flusseinzugsgebiete im südlichen Afrika. PhD-thesis, Friedrich-Schiller-Universität, Jena, Germany.

Martínez-Carreras, N., Soler, M., Hernández, E., Gallart, F., 2007. Simulating badland erosion with KINEROS2 in a small Mediterranean mountain basin (Vallcebre, Eastern Pyrenees). *Catena* 71, 145–154.

Martínez-Casasnovas, J., Poch, R. 1997. Estado de conservación de los suelos de la cuenca del embalse 'Joaquín Costa'. In: Proceedings of 'Encuentro científico-técnico sobre el vaciado total y prolongado del embalse de Joaquin Costa', Zaragoza, Spain.

MATHWORKS, 2002. MatLab—The Language of Technical Computing. Version 6.5, The MathWorks, Natick, MA, USA

Maurer, T., 1997, *Physikalisch begründete, zeitkontinuierliche Modellierung des Wassertransports in kleinen ländlichen Einzugsgebieten.* , Vol. H. 61, Mitteilungen Inst. f. Hydrologie u. Wasserwirtschaft, H. 6. Universität Karlsruhe, Germany

McBratney, A. B., Odeh, I. O. A., Bishop, T. F. A., Dunbar, M. S., Shatar, T. M., 2000. An overview of pedometric techniques for use in soil survey. *Geoderma* 97 (3-4), 293 - 327.

McKay, M. D., Beckman, R. J., Conover, W. J., May, 1979. A Comparison of Three Methods for Selecting Values of Input Variables in the Analysis of Output from a Computer Code. *Technometrics* 21 (2), 239 - 245.

Meade, R., Yuzyk, T., Day, T., 1990. Movement and storage of sediment in rivers of the United States and Canada. In: Wolman, M. G., Riggs, H. C.(eds.): *Surface Water Hydrology, The Geology of North America, vol. O-1*. Geol. Soc. of Am., Boulder, CO, USA, pp. 255-280.

Medeiros, P., Güntner, A., Francke, T., Mamede, G. de Araujo, J. C. (*submitted*). Spatial and temporal patterns of sediment yield and connectivity at the catchment scale: an application of WASA-SED model to a semi-arid environment. *Journal of Hydrology*

Meinshausen, N., 2006. Quantile Regression Forests. *Journal of Machine Learning Research* 7, 983-999.

Meinshausen, N., 2007. quantregForest: Quantile Regression Forests; R package version 0.2-2.

Meischner, P. (ed.), 2007. *Weather Radar: Principles and Advanced Applications*. 2nd Edition. Springer, Berlin, Germany

Messer, H. A., Zinevich, A., Alpert, P., 2006. Environmental monitoring by wireless communication networks. *Science*, 312, 713.

Meyer-Peter, E., Müller, R., 1948. Formulas for bedload transport. *Proc. International Association of Hydraulic Research*. 3rd Annual Conference, Stockholm, Sweden, 39-64.

Miller, T., Lumley, A., 2006. leaps: regression subset selection; R package version 2.7.

Moreno, J. M., Aguiló, E., Alonso, S., Álvarez Cobelas, M., Anadón, C., 2005. A Preliminary Assessment of the Impacts in Spain due to the Ef-

fects of Climate Change. J.M. Moreno Rodríguez. ECCE Project - Final Report, Ministerio de Medio Ambiente.

Morgan, R.P.C., 1995. Soil erosion and conservation Longman Group, UK Limited.

Morgan, R. P. C., 2005. Soil erosion and conservation. Blackwell, Oxford, UK.

Morgan, R. P. C, Quinton, J. N., Smith, R. E., Govers, G., Poesen, J. W. A., Auerswald, K., Chisci, G., Torri, D., Styczen, M. E., 1998. The European Soil Erosion Model (EUROSEM): a dynamic approach for predicting sediment transport from fields and small catchments. *Earth Surface Processes and Landforms* 23, 527-544.

Mosley, M. P., McKerchar, A., 1993. Streamflow. In: Maidment, D. R.(eds.): *Handbook of Hydrology*. McGraw-Hill, New York, USA, pp. 8.1-8.39.

Mueller, E., submitted. Quantification of the transient sediment storage in the riverbed for a dryland setting in NE Spain. *International Journal of River Basin Management*.

Mueller, E. N., Batalla, R. J., Garcia, C., Bronstert, A., 2008. Modelling bedload rates from fine grain-size patches during small floods in a gravel-bed river. *Journal of Hydraulic Engeneering* in press

Müller, E., Francke, T., 2006. Parameterisation of the Ésera Catchment, NE Spain; Jan 2009. SESAM-project, internal working report; http://brandenburg.geoecology.uni-potsdam.de/projekte/sesam/download/workingpapers/Esera_Parameterisation_Doku.pdf (accessed 30. Jan. 2009)

Mueller, E. N., Francke, T., Batalla, R. J., Bronstert, A. (submitted) Modelling the effects of land-use change on runoff and sediment yield for a meso-scale catchment in the Southern Pyrenees. *Catena*

Mueller, E. N., Güntner, A., Francke, T., Mamede, G., 2008. Modelling water availability, sediment export and reservoir sedimentation in drylands with the WASA-SED Model. *Geoscientific Model Development Discussions* 1 (1), 285 - 314.

Mueller, E. N., Wainwright, J., Parsons, A. J., 2007. The Impact of Connectivity on the Modelling of Overland Flow within Semi-Arid Shrubland Environments, *Water Resources Research* 43, W09412

Mulligan, M., Wainwright, J., 2004. Modelling and model Building. In: Wainwright, J., Mulligan, M. (eds.): *Environmental modelling. Finding simplicity in complexity*. Wiley, Chichester, UK

Nagy, H. M., Watanabe, K., Hirano, M., 2002. Prediction of Sediment Load Concentration in Rivers using Artificial Neural Network Model. *Journal of Hydraulic Engineering* 128 (6), 588-595.

Nash, E., 2007 Spanish wine-makers forced into Pyrenees by global warming. *The Independent* 27.09.2007.

Nash, J. E., Sutcliffe, V., 1970. River flow forecasting through conceptual models, I. A discussion of principles. *Journal of Hydrology* 10, 282-290.

Navas, A., Valero-Garcés, B. L., Machín, J., 2004. Research Note: An approach to integrated assessement of reservoir siltation: the Joaquín Costa reservoir as a case study. *Hydrology and Earth System Sciences* 8 (6), 1193-1199.

Nearing, M. A., 1998. Why soil erosion models over-predict small soil losses and under-predict large soil losses. *Catena* 32 (1), 15 - 22.

Neitsch, S., Arnold, J., Kiniry, J., Williams, J., King, K., 2002, *Soil and water assessment tool-theoretical documentation, version 2000.* , TWRI Report TR-191, Texas Water Resources Institute.

Onstad, C., Foster, G., 1975. Erosion modeling on a watershed. *Trans. Amer. Soc. Civ. Engrs* 18 (2), 288-292.

Ortigosa, L. M., Garcia-Ruiz, J. M., Gil, E., 1990. Land reclamation by reforestation in the central Pyrenees. *Mountain Research and Development* 10, 281-288.

Ortigosa, L. M., Garcia-Ruiz, J. M., 2000. Geomorphological consequences of afforestation at a basin scale, an example from the Central Pyrenees. *Physics and Chemistry of the Earth* 20, 345-349.

Pistocchi, A., Cassani, G., Zani, O. 2002. Use of the USPED model for mapping soil erosion and managing best land conservation practices. In: 1st Biennial Meeting of the iEMSs, vol. 3.

Prasad, A., Iverson, L., Liaw, A., 2006. Newer Classification and Regression Tree Techniques: Bagging and Random Forests for Ecological Prediction. *Ecosystems* 9 (2), 181 - 199.

Quinn, G. P., Keough, M. J., 2002. Experimental design and data analysis for biologists. Cambridge Univ. Press, Cambridge, UK.

Quinton, J., 2004. Erosion and sediment transport. In: Wainwright, J., Mulligan, M. (eds.): *Environmental modelling. Finding simplicity in complexity.* Wiley, Chichester, UK

Regüés, D., Balasch, J., Castelltort, X., Soler, M., Gallart, F., 2000a. Relación entre las tendencias temporales de producción y transporte de sedimentos y las condiciones climáticas en una

pequeña cuenca de montaña mediterránea (Vallcebre, Eastern Pyrenees). *Cuadernos de Investigación Geográfica* 26, 24-41.

Regüés, D., Guàrdia, R., Gallart, F., 2000b. Geomorphic agents versus vegetation spreading as-causes of badland occurrence in a Mediterranean-subhumid mountainous area. *Catena* 40, 173-187.

Reineking, B., Schröder, B., 2006. Constrain to perform: Regularization of habitat models. *Ecological Modelling* 193 (3-4), 675-690.

Renschler, C. S., Mannaerts, C., Diekkrüger, B., 1999. Evaluating spatial and temporal variability in soil erosion risk -- rainfall erosivity and soil loss ratios in Andalusia, Spain. *Catena* 34 (3-4), 209 - 225.

Reusser, D., Kneis, D., Francke, T., 2008. Manual for GOLM_db (General Observation and Location data Management). Technical report. URL: http://brandenburg.geoecology.uni-potsdam.de/projekte/sesam/download/software (accessed 17 Nov 2008)

Rickenmann, D., 2001. Comparison of bed load transport in torrents and gravel bed streams. *Water Resources Research* 37, 3295-3305.

Rius, J., Batalla, R., Poch, R. M., 2001. Monitoring water and sediment yield in Mediterranean mountainwatersheds: preliminary results. In Stott, D. E., Mohtar, R. H., Steinhardt, G. C. (eds.): *Sustaining the global farm*, selected papers from the 10th International Soil Conversation Organisation Meeting held May 24-29, 1999 at Purdue University, pp. 223-228.

R-Team Development Core, 2006. R: A Language and Environment for Statistical Computing. R Foundation for Statistical Computing, Vienna, Austria.

Rudra, R. D. W. T., Wall, G. L., 1998. Problems Regarding the Use of Soil Erosion Models. In: Boardman, J., Favis-Mortlock, D.(eds.): *Modelling soil erosion by water*. Springer, Berlin, London, pp. 175-190.

Saavedra, C., Mannaerts, C. 2005. Erosion estimation in an Andean catchment combining coarse and fine resolution satellite imagery. In Proceedings of the 31st International Symposium on Remote Sensing of Environment : global monitoring for sustainability and security, Saint Petersburg.

Sanz Montero, M., Cobo Rayán, R., Avendaño Salas, C., Gómez Montaña, J. 1996. Influence of the drainage basin area on the sediment yield to Spanish reservoirs. In: Proceedings of the First European Conference and Trace Exposition on Control Erosion.

Schaap, M. G., Leij, F. J., van Genuchten, M. Th. (2001): ROSETTA: a computer program for estimating soil hydraulic parameters with hierarchical pedotransfer functions. *Journal of Hydrology* 251, 163-176

Scherrer, S., Naef, F., 2003. A decision scheme to indicate dominant hydrological flow processes on temperate grassland. *Hydrological Processes* 17 (2), 391-401.

Schmidt, J., 1991. A mathematical model to simulate rainfall erosion. *Catena Suppl.* 19, 101-109.

Schmidt, J., Dikau, R., 1999. Extracting geomorphometric attributes and objects from digital elevation models - semantics, methods, future needs. In: Dikau, R., Saurer, H.(eds.): *GIS for earth surface systems : analysis and modelling of the natural environment.* Gebrüder Bornträger, pp. 153-173.

Schnabel, S., Maneta, M., 2005. Comparison of a neural network and a regression model to estimate suspended sediment in a semiarid basin. In: Batalla, R. J., Garcia, C.(eds.): *Geomorphological Processes and Human Impacts in River Basins.* IAHS Publications, 299: pp. 91-100.

Schoklitsch, A., 1950. *Handbuch des Wasserbaus.* 2nd ed., Springer, Vienna, Austria.

Schoorl, J. M., Boix Fayos, C., de Meijer, R. J., van der Graaf, E. R., Veldkamp, A., 2004. The 137Cs technique applied to steep Mediterranean slopes (Part I): the effects of lithology, slope morphology and land-use. *Catena* 57 (1), 15-34.

SESAM, 2006. SESAM – Sediment Export from large Semi-Arid Catchments: Measurement and Modelling. Interim Report 2006. URL: http://brandenburg.geoecology.uni-potsdam.de/projekte/sesam/reports.php (accessed 23. Aug. 2007)

SESAM, 2008. SESAM – Sediment Export from large Semi-Arid Catchments: Measurement and Modelling. make_wasa_input: toolset for generating the WASA-SED input files from a database. Technical report. URL: http://brandenburg.geoecology.uni-potsdam.de/projekte/sesam/download/software/make_wasa_input.zip (accessed 13. Nov. 2008)

Shuttleworth, J., Wallace, J. S., 1985. Evaporation from sparse crops – an energy combination theory. *Quarterly Journal of the Royal Meteorological Society* 111, 839-855

Sidorchuk, A. 1998. A dynamic model of gully erosion. In: Boardman, J., Favis-Mortlock, D. (eds.): *Modelling soil erosion by water*. NATO-

Series I, Vol. 55, pp. 451-460, Berlin, Heidelberg, Germany.

Sidorchuk, A., Sidorchuk, A., 1998. Model for estimating gully morphology. IAHS Publ., 249, pp. 333-343, Wallingford, UK

Sidorchuk, A., Walling, D., Wasson, R., 2003. A LUCIFS Strategy: Modelling the Sediment Budgets of Fluvial Systems. In: Lang, A., Hennrich, K., Dikau, R.(eds.): *Long Term Hillslope and Fluvial System Modelling*. Springer, Berlin, Heidelberg, pp. 19-35.

Sivakumar, B., Wallender, W. W., 2005. Predictability of river flow and suspended sediment transport in the Mississippi River basin: a non-linear deterministic approach. *Earth Surface Processes and Landforms* 30 (6), 665-677.

Sivapalan, M., Viney, N. R., Jeevaraj, C. G., 1996. Water and salt balance modelling to predict the effects of land-use changes in forested catchments. 3. The large scale model. *Hydrological Processes* 10: 429-446.

Smart, G. M., Jaeggi, M. N. R., 1983. Sediment transport on steep slopes. Mitteil. 64, Versuchsanstalt für Wasserbau, Hydrologie und Glaziologie, ETH-Zürich, Switzerland.

Smith, C., Croke, B., 2005. Sources of uncertainty in estimating suspended sediment load. In: Horowitz, A. J., Walling, D. E.(eds.): *Sediment Budgets 2*. IAHS, 292: pp. 136-143.

Strauss, P., Klaghofer, E., 2003. Scale considerations for the estimation of processes and effects of soil erosion in Austria. In: Francaviglia R.(eds.): *Agricultural Impacts on Soil Erosion and Soil Biodiversity: Developing Indicators for Policy Analysis. Proceedings from an OECD Expert Meeting - Rome, Italy, March 2003*. pp. 229-238.

Tamene, L., Park, S. J., Dikau, R., Vlek, P. L. G., 2006. Reservoir siltation in the semi-arid highlands of northern Ethiopia: sediment yield-catchment area relationship and a semi-quantitative approach for predicting sediment yield. *Earth Surface Processes and Landforms* 31 (11), 1364-1383.

Thapa, P. K., Bardossy, A., 2008. Very good prediction of a distributed rainfall runoff model but for all wrong reasons. Poster presentation at: The court of Miracles of Hydrology. Cemagref and ENGREF-AgroParistech, Paris, 18-20 June 2008.

Ubalde, J. M., Rius, J., Poch, R., 1999. Monitorizacion de los cambios de uso del suelo en la cabecera de cuenca de la Ribera Salada mediante fotografia aerea y S.I.G. (El Solsones, Lleida, España), *Pirineos* 153-154, 101-122.

USDA-SCS, 1992. USDA-SCS, 1992. Ephemeral Gully Erosion Model. EGEM. Version 2.0 DOS User Manual. Washington, USA.

Valero-Garcés, B. L., Navas, A., Machín, J., Walling, D., 1999. Sediment sources and siltation in mountain reservoirs: a case study from the Central Spanish Pyrenees. *Geomorphology* 28, 23–41.

Venables, W. N., Ripley, B. D., 2002. Modern Applied Statistics with S. Springer, New York, USA.

Verdú, J. M., Batalla, R. J., Poch, R. M., 2000. Dinamica erosiva y aplicabilidad de modelos fisicos de erosion en una cuenca de montana mediterranea (Ribera Salada, Cuenca del Segre, Lleida, Espana). *Pirineos* 155, 37-57.

Verdú, J., 2003. Analysis and modelling of the hydrological and fluvial response of a largemountainous Mediterranean catchment (Isabena River, Pre-Pyrenees). Unpublished PhD-thesis, Universitat de LleidaUniversitat de LleidaUniversitat de Lleida, Catalonia, Spain.

Verdú, J., Batalla, R., Martínez-Casasnovas, J., 2006a. Estudio hidrológico de la cuenca del río Isábena (Cuenca del Ebro). I: Variabilidad de la precipitación. *Ingeniería del Agua* 13 (4), 321-330

Verdú, J., Batalla, R., Martínez-Casasnovas, J., 2006b. Estudio hidrológico de la cuenca del río Isábena (Cuenca del Ebro). II: Respuesta hidrológica. *Ingeniería del Agua* 13 (4), 331-343.

Vericat, D., Batalla, R., 2006. Balance de sedimentos en el tramo bajo del Ebro. *Cuaternario y Geomorfología* 20 (1-2), 79-90.

Von Werner, K., 1995. GIS-orientierte Methoden der digitalen Reliefanalyse zur Modellierung von Bodenerosion in kleinen Einzugsgebieten. PhD-thesis, TU Berlin, Germany.

Wainwright, J., Parsons, A. J., 1995. Sensitivity of sediment-transport equations to errors in hydraulic models of overland flow. In: Boardman, J., Favis-Mortlock, D. (eds.): *Modelling soil erosion by water*. NATO ASI Series, Springer, Berlin, Germany. pp. 271-284.

Walling, D. E., 1977. Limitations of the rating curve technique for estimating suspended sediment loads, with particular reference to British rivers. In: *Erosion and Solute Matter Transport in Inland Waters*. pp. 34-38.

Walling, D. E., 1984. Dissolved loads and their measurements. In: Hadley, R. F., Walling D. E. (eds.): *Erosion and sediment yield: Some methods*

of measurements and modelling. Geo Books, London, pp. 111-117.

Walling, D. E., 1984. Dissolved load and their measurements. In: Hadley, R., Walling, D.(eds.): *Erosion and sediment Yield*. Cambridge University Press, pp. 111-178.

Walling, D. E. 2004. Quantifying the fine sediment budgets of river basins. In: Proceedings Irish National Hydrology Seminar.

Walling, D. E., Collins, A., Sichingabula, H., Leeks, G., 2001. Integrated assessment of catchment suspended sediment budgets: a Zambian example. *Land Degradation and Development* 12, 387-415.

Wang, G., Wente, S., Gertner, G., Anderson, A., 2002. Improvement in mapping vegetation cover factor for the universal soil loss equation by geostatistical methods with Landsat Thematic Mapper images. *International Journal of Remote Sensing* 23 (18), 3649–3667.

Williams, G., 1989. Sediment concentration versus water discharge during single hydrologic events in rivers. *Journal of Hydrology* 111, 89-106.

Williams, J. R., 1995. The EPIC Model. In: Singh, V. P. (ed.): *Computer Models of Watershed Hydrology*. Water Resources Publications, Highlands Ranch, CO, USA, pp. 909-1000.

Wischmeier, W., Smith, D., 1978. Predicting rainfall erosion losses. U.S. Gov. Print. Off, Washington.

Wood, P., 1977. Controls of variation in suspended sediment concentration in the River Rother, West Sussex, England. *Sedimentology* 24, 437-445.

Woolhiser, D., Smith, R., Goodrich, D., 1990, *KINEROS, A Kinematic Runoff and Erosion Model: Documentation and User Manual.* , Vol. ARS-77, U S. Department of Agriculture, A. R. S.

Wren, D. G., Barkdoll, B. D., Kuhnle, R. A., Derrow, R. W., 2000. Field Techniques for Suspended-Sediment Measurement. *Journal of Hydraulic Engineering* 126 (2), 97-104.

Wu, W., Rodi, W., Wenka, T., 2000. 3D numerical modeling of flow and sediment transport in open channels. *Journal of Hydraulic Engeneering* 126, 4-15.

Yang, C.T., Simoes, F.J.M., 2002. User's manual for GSTARS3 (Generalized Sediment Transport model for Alluvial River Simulation version 3.0). U.S. Bureau of Reclamation Technical Service Center, Denver, CO, USA.

Zapata, F., 2002. Handbook for the assessment of soil erosion and sedimentation using environmental radionuclides. Kluwer Academic Publ, Dordrecht, The Netherlands.

Zhang, X., Srinivasan, R., Zhao, K., Liew, M. V., 2008. Evaluation of global optimization algorithms for parameter calibration of a computationally intensive hydrologic model. *Hydrological Processes* (online preview).

Acknowledgements

During my PhD, I had the pleasant experience of lots of support from many different people, all of which deserve my gratitude.
First of all, I would like to thank my supervisor Axel Bronstert for giving me the opportunity to work on an inspiring subject with all the scientific freedom and support one could wish for. Likewise, I am deeply indebted to Ramon Batalla, who provided invaluable support during fieldwork, lots of crucial input and taught me to "eat a lot of soup before challenging the big cheeses".
I am very grateful for having been a part of the SESAM-project. Thanks to Eva Müller, José Carlos de Araújo and Andreas Güntner, I was able to enjoy a highly-experienced yet laid-back working atmosphere with always enough time for discussions. This also includes Boris Schröder, Damià Vericat and Nicholas Meinshausen, who were never short of an inspiring answer to a given question.
I would like to thank my fellow PhD-students associated with the project who collaborated with me: George Mamede, who taught me Brazilian children's songs in the midst of the Caatinga; José López-Tarazón, for proving that 2 am is the best time to go taking water samples and Benjamin Creutzfeldt, for making German scientists legendary long before I arrived in Aiuaba. Special thanks go to Pedro Medeiros, one of the most inspiring persons I have worked with, whose sharp wits helped me unravel many *USLE-related questions.
Working at the Institute for Geoecology was always a pleasure for me thanks to the scientific and technical staff that helped me to accept the mysteries of ArcMap, provided key knowledge on the hood infiltrometer, replaced CPU-fans during model-runs, almost converted me to Linux (LateX still pending), etc.: Damaris, Theresa, Saskia, Andi, Daniel, David, Dominik, Erwin, Hauke, Jan and Thomas made every lunch-break a dinner with friends. My utmost gratitude goes to my office-mate Maik who introduced me to maieutics and endured countless swear words and some strange habits of mine. Without the Master students Katharina, Conrad and Christian, WASA-SED and the accompanying scripts would still hold twice as many bugs. Kudos to all the students we recklessly exploited in the field or in the laboratory.
I am deeply indebted to Wolfgang Regenstein, who never lost his generosity towards us Geoecologists despite all the bad luck with the Gamma spectrometer.
Thanks are due to Celia Kirby for proof-reading all my manuscripts in record time. I hope one day I will also get the chance to have my pronunciation corrected.
Finally, I am most grateful for the support of my family, namely my father and my brother, who were never more than a phone-call or instant-message away and always made me feel that a profound knowledge of physics and the dark sides of operating systems toughen you for scientific life. Thanks to my wife for bearing with an often absent-minded or frustrated husband – I promise, this is the last PhD (at least for this year). At last, my marvellous daughters deserve all the credit for reassuring me every day that modelling is merely poor reflection of true life.
I am very grateful for being blessed with all these people.